INFORMATION TO USERS

This manuscript has been reproduced from the microfilm master. UMI films the text directly from the original or copy submitted. Thus, some thesis and dissertation copies are in typewriter face, while others may be from any type of computer printer.

The quality of this reproduction is dependent upon the quality of the copy submitted. Broken or indistinct print, colored or poor quality illustrations and photographs, print bleedthrough, substandard margins, and improper alignment can adversely affect reproduction.

In the unlikely event that the author did not send UMI a complete manuscript and there are missing pages, these will be noted. Also, if unauthorized copyright material had to be removed, a note will indicate the deletion.

Oversize materials (e.g., maps, drawings, charts) are reproduced by sectioning the original, beginning at the upper left-hand corner and continuing from left to right in equal sections with small overlaps. Each original is also photographed in one exposure and is included in reduced form at the back of the book.

Photographs included in the original manuscript have been reproduced xerographically in this copy. Higher quality 6" x 9" black and white photographic prints are available for any photographs or illustrations appearing in this copy for an additional charge. Contact UMI directly to order.

UMI

A Bell & Howell Information Company
300 North Zeeb Road, Ann Arbor MI 48106-1346 USA
313/761-4700 800/521-0600

NMR STUDY OF NITROGEN INVERSION AND N-O BOND ROTATION AND ANOMERIC EFFECT IN HYDROXYLAMINE DERIVATIVES

BY

Azfar Hassan

A Dissertation Presented to the

FACULTY OF THE COLLEGE OF GRADUATE STUDIES

KING FAHD UNIVERSITY OF PETROLEUM & MINERALS

DHAHRAN, SAUDI ARABIA

In Partial Fulfillment of the
Requirements for the Degree of

DOCTOR OF PHILOSOPHY
In
CHEMISTRY

NOVEMBER, 1996

IN THE NAME OF ALLAH
THE MOST BENEFICENT THE MOST MERCIFUL

KING FAHD UNIVERSITY OF PETROLEUM AND MINERALS DHAHRAN 31261, SAUDI ARABIA

COLLEGE OF GRADUATE STUDIES

This dissertation, written by Mr. Azfar Hassan under the direction of his Dissertation advisor and approved by his Dissertation Committee, has presented to and accepted by the Dean of College of Graduate Studies, in partial fulfillment of the requirements for the degree of DOCTOR OF PHILOSOPHY in chemistry.

Dissertation committee:

Professor M. I. M. Wazeer
Dissertation Advisor

Professor S. A. Ali
Dissertation Co-Advisor

Professor A. A. Isaab
Member

Dr. H. P. Perzanowski
Member

Professor U. Klein
Member

Dr. E. Y. Osei.-Twum
Member

Dr. Abdulrehman. A. Al-Arfaj
Department Chairman

Dean, College of Graduate Studies

Date: 30-4-97

To

My Parents

ACKNOWLEDGMENT

*All praises to Almighty **Allah** for His guidance and bounties and all respects to our Holy prophet **Hazrat Muhammad** (peace be upon him) .*

I would like to express my sincere gratitude and appreciation to my dissertation advisor Prof. M. I. M. Wazeer, and co-advisor Prof Sk. Asrof Ali for their able guidance and encouragement during the research work. Their cooperation, in and out of the lab always remained a source of inspiration for me.

I thank and eulogize the other members of my dissertation committee, Prof. A. A. Isaab, Prof. U. Klein, Dr. H. P. Perzanowski and Dr. E. Y. Osei-Twum for their positive criticism and helpful suggestions.

I am grateful to Dr. Abdulrehman A. Al-Arfaj, Chairman Chemistry Department, for providing the available facilities and extending all possible help and support necessary to carry out my research work.

I am thankful to the technical staff of the Chemistry Department, for their help and assistance.

I am also thankful to my colleagues and friends for their help during the course of my work. I wish to mention Arshad, Asad, Atif, Fahim, Imran, Naseem, Shakil, Shariq, Shazada, Tiwana, and Zaka.

Finally, I wish to thank my family members, for their prayers, love and support . This achievement wouldn't have been possible without their contribution in so many different ways.

May Allah Bless them all (Ameen).

TABLE OF CONTENTS

LIST OF TABLES

LIST OF FIGURES

LIST OF SCHEMES

LIST OF PUBLICATIONS

Sk. Asrof Ali, **Azfar Hassan,** Mohammad I. M. Wazeer," NMR study of the anomeric effect and nitrogen inversion in some isoxazolidines." ***Spectrochimica Acta Part A*** , **51**, 2279-2287, 1995.

Sk. Asrof Ali, **Azfar Hassan,** Mohammad I. M. Wazeer," Nitrogen inversion and N-O bond rotation processes in di- and tri-substituted hydroxylamines. A dynamic NMR study." ***J.Chem. Soc. Perkin Transactions 2*** , 1479-1483, 1996.

Azfar Hassan, Mohammad I. M. Wazeer, H. P. Perzanowski, Sk. A. Ali," Nitrogen inversion and N-O bond rotation in some hydroxylamine and isoxazolidine derivatives". *J. Chem. Soc. Perkin Transactions 2*, 411-418, 1997.

DISSERTATION ABSTRACT

NAME	AZFAR HASSAN
TITLE OF STUDY	NMR STUDY OF NITROGEN INVERSION, AND N-O BOND ROTATION AND ANOMERIC EFFECT IN HYDROXYLAIME DERIVATIVES
MAJOR FIELD	CHEMISTRY
DATE OF DEGREE	November, 1996

A multitude of nitrones are prepared by the condensation of aldehydes and hydroxylamines, which on reduction with $NaBH_4$ gave the required hydroxylamines. The barriers to inversion in these acyclic di- and tri- substituted hydroxylamines are determined by ^1H NMR bandshape analysis. The barriers range from 49.1 to 66.8 kJ mol^{-1}. The magnitude of the barriers are discussed in terms of a conformational process which involves nitrogen inversion and rotation around N-O bond. The N-benzyl group with an *ortho* hydroxy substituent increases the nitrogen inversion barrier by 10 kJ mol^{-1}, which indicates the requirement of breaking of the intramolecular hydrogen bond prior to inversion. In several series of compounds, having $XC_6H_4CH_2$ substituents attached to nitrogen, Hammet free energy correlations are obtained with positive ρ values, indicating increased electron density at the transition state for the inversion process. To shed more light on the nitrogen inversion process and anomeric effect a series of isoxazolidines are also synthesized, and their ^1H and ^{13}C NMR spectra recorded over a range of temperatures. Hammet plots were obtained to quantify the reaction constant ρ. Isoxazolidines with C(5) ethoxy substituents demonstrate a strong anomeric effect. Kinetic studies involving HgO and *para* benzoquinone oxidation of hydroxylamines to nitrones provided an insight to the mechanistic pathway the oxidation process traverses. The formation of E nitrones which quickly isomerize to the Z nitrone was also observed. This isomerization appears to be a bimolecular process.

DOCTOR OF PHILOSOPHY DEGREE
KING FAHD UNIVERSITY OF PETROLEUM AND MINERALS
DHAHRAN, SAUDI ARABIA

خلاصة الرسالة

الاسم : أظفر حسن

عنوان الرسالة : دراسة انقلاب النيتروجين وحاجز الدوران في N-O بواسطة مطيافية NMR والتأثير الحثي في مشتقات الهيدروكسيل الامين .

التخصص : كيمياء

التاريخ : نوفمبر ١٩٩٦

لقد تم تحضير العديد من مركبات النيترون بتفاعل تكاثف الألدهيد مع هيدروكسيل الأمين الذي عند اختزاله بواسطة $NaBH_4$ يعطي الهيدروكسيل أمين المطلوب . وقد تم تعيين حاجز الانقلاب في بدائل الهيدروكسيل أمين الثنائية والثلاثية بواسطة تحليل طيف الرنين النووي المغناطيسي ^1HNMR ووجد أن قيمته تتراوح بين ٤٩،١ - ٦٦،٨ كيلوجول / مول . يمكن تفسير قيمة الحاجز بعمليات التعديل التي تتضمن انقلاب النيتروجين ودوران حول الرابطة N-O . مركبات ن - بنزايل المحتوية على مجموعة هيدروكسيل في الوضع أورثو تزيد حاجز انقلاب النيتروجين بمقدار ١٠ كيلو جول /مول مما يدل على انكسار الرابطة الهيدروجينية قبل انقلاب النيتروجين . في مجموعة من المركبات المحتوية على بدائل $xC_6H_4CH_2$ المرتبطة بالنيتروجين فان طاقة الربط الحرة Hammett Plot لها قيمة موجبة مما يدل على زيادة الكثافة الإلكترونية للحالة الانتقالية عند الانقلاب . ولإلقاء ضوء أكثر على عمليات انقلاب النيتروجين تم تحضير سلسلة من مركبات أيزوأوكسازوليدين وتم دراسة الرنين النووي المغناطيسي $^{13}CNMR$ و^1H في مدى من درجات الحرارة ، كما تم رسم أشكال هاميت لتعيين الثابت ρ ، ومن خلال دراسة ديناميكية أكسدة الهيدروكسيل أمين إلى نيترون بواسطة أكسيد الزئبق٣

وبارابنزوكينون تم معرفة المسار الميكانيكي الذي يسلكه تفاعل الأكسدة . وقد تم ملاحظة نيترون $E-$ الذي يتحول إلى نيترون $Z-$ من خلال عملية ثنائية الجزيء .

درجة الدكتوراه في الفلسفة

جامعة الملك فهد للبترول والمعادن

الظهران - المملكة العربية السعودية

1

INTRODUCTION

1.1 Introduction

A trivalent nitrogen cannot maintain its chiral nature because of nitrogen inversion.[1] While the elec ronegative substituents on nitrogen increase the inversion barrier by their σ inductive electron withdrawing ability and π repulsive character due to the lone pairs, the relative contribution of these two effects still remains a challenging question. Hydroxylamine, owing to its unique properties, have acquired a place of distinction in conformational analysis. Barrier to nitrogen inversion is considered as a useful probe for understanding structural effects in organic molecules.

In hydroxylamines nitrogen inversion is also accompanied by N-O bond rotational process. The barrier of nitrogen inversion and N-O rotation in acyclic systems is of comparable magnitude (~50 kJ/mol). This has given rise to nitrogen inversion and N-O bond rotation dichotomy. It is quite often difficult to distinguish bet veen the two processes as far as the determination of the rate limiting step is concerned. Rotation about an N-O bond may be eliminated by incorporation into a ring (3-, 4- or 5- membered) or into a bicyclic frame work.

1.2 Objectives

The main objectives of this work can be divided into three main parts.

1.2.1 Part A

A multitude of nitrones will be prepared by the condensation of aldehyde and hydroxylamines. The nitrone on reduction is expected to give the required hydroxylamines which will be converted to acetyl and silyl derivatives. Variable temperature ^1H NMR spectra of the hydroxylamines will be recorded and by using the NMR simulation programs the barriers will be determined. The effects of size and nature of various groups on the inversion (or rotation) barrier will be studied in great depth.

It would indeed be interesting if the proposed study can demarcate between the two processes using judicious selection of the substituents attached to nitrogen. The sensitivity of the barrier to the *ortho*, *para*, and *meta* substituents in the aromatic molecules will be closely monitored. Hammett plot of the free energies of activation with substituent constant σ would shed light on the electronic requirements in the transition state. Close attention will be paid to the particular hydroxylamine to study the effects of hydrogen bonding on the inversion - rotation process. While the nitrogen inversion process is expected to slow down, the effect of hydrogen bonding on the N-O rotation will presumably be marginal. X-ray structure of hydroxylamine will be determined to find out the strength and extent of the hydrogen bonding (if any).

1.2.2 Part B

The objective in this part is to completely freeze the N-O rotation process by inserting both N and O in a ring skeleton. The ring should not be six-membered since ring inversion will compete and complicate the study of nitrogen inversion. Several nitrone cycloaddition products will be synthesized. Dynamic NMR study would help us to

determine nitrogen inversion barrier without any contribution from N-O torsion. The study would help us to identify or even find out the relative contribution of nitrogen inversion and N-O rotation processes (as described in part A) in a common transition state. The study would also shed light on the conformational stability of the axial versus equatorially oriented nitrogen substituent in the diastereomers. Crystalline compound (if any) will be studied by X-ray crystallography.

1.2.3 Part C

Inversion of the nitrogen and its oxidation are closely related in the sense that both the processes go through a sp^2 transition state. Therefore the structural effects that make the inversion easier should also make the oxidation process easy. A kinetic study of the oxidation process in hydroxylamines would help us to determine the mechanistic pathway this synthetically versatile process traverses. Among the plethora of functional groups nitrone functionality has etched an important place in the organic synthesis. The sterically favoured *Z* nitrone are reported to be formed in the oxidation process. It is possible that the initial product of the oxidation may not be the thermodynamic product alone. Using various oxidants the original composition of the product mixture will be analyzed. A kinetic study of *E*-*Z* isomerization will be undertaken. Successful isolation of the less stable *E* isomer would pave the way of better utilization of the nitrone cycloaddition reaction.

2

HISTORICAL

2.1 Nitrogen Inversion

As early as 1924, it was suggested [1] that an inversion process was responsible for the inability of the trivalent nitrogen to sustain optical activity (Scheme 2.1).

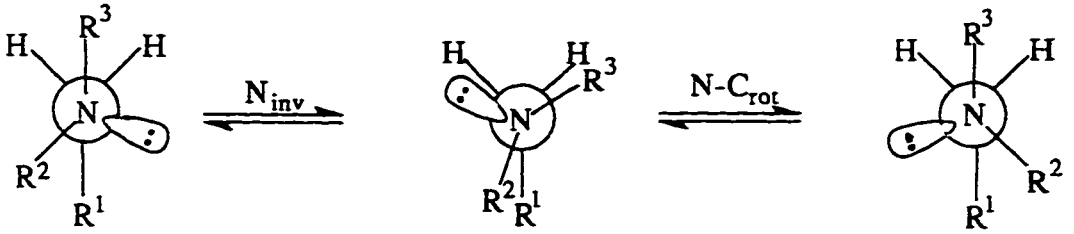

Scheme 2.1: Nitrogen inversion followed by N-C rotation.

The first thoroughly documented case of atomic inversion in ammonia is explained in terms of quantum mechanical tunneling through the barrier rather than by a classical traversal over it [2,3]. Quantum mechanical tunneling is important only for cases with very light substituent atoms, such as protons.

An sp^3 hybridized nitrogen atom with a pyramidal geometry **1a** is capable of inverting its configuration. The transition state has an sp^2 hybridized nitrogen with the lone pair in an unhybridized p orbital. The rate of nitrogen inversion depends on the steric, conjugative, inductive and angle constraints effects of substituents [4-7].

Electronegative heteroatoms attached to nitrogen increase the barriers to nitrogen inversion. The higher the electronegativity the higher is the barrier to inversion.

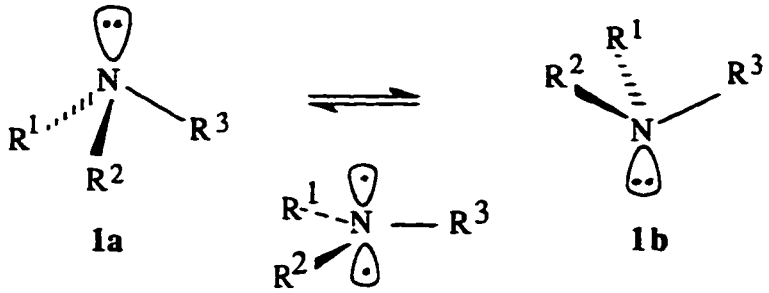

Transition State

Scheme 2.2: Nitrogen inversion.

Amines with pyramidal geometry are expected to invert via the planar transition state. The rates of inversion of this type vary over a considerable range and depend on the nature of the substituents attached to nitrogen; while the electronegative and π-donor substituents raise the inversion barrier, the π-acceptor substituents lower the barrier.

An analysis using molecular orbitals describes the effect of various types of substituents on the inversion barrier of the seven molecular orbitals that describe NH_3 [8]. Three orbitals, all having the same three fold rotation axis, are shown in Figure 2.1. These orbitals are responsible for the energy changes associated with the pyramidal inversion of the sp^3 hybridized nitrogen through planar transition state with sp^2 hybridized nitrogen. Energy changes of four other orbitals do not control the inversion process and are not shown in the figure. As the hydrogen atoms are moved out of the plane (at the left), three orbitals interact with each other and their relative energies change. The strongest interaction is between the HOMO a_n and LUMO a^* since these two have the smaller energy gap. The nonbonding orbital a_n gains a bonding interaction from the central p orbital and the antibonding orbital a^* gains an antibonding contribution from the central p orbital. There is a smaller interaction between a and a_n.

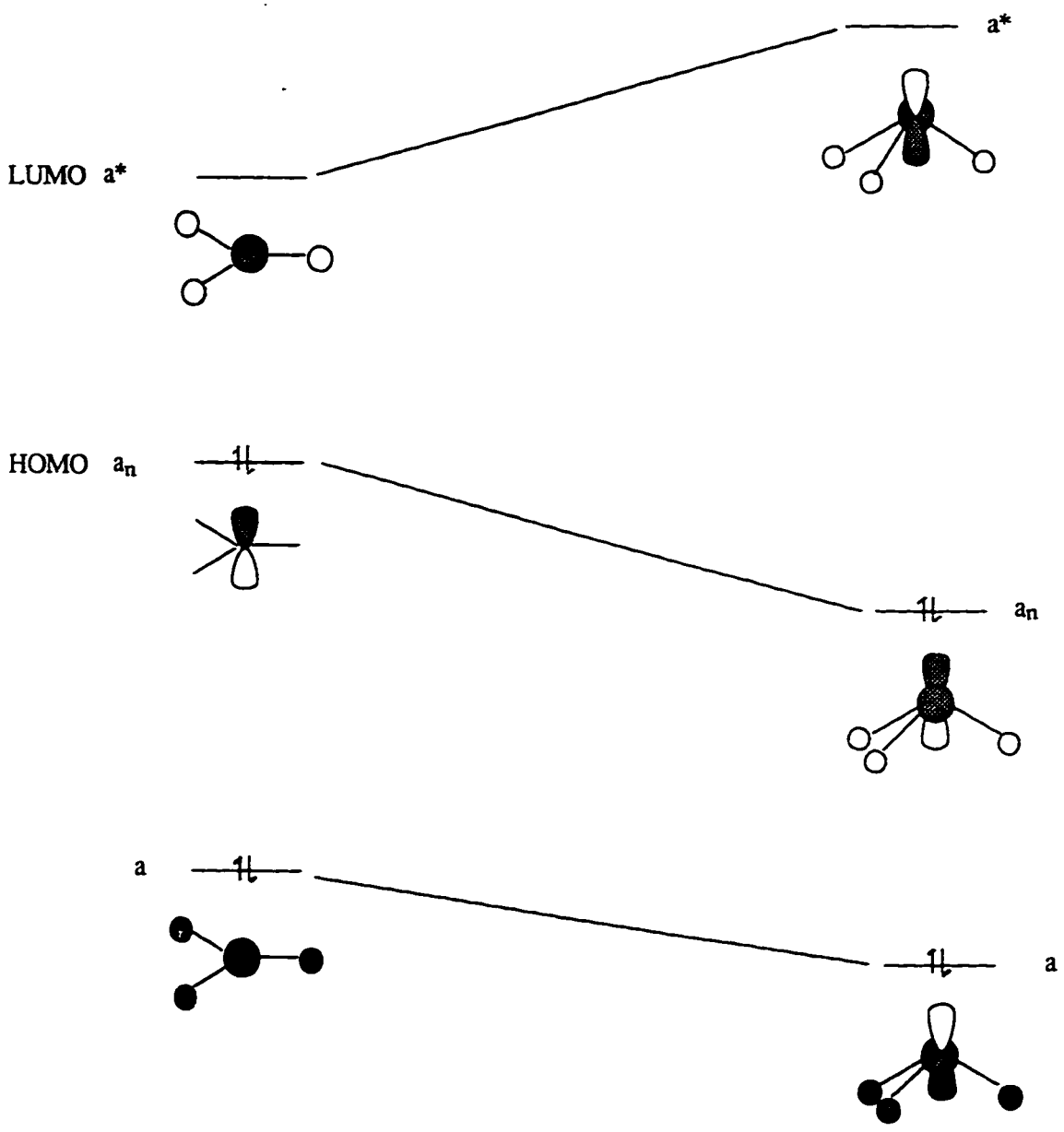

Figure 2.1: MO diagram of the three orbitals involved in the inversion process.

The most dominant interaction between a_n and a^* lowers the energy of the a_n considerably. The pyramidal structure is more stable than the planar structure as a result of energy decrease of a_n molecular orbital in going from the pyramidal to the planar geometry.

A π-donor substituent as in **2** can interact through its π-orbitals but cannot interact with a^* molecular orbital because of symmetry mismatch.

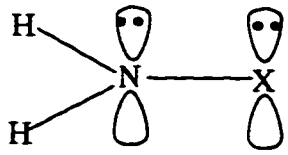

2

The interaction between the filled orbitals of the π-donor and a_n will raise the energy of the planar structure by raising the energy of the a_n (Figure 2.2). Decreased

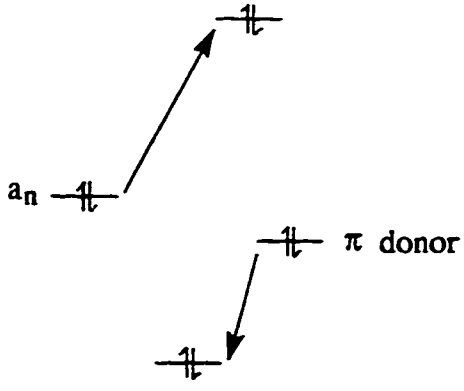

Figure 2.2: Energy changes due to the interaction of a_n and filled orbital of a π donor.

energy gap between a_n and a^* would lead to enhanced interaction which would in turn lead to larger stabilization as there is a change towards the pyramidal structure. In the pyramidal structure the unfavourable a_n-π donor interaction would be diminished due to

the p character and increased s character of the a_n orbital. A π-donor, therefore, destabilzes the planar structure and stabilizes pyramidal geometry hence increases the inversion barrier.

A π-acceptor substituent in **3** lowers the energy of a_n in the planar structure hence increases the energy gap between a_n and a^*.

3

Strongly stabilizing filled (a_n) -unfilled (π^*) interaction which is maximum for maximum p character of a_n diminishes a_n-a^* interaction and hence favours the planar geometry and lowers the inversion barrier (Figure 2.3). The acceptor argument put forward by molecular orbital (MO) treatment can be understood using the familiar resonance argument for planarity in such systems.

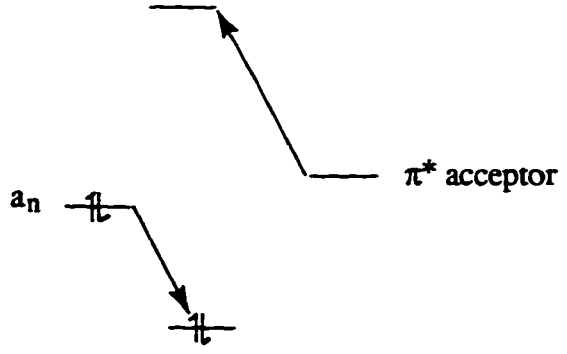

Figure 2.3: Energy changes during the interaction of a_n and an empty orbital of a π acceptor.

The effect of electronegative substituent on nitrogen can be understood in the following way. Inductive electron withdrawal through σ orbitals will lower the energy of

a and a* orbital but the energy of the a_n orbital will not be affected to the same extent due to the π-symmetry of the a_n orbital. The energy gap between a_n and a* is reduced in planar geometry and change to a pyramidal structure is strongly favoured and the inversion barrier is raised. The converse is true for the inductive electron donating substituent. Electronegativity of the central atom also affects the inversion barrier but in the opposite sense of the electronegative substituents. Thus increasing the electronegativity of the central atom lowering the inversion barrier.

The inversion rate of amines is usually so high that resolution of racemic mixtures of optically active amines cannot be achieved. The inversion rate is usually measured by NMR spectroscopy. Asymmetric amines having a benzyl group would display methylene protons as AB quartet at low temperature but will coalesce at temperature where inversion is sufficiently rapid [9]. If the inversion is too rapid even at low temperatures, it can be effectively slowed down by use of appropriate amounts of acid to convert a large fraction of the amine to ammonium ion which cannot invert at all [10].

Experimental evidence reveals that the inversion rates are influenced by various factors. If one or more substituents is hydrogen, the inversion rates are too fast to be seen by NMR. The rapid inversion in the gas phase is attributed to tunneling [11]. Inversion in solution is complicated by proton exchange.

Tertiary amines with bulky substituents are expected to be crowded more severely in pyramidal geometry than in the planar transition state. Hence, amines with larger groups tend to undergo faster inversion.

Small cyclic amines are expected to invert slowly. In the pyramidal geometry, at least two bond angles are normal but in planar geometry all the three bond angles at the nitrogen deviate greatly from their normal values. From the temperature dependence of the NMR spectrum of 1,2,2-trimethyl aziridine **4** the barrier to nitrogen inversion has been found to be 83.7 kJ/mol, whereas that for N-methyl pyrrolidine **5** is only 29.3 kJ/mol [12].

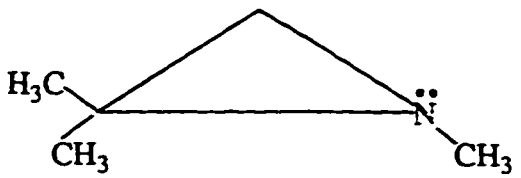

4

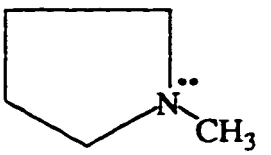

5

Amides are, as a rule, characterized by planar nitrogen due to resonance. No temperature dependence has been noted for N-acetyl aziridine **6** even though the planar geometry introduces severe angular constraints [13].

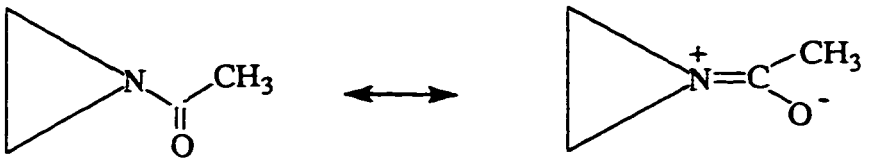

6

Substitution by atoms other than hydrogen and carbon tend to lower the inversion rates and hence increase the inversion barrier. The *cis* and *trans-N*-chloro aziridine **7**

7

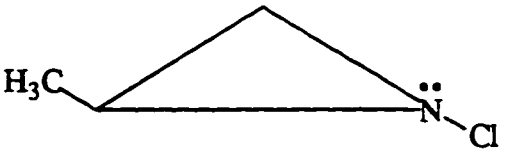

8

and **8**, respectively, have very high inversion barriers and have infact been separated. This is the first example of a non bridgehead amine stable to inversion at room temperature [14]. If the central nitrogen atom is attached to two hetero atoms, even the three-membered ring is no longer a requirement for slowing down the nitrogen inversion rate. The isoxazolidines **9** and **10** can be separated; the activation energy of inter conversion is found to be 125.5 kJ/mol [15].

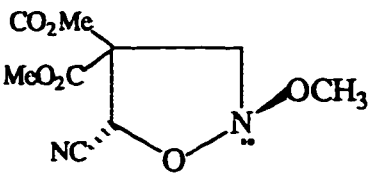

9

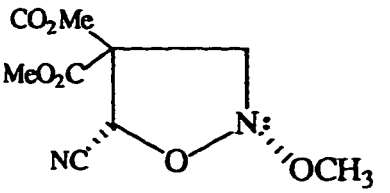

10

2-Methyl-3,3-diphenyloxaziridine **11** in which a pyramidal nitrogen atom is the chiral centre, has been isolated [16].

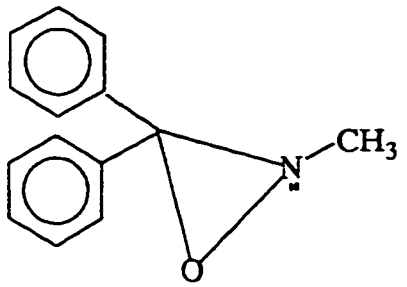

11

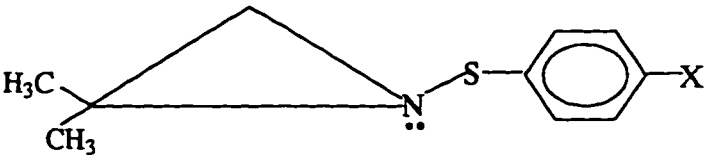

12

The N-silylamines and several N-sulfuramines are found to be planar [17]. Availability of low lying vacant d orbitals, presumably makes the planar geometry more attractive due to dπ-pπ bonding (Figure 2.4).

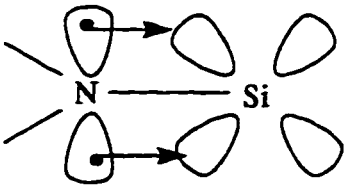

Figure 2.4: dπ-pπ bonding in N-Silylamines.

However, the sulfuramine **12** is found to exhibit inversion as indicated by coalescence of the NMR spectrum. Both nitro and methoxy groups lead to a barrier of 52.3 kJ/mol indicating the insensitivity of the inversion rate to the nature of X [18].

The presence of electronegative hetero atoms attached to the central nitrogen slows down the rate of inversion. This is at present best explained by the statement that the planar transition state has maximum s character in the bonds to the nitrogen atom and an electronegative substituent is least likely to tolerate that situation.

In phosphines and arsines, with bond angle lower than those of ammonia, inversion is very slow. Silicon attached to these atoms lowers the energy of the planar transition state, hence lowers the inversion barrier. In many phosphines the inversion barrier is about 146 kJ/mol, however the barrier is decreased to about 83.7 kJ/mol if one of the substituents is silicon [19]. For the tris silylphosphene **13** no resolution of the $SiMe_2$ signal was observed even at -80°C and $\Delta G^{\#}$ must be less than 41.8 kJ/mol [20].

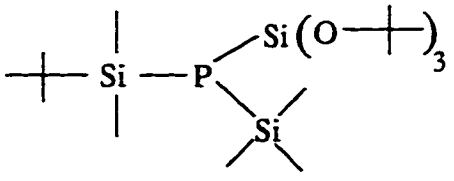

13

The inversion barrier of phosphorus and arsenic atoms can be lowered by making it a part of an aromatic system. The barrier in acyclic arsenes is as high as 188 kJ/mol, however in arsoles **14** it is only about 146 kJ/mol. In spite of the difference in size, the planar state is stabilized by 4p-2p conjugation [21].

Inversion at oxygen can also be monitored by NMR spectroscopy. The methyl oxonium salt of oxirane **15** has an inversion barrier of 41.8 kJ/mol. However, the analogous salt **16** with six-membered ring does not show this phenomenon [22].

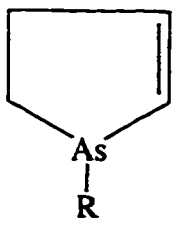

14

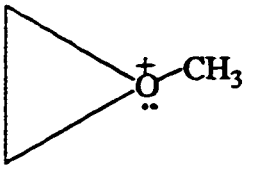

15

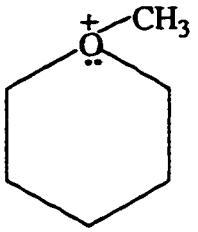

16

Related to pyramidal atomic inversion are interconversion exemplified by methyl phenyl ether **17**, acetone oxime **18** etc. [23] In atomic inversion, one of the most subtle of molecular processes, only a reversal of configuration results; no bonds are broken and no second chemical reactant is required. The two processes shown may occur either by a "lateral shift" or by a simple bond rotation. In the lateral shift mechanism the central atom and its two substituent atoms remain in the same plane when passing through the sp-hybridized transition state. This mechanism is a two dimensional analog of the pyramidal atomic inversion. Divalent oxygen R_2O may invert through linear sp or sp^2 transition state. The later process is similar to bond rotation. However linear inversion has been found to be relatively high energy process (about 142 kJ/mol in H_2O) [23] compared with almost negligible barrier to pyramidal inversion in H_3O^+. Therefore the process depicted below must occur by a torsional mechanism rather than by a linear inversion [23].

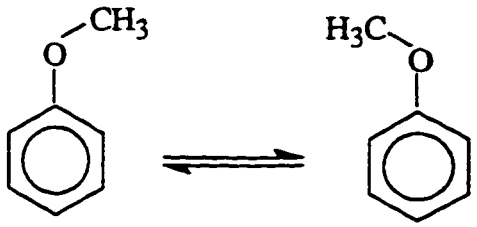

17

18

Geometric constraints, however, do not permit nitrogen inversion in amines where nitrogen atom occupies bridgehead position in such compounds as exemplified by **19**.

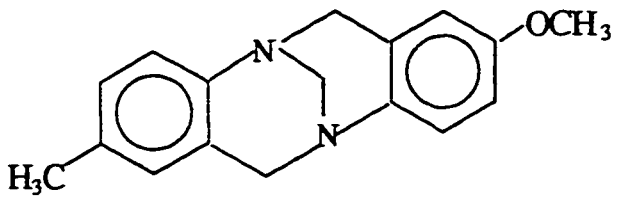

19

The rate of inversion varies over a considerable range as discussed before. To give an idea of such variation, several compounds are listed below along with their inversion barriers.

In ammonia, primary and secondary amines, the rates of inversion are too fast to be seen by NMR scale. For ammonia, there are 2×10^{11} inversions per second in gas phase and this rapid inversion has been attributed to tunneling [11]. The inversion is less rapid in substituted ammonia (amines).

NH_3

20

24 kJ/mol

CH_3NH_2

21

20 kJ/mol

NF_3

22

209 kJ/mol

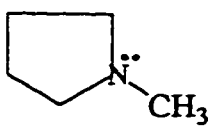

23

29 kJ/mol

24

44 kJ/mol

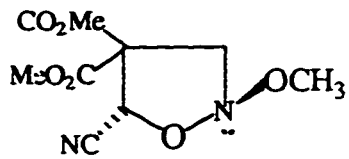

9

126 kJ/mol

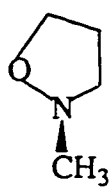

25

65 kJ/mol

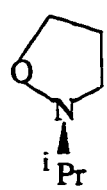

26

62 kJ/mol

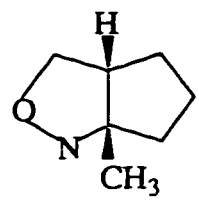

27

57 kJ/mol

Nitrogen trifluoride has an exceptionally high inversion barrier [17] of 209 kJ/mol. While N-methyl pyrrolidine **23** has an inversion barrier of 29 kJ/mol [12], N-methylisoxazolidine **25** in contrast, has a considerably higher barrier of 65 kJ/mol [24]. The inversion barrier increases considerably when the nitrogen is a part of a three membered ring such as 1,2,2-trimethyl aziridine **24** [12].

2.1.1 N-O Rotation

There is a three-fold barrier to rotation in ethane with staggered and eclipsed conformations occupying the energy minima and maxima positions, respectively. Methylamine, methanol, and their higher homologous also show three fold periodicity in their bond rotation behaviour. Both MO calculations and experimental evidence on hydroxylamines and its derivatives point toward a completely different picture of the conformational behaviour. Hydroxylamine has two maxima and two minima on its potential function for N-O bond rotation and the barrier to rotation is huge, several times larger than in ethane and related compounds.

The results of MO calculations [25] on the conformational behaviour of hydroxylamine **28** is presented in Figure 2.5 which shows the variation of molecular energy with N-O bond rotation. The barriers to rotation were calculated to be 50 kJ/mol and 4.85 kJ/mol. The two stable conformers **28a** and **28d** were thus calculated to be

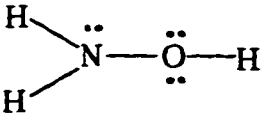

28

45.15 kJ/mol apart. In complete contrast to the conformational stability of ethane, methanol and methylamine the stable conformation of hydroxylamine was determined to be **28a** with the lone pairs and bonds formally eclipsed. The less stable conformation **28d** has the formal bonds and lone pairs staggered. The other staggered conformation **28b** does not occupy a potential energy minimum.

Pople et al [26] have also reported the results of molecular orbital calculation on hydroxylamine and monoethyl derivatives. The calculations agree with those of the

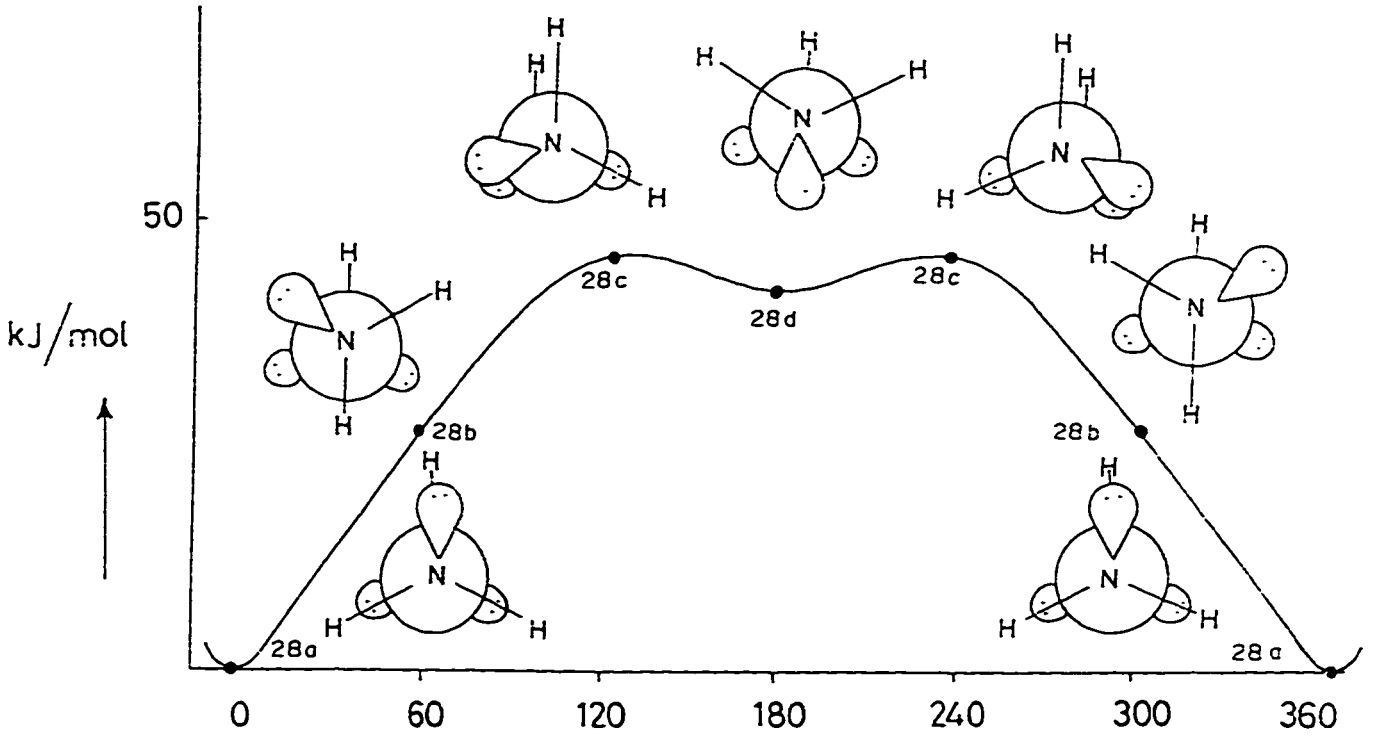

Figure 2.5 Energy changes involved in rotation around the N-O bond of hydroxylamines.

earlier workers. While the higher barrier to rotation was calculated to be 49 kJ/mol the energy difference between the stable conformers **28a** and **28d** was calculated to be 33.5 kJ/mol. Calculations on the methyl derivatives **29** and **30** revealed an almost identical rotational barrier but the energy difference is almost 4.18 kJ /mol lower.

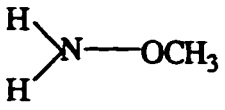

29

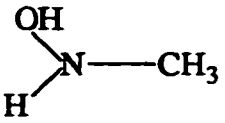

30

Experimental evidence [27] accumulated from IR study and microwave investigation on hydroxylamine strongly support the results of molecular orbital calculations that the *trans* conformer **28a** is the strongly preferred conformation.

For methylated derivatives **31** dipole moment data [28] and an electron diffraction study [29] reveals the presence of two conformations for the N-O dimethyl and trimethyl derivatives with the *trans* form **31a** as the major conformer. For the compound **31** the energy difference is found to be about 2.5 kJ/mol which is rather lower than that proposed from molecular orbital calculations [26].

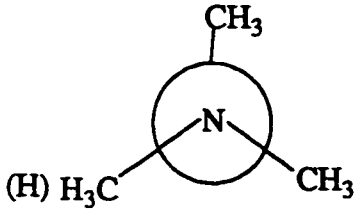

31a

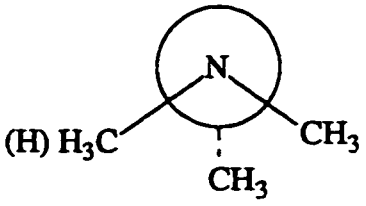

31b

2.1.2 Nitrogen Inversion and N-O Bond Rotation Dichotomy

NMR spectra of many hydroxylamine derivatives show temperature dependence attributed either to inversion at nitrogen or N-O bond rotation. Griffith and Roberts [30] studied the process in **32** and the barrier to the process was attributed to the nitrogen

inversion. They reached this conclusion based on the evidence that the barrier decreased as the polarity of the solvent is increased. The sp^2 hybridized planar transition state should be more polar than the ground state and as such polar solvents should stabilize the transition states, thus lowering the energy barrier.

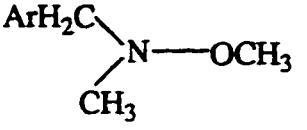

32

However, other investigators [31] questioned the view presented above. They found out that by increasing the bulk around nitrogen in a series of compounds like **32**, a small steric retardation of the process [30] was observed which is consistent with N-O bond rotation being the rate limiting process.

Fletcher and Sutherland [32] however supported the view that nitrogen inversion is the origin of the observed process since changing the size of the O-substituent in **32** from alkyl to acyl to hydrogen the observed barrier changed very little. The variation in the size of the substituents should have caused a substantial variation in the observed barrier, were the N-O bond rotation be the rate limiting process.

Works on compound **32**, with aromatic rings having *ortho* substituents, firmly suggest nitrogen inversion as the rate limiting process [33]. *Ortho* substituents were found to cause a steric acceleration which is consistent with the nitrogen inversion being the rate limiting process.

Attachment of nitrogen to a π acceptor substituent, however, makes the nitrogen inversion an easy process. The rate limiting process in compounds **33-36** was ascribed to the N-O bond rotation [34].

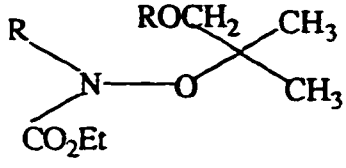

33

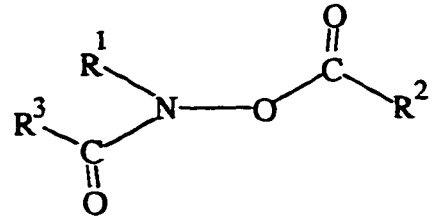

34

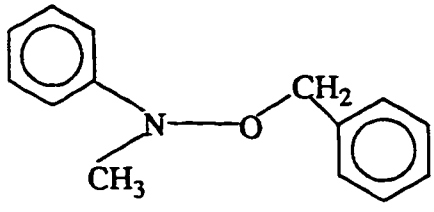

35

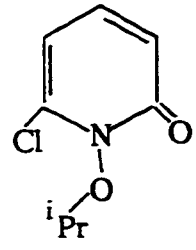

36

Inclusion of N-O bond in the ring skeleton removes the possibility of bond rotation as the rate limiting process [35]. The inclusion of both N and O in a 3-membered ring **37** slows down the inversion process with a $\Delta H^{\#}$ of 142.7 kJ/mol for R = CH_3 and 116 kJ/mol for R = *tertiary* butyl. A barrier ($\Delta G^{\#}$) of 41.8 kJ/mol was found [36] for the 4 membered ring compound **38**. The presence of fluoro alkyl groups tend to increase the rate of nitrogen inversion and lower the barrier.

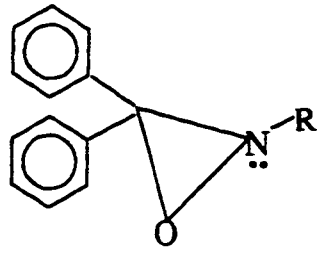

37

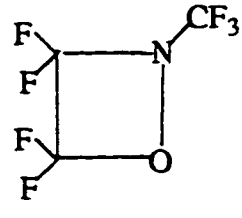

38

The inversion barrier ($\Delta G^{\#}$) in 5-membered isoxazolidine **39** was determined to be 65.3 kJ/mol [37]. The energy barrier is observed to decrease when the methyl in **39** is replaced by bulkier *iso-* propyl group [30]. The barrier is also decreased by the ß-O atom in **40** ($\Delta G^{\#}$= 43.1 kJ/mol).

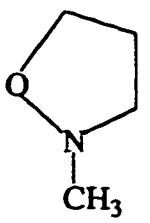

39

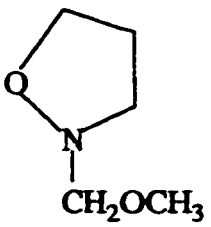

40

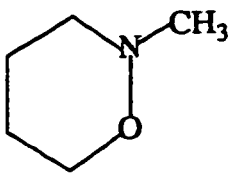

41

2.1.3 Application of NMR Spectroscopy in the Study of Inversion-Rotation Process

The stereochemistry of the chiral nitrogen centre cannot be developed using classical methods based on chiroptical properties that are used for the investigation of stereostable configuration of enantiomers having chiral carbon. NMR technique is a convenient tool to study the stereolabile chiral units with asymmetric nitrogen [39]. While the stereomutations in chiral carbon usually require the breaking and making of σ bonds catalytically or photochemically, stereomutation in asymmetric nitrogen occurs thermally (uncatalyzed). NMR spectroscopy can probe stereochemical relationships between individual groups in the same molecule. The stereochemical relationships between paired groups can be described as homotopic (indistinguishable), enantiotopic, and diastereotopic. Incorporation of a prochiral [40] group of the form —CX_2Y (e.g., —CH_2CH_3, —$CH(CH_3)_2$, —CH_2Ph etc.) in a molecule RCX_2Y **42** can serve as a probe for the chirality or lack of chirality of the group R.

For instance the molecule **43**, where 'R' in **42** is achiral $(CH_3)_2N$, symmetry σ is in the plane of the paper containing N—C—Y. Reflection through the plane interchanges the two X substituents and as such these groups are enantiotopic and will have the

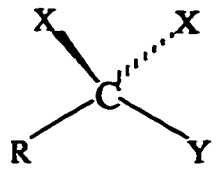

42

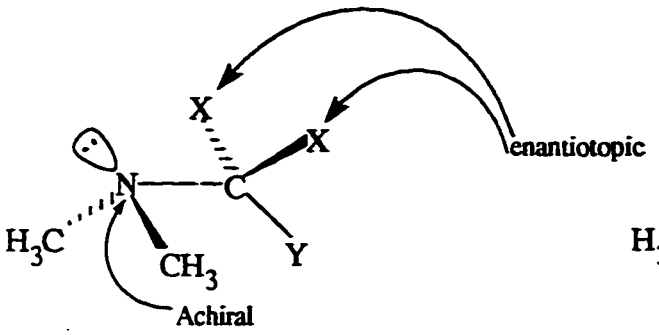

43

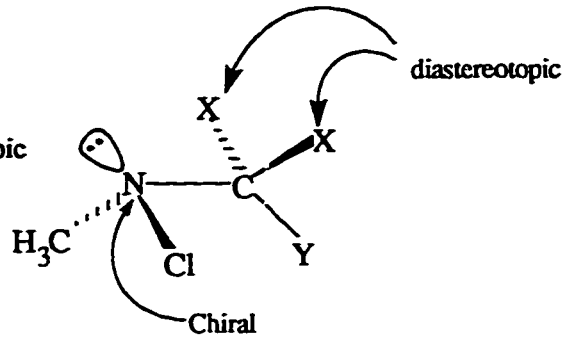

44

identical chemical shifts. However when R in **42** is chiral as exemplified by compound **44**, the plane of the paper is no longer the symmetry plane and as a result the X groups are diastereotopic and will exhibit chemical shift nonequivalence. Chemical shift nonequivalence of the X groups confirms the chirality of the R group but the opposite, i.e., chemical shift equivalence of the X groups does not necessarily confirm the lack of chirality of the R group. Accidental degeneracy or too small a difference in chemical shifts might lead to incorrect conclusions.

If R is a chiral group in **42** it does not mean that the molecule must be chiral. The compound **45** is achiral even though the group CCl_3SNCH_2Ph (R) is chiral. The molecule has a σ plane perpendicular to the plane of the paper (containing CSN) which interchanges the benzyl group as a whole thus making them enantiotopic. However, the plane does not interchange the two methylene protons H_A, H_B in each benzyl group thus making H_A and H_B diastereotopic and the NMR spectrum displays the simple AB quartet [41].

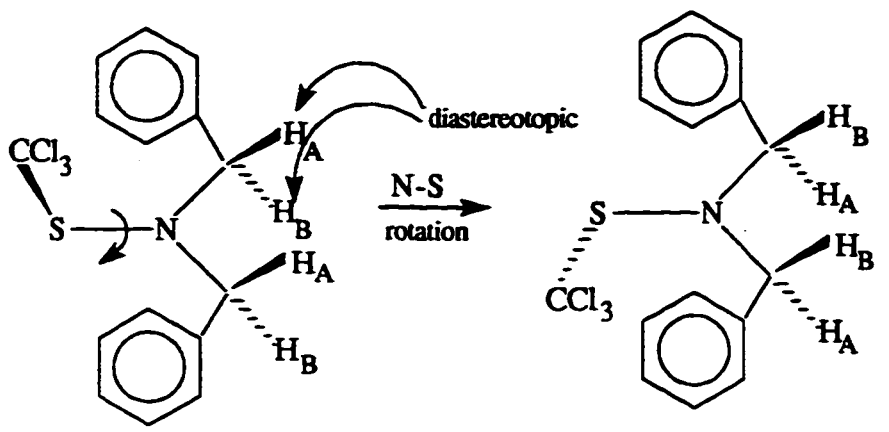

45

In compound **46** with a σ plane (the plane of the paper) the two hydrogen atoms in each benzyl group are enantiotopic (reflection through the plane exchanges the hydrogen), however the benzyl groups, as a whole, are not exchangeable hence diastereotopic and as such benzyl protons appear as two singlets in the NMR spectrum [42].

The spectral characteristics in **45** and **46** are observed when the rate of N—S or N—C bond rotations are slower relative to the NMR time scale (bond angles do not change but dihedral angle changes in the transition state). However increasing the temperature the rate of H_A becoming H_B and vice versa after rotation becomes faster on the NMR time scale. As such the NMR spectrum of **45** reveals the time average signal of methylene protons, which gradually changes with increasing temperature from AB quartet (diastereotopic protons) to a singlet (enantiomeric protons). This averaging of stereochemical relationship or the exchange phenomenon is termed topomerization [43]. During the process the topomerization of benzyl groups is also affected. On time average the whole benzyl groups become homotopic rather than enantiotopic.

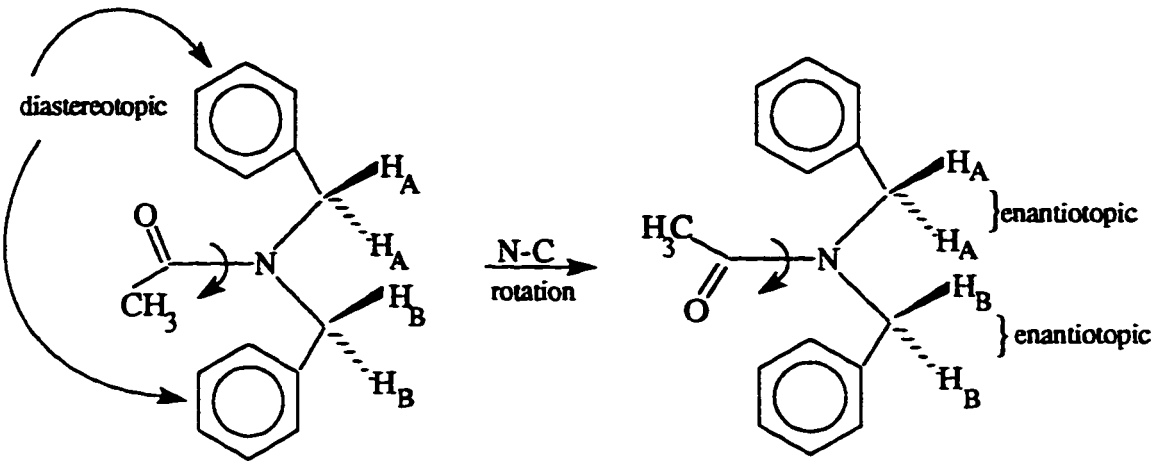

46

In the topomerization of compound **46** rapid rotation around the amide bond changes the diastereotopic benzyl groups to homotopic on time average. The stereochemical relationship between methylene protons in each benzyl group however remain enantiotopic and the benzyl protons coalesce into one singlet. It may be noted that only topomerization which transforms diastereo groups to either enantiotopic or homotopic, lead to coalescence and can be studied by the NMR technique.

Stereomutation of nitrogen and other stereolabile configurational units involve geometry changes rather than bond breaking or making at the transition state (Scheme 2.3). Changes in bond angles in **1a** having a chiral nitrogen configurational unit from pyramidal ground state to planar transition state leads to interconversion of enantiomers **1a, 1b**. However stereomutation of an achiral N-O configurational unit (rather conformational unit) causes changes in dihedral angles (torsion) in the transition state and stereomutation interconvert the diastereomers **47a** and **47b**.

The presence of both chiral nitrogen and achiral N—O unit in the same molecule (as exemplified by hydroxylamine derivative) provided a long, lively, and still continuing debate on the inversion and torsion mechanistic dichotomy. The interconversion of one ground structure **1a** to its enantiomer **1b** (degenerate

racemization) requires both inversion at nitrogen (to give the diastereomer **47a**) followed by N—O bond rotation.

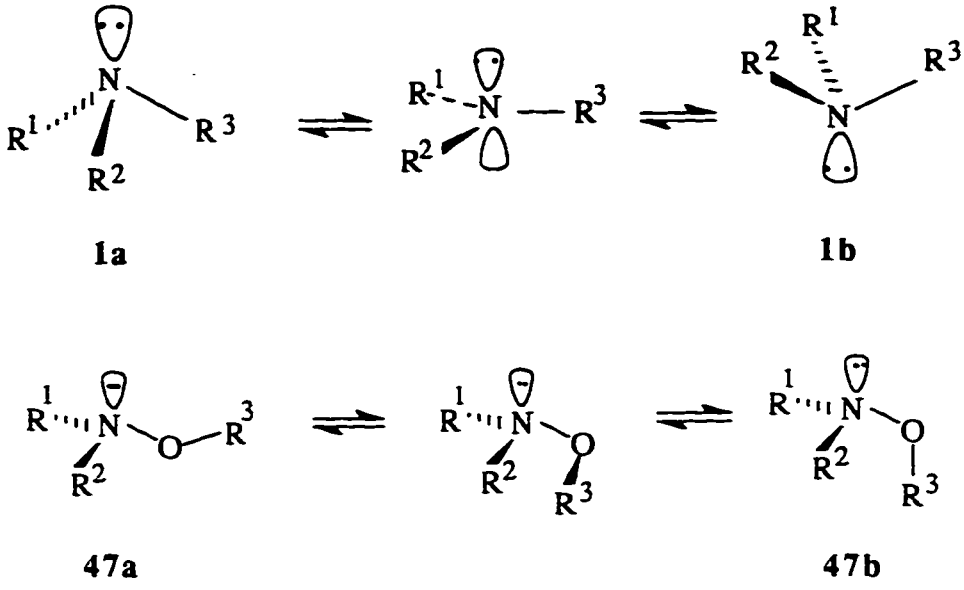

1a **1b**

47a **47b**

Scheme 2.3: Stereomutation of N & N-O configurational unit.

Most likely the inversion and torsion happen in sequence. Combined composite of the two processes in a complex single step would require a higher energy transition state (corresponding to direct **a** ⟷ **b** interconversion). If the two processes were independent the energy of activation for the combined process will be the sum of energy requirements for the two individual processes. Experimental and theoretical evidence [44], however, indicate that the torsional barrier is increased at the inversion transition state and that the inversion barrier is increased at the torsional transition state. In such a situation, the two processes are not quite independent of each other and become more dependent as the energy of activation increases.

With sequential inversion and torsion, the process with the higher energy of activation represents the rate determining step for stereomutation, **48** (Scheme 2.4). Barriers measured from the coalescence of the NMR signals due only to degenerate racemization (A = A*) of the prochiral probe shed light on the slower process but failed

to provide information about the faster process. However, if the minor diastereomer (**B** and **B***) is populated sufficiently to permit detection by NMR, the coalescence associated with interconversion of the diastereomers (**A**,**A*** **B**,**B***) would provide the energy barrier for the second of the two first order interconversions. Experimentally this situation has not so far arisen in the study of hydroxylamines, sulfenamides, and hydrazines so far. The inability to observe the minor diastereomer may arise from any of the following reasons:

An unfavourable equilibrium constant (K=[A]/[B]>>10) or a small free energy of activation ($\Delta G^{\neq} < 21$ kJ/mol) for the fast process below the lower limit of the dynamic NMR method or accidental degeneracy of the signals due to two diastereomers. Where the rate determining step is nitrogen inversion the process is called inversion dominant and if N—O rotation is the limiting step the process is called rotation dominant.

Experimental evidence indicates that comparable barriers have been measured for both inversion and the rotation processes. There is a long literature controversy over the dominance of the barrier in hydroxylamines [45].

In some cases the slower step can be unambiguously assigned. In compounds (**33, 35, 49, 50**) [46] attachment of the π-acceptor substituent to nitrogen makes the nitrogen planar or nearly planar and as such the inversion process will be faster. In these molecules the NOC plane is perpendicular to the plane of containing NCC and as such have N—O chiral axis (much like the chiral axis in allenes) as shown in compound **35**. The nonequivalence of the diastereotopic groups can be attributed to the axial chirality at the nitrogen-oxygen bond and the observed energy barrier can be confidently assigned to N—O torsional process leading to degenerate racemization.

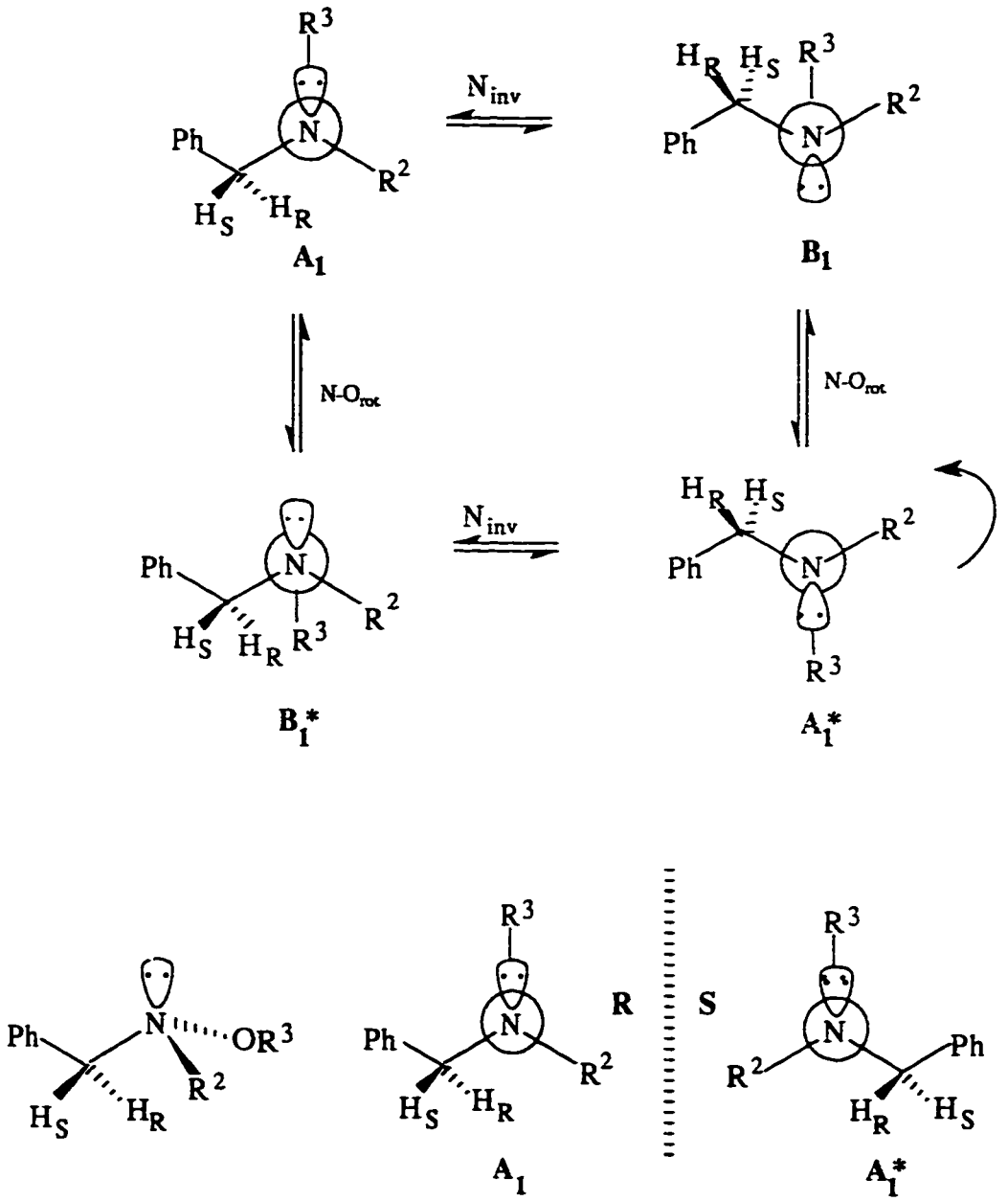

48

Scheme 2.4: Interconversion of the diastereomers.

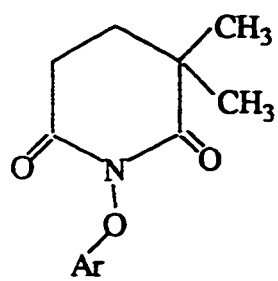

49

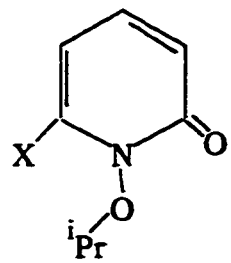

50

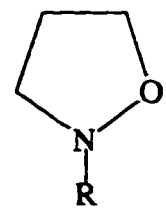

51

Incorporation of N and O into a small ring (3, 4, 5-membered) increases the inversion barrier and at the same time fixes the CONC dihedral angle at (~0°) or near the geometry of N—O rotational transition state. In compounds **37, 41, 51** the barrier must be due to inversion process and nonequivalence of diastereotopic groups is due to chirality at nitrogen [47,48].

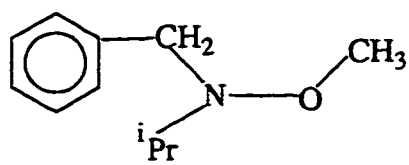

52

The situation in simple trialkyl hydroxyl amines like **52** is more complicated. The rotation-inversion dichotomy in simple N,N-dialkyl and acyclic trialkyl hydroxylamines has been the subject of considerable controversy in the literature. The torsional barriers in **49** and **33** are in the range 50-63 kJ/mol which are comparable to those of normal trialkyl hydroxylamines. The torsional barriers, thus, cannot be ignored. The steric effects and solvent effects are often used to differentiate between the two processes. Steric effects take into account the fact that increasing bulk around N and O would crowd the pyramidal ground state (109°) and for the inversion process this crowding would be relieved in the planar transition state (120°) due to an increase in the distances between substituents on nitrogen. The transition state for the torsional process on the other hand requires eclipsing of the nitrogen and O substituents. Thus any increase in the steric

hindrance in the ground state would lead to steric acceleration [24] of the process if it is inversion dominated and to steric deceleration if it is rotation dominated. However the application of this factor has led to conflicting results from various authors [24,45]. Solvent effects on barriers have been neither extensively studied nor well understood [39]. In some cases an increase in polarity leads to rate acceleration and in some cases to rate deceleration. The evidence so far indicates that the magnitude of both the inversion and rotation are similar and substantial. While the presence of conjugative interactions with the N make the process rotation dominated, in absence of conjugative interactions substituents and solvent effects can change the shape of the energy surface in acyclic system and as such can shift the mechanism for topomerization from inversion to rotation or vice versa.

The presence of intramolecular H-bonding has been shown [49] to increase the nitrogen inversion barrier. The nitrogen inversion in amine **53** has been shown to require a preliminary stage of intramolecular H-bond breaking prior to nitrogen inversion and the barrier $\Delta G^{\#}$ of the total process was determined to be 54.7 kJ/mol (compared to 29-34 kJ/mol for Me_3N).

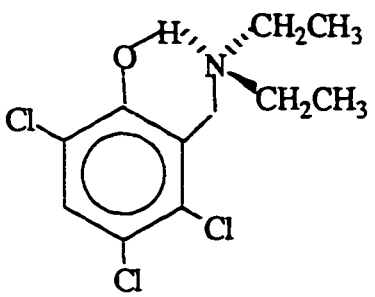

53

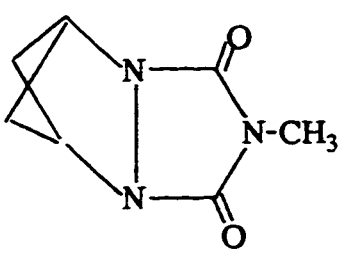

54

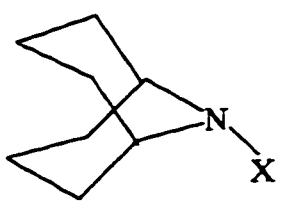

55

Restriction of the CNN angle of **54** causes the nitrogen to be pyramidal and the low temperature ^{13}C NMR spectrum of **54** reveals two CH_2 signals when double nitrogen inversion is slow on NMR time scale. The inversion barrier ($\Delta G^{\#}$) has been shown [50] to be 36.4 kJ/mol at -72°C.

N-substituted dialkylamines of general formula R_2N-X exhibit parallel behaviour for cation radical formation and kinetics for nitrogen inversion [51]. Changes in the structure of "R" that raise the nitrogen inversion barrier also make the electron removal to form a cation radical more difficult. Even though the two processes appear to be quite different they are similar in the sense that flattening at nitrogen occurs in both of them.

The relationship between the nitrogen inversion barrier and the ease of electron loss for the haloamines **55** has been determined.

The phosphinoyl oxaziridines **56** have much lower barriers [52] to inversion at nitrogen ($\Delta G^{\#}$ 52.7-55.6 kJ/mol) than that in 2-sulphonyl oxaziridines [53] ($\Delta G^{\#}$ 84-88 kJ/mol) and N-alkyl oxaziridines ($\Delta G^{\#}$ 105-142 kJ/mol), and this is attributed to a much stronger conjugative interaction between nitrogen and phosphorous than between nitrogen and sulphur in the trigonal state for nitrogen inversion.

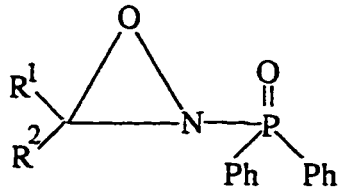

56

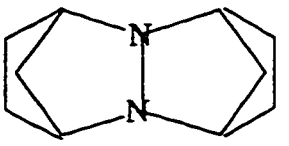

57

The barrier to double nitrogen inversion in **57** is determined to be 113 kJ/mol. [54] The σ-inductive effect of electronegative substituents increases the barrier to nitrogen inversion. The presence of a lone pair on an atom adjacent to nitrogen also raises the barrier since the lone pair repulsion is maximum in the sp^2-hybridized transition state where the overlap with a pure 'p' orbital is maximum. According to simple rules of hybridization as the electronegativity of the atom (attached to nitrogen) increases the nitrogen orbital directed towards the electronegative orbital will have higher p character resulting in the higher 's' character in the nitrogen lone pair which in the transition state must occupy a pure p orbital. The σ-inductive effect of an electronegative substituent therefore increases the barrier to inversion. The relative contribution of these two effects to the inversion barrier is still a long standing question and many researchers despaired

addressing this challenge [55]. MO calculations can reproduce the trends observed experimentally but they cannot distinguish the origin [56]. A quantum mechanical study describes the effect of through-bond electron donor-acceptor interaction on nitrogen inversion in *p*-pipridine derivatives [57]. A recent study [58] uses nitrogen inversion to describe the molecular flexibility in the anti-depressant drug trimipramine maleate **58**.

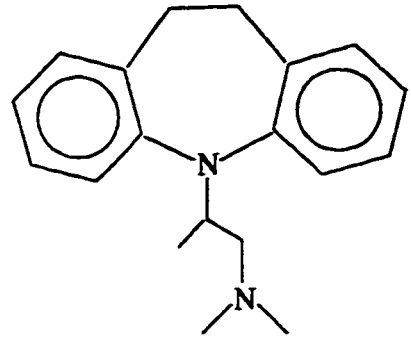

58

Restricted nitrogen inversion in the bicyclic amine **59** gave a very high barrier of 59 kJ/mol [59] . The origin of this bicyclic effect is attributed to the extreme rigidity of the framework which prevents the highly strained internal C-N-C bond angle (96°) from opening in the quasitrigonal transition state.

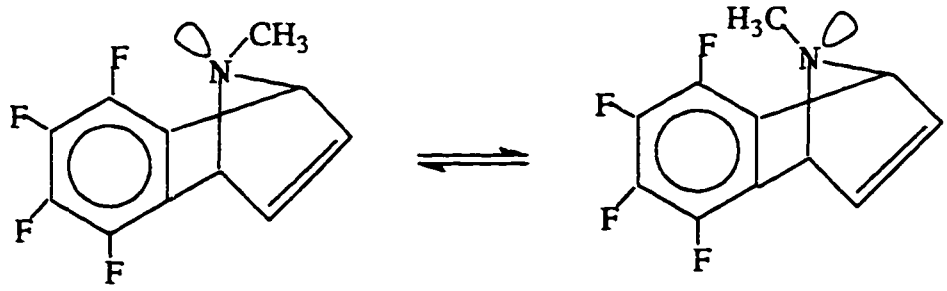

59

A rotation dominated inversion process [60] has been found to be the case in the piperidine derivative **60**.

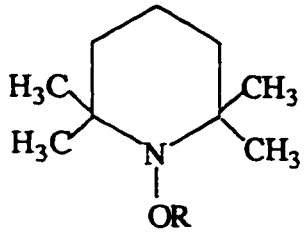

60

Recent studies [60-64] on nitrogen inversion processes in several classes of isoxazolidines **61-65** shed valuable light on the conformation. Effects of ring size and

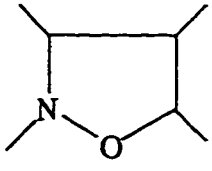

61

$\Delta G^{\#}$ 59-60 kJ/mol

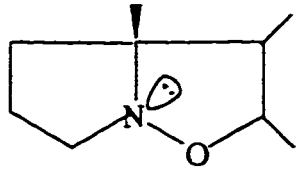

62

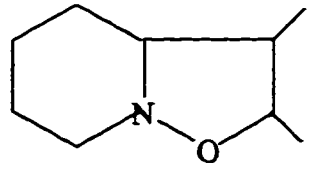

63

$\Delta G^{\#}$ 65.2–69.0 kJ/mol

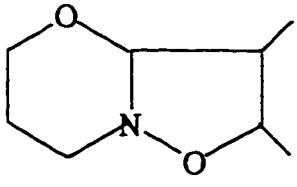

64

$\Delta G^{\#}$ 66.3-72.9 kJ/mol

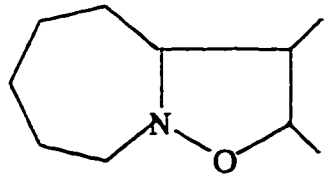

65

$\Delta G^{\#}$ 53-56 kJ/mol

substituents on the inversion have been studied at great length. Because of geometric constraints the isoxazolidines **62** cannot undergo nitrogen inversion and *cis* geometry is the only stable isomer. However in **63-65** the nitrogen inversion processes have been studied by DNMR method. Recently, the nitrogen inversion process has been used to unlock one interesting mechanism [65].

2.2 Anomeric Effect

It is well known in carbohydrate chemistry that pyranose sugars having electron withdrawing substituents (like halogen, alkoxy and acetoxy) at the anomeric carbon (i.e. C-1) are very often more stable when the C-1 substituent is in the axial orientation (α-anomers) rather than the equatorial orientation. Anomers are stereoisomers differing in their configuration only at the anomeric carbon.

This axial preference of the substituents is not limited to carbohydrates only but also observed in 2-substituted pyrans. This phenomenon is known as anomeric effect [66], since it involves the anomeric carbon in the carbohydrate pyranose ring.

All the equilibria between diastereomers **66**α, **66**β [67]; **67**α, **67**β [68]; **68** α, **69**β [69] reveal that the major isomers are those with axially oriented substituents at the anomeric carbon, thus the α-anomers are more stable in each case. For a conformationally mobile system the compound **69** with all axially oriented substituents reveals the powerful demonstration of the anomeric effect [70].

The nature of the substituent at C-1 and the dielectric constant determines the magnitude of the anomeric effect. The 2-chloro substituent **70** exhibit greater preference for axial orientation than C-2 methoxy **71**. The magnitude of the anomeric effect decreases with increasing dielectric constant of the solvent.

Several structural factors have been considered to put forward a plausible explanation of the anomeric effect. In the valence bond approach the β anomer experiences unfavourable dipole-dipole interaction between the polar bonds at the anomeric carbon. This interaction is reduced in the α anomer. The β-anomer, with higher dipole moment is expected to be stabilized in solvents with higher dielectric constant.

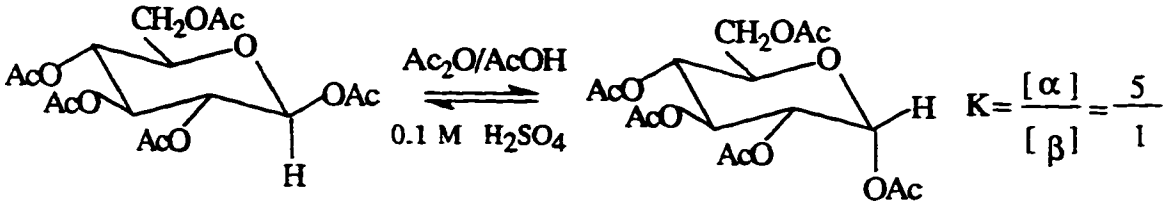

β α

66

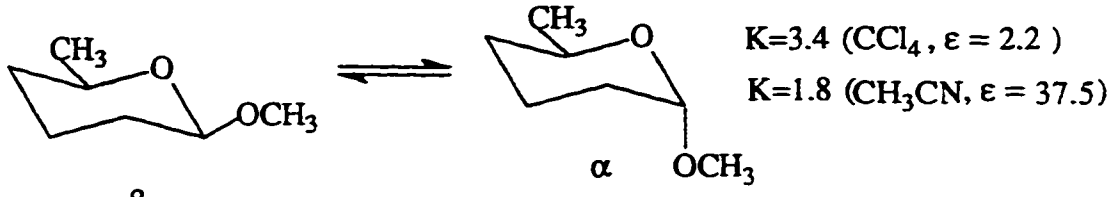

β

67

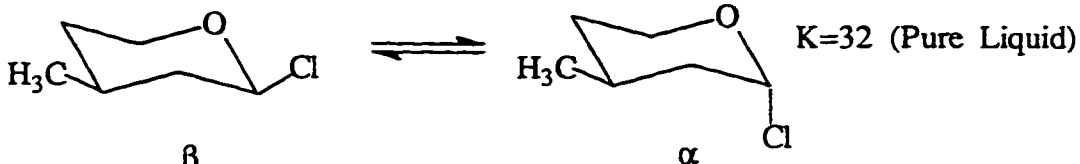

β α

68

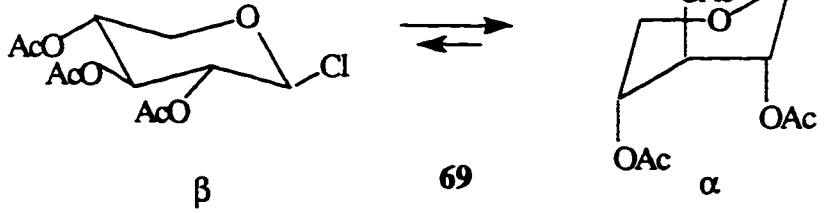

β

69

α

Strongly favoured

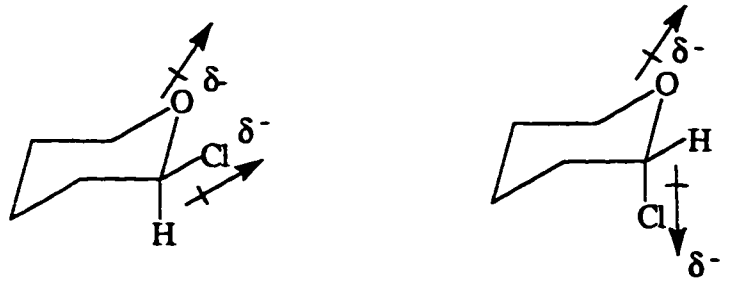

β α

70

From MO view point [71], the axial lone pair on ring oxygen is antiperiplanar to the C-Cl (or C-OR) bond and such delocalization of the ring lone pair by interaction with the σ* of exocylic C-X stabilizes the anomer. With increased electronegativity of the C-2 substituents such interaction also increases. This interaction is expected to shorten the C-O bond and lengthen the exocylic C-X bond.

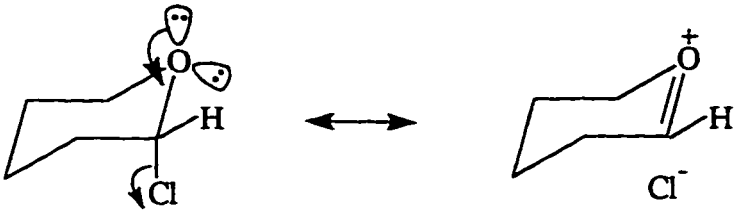

71

The anomeric effect can also operate in acyclic system in which a particular conformation is stabilized by antiperiplanar arrangement of a lone pair orbital on a heteroatom with C-X bond. For the donation of the lone pair the anomeric effect increases in the order F < O < N and for accepting the lone pair the effect increases with the increase in the electronegativity of the C-X system.

Acyclic acetals can possess various conformations among which **72** is the preferred conformation where the number of antiperiplanar arrangements between nonbonded electron pairs and C-O bonds is maximum.

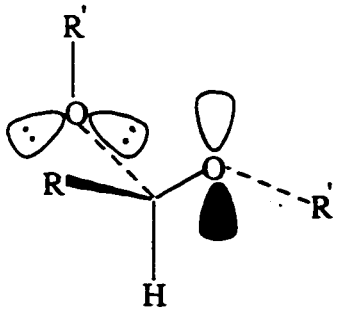

72

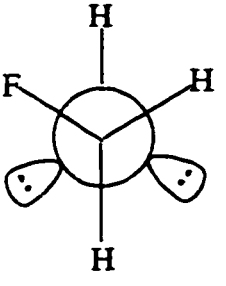

A

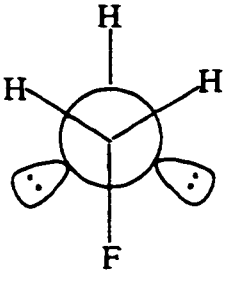

B

73

The molecular orbital approach is indeed very useful in identifying the rotational barriers in fluoromethanol **73** [72]. The conformation **A** (with gauche F, H) is calculated to be more stable than **B** (with anti F, H) by 52.7 kJ/mol. This is an example of the anomeric effect; one of the oxygen lone pair is anti to F in conformation **A**.

The conformational properties of monosubstituted tetrahydropyrans have been summarized by Eliel and coworkers [73] with special attention to electron-withdrawing substituents at C-2 which prefer the axial orientation [74] as a result of the anomeric effect[75]. Nonpolar substituents prefer equatorial orientation at C-2; the axial substituents experiences unfavourable 1,3-diaxial interactions which is further aggravated due to shorter C-O bond distances [76].

With electronegative substituents at C-2, the axial preference increases in less polar solvents [77]. In MO terms [78] mixing of the lone pair orbital at oxygen and the antiperiplanar C-X antibonding orbital in the axial form is responsible for the observed anomeric effect.

The discovery [79] of the anomeric effect in 1955 and subsequent experiments and theoretical calculations demonstrated the powerful effect of lone electron pairs in determining conformational preferences. The origin of the anomeric effect has been the cause of considerable debate. The cause of the anomeric effect has been explained in terms of following models:

1) Unfavourable dipole-dipole interactions (Electrostatic Model).
2) n-σ^* interaction (Negative Hyperconjugation Model).
3) "Principle of least nuclear motion" model.
4) Lone pair interaction model.

The stabilizing n-σ^* interaction is inversely proportional to the energy difference between the interacting orbitals.

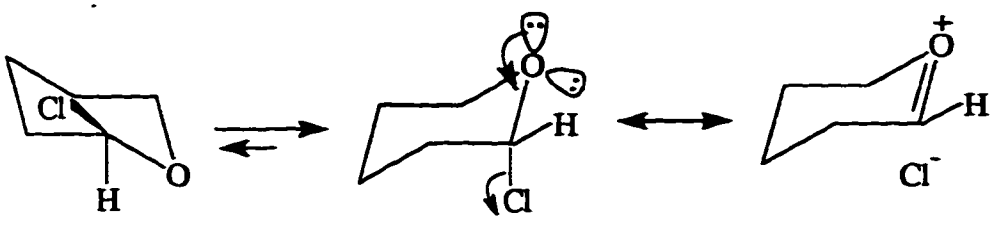

70

In the language of valence bond theory, the negative hyperconjugation model is expressed as two resonance structures (double bond - no bond resonance). In molecular orbital terms, the axial form is energetically preferred because it gains stabilization from a two-electron interaction (n-σ^*) between an occupied high energy donor orbital and an empty low energy unoccupied orbital [80] (Figure 2.6).

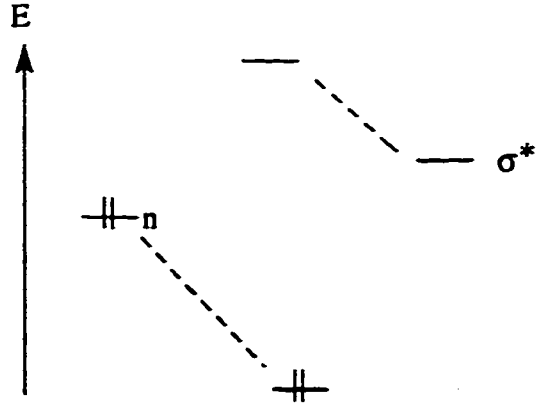

Figure 2.6: Energy level diagram showing n -σ^* interaction.

For the correct understanding of the electron pairs Kirby [81] has presented evidence which suggests that the nonbonding electrons in oxygen are directionally nonequivalent and should be in canonical n_σ and n_p orbital rather than in localized sp^3 orbitals in tetrahedral centres (Figure 2.7).

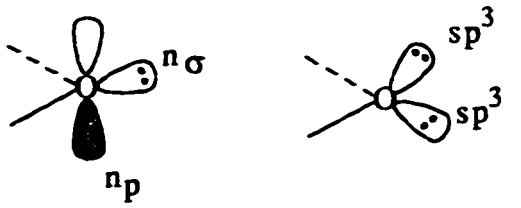

Figure 2.7: n_σ, n_p and sp^3 orbitals in oxygen.

The photoelectron spectrum of water [82] affords four well defined bands at 12.6, 13.7, 17.2 and 32 eV which were assigned to the p-type lone pairs, two bonding molecular orbitals and s-type lone pairs respectively. By contrast the sp^3 model of water will have two bands one for the bond pairs and the other for the lone pair. It has been shown [83, 84] that the anomeric effect is much stronger in the 5-membered furanose ring **74** (95% axial) than in the 6-membered pyranose ring **75** (56%).

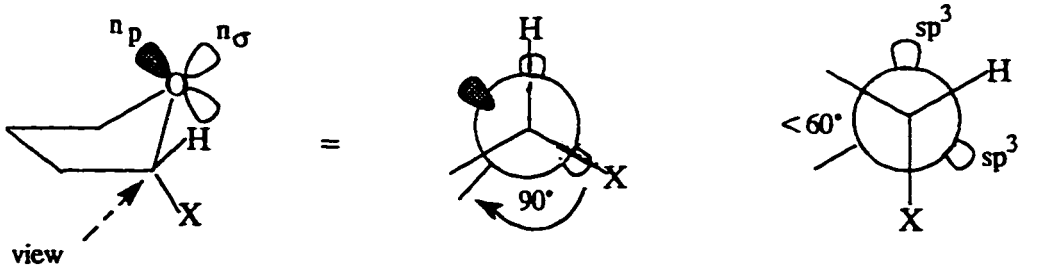

74

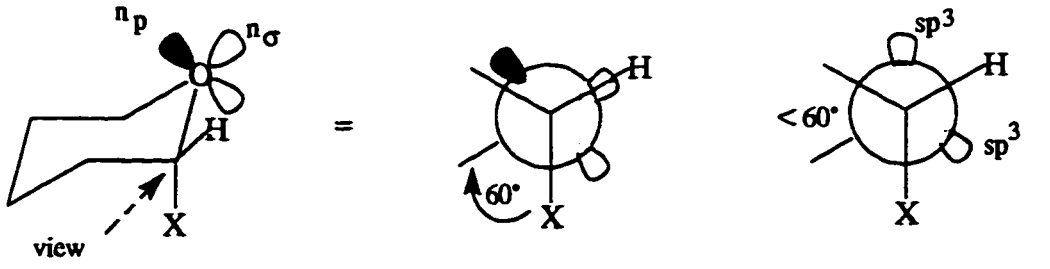

75

The stereoelectronic effect is expected to be strongest with the C-O-C-X torsional angle of 90° in which the n_p and the $\sigma^*_{C\text{-}X}$ will be eclipsed. In the sp^2-hybrid model of the

endocyclic oxygen a torsion angle of 90° allows maximum n_p -> σ^*_{C-X} overlap for the 5-membered system. Had it been the sp^3-hybrid model (in which torsion of 60° is the requirement for maximum n_{sp^3} -> σ^*_{C-X} overlap) six membered systems should show the maximum anomeric effect. In the sp^2-hybrid model n_p being the higher energy orbital than the n_{sp^3} becomes a better donor. Stereoelectronic effects also influence the orientation of the aglycon (exo anomeric effect). Exo anomeric effect delocalizes electron density from the exocyclic substituent which is maximum when the p-type orbital is antiperiplanar to the ring C-O bond. Rotomeric behavior of 2-methoxytetrahydropyran **76** has been studied [85]. Of the six staggered conformation a_3 is discarded on steric grounds. Of the remaining five rotamers, three rotamers a_1, e_1 and e_3 make important contributions for having n_p orbital antiperiplanar to the ring C-O bond. In a_1, both exo- and endo-anomeric effect compete for

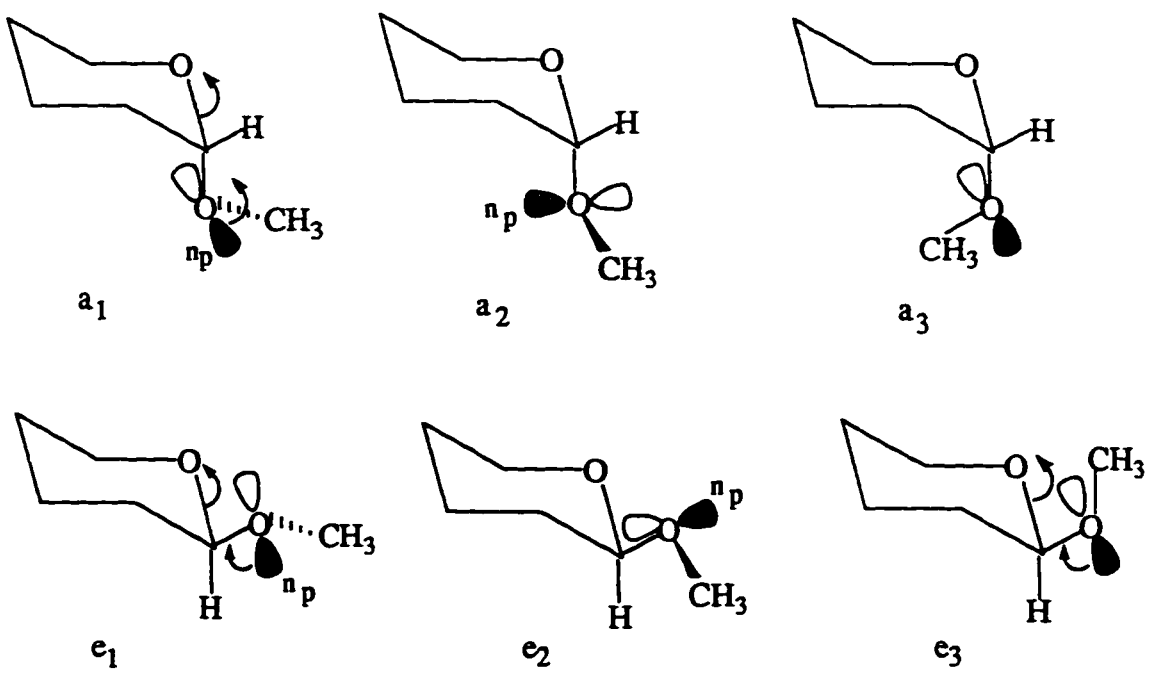

76

electron delocalization towards carbon whereas in e_1 and e_3 only exo anomeric effect operate.

The overall anomeric effect (AE), which determines the preference of the axial (or equatorial) conformer should be the difference of the anomeric effect in the equatorial and the axial conformer [86] [AE = exo-AE_{eq} - (exo-AE_{ax} + endo-AE_{ax})]. Since the axial conformer is strongly favoured, the term exo-AE_{eq} must be less stabilizing than (exo-AE_{ax} + endo-AE_{ax}), giving a positive anomeric effect. In the following example **77** the anomeric effect is negative [87]. Here nitrogen is a better donor, thus, exhibiting strong exo-AE_{eq} which should then be greater than exo-AE_{ax} and may even be greater than (exo-AE_{ax} + endo-AE_{ax}).

In spite of the evidence pointing towards nonequivalent lone pair orbitals many theoreticians advise that the partitioning of the lone pair density is difficult. Several reports disclose examples of the compounds where the axial anomer is preferentially stabilized in more polar solvents [88] contrary to the understanding presented by the electrostatic model.

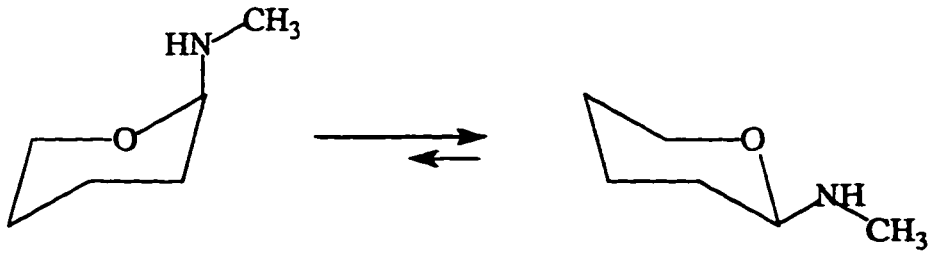

77

A major failure of the negative hyperconjugation model is the example of several compounds which show an unexpected "Reverse anomeric effect" [81,89]. The opponents of the frontier orbital interactions put forward and alternative model the "principle of least molecular deformation" [90] to rationalize the anomeric effect. There are cases of molecules which do not support the n-σ^* model of the anomeric effect, and a new model based on dominant n-n interaction through space is proposed [91]. Hence even to date the lively debate on how to rationalize the anomeric effect continues.

2.3 *E-Z* Isomerization in Nitrones

The barrier to *E-Z* isomerization about the C=N double bond is very sensitive to the nature of the substituents [92]. The barrier is usually high (780 kJ/mol) in simple N-alkylimines and can be conveniently followed by NMR techniques.

E	*Z*	Equlibrium E/Z
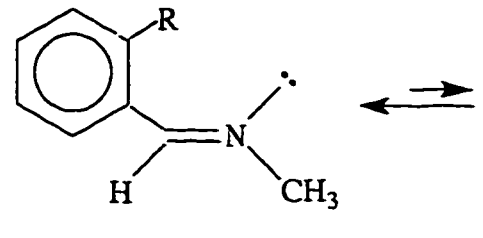	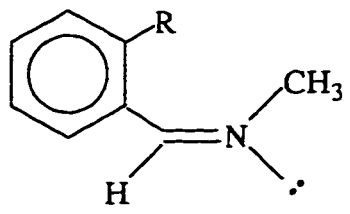	
78 R=H		> 99:1
79 R=CH_3		> 99:1
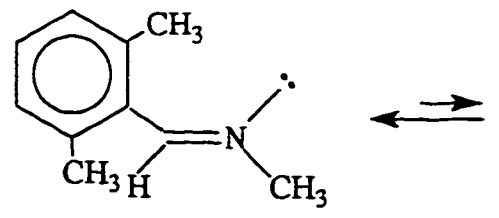	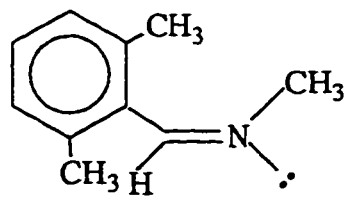	94:6

80

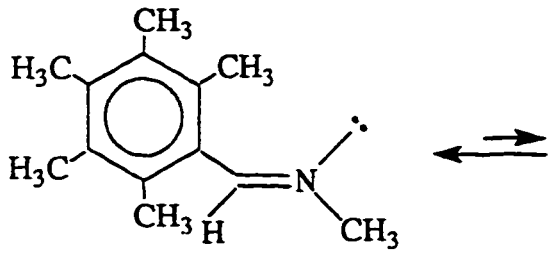
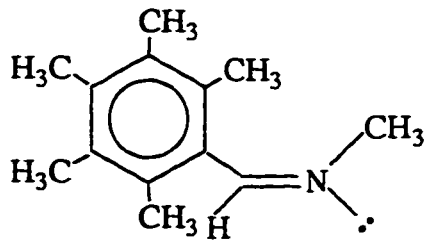

79:21

81

Usually ketimines exist as a mixture of *E, Z* isomers, however, normal aldimines tend to exist completely (>99%) in the *E* configuration. N-methylimines **78** and **79** derived from benzaldehyde or *o*-methyl benzaldehyde exist as *E* isomer. Surprisingly however, in imines with both *ortho* position substituted **80**, a considerable portion exist as the *Z* isomer. The N-methyl proton signals of the *Z* isomer appear upfield due to increased deshielding by the proximate benzene ring. The HC+NCH coupling constants for the *E* and *Z* isomer were found to be 1.6 and 2.2 Hz respectively. Imines **82** from alkylaldehydes exist exclusively in the *E* form and classical nonbonded interaction between alkyl substituents preclude the presence of the *Z* isomer. However the effective size of the aryl group is strongly conformation dependent. Substituents at *ortho* position exert unfavorable

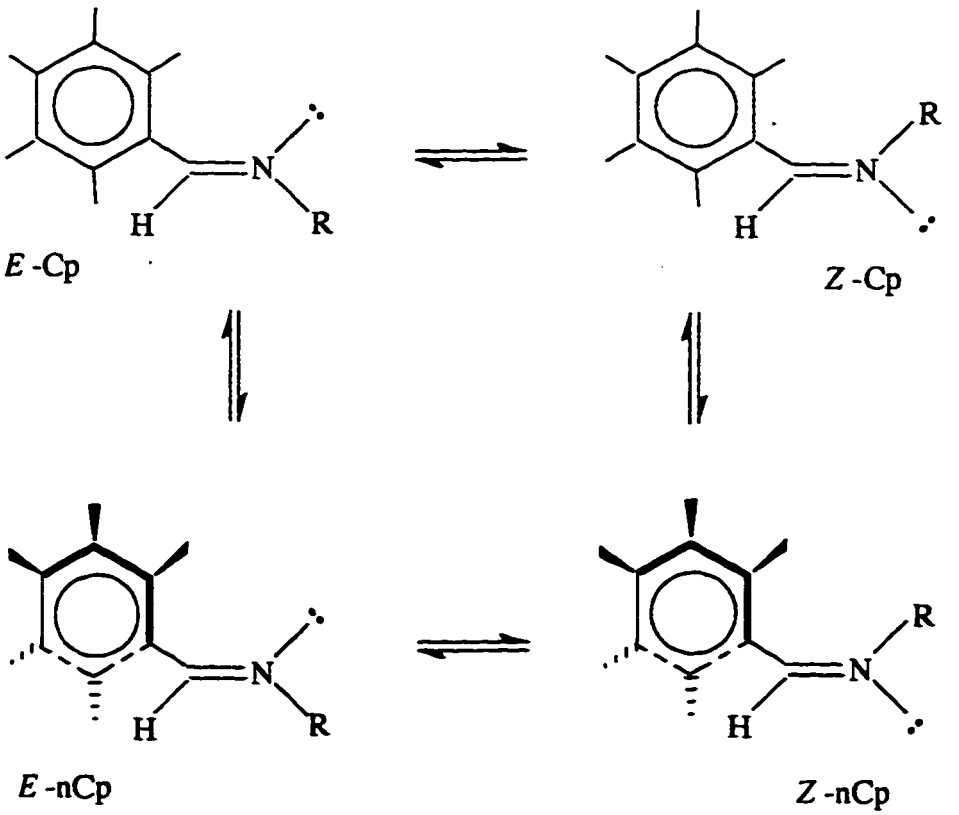

82

Scheme 2.5: Dynamic stereochemistry of imines.

steric interactions with the vinyl "H" and N-alkyl substituents. The steric interactions, thus force the aryl group to twist out of the imino-plane to adopt a noncoplanar (ncp) arrangement as depicted in Scheme 2.5. However the conjugate stabilization of the coplanar (cp) conformation opposes the twisting out of the imino-plane. It is suggested that n-p repulsion between the nitrogen lone pair and the aromatic π-cloud in *E* -"ncp" would destabilize this conformation in comparison to *Z* -"ncp". Increasing orthogonality will decrease the proportion of the *E* isomer. The "buttressing" effect of *meta* and *para* substituents along with increased π-electron density increases the orthogonality. Another contributing factor is suggested to be attractive non-bonded interactions between the aryl and N-aryl groups to stabilize the *Z* form. The presence of small amounts of acid catalyst increases the rate of isomerization whereas the presence of base suppresses the isomerization process.

E, Z isomers of ketimine and ketonitrones are known and easily separable. N-alkylketimines have been shown by NMR spectroscopy to have $\Delta G^{\#}$ values of 110-120 kJ/mol at 200°C in biphenyl solution [93]. However the aldimine **81** is shown [92] to have a free energy of activation of 89 kJ/mol (mean of the forward and reverse reactions).

The aldonitrones, like aldimines, is known to exist in the preferred *Z* form. However, aldonitrones **83** with both *ortho* positions substituted exist in both *Z* and *E* forms at equilibrium [94]. The NMR signal of **83b** appeared at upfield due to the shielding influence of the proximate aryl group (Table 2.1).

The aldehyde-hydroxylamine condensation leading to the formation of the nitrone, was found to be kinetically controlled. The nitrone **83b** was formed in the unstable *"E"* form with a stereo preference to a *Z:E* ratio of 83:17. The interconversion rate and barrier of the *E* and *Z* isomers of **83b** obtained by thermal stereomutation in diphenyl ether at 147°C were found to be $k_f = 5.3 \times 10^{-5}\ s^{-1}$ $\Delta G_f^{\#} = 138.5$ kJ/mol; $k_r = 0.9 \times 10^{-5}\ s^{-1}$, $\Delta G_r^{\#} = 144.8$ kJ/mol respectively. With traces of benzoic acid increasing the rate of interconversion drastically (at 64°C, $k_f = 2.1 \times 10^{-3}\ s^{-1}$, $\Delta G_f^{\#} = 100$ kJ/mol;

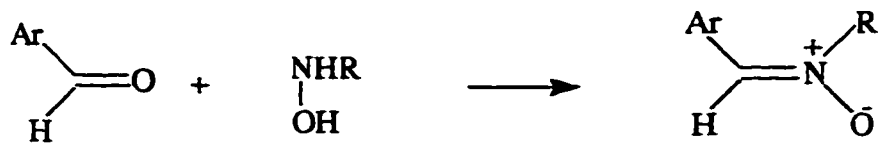

(E) **83**

$k_r = 2.6 \times 10^{-4}\ s^{-1}$, $\Delta G_r^{\#} = 106$ kJ/mol). The presence of trace amounts of bases decelerates the rate of isomerization. A consistent downfield shift [94] of the methine (CH=N) proton signal in the **83***E* nitrone is attributed to the fact that proton is adjacent to the negatively charged oxygen atom of the N-oxide. The conformation of the aryl ring which

E *Z*

83

Table 2.1: ^{1}H NMR chemical shifts of *E* and *Z* nitrones.

Nitrone **83**	Ar	R	%E at Eq	δE_R	$\delta E_{CH=N}$	δZ_R	$\delta Z_{CH=N}$
a	2,6-$Me_2C_6H_3$	Me	9	3.40	7.87	3.82	7.52
b	C_6Me_5	Me	17	3.40	7.90	3.89	7.59
c	C_6Me_5	Et	12	1.32	7.88	1.58	7.64
d	C_6Me_5	^{i}Pr	8	1.29	7.83	1.49	7.63
e	C_6Me_5	^{t}Bu	<1	-	-	1.62	7.67

is almost orthogonal for both *E*- and *Z*- isomers of **83** will also affect the methine proton chemical shift. While the resonance stabilization would prefer **83** *E* and *Z* coplanar (cp) conformation (Scheme 2.6), the presence of non-bonded steric interactions between *ortho* substituents and N-alkyl group in *Z* (cp) and between *ortho* substituents and methine proton in both *E* (cp) and *Z* (cp) will favour the orthogonal (non coplanar, ncp) conformers. Non-bonded attraction between Ar and N-alkyl will also favour *E* (ncp). However repulsion between the aromatic π-cloud and oxygen lone pair would destabilize *Z* (ncp). The net effect of all these factors would decide the equilibrium ratios of the isomer and also the magnitude of twisting out of the imino-plane. Oxygen also exerts non-bonded interaction (this interaction is less severe in the corresponding imine).

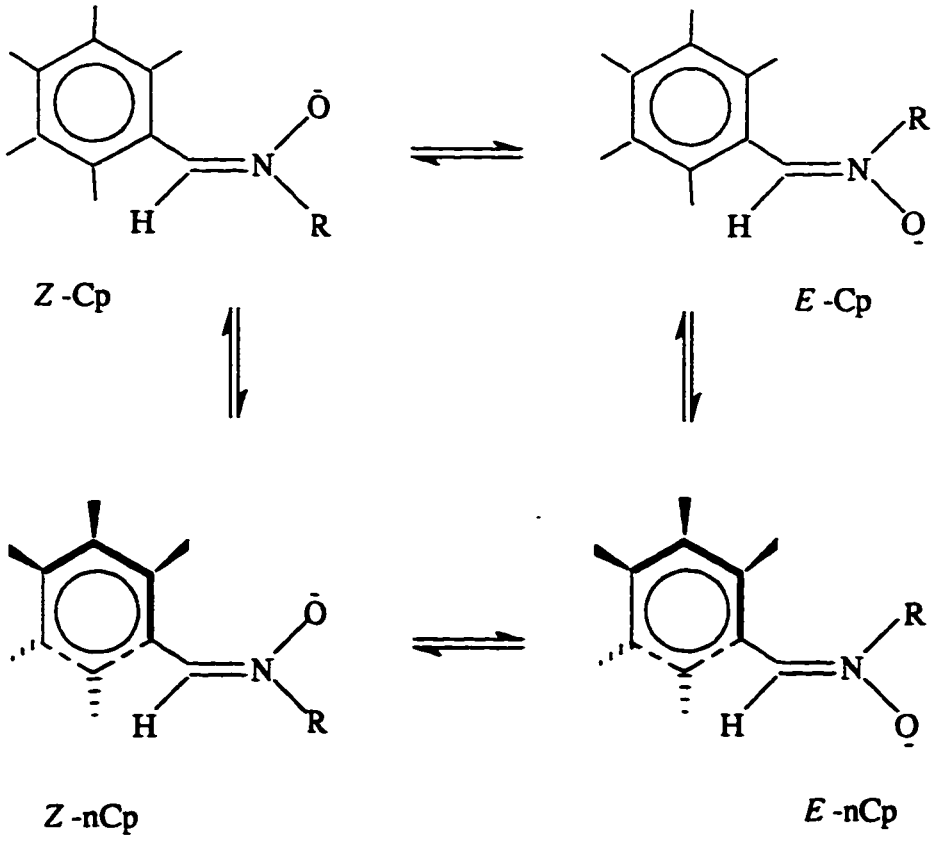

83

Scheme 2.6: Dynamic stereochemistry of nitrones (the extreme conformations).

The free energy of activation for the rotational barrier of the nitrone **84** at 180°C in nitrobenzene solution has been determined [95] to be 97 kJ/mol.

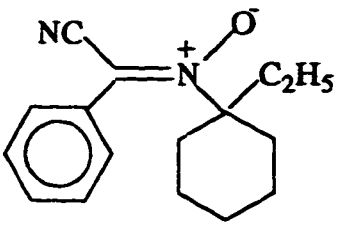

84

For the stereoisomeric ketonitrone **85** the energy of activation was found [96] to be 103 kJ/mol at 117°C.

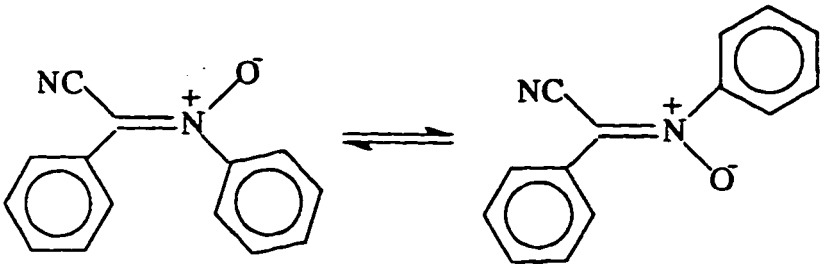

Z *E*

85

The energy barriers for the *Z, E* isomerization in nitrones are found to be considerably lower than the barriers observed in alkenes **86** and **87**.

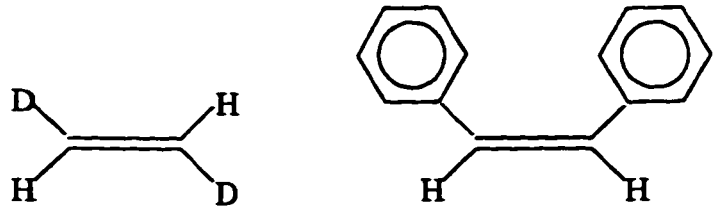

E_a 272 kJl/mol 176 kJ/mol

86 **87**

Interconversion in imines can take place by rotation through 180° around the double bond by nitrogen inversion (planar inversion, lateral shift) or by imine-enamine tautomerism [98]. In the case of nitrones the inversion mechanism is not available. MO calculations [99] tried to shed light on the *E, Z* isomerization process. The structure of nitrones is usually represented as a hybrid **90** between the valence bond structures **88** and **89**. The calculation on the ground state indicates a high charge density at oxygen and a CN π-bond order of 0.86 and a NO π-bond order of 0.50.

The transition state **90** places a high charge density at the carbon with a tetrahedral geometry at carbon and a NO π-bond order of 0.94. The calculated rotational barrier in **88** was estimated to be 251 kJ/mol (by CNDO/2) and 335 kJ/mol (by INDO). These barriers are clearly higher than the experimentally observed barriers in several nitrones (96-146 kJ/mol).

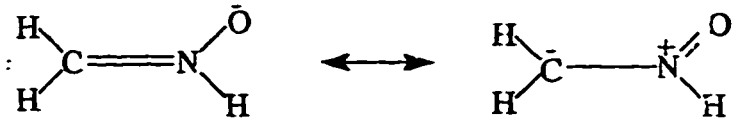

88 **89**

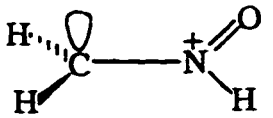

90

Conjugating substituents, however, might be expected to lower the energy barrier of rotation around the CN bond. The anomalous behavior of *ortho*-disubstituted C-aryl nitrones which show a significant proportion of the *E* isomer at equilibrium [94] has been accounted for, in molecular orbital terms [99]. The potential energy difference between the orthogonal *Z* and *E* at the ground state has been estimated to be 0.6 (CNDO) and 5.44 kJ/mol (INDO) corresponding to an equilibrium proportion of 25 or 10% *E* at equilibrium. These estimates are surprisingly close to the observed isomeric distribution [94]. However, the observed barrier for the isomerization of the nitrone **83b** was found to be 145 kJ/mol

even though the free energy barrier was estimated to be 213 (CNDO) or 285 kJ/mol (INDO). It would appear that either the MO calculations overestimates the CN rotational barrier or the *E-Z* isomerization occurs via another route. It is difficult to rationalize why the rotational barrier in the case of nitrone **84** (97 kJ/mol) [95] is about 41.8 kJ/mol lower than in **83b** (145 kJ/mol) [96]. It should also be noted that traces of benzoic acid lower the energy barrier by about 38 kJ/mol [94]. It has been suggested that the isomers may inter convert via an intermediate with a CN single bond where rapid rotation around CN is possible [100]. First order thermal isomerization is expected to have an entropy of activation close to zero,[101,102] whereas acid catalyzed second order isomerization should have large negative entropy of activation [100].

The energy barrier for the *Z-E* isomerization of nitrone **91** under acid free conditions in $CDCl_3$ is measured [99] to be 134 kJ/mol. Near zero entropy of activation ($\Delta S^{\#}$, -10.5 kJ/mol) is quite consistent with an intermolecular bond rotational forces.

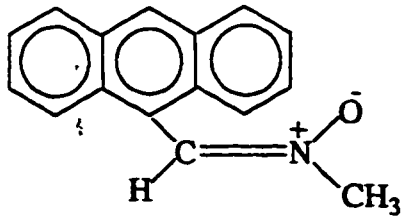

91

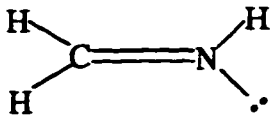

92

CNO/2 calculations on methyleneamine **92** have given a CN rotational barrier of 255 kJ/mol and a barrier to nitrogen inversion of 130 kJ/mol.[103] Measured *E-Z* isomerization barriers in N-alkylimines in the range of 105-117 kJ/mol supported the view that the interconversion might be happening via planar nitrogen inversion. A sample of **93** in acid-free diphenyl ether undergoes isomerization at 35°C with a half life of 35 h. The rate of isomerization is considered to be that of an uncatalyzed intramolecular process (probably nitrogen inversion). However the presence of benzoic acid (1 mg per 15 mg of **93** in

diphenyl ether (0.5 ml) reduced the half life to < 1 min. Half lives depend on the amount of acid added.

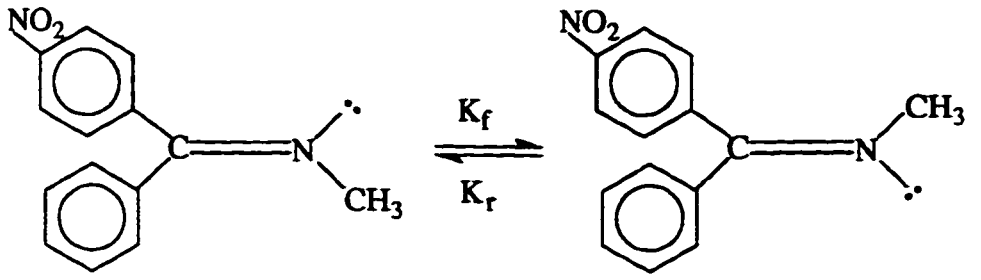

E **93** *Z*

The $\Delta H^{\#}_f$ of the non catalyzed isomerization [100] determined to be 107.5 kJ/mol and the near zero entropy of activation ($\Delta S^{\#}_f$ = -4.18 J/mol K) is quite consistent with planar

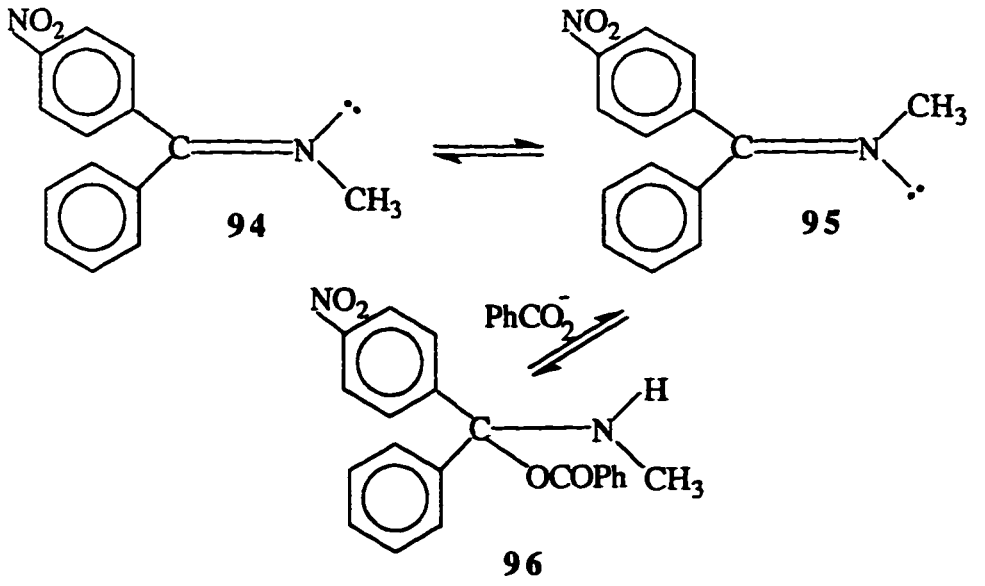

96

inversion forces. However in the presence of benzoic acid as catalyst, $\Delta S^{\#}_f$ was found to be -126 J/mol K. It was suggested that a small fraction of the imine will be protonated reversibly to give the immonium salt which on reversible nucleophilic addition would afford **97** where the rotation around CN will be much faster.

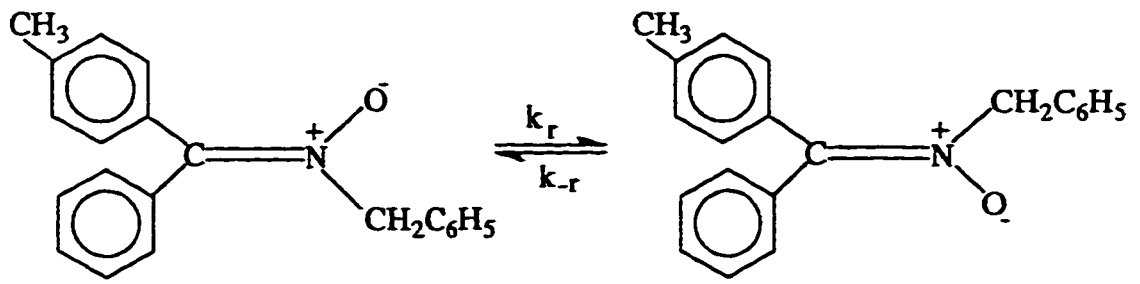

97

The activation parameters [104] for the E-Z isomerization of ketonitrones **97** were determined to be 141 kJ/mol (E_a) and $\Delta S^{\#}$ of -16.7 cal / mol K, indicates the process as a intramolecular one.

3

BANDSHAPE ANALYSIS

Dynamic NMR (DNMR) deals with the effects of chemical exchange processes on the NMR spectra. The most important kind of information that can be obtained is the rate constant for the processes studied. The first order, or pseudo first order, rate constants in the range 10^{-1}-10^{5} or 10^{6} s^{-1} can be measured. This desired kinetic information is obtained by the analysis of exchange broadened spectra, the so-called band shape analysis technique.

When the bandshape at a known temperature has been secured the corresponding rate constant can be derived. With the aid of the known parameters; the chemical shift difference $\delta\nu$, the coupling constant J, the transverse relaxation time T_2, and by the systematic variation of the rate constant, theoretical band shapes are calculated. The best curve with the best rate constant is found by comparison with the experimental curve, either by a visual inspection or by a computerized least-squares adaptation.

When rate constants are obtained at several temperatures, it is possible to calculate thermodynamic parameters such as enthalpies, entropies and free energy of activation.

3.1 Band Shape Equations

There are two approaches to the bandshape equations, the classical and quantum mechanical approaches. For the study of exchange between uncoupled sites, the simpler

classical bandshape theory based on suitably modified Bloch equations can be applied. For deriving bandshape equations for second order coupled systems the quantum mechanical approach must be used.

3.1.1 The Bandshape Equation for the Exchange Between Two Uncoupled Sites

The suitable forms of the Bloch equations for the consideration of the effect of chemical exchange upon the bandshape are:

$$\frac{dG}{dt} = i(w_o - w)G - i\gamma B_1 M_z - \frac{G}{T_2} \qquad (3.1)$$

$$\frac{dM_z}{dt} = \gamma v B_1 - \frac{(M_z - M_o)}{T_1} \qquad (3.2)$$

where G is the complex magnetization in the xy plane and M_z is the macroscopic magnetization in the z direction.

Consider the exchange between two sites A and B

$$A \underset{k_B}{\overset{k_A}{\rightleftharpoons}} B$$

with site populations p_A and p_B. The kinetics of the process may be described in terms of two first order rate constants, k_A for transfer from site A to site B and k_B for the transfer from site B to site A. At equilibrium

$$k_A p_A = k_B p_B \qquad (3.3)$$

The lifetime of nuclei at each site is given by the reciprocal rate constant. i.e.

$$\tau_A = \frac{1}{k_A}; \ \tau_B = \frac{1}{k_B} \qquad (3.4)$$

The effect of the exchange process on the NMR spectrum can be considered using the approach described by Hahn, Maxwell and McConnell (HMM) [105,106]. It is assumed that jumps of nuclei between sites are fast so that no nuclear precession occurs during the jump. For the two-site case there are two independent transverse magnetizations, G_A and G_B. The effect of exchange between the two sites is to decrease the transverse magnetization of site A at a rate equal to $k_A G_A$ and increase it at a rate $k_B G_B$. The changes may be incorporated into the Bloch equation (3.1) to give,

$$\frac{dG_A}{dt} + \alpha_A G_A = -i\gamma B_1 M_{zA} + k_B G_B - k_A G_A \qquad (3.5a)$$

$$\frac{dG_B}{dt} + \alpha_B G_B = -i\gamma B_1 M_{zB} + k_A G_A - k_B G_B \qquad (3.5b)$$

where

$$\alpha_A = \frac{1}{T_{2A}} - 2\pi i(\nu_A - \nu)$$
$$\alpha_B = \frac{1}{T_{2B}} - 2\pi i(\nu_B - \nu) \qquad (3.5c)$$

Generally NMR spectra are measured under 'steady state' conditions, i.e. the spectra are swept slowly so that dG_A / dt and dG_B / dt may be set equal to zero. Hence the two equations (3.5a) and (3.5b) can be solved to give G_A and G_B. The absorption intensity at an angular frequency w is proportional to the imaginary component of G. For the exchange between two unequally populated sites having equal transverse relaxation time, T_2, the imaginary part of G is given by Eq. (3.6).

$$\mathrm{Im}(G) = \frac{-\gamma B_1 M_o \left(1 + \tau/T_2\right) P + QR}{Q^2 + R^2} \qquad (3.6)$$

where

$$\tau = \frac{\tau_A \tau_B}{\tau_A + \tau_B} \tag{3.6a}$$

$$Q = \tau\left\{\left(\frac{w_A + w_B}{2}\right) - w - \left(\frac{(p_A - p_B)(w_A - w_B}{2}\right)\right\} \tag{3.6b}$$

$$P = \tau\left\{\left(\frac{1}{T_2}\right)^2 - \left(\frac{w_A + w_B}{2} - w\right)^2 + \left(\frac{(w_A - w_B}{4}\right)^2\right\} + \frac{1}{T_2} \tag{3.6c}$$

$$R = \left\{\left(\frac{w_A - w_B}{2} - w\right)\left(1 + \frac{2\tau}{T_2}\right) + \left(\frac{(p_A - p_B)(w_A - w_B}{2}\right)\right\} \tag{3.6d}$$

M_o is the equilibrium value of the z component of the magnetization, w is the frequency in radians per second, and w_A and w_B are the resonant frequencies corresponding to the sites A and B.

Equation (3.6) can be simplified in the two limiting cases; the slow exchange limit i.e. $k << v_{AB}$ and the fast exchange i.e. $k >> v_{AB}$. The simplified expressions are subject to serious systematic errors in the region of intermediate exchange rates. Eq. (3.6) can be extended to allow for unequal transverse relaxation times i.e. $T_{2A} \neq T_{2B}$.

For $p_A = p_B = 0.5$, the exchange rate, k_C, at the coalescence is given by,

$$k_C = \frac{\pi(v_A - v_B)}{\sqrt{2}} \tag{3.7}$$

The coalescence point is defined as that point where there no longer exists a minimum between the two peak maxima, and the bandshape is that of one flat-topped peak. Eq. (3.7) is applicable only when the line-widths are smaller than $v_A - v_B$.

When the populations are unequal, e.g. $p_A > p_B$, the smaller peak B shifts more as well as broadens more rapidly as the exchange rate increases. The coalescence point in these cases is the disappearance of the B peak. The expression for the rate at coalescence is given by [107],

$$k_A = p_B\, k = \frac{p_B\, 2\pi\Delta\nu}{X} \tag{3.8}$$

where X is the solution of

$$\Delta p = p_A - p_B = \left(\frac{X^2-2}{3}\right)^{3/2} \frac{1}{X} \tag{3.9}$$

3.1.2 The Bandshape Equations for Exchange in the Presence of Coupling

The system studied in this work include intramolecular exchange between two coupled nuclei

$$AB \rightleftharpoons BA$$

The presence of coupling requires the use of the quantum mechanical approach to calculate the bandshapes. This has been carried out successfully using density matrix methods [108,109].

3.2 Computer Programs

The computer programs used in this work were obtained from Science & Engineering Research Council, UK [110]. These main frame programs were modified into PC versions before use.

3.2.1 The "NCSHAPE" Program

This program deals with the exchange between two non-coupled sites of unequal populations, but with equal transverse relaxation times T_2. The equation used is that of HMM given as Eq. (3.6). The intensity of the absorption spectrum is calculated over a required number of points (e.g. 500). The intensities calculated are then normalized, so that the spectrum can be plotted in the required dimensions for direct comparison with the observed spectrum. The parameters required for the computation are, the peak separation (chemical shift difference), the width at half height of a non-exchange line (w), initial final and incremental lifetimes (TI, TF and TT), initial, final, and incremental populations of the high frequency site (PI, PF, PP) and the plot parameters. The plot of the computer spectrum is compared directly with the observed spectrum by superposition using a light box. The mean lifetime is varied to give the best fit of the computer to the observed spectrum by eye.

3.2.2 The "CSHAPE" Program

For first order spectra showing couplings, we modified the library NCSHAPE program described above. The first order couplings of the protons was simply assumed as giving overlapping two-site exchanges, with same population ratios and equal rates of exchanges. The intensity at each point was calculated by applying HMM equation for two-site exchange, for each of the overlapping cases, which were displaced from one another by certain frequencies corresponding to coupling constant, and then the intensities were summed to give band shape at that point. For cases of coupling to two and three equivalent protons, appropriate intensity ratios were taken into account.

3.2.3 The "ABSHAPE" Program

This calculates the band shape for mutually exchanging AB = BA system where at low temperature we observe the AB pattern and at high temperature it is a single line. Program employs density matrix method for the simulation of band shape.

3.2.4 The "ABEX" Program

This program calculates the band shapes for the system of two exchanging AB spin system with unequal populations

$$AB \rightleftharpoons A'B'$$

So the low temperature spectrum shows two AB quartets and at high temperature they coalesce to give one average AB quartet.

3.2.5 The "AXEX" Program

This program deals with the exchange between two non-coupled sites of unequal populations, but with equal transverse relaxation time T_2. The equation used is that of HMM given as equation 3.6.

3.3 Calculation of the Activation Parameters

The measurement of exchange rate constants as a function of temperature offers the possibility of calculating the activation parameters for the underlying process. A free energy of activation may be calculated from a rate constant at a single temperature by means of the Eyring equation.

$$k = \kappa(k_B T / h)e^{\left(\frac{-\Delta G^{\#}}{RT}\right)} \qquad (3.10)$$

where κ is the transition coefficient and k_B is the Boltzmann constant.

Rate constants measured over a range of temperatures may be converted to Arrhenius activation energies (E_a) and frequency factor (A) or to enthalpies and entropies of activation by formulae given below:

$$k = A e^{\left(\frac{-E_a}{RT}\right)} \qquad (3.11)$$

$$k = \kappa(k_B T / h)e^{\left(\frac{-\Delta H^{\#}}{RT}\right)} e^{\left(\frac{\Delta S^{\#}}{RT}\right)} \qquad (3.12)$$

$$\Delta G^{\#} = \Delta H^{\#} - T\Delta S^{\#} \qquad (3.13)$$

The Eyring equation was originally developed as an approximation for bimolecular processes in the gas phase, but it has been argued that it is valid for unimolecular processes as well [111]. It has been shown [112] that it is advantageous to discuss the results in terms of the free energy of activation $\Delta G^{\#}$ because it is accepted that $\Delta G^{\#}$ is far less influenced by systematic errors than the Arrhenius activation energy E_a. Moreover, in the discussion of barriers to C-N internal rotation in amides, a comparison of E_a values may obscure the true situation [112] because E_a is easily influenced by entropy effects. The use of Eyring equation to obtain $\Delta H^{\#}$ and $\Delta S^{\#}$ has also been favoured [113] because this has the advantage of assumption with clear-cut thermodynamic implications e.g. that $\Delta H^{\#}$ and $\Delta S^{\#}$ are temperature independent.

The activation parameters $\Delta H^{\#}$ and $\Delta S^{\#}$ obtained from NMR bandshapes are subject to large systematic errors, unless very accurate rate constants and temperature measurements are made. Since the temperature measurements in the NMR probe are made in the gas steam they are not very accurate (±0.5°C). Also for simple exchanging spin

systems the precision of the rate constants decreases with the distance from the coalescence region.

Further systematic errors are introduced by incorrect use of chemical shift difference ($\delta\nu$) and line width in the absence of exchange (T_2) values. We have taken care to minimize these errors by extrapolating low temperature $\delta\nu$ values to higher temperatures and using the non-exchanging signal line width (e.g. TMS) to estimate T_2. Major systematic errors could also arise due to the small $\delta\nu$ observed in some of the systems, which allow only a small temperature range to be studied (~50°C)

Even though $\Delta H^{\#}$ and $\Delta S^{\#}$ have large errors, the $\Delta G^{\#}$ at the coalescence temperature, T_c, ($\Delta G_c^{\#}$) is usually more accurate. It is clear that discrepancies in the value of $\Delta H^{\#}$ and $\Delta S^{\#}$ have a tendency to be mutually compensating; for example a $\Delta H^{\#}$ that is too small tends to be associated with a $\Delta S^{\#}$ that is too negative and too large $\Delta H^{\#}$ with a $\Delta S^{\#}$ too positive etc. Small errors involved in $\Delta G^{\#}$ are shown by analyzing the Eyring equation (3.10). The formula for the linearized relative statistical error in $\Delta G^{\#}$ is given by:

$$\left(\frac{\sigma_{\Delta G^{\#}}}{\Delta G^{\#}}\right)^2 = \left[\ln\left(\frac{k_B T}{hk}\right)\right]^{-2}\left(\frac{\sigma_k}{k}\right)^2 + \left[1+\ln\left(\frac{k_B T}{hk}\right)^{-1}\right]^2\left(\frac{\sigma_T}{T}\right)^2$$

$$\equiv \left[\ln\left(\frac{k_B T}{hk}\right)\right]^{-2}\left(\frac{\sigma_k}{k}\right)^2 + \left(\frac{\sigma_T}{T}\right)^2$$

For a typical case with T = 300°C and k = 100 s^{-1} a relative statistical error of 100% in the rate constant introduces a relative error of 4% in $\Delta G^{\#}$. A temperature error of 6°, introduces an error of 2% in $\Delta G^{\#}$, which adds up to a total standard deviation of 4.5%;

or for a typical $\Delta G^{\#}$ of 62.76 kJ/mol to ± 2.9 kJ/mol. Similarly errors in k and T of 25% and 3% respectively yield a $\Delta G^{\#}$ with a precision of ± 0.8 kJ/mol.

This can also be discussed in terms of the covariance of $\Delta H^{\#}$ and $\Delta S^{\#}$. This covariance measures the degree to which the values of the variables or parameters depends on the values of other variables or parameters. It can be shown that

$$\left(\sigma_{\Delta G^{\#}}\right)^2 = \left(\sigma_{\Delta H^{\#}}\right)^2 + \left(T\,\sigma_{\Delta S^{\#}}\right)^2 - 2T\,\sigma_{\Delta H^{\#}}\,\sigma_{\Delta S^{\#}}$$

So it follows that contribution to $\sigma_{\Delta G^{\#}}$ from errors in $\Delta H^{\#}$ and $\Delta S^{\#}$ are compensated by the covariance term. The correlation increases with increasing experimental errors. This effect is amply demonstrated [114] by data from the DNMR literatures where different authors report extremely different values for $\Delta H^{\#}$ and $\Delta S^{\#}$ but nearly the same $\Delta G^{\#}$ for such processes as internal rotation in N, N- dimethylformamide.

Although the values of $\Delta H^{\#}$ and $\Delta S^{\#}$ were obtained by Eyring plots, little significance was given on these, for reasons stated above and therefore they are not reported and discussed. In the light of above, the attention was directed to the use of bandshape fitting as a means of improving the accuracy of $\Delta G^{\#}$ (± 0.3 kJ/mol) at near coalescence temperature.

4

EXPERIMENTAL

4.1 Instrumentation

4.1.1 Variable Temperature NMR Measurements

Variable temperature ^{1}H NMR spectra were recorded on a Varian XL 200 NMR spectrometer operating at 200.05 MHz in the Fourier transform mode. The compounds were examined in $CDCl_3$ solutions at 0.15 M concentrations. Temperature control was achieved using the XL-200 temperature controller and calibrated using standard chemical shifts of methanol for low temperatures. The temperatures are accurate to ±0.5°C.

Simulations of exchange affected NMR spectra were carried out using the library program ABSHAPE [110] which calculates the band shapes for the mutually exchanging spin system of AB going to BA. The matching of simulated and experimental spectra were carried out by superposition of calculated and experimental spectra by eye. In the isoxazolidines, the exchange of benzylic CH_2 protons can be depicted as AB<-> A'B' (exchange between two AB systems with unequal populations). Computer program ABEX [110] was used to calculate the rate constants.

Variable temperature ^{13}C NMR spectra were recorded on the same Varian XL-200 NMR spectrometer, operating in the Fourier transform mode, with a digital resolution of 0.31 Hz at 50.3 MHz. The isoxazolidines were studied as 25 mg ml^{-1} solutions in $CDCl_3$ with TMS as internal standard. The spectra were obtained in the usual way with wide band proton decoupling and off-resonance decoupling to determine multiplicities of signals. Temperature control was achieved using the XL-200 temperature controller and calibrated

using standard chemical shifts of methanol and glycol for low and high temperatures respectively. The temperature were accurate to ±0.5°C.

Simulations of exchange affected ^{13}C NMR spectra for **123b** and **123c** were carried out using a computer program, AXEX [110], corresponding to a two non-coupled sites exchange with unequal populations. At least three carbon resonances were utilized at each temperature, and the matching of simulated and experimental spectra was carried out by eye (by superposing calculated spectra over the experimental spectra). The rate constant obtained at each temperature was an average of three calculated values.

4.1.2 Elemental and IR Analyses

Elemental analyses were performed on a Fisons Instruments Elemental Analyser 1108 and Carlo-Erba Elemental Analyser 1106. Elemental analyses are not provided for the compounds **123a**, **123b**, and **123c** due to their volatile nature; instead molecular ion peaks are provided. IR spectra were recorded on a Nicolet 5 DXB FTIR and Shimadzu instrument model IR-408, and are reported in wave numbers (cm^{-1}).

Silica gel chromatographic separations were performed with flash silica gel (Baker Chemicals Co). All melting points are uncorrected.

4.2 General Synthetic Procedures & Experimental Parameters

4.2.1 The Hydroxylamines

Aldehyde (5.5 mmol) was added to a solution of the hydroxylamine (5.0 mmol) in ethanol ($10cm^3$) . The reaction mixture was stirred at 50-60°C for 5 h and TLC experiment (silica, ether) was used to determine the complete formation of the nitrone. To this solution was added $NaBH_4$ (10 mmol) and the mixture was then stirred at 50°C for 5 h. Another 10 mmol of $NaBH_4$ was added and the reaction mixture was stirred at 20°C for 24 h to

ensure complete reduction of the nitrone (checked by TLC experiment). After removal of the ethanol by a gentle stream of N_2 the reaction mixture was taken up in H_2O (15 cm^3) and extracted with $CHCl_3$ (3 x 25 cm^3). Removal of the solvent followed by passing through a silica column using hexane-ether mixture (3:1) as eluent afforded the hydroxylamines in 70-85% yield. While the hydroxylamines were used as their free bases, *N*-methylhydroxylamine was introduced as its hydrochloride and the base was liberated from its salt by adding 1.1 equivalent of sodium acetate in the reaction mixture. After removal of the solvent by a gentle stream of N_2 the residual mixture was taken up in H_2O (15 cm^3) and extracted with $CHCl_3$ (3 x 25 cm^3). The organic layer was dried (Na_2SO_4), concentrated, and reduced with $NaBH_4$ in ethanol as described above.

Sodiumborohydride reduction of the nitrone derived from *p*- hydroxy benzaldehyde and N-*iso*propylhydroxylamine was unsuccessful. The nitrone remained unreacted and only minor amounts of the product hydroxylamine was obtained. However, catalytic hydrogenation (1atm, PtO_2, ethanol, 3 h, 20°C) afforded the hydroxylamine after silica gel chromatography in 65% yield.

N-Benzyl-N-methylhydroxylamine (108a). Purified by chromatography using 1:1 hexane - ether mixture as eluent. Colourless needles m.p. 40-41°C (ether-hexane) Found: C, 70.6; H, 8.0; N, 10.2. $C_8H_{11}NO$ requires C, 70.05; H, 8.08; N, 10.21); ν_{max} (KBr) 3175, 2850, 1458, 1365, 1192, 1081, 1058, 963, 831, 745 and 703 cm^{-1}; δ_H ($CDCl_3$, +22°C) 2.49 (3 H, s), 3.70 (2 H, s), 7.32 (5 H, s), OH proton signal was not observed; δ_H (-55°C) 2.36 (3 H, s), 3.60 (2 H, AB, J 12.5 Hz), 7.2-7.4 (5 H, m), 9.50 (1 H, broad s).

N-p-Nitrobenzyl-N-methylhydroxylamine (108b). Purified by chromatography using 4:1 hexane - ether mixture as eluent . Pale yellow plates, m.p. 134-136°C (ether-hexane) (Found: C, 52.8; H, 5.5; N, 15.6. $C_8H_{10}N_2O_3$ requires C, 52.75; H, 5.53; N, 15.38%);

ν_{max} (KBr) 3225, 2850, 1514, 1344, 1320, 1109, 1067, 972, 957, 861, 805, and 748 cm^{-1}; δ_H ($CDCl_3$, +22°C) 2.62 (3 H, s), 3.84 (2 H, s), 7.52 (2 H, d, J 10.0 Hz), 8.23 (2 H, d, 10.0 Hz); OH proton signal was not observed; δ_H (-40°C) 2.42 (3 H, s), 3.72 (1 H, d, J 13.0 Hz), 3.84 (1 H, d, J 13.0 Hz), 7.54 (2 H, d, J 10.0 Hz), 8.25 (2 H, d, J 10.0 Hz); 8.60 (1 H, broad s).

*N-p-Chlorobenzyl-N-methylhydroxylamine (**108c**).* Purified by chromatography using 1:1 hexane - ether mixture as eluent. White needles m.p. 88-90°C (ether-hexane) (Found: C, 56.2; H, 5.9; N, 8.2. $C_8H_{10}NOCl$ requires C, 55.98; H, 5.87; N, 8.16%); ν_{max} (KBr) 3237, 3000, 2900, 1490, 1437, 1362, 1195, 1084, 1016, 969, 849 and 796 cm^{-1}; δ_H ($CDCl_3$, +20°C) 2.52 (3 H, s), 3.67 (2 H, s), 7.25 (2 H, d, J 8.0 Hz), 7.34 (2 H, d, J 8.0 Hz), 7.52 (1 H, broad s); δ_H (-50°C) 2.32 (3 H, s), 3.55 (2 H, AB, J 12.3 Hz), 7.18 (2 H, d, J 8.0 Hz), 7.30 (2 H, d, J 8.0 Hz), 8.24 (1 H, s).

*N-p-Methoxybenzyl-N-methylhydroxylamine (**108d**).* Purified by chromatography using 1:1 hexane - ether mixture as eluent. Colourless plates, m.p. 52-54°C (ether-hexane) (Found: C, 64.7; H, 7.9; N, 8.5. $C_9H_{13}NO_2$ requires C, 64.66; H, 7.84; N, 8.38%); ν_{max} (KBr) 3200, 2950, 2825, 1618, 1520, 1463, 1445, 1362, 1280, 1177, 1040, 960, 855, 802, and 748 cm^{-1}; δ_H ($CDCl_3$, +22°C) 2.56 (3 H, s), 3.68 (2 H, s), 3.80 (3 H, s), 6.90 (2 H, d, J 10.0 Hz), 7.27 (2 H, d, 10.0 Hz) ; OH proton signal not observed. δ_H (-40°C) 2.42 (3 H, s), 3.65 (2 H, s), 3.83 (3 H, s), 6.93 (2 H, d, J 10.0 Hz), 7.28 (2 H, d, J 10.0 Hz); 9.33 (1 H, broad s).

*N-p-Methylbenzyl-N-methylhydroxylamine (**108e**).* Purified by chromatography using 9:1 CH_2Cl_2 - methanol mixture as eluent. White crystals m.p. 56-58°C (ether-hexane) (Found: C, 71.6; H, 8.7; N, 9.3. $C_9H_{13}NO$ requires C, 71.49; H, 8.66; N, 9.26%); ν_{max} (KBr) 3225, 2863, 2825, 1517, 1350, 1144, 1067, 960, 852, 793, and 760 cm^{-1}; δ_H

($CDCl_3$, +20°C) 2.30 (3 H, s), 2.60 (3 H, s), 3.70 (2 H, s), 7.15 (2 H, d, J 9.0 Hz), 7.22 (2 H, d, 9.0 Hz), OH proton signal was not observed; δ_H (-50°C) 2.30 (3 H, s), 2.44 (3 H, s), 3.64 (2 H, AB, J 12.2 Hz), 7.20 (4 H, s), 9.18 (1 H, broad s).

N-p-N,N-dimethylbenzyl-N-methylhydroxylamine (108f). Purified by chromatography using 1:1 hexane - ether mixture as eluent. White crystals m.p. 75-77°C (ether-hexane) (Found: C, 66.6; H, 9.1; N, 15.65. $C_{10}H_{16}N_2O$ requires C, 66.64; H, 8.95; N, 15.54); ν_{max} (KBr) 3250, 3000, 2950, 2850, 1619, 1526, 1365, 1237, 1192, 1073, 972, 924, 808, and 733 cm^{-1}; δ_H ($CDCl_3$, +20°C) 2.59 (3 H, s), 2.99 (6 H, s), 3.67 (2 H, s), 6.70 (2 H, d, J 9.0 Hz), 7.18 (2 H, d, J 9.0 Hz), OH proton signal was not observed ; δ_H (-50 °C) 2.45 (3 H, s), 2.90 (6 H, s), 3.55 (1 H, d, J 12.1 Hz), 3.70 (1 H, d, J 12.1 Hz), 6.70 (2 H, d, J 9.0 Hz), 7.19 (2 H, d, J 9.0 Hz), 9.45 (1 H, s).

N-m-Nitrobenzyl-N-methylhydroxylamine (108g). Purified by chromatography using 1:1 hexane - ether mixture as eluent White crystals m.p. 88-90°C (ether-hexane) (Found: C, 52.8; H, 5.5; N, 15.6. $C_8H_{10}N_2O_3$ requires C, 52.75; H, 5.53; N, 15.38%); ν_{max} (KBr) 3150, 2863, 1526, 1347, 1186, 1084, 984, 950, 805, 739, and 694 cm^{-1}; δ_H ($CDCl_3$, +20°C) 2.65 (3 H, s), 3.82 (2 H, s), 5.60 (1 H, broad s), 7.5 (1 H, t, J 8.5 Hz), 7.65 (1 H, d, J 8.0 Hz), 8.14 (1 H, d, J 8.0 Hz), 8.24 (1 H, s); δ_H (-50°C) 2.40 (3 H, s), 3.68 (1 H, d, J 12.5 Hz), 3.80 (1 H, d, J 12.5 Hz), 7.57 (1 H, t, J 8.0 Hz), 7.68 (1 H, d, J 8.0 Hz), 8.21 (1 H, d, J 8.0 Hz), 8.50 (1 H, s), OH proton signal was not observed.

N-o-Hydroxybenzyl-N-methylhydroxylamine (108h). Colourless crystals, m.p. 108-109°C (CH_2Ci_2-hexane) (Found: C, 62.7; H, 7.2; N, 9.1. $C_8H_{11}NO_2$ requires C, 62.72; H, 7.24; N, 9.15); ν_{max} (KBr) 3256, 3060, 2995, 2873, 1598, 1465, 1378, 1357, 1273, 1248, 1109, 959, 812, 758 and 730 cm^{-1}; δ_H ($CDCl_3$, +25°C) 2.72 (3 H, s), 4.01 (2 H,

s), 6.84-7.32 (4 H, m, 2 H, hydroxyl underneath); δ_H (-50°C) 2.72 (3 H, s), 3.94 (1 H, d, J 14.0 Hz), 4.06 (1 H, d, J 14.0 Hz), 6.88-7.37 (4 H, m) , 8.87 (2 H, broad).

N-o-Methoxybenzyl-N-methylhydroxylamine (108i). Purified by chromatography using 1:1 hexane - ether mixture as eluent. White crystals, m.p. 88-90°C (ether-hexane) (Found: C, 64.5; H, 7.7; N, 8.3. $C_9H_{13}NO_2$ requires C, 64.66; H, 7.84; N, 8.38%); ν_{max} (KBr) 3225, 3000, 2850, 1687, 1428, 1329, 1294, 1186, 939, 811, 712 and 670 cm^{-1}; δ_H ($CDCl_3$, +20°C) 2.56 (3 H, s), 3.81 (2 H, s), 3.83 (3 H, s), 6.86-7.41(4 H, m, 1 H, hydroxyl underneath); δ_H (-50°C) 2.33 (3 H, s), 3.54 (1 H, d, J 12.2 Hz), 3.80 (1 H, d, J 12.2 Hz), 3.81 (3 H, s), 6.82-6.98 (2 H, m), 7.22-7.38 (2 H, m), 8.84 (1 H, broad s).

N-Benzyl-N-ethylhydroxylamine (109). Purified by chromatography using 4:1 hexane - ether mixture as eluent . Colourless liquid, (Found: C, 71.3; H, 8.8; N, 9.2. $C_9H_{13}NO$ requires C, 71.49; H, 8.67; N, 9.26%); ν_{max} (neat) 3222, 3026, 2960, 2829, 1496, 1454, 1341, 1090, 1031, 983, 909, 825, 742, and 700 cm^{-1}; δ_H ($CDCl_3$, +20°C) 1.12 (3 H, t, J 7.0 Hz), 2.80 (2 H, q, J 7.0 Hz), 3.84 (2 H, s), 7.45 (5 H, s, 1 H, hydroxyl proton underneath); δ_H (-50°C) 1.10 (3 H, t, J 7.0 Hz), 2.55 (1 H, m), 2.76 (1 H, m), 3.66 (2 H, s), 7.38 (5 H, s); 8.20 (1 H, s); mass spectrum: *m/z* 151 (M^+ 28%).

N-p-Nitrobenzyl-N-isopropylhydroxylamine (110b). Purified by chromatography using 1:1 hexane - ether mixture as eluent .Colourless plates, m.p. 83-85°C (ether-hexane) (Found: C, 57.0; H, 6.9; N, 13.4. $C_{10}H_{14}N_2O_3$ requires C, 57.13; H, 6.71; N, 13.33%); ν_{max} (KBr) 3200, 3069, 2971, 2873, 1069, 1529, 1347, 1174, 1117, 1019, 954, 879, 864, 817, and 745 cm^{-1}; δ_H ($CDCl_3$, +24°C) 1.08 (6 H, d, J 6.0 Hz), 3.02 (1 H, hept, J 6.0 Hz), 3.89 (2 H, s), 4.77 (1 H, s), 7.58 (2 H, d, J 9.0 Hz), 8.24 (2 H, d, J 9.0 Hz); δ_H (-45°C) 1.07 (6 H, d, J 6.0 Hz), 2.81 (1 H, hept, J 6.0 Hz), 3.68 (1 H, d, J

13.0 Hz), 3.92 (1 H, d, J 13.0 Hz), 6.74 (1 H, broad s), 7.56 (2 H, d, J 9.0 Hz), 8.27 (2 H, d, J 9.0 Hz).

*N-p-Chlorobenzyl-N-isopropylhydroxylamine (**110c**).* Purified by chromatography using 1:1 hexane - ether mixture as eluent. White crystals, m.p. 72-74°C (ether-hexane) (Found: C, 60.1; H, 7.2; N, 7.0. $C_{10}H_{14}NOCl$ requires C, 60.15; H, 7.07; N, 7.01%); ν_{max} (KBr) 3212, 2972, 2873, 1493, 1377, 1126, 1094, 1019, 936, 888, 843, 825, and 748 cm^{-1}; δ_H ($CDCl_3$, +22°C) 1.13 (6 H, d, J 6.0 Hz), 2.97 (1 H, hept, J 6.0 Hz), 3.77 (2 H, s), 5.29 (1 H, broad s), 7.35 (4 H, s); δ_H (-40°C) 1.05 (6 H, d, J 6.0 Hz), 2.74 (1 H, hept, J 6.0 Hz), 3.48 (1 H, d, J 13.0 Hz), 3.76 (1 H, d, J 13.0 Hz), 7.29 (2 H, d, J 8.0 Hz), 7.37 (2 H, d, J 6.0 Hz), 7.90 (1 H, broad s).

*N-p-Methoxybenzyl-N-isopropylhydroxylamine (**110d**).* Purified by chromatography using 1:1 hexane - ether mixture as eluent. White crystals m.p. 49-51°C (ether-hexane) (Found: C, 67.6; H, 8.9 ; N, 7.2 $C_{11}H_{17}NO_2$ requires C, 67.66; H, 8.78; N, 7.17%); ν_{max} (KBr) 3212, 2839, 2835, 2829, 1517, 1371, 1255, 1186, 1040, 930, 799, and 754 cm^{-1}; δ_H ($CDCl_3$, +20°C) 1.18 (6 H, d, J 7.0 Hz), 2.98 (1 H, hept, J 7.0 Hz), 3.76 (2 H, s), 3.82 (3 H, s), 5.27 (1 H, s), 6.94 (2 H, d, J 10.0 Hz), 7.36 (2 H, d, 10.0 Hz) ; δ_H (-50°C) 1.08 (3 H, d, J 7.0 Hz), 1.12 (3 H, d, J 7.0 Hz), 2.83 (1 H, hept, J 7.0 Hz), 3.48 (1 H, d, J 13.0 Hz), 3.75 (1 H, d, J 13.0 Hz), 3.82 (3 H, s), 6.93 (2 H, d, J 10.0 Hz), 7.32 (2 H, d, J 10.0 Hz), 8.26 (1 H, broad s).

*N-p-Methylbenzyl-N-isopropylhydroxylamine (**110e**).* Purified by chromatography using 1:1 hexane - ether mixture as eluent. White plates, m.p. 79-81°C (ether-hexane) (Found: C, 73.8; H, 9.7; N, 7.8. $C_{11}H_{17}NO$ requires C, 73.70; H, 9.56; N, 7.81%); ν_{max} (KBr) 3222, 2971, 2002, 1517, 1457, 1362, 1121, 1082, 1028, 933, 882, 843, 817, and 745 cm^{-1}; δ_H ($CDCl_3$, +23°C) 1.16 (6 H, d, J 7.0 Hz), 2.36 (3 H, s), 2.96 (1

H, hept, J 7.0 Hz), 3.78 (2 H, s), 5.29 (1 H, broad s), 7.18 (2 H, d, J 9.0 Hz), 7.30 (2 H, d, J 9.0 Hz); δ_H (-40°C) 1.10 (6 H, d, J 7.0 Hz), 2.34 (3 H, s), 2.82 (1 H, hept, J 7.0 Hz), 3.53 (1 H, d, J 13.0 Hz), 3.77 (1 H, d, J 13.0 Hz), 7.20 (2 H, d, J 9.0 Hz), 7.28 (2 H, d, J 9.0 Hz), 8.23 (1 H, broad s).

*N-p-N,N-dimethylbenzyl-N-isopropylhydroxylamine (**110f**)*. Purified by chromatography using 1:1 hexane - ether mixture as eluent. Yellow crystals, m.p. 66-68°C (ether-hexane) (Found: C, 69.1; H, 9.8; N, 13.6. $C_{12}H_{20}N_2O$ requires C, 69.19; H, 9.68; N, 13.45%); ν_{max} (KBr) 3200, 2971, 2884, 1624, 1606, 1529,1443, 1353, 1129, 1064, 951, 882, 846, 820, and 751 cm^{-1}; δ_H (+24°C) 1.16 (6 H, d, J 6.0 Hz), 2.97 (6 H, s, and 1 H, hept, J 6.0 Hz underneath), 3.74 (2 H, s), 5.98 (1 H, broad s), 6.77 (2 H, d, J 8.0 Hz), 7.27 (2 H, d, J 8.0 Hz); δ_H (-50°C) 1.10 (3 H, d, J 6.0 Hz), 1.14 (3 H, d, J 6.0 Hz), 2.84 (1 H, hept, J 6.0 Hz), 2.93 (6 H, s), 3.58 (1 H, d, J 12.3 Hz), 3.66 (1 H, d, J 12.3 Hz), 6.75 (2 H, d, J 9.0 Hz), 7.28 (2 H, d, J 9.0 Hz), 8.58 (1 H, broad s).

*N-m-Nitrobenzyl-N-isopropylhydroxylamine (**110g**)*. Purified by chromatography using 9:1 hexane - ether mixture as eluent. Pale yellow crystals m.p. 79-81°C (ether-hexane) (Found: C, 57.2; H, 6.8; N, 13.2. $C_{10}H_{14}N_2O_3$ requires C, 57.13; H, 6.71; N, 13.33%); ν_{max} (KBr) 3212, 2961, 2917, 1586, 1532, 1371, 1347, 1231, 1177, 1085, 1031, 954, 817, and 796 cm^{-1}; δ_H ($CDCl_3$, +23°C) 1.17 (6 H, d, J 6.0 Hz), 3.02 (1 H, hept, J 6.0 Hz), 3.87 (2 H, s), 4.80 (1 H, broad s), 7.46-8.38 (4 H, m); δ_H (-40°C) 1.07 (6 H, d, J 6.0 Hz), 2.80 (1 H, hept, J 6.0 Hz), 3.66 (1 H, d, J 13.0 Hz), 3.88 (1 H, d, J 13.0 Hz), 6.77 (1 H, broad s), 7.48-8.34 (4 H, m).

*N-m-Bromobenzyl-N-isopropylhydroxylamine (**110h**)*. Purified by chromatography using 1:1 hexane - ether mixture as eluent .White crystals, m.p. 78-80°C (ether- hexane) (Found: C, 49.1 ; H, 5.9 ; N, 5.7. $C_{10}H_{14}NOBr$ requires C, 49.20 ; H, 5.78 ; N, 5.74

%); ν_{max} (KBr) 3189, 2971, 2895, 1576, 1478, 1427, 1368, 1177, 1129, 1073, 992, 957, 939, 894, 859,775, 697, and 673 cm^{-1}; δ_H ($CDCl_3$, +23°C) 1.15 (6 H, d, J 7.0 Hz), 2.95 (1 H, hept, J 7.0 Hz), 3.73 (2 H, s), 5.08 (1 H, broad s), 7.13- 7.59 (4 H, m); δ_H (-35°C) 1.07 (6 H, d, J 7.0 Hz), 2.75 (1 H, hept, J 7.0 Hz), 3.47 (1 H, d, J 13.0 Hz), 3.74 (1 H, d, J 13.0 Hz), 7.20- 7.60 (4 H, m), hydroxyl proton signal was not observed.

N-p-Bromobenzyl-N-isopropylhydroxylamine (110i). Purified by chromatography using 1:1 hexane - ether mixture as eluent. White crystals, m.p. 76-78°C (ether-hexane) (Found: C, 49.3; H, 5.8; N, 5.8. $C_{10}H_{14}NOBr$ requires C, 49.20; H, 5.78; N, 5.74 %); ν_{max} (KBr) 3233, 2960, 2906, 1490, 1368, 1174, 1073, 1016, 957, 807, and 784 cm^{-1}; δ_H ($CDCl_3$, +24°C) 1.11 (6 H, d, J 6.0 Hz), 2.00 (1 H, s), 2.95 (1 H, hept, J 6.0 Hz), 3.94 (2 H, s), 7.26 (2 H, d, J 10.0 Hz), 7.48 (2 H, d, J 10.0 Hz); δ_H (-50°C) 1.04 (6 H, d, J 6.0 Hz), 2.71 (1 H, hept, J 6.0 Hz), 3.44 (1 H, d, J 13.0 Hz), 3.73 (1 H, d, J 13.0 Hz), 7.23 (2 H, d, J 10.0 Hz), 7.50 (2 H, d, J 10.0 Hz), 8.07 (1 H, s).

N-2,4,5-trimethoxybenzyl-N-isopropylhydroxylamine (110j). Purified by chromatography using 2:1 hexane - ether mixture as eluent . White crystals m.p. 87-89°C (ether-hexane) (Found: C, 61.0; H, 8.3; N, 5.5. $C_{13}H_{21}NO_4$ requires C, 61.16; H, 8.29; N, 5.49%); ν_{max} (KBr) 3222, 2961, 2851, 1612, 1526, 1469, 1407, 1308, 1216, 1180, 1040, 981, 885, 861, 817, and 754 cm^{-1}; δ_H ($CDCl_3$, +22°C) 1.10 (6 H, d, J 6.0 Hz), 2.83 (6 H, s), 3.76 (2 H, s), 3.80 (3 H, s), 3.85 (3 H, s), 3.89 (3 H, s), 5.89 (1 H, s), 6.58 (1 H, s), 6.99 (1 H, s); δ_H (-40°C) 0.93 (6 H, broad, app. t), 2.38 (1 H, hept, J 7.0 Hz), 3.32 (1 H, d, J 14.0 Hz), 3.83 (3 H, s), 3.89 (3 H, s), 3.96 (3 H, s, and 1 H underneath), 6.57 (1 H, s), 6.93 (1 H, s), 8.16 (1 H, broad s).

*N-p-hydroxybenzyl-N-isopropylhydroxylamine (**110k**)*. White crystals, m.p. 147-148.5°C (ether) (Found: C, 66.4; H, 8.3; N, 7.7. $C_{10}H_{15}NO_2$ requires C, 66.27; H, 8.34; N, 7.73); ν_{max} (KBr) 3305, 2969,1615, 1519, 1270, 1226, 1169 and 791 cm^{-1}. δ_H ($CDCl_3$, +23°C) 1.17 (6 H, d, J 14.0 Hz), 3.0 (1 H, m), 3.75 (2 H, s), 6.84 (2 H, d, J 8.0 Hz), 7.29 (2 H, d, J 8.0 Hz), hydroxyl proton signal not observed; δ_H (-30°C) 1.15 (6 H, broad), 3.0 (1 H, m), 3.54 (1 H, d, J 11.5 Hz), 3.86 (1 H, d, J 11.5 Hz), 6.0 (2 H, broad), 6.94 (2 H, d, J 8.0 Hz), 7.15 (2 H, d, J 8.0 Hz).

*N-o-hydroxybenzyl-N-isopropylhydroxylamine (**110l**)*. Colourless crystals, m.p. 140 -142°C (CH_2Cl_2-ether) (Found: C, 66.5; H, 8.4; N, 7.5. $C_{10}H_{15}NO_2$ requires C, 66.27; H, 8.34; N, 7.73); ν_{max} (KBr) 3238, 2957, 2864, 1598, 1462, 1374, 1277, 1174, 1106, 987, 859, 752 and 726 cm^{-1}; δ_H ($CDCl_3$, +25°C) 1.2 (6 H, d, J 12.0 Hz), 1.95 (1 H, s), 3.15 (1 H, m), 4.05 (2 H, s), 6.70-7.35 (4 H, m), hydroxyl protons signal not observed; δ_H (-40°C) 1.24 (6 H, q, J 8.0 Hz), 2.12 (1 H, s), 3.17 (1 H, m), 4.02 (1 H, d, J 14.0 Hz), 4.23 (1 H, d, J 14.0 Hz), 6.82-7.38 (4 H, m), 7.48 (1 H, s).

*N-o-methoxybenzyl-N-isopropylhydroxylamine (**110m**)*. Colourless crystals, m.p. 79 - 81°C (ether-hexane) (Found: C, 68.8 ; H, 8.9; N, 7.3. $C_{11}H_{17}NO_2$ requires C, 67.66 ; H, 8.78; N, 7.18) ν_{max} (KBr) 3219, 2967, 2892, 2827, 1604, 1497, 1464, 1438, 1428, 1363, 1249, 1118, 1033, 751 and 724 cm^{-1}; δ_H ($CDCl_3$, +17.6°C) 1.13 (6 H, d, J 6.0 Hz), 2.88 (1 H, m), 3.84 (2 H, s), 3.87 (3 H, s), 6.02 (1 H, s), 6.9-7.48 (4 H, m); δ_H (-49°C) 0.97 (6 H, t, J 6.0 Hz), 2.48 (1 H, m), 3.37 (1 H, d J 14.0 Hz), 3.86 (3 H, s), 4.01 (1 H, d, J 14 .0 Hz), 6.9-7.44 (4 H, m), 8.45 (1 H, s).

*N-Benzyl-N-^{t}butylhydroxylamine (**111a**)*. Purified by chromatography using 4:1 hexane - ether mixture as eluent. White crystals m.p. 59-61°C (ether-hexane) (Found: C, 73.5; H, 9.8; N, 7.7. $C_{11}H_{17}NO$ requires C, 73.70; H, 9.98; N, 7.81%); ν_{max} (KBr) 3400, 2975,

2925, 1362, 1207, 1055, 910, 894, 820, 727, and 697 cm^{-1}; δ_H (+20°C); 1.24 (9 H, s), 3.84 (2 H, s), 7.32-7.52 (5 H, m); δ_H (-50°C) 1.21 (9 H, s), 3.60 (1 H, d, J 13.0 Hz), 4.02 (1 H, d, J 13.0 Hz), 4.75 (1 H, s), 7.40 (5 H, m).

N-o-Hydroxybenzyl-N-^{t}butylhydroxylamine (111b). Colourless crystals, m.p. 101-103°C (ether) (Found: C, 68.84; H, 8.88; N, 7.35. $C_{11}H_{17}NO_2$ requires C, 67.66; H, 8.78; N, 7.18); ν_{max} (KBr) 3349, 2985, 2967,1592, 1494,1481,1403,1387,1361, 1252, 1211, 918, 761, and 750 cm^{-1} ; δ_H ($CDCl_3$, +24.2°C) 1.26 (9 H, s), 2.54 (1 H, s), 4.1(2 H, broad), 6.72-7.32 (4 H, m), hydroxyl proton signal not observed ; δ_H (-39°C) 1.3 (9 H, s), 2.63 (1 H, s), 3.85 (1 H, d J 15.0 Hz), 4.42 (1 H, d, J 15.0 Hz), 6.5-7.36 (4 H, m), 10.5 (1 H, broad).

4.2.2 The Acetyl Derivatives

Acetic anhydride (2.4 mmol) was added to a solution of the *N*-hydroxylamine (2.0 mmol) in CH_2Cl_2 (3 cm^3) at 0°C and the mixture stirred at 0°C for 1 h. TLC (ether-hexane) was taken to ensure the completion of the reaction. The reaction mixture was taken up in 5% $NaHCO_3$ solution (10 cm^3) and extracted with CH_2Cl_2 (3 x 20 cm^3). The organic layer was dried (Na_2SO_4), filtered and the solvent was removed by a gentle stream of N_2 at 10°C to give the acetate which was further purified by crystallization. However the acetate was purified by passing through a short column of silica using ether-hexane as the eluant to give the acetate as colourless liquid.

The acetate solution should not be warmed since heating leads to decomposition. These samples were kept in the freezer to eliminate any decomposition.

O-Acetyl-N-o-hydroxybenzyl-N-methylhydroxylamine (115). Colourless Plates, m.p. 73-74°C (ether-hexane) (Found: C, 62.6; H, 6.8; N, 7.2. $C_{10}H_{13}NO_3$ requires C, 61.52; H, 6.71; N, 7.18); ν_{max} (KBr) 3302, 3060, 2883, 1742, 1585, 1491, 1371, 1243, 1197,

1081, 903 and 758 cm^{-1}; δ_H ($CDCl_3$, +23°C) 2.1 (3 H, s), 2.74 (3 H, s), 4.08 (2 H, broad), 6.80-7.38 (4 H, m), 9.01(1 H, s); δ_H (-29°C) 2.14 (3 H, s), 2.74 (3 H, s), 3.76 (1 H, d, J 12.0 Hz), 4.42 (1 H, d, J 12.0 Hz), 6.82-7.4 (4 H, m), 9.2 (1 H, s).

*O-Acetyl-N-p-nitrobenzyl-N-isopropylhydroxylamine (**116b**)*. Purified by chromatography using 9:1 hexane - ether mixture as eluent. White crystal m.p. 40.5-42°C (ether-hexane) (Found: C, 57.2; H, 6.4; N, 11.2. $C_{12}H_{16}N_2O_4$ requires C, 57.13; H, 6.39; N, 11.10%); ν_{max} (KBr) 3075, 2975, 1771, 1612, 1526, 1350, 1201, 1118, 1001, 957, 903, 864, 819, and 754 cm^{-1}; δ_H ($CDCl_3$, +23°C) 1.22 (6 H, d, J 7.0 Hz), 1.85 (3 H, s), 3.28 (1 H, hept, J 7.0 Hz), 4.12 (2 H, s), 7.64 (2 H, d, J 10.0 Hz), 8.24 (2 H, d, J 10.0 Hz); δ_H (-40°C) 1.27 (6 H, d, J 7.0 Hz), 1.78 (3 H, s), 3.33 (1 H, hept, J 7.0 Hz), 4.09 (1 H, broad), 4.23 (1 H, broad), 7.67 (2 H, d, J 10.0 Hz), 8.30 (2 H, d, J 10.0 Hz).

*O-Acetyl-N-p-chlorobenzyl-N-isopropylhydroxylamine (**116c**)*. Purified by chromatography using 1:1 hexane - ether mixture as eluent. Colourless liquid. (Found: C, 59.5; H, 6.7; N, 5.8. $C_{12}H_{16}NO_2Cl$ requires C, 59.63; H, 6.67; N, 5.8%); ν_{max} (neat) 2972, 1765, 1493, 1385, 1368, 1210, 1091, 1016, 1001, 906, 804, and 736 cm^{-1}; δ_H ($CDCl_3$, +24 °C) 1.20 (6 H, d, J 6.0 Hz), 1.84 (3 H, s), 3.21 (1 H, hept, J 6.0 Hz), 3.97 (2 H, s), 7.35 (4 H, AB, J 9.0 Hz); δ_H (-50°C) 1.21 (3 H, d, J 7.0 Hz), 1.26 (3 H, d, J 7.0 Hz), 1.90 (3 H, s), 3.24 (1 H, m), 3.85 (1 H, d, J 13.0 Hz), 4.13 (1 H, d, J 13.0 Hz), 7.36 (4 H, s).

*O-Acetyl-N-p-methoxybenzyl-N-isopropylhydroxylamine (**116d**)*. Purified by chromatography using 1:1 hexane - ether mixture as eluent. Colourless liquid. (Found: C, 65.6; H, 8.1; N, 5.9. $C_{13}H_{19}NO_3$ requires C, 65.80; H, 8.07; N, 5.9%); ν_{max} (neat) 2972, 2829, 1762, 1615, 1517, 1368, 1262, 1207, 1177, 1034, 1001, 909, 825, and 808 cm^{-1}; δ_H ($CDCl_3$, +18°C) 1.22 (6 H, d, J 6.0 Hz), 1.88 (3 H, s), 3.22 (1 H, hept, J 6.0 Hz), 3.83

(3 H, s), 3.98 (2 H, s), 6.92 (2 H, d, J 10.0 Hz), 7.36 (2 H, d, 10.0 Hz) ; δ_H (-50 °C) 1.17 (3 H, d, J 7.0 Hz), 1.23 (3 H, d, J 7.0 Hz), 1.89 (3 H, s), 3.18 (1 H, hept, J 7.0 Hz), 3.79 (1 H, d, J 12.5 Hz), 3.82 (3 H, s), 4.08 (1 H, d, J 12.5 Hz), 6.90 (2 H, d, J 10.0 Hz), 7.34 (2 H, d, J 10.0 Hz); mass spectrum: m/z 237 (M+ 2%).

O-Acetyl-N-p-methylbenzyl-N-isopropylhydroxylamine (116e). Colourless liquid, (Found: C, 70.4; H, 8.4; N, 6.4. $C_{13}H_{19}NO_2$ requires C, 70.56; H, 8.65; N, 6.33%); ν_{max} (neat) 2971, 1764, 1526, 1368, 1210, 998, 909, and 798 cm^{-1}; δ_H ($CDCl_3$, +23°C) 1.27 (6 H, d, J 6.0 Hz), 1.73 (3 H, s), 2.43 (3 H, s), 3.28 (1 H, hept, J 6.0 Hz), 4.07 (2 H, s), 7.26 (2 H, d, J 9.0 Hz), 7.40 (2 H, d, J 9.0 Hz); δ_H (-45°C) 1.21 (3 H, d, J 6.0 Hz), 1.27 (3 H, d, J 6.0 Hz), 1.90 (3 H, s), 2.36 (3 H, s), 3.24 (1 H, hept, J 6.0 Hz), 3.88 (1 H, d, J 13.0 Hz), 4.16 (1 H, d, J 13.0 Hz), 7.21 (2 H, d, J 9.0 Hz), 7.33 (2 H, d, J 9.0 Hz).

O-Acetyl-N-p-N,N-dimethylbenzyl-N-isopropylhydroxylamine (116f). Purified by chromatography using 1:1 hexane - ether mixture as eluent. Colourless liquid, (Found: C, 67.0; H, 8.7; N, 11.2. $C_{14}H_{22}N_2O_2$ requires C, 67.17; H, 8.86; N, 11.19%); ν_{max} (neat) 2949, 2775, 1761, 1618, 1526, 1365, 1213, 1165, 1126, 998, 948, 903, and 811 cm^{-1}; δ_H ($CDCl_3$, +24°C) 1.17 (6 H, d, J 6.0 Hz), 1.87 (3 H, s), 2.94 (6 H, s), 3.15 (1 H, hept, J 6.0 Hz), 3.92 (2 H, s), 6.70 (2 H, d, J 10.0 Hz), 7.24 (2 H, d, J 10.0 Hz); δ_H (-40°C) 1.18 (3 H, d, J 7.0 Hz), 2.03 (3 H, d, J 7.0 Hz), 1.91 (3 H, s), 2.95 (6 H, s), 3.19 (1 H, hept, J 7.0 Hz), 3.83 (1 H, d, J 13.0 Hz), 4.09 (1 H, d, J 13.0 Hz), 6.73 (2 H, d, J 10.0 Hz), 7.27 (2 H, d, J 10.0 Hz).

O-Acetyl-N-m-nitrobenzyl-N-isopropylhydroxylamine (116g). Purified by chromatography using 9:1 hexane - ether mixture as eluent . Colourless liquid, (Found: C, 57.0; H, 6.4; N, 11.1. $C_{12}H_{16}N_2O_4$ requires C, 57.13; H, 6.39; N, 11.10%); ν_{max} (neat) 2977,

1764, 1532, 1353, 1204, 1094, 998, 897, 810 and 736 cm^{-1}; δ_H ($CDCl_3$, +20°C) 1.23 (6 H, d, J 6.0 Hz), 1.86 (3 H, s), 2.99 (1 H, hept, J 6.0 Hz), 4.10 (2 H, s), 7.47-8.35 (4 H, m) ; δ_H (-50°C) 1.27 (6 H, broad), 1.92 (3 H, s), 3.33 (1 H, hept, J 7.0 Hz), 4.01 (1 H, d, J 13.0 Hz), 4.26 (1 H, d, J 13.0 Hz), 7.55-8.39 (4 H, m); mass spectrum: *m/z* 252 (M^+ 5%)

*O-Acetyl-N-m- bromobenzyl - N- isopropylhydroxylamine (**116h**)*. Purified by chromatography using 1:1 hexane - ether mixture as eluent . Colourless liquid, (Found: C, 50.2; H, 5.6; N, 4.9. $C_{12}H_{16}NO_2Br$ requires C, 50.37; H, 5.64; N, 4.89 %); ν_{max} (neat) 2972, 2862, 1765, 1571, 1472, 1371, 1204, 1070, 998, 906, and 778 cm^{-1}; δ_H ($CDCl_3$, +24°C) 1.22 (6 H, d, J 7.0 Hz), 1.90 (3 H, s), 3.24 (1 H, hept, J 7.0 Hz), 3.98 (2 H, s), 7.17-7.65 (4 H, m); δ_H (-50°C) 1.24 (6 H, t, J 7.0 Hz), 1.94 (3 H, s), 3.24 (1H, hept, J 7.0 Hz), 3.85 (1 H, d, J 13.0 Hz), 4.13 (1 H, d, J 13.0 Hz), 7.24-7.64 (4 H, m).

*O-Acetyl-N-p-bromobenzyl-N-isopropylhydroxylamine (**116i**)*. Purified by chromatography using 1:1 hexane - ether mixture as eluent. Colourless crystals, m.p. 34-36°C (ether-hexane) (Found: C, 50.2; H, 5.6; N, 4.9. $C_{12}H_{16}NO_2Br$ requires C, 50.37; H, 5.64; N, 4.89%); ν_{max} (KBr) 3000, 1765, 1490, 1368, 1210, 1174, 1070, 1013, 906, and 799 cm^{-1}; δ_H ($CDCl_3$, +24°C) 1.20 (6 H, d, J 7.0 Hz), 1.84 (3 H, s), 3.21 (1 H, hept, J 7.0 Hz), 3.95 (2 H, s), 7.31 (2 H, d, J 10.0 Hz), 7.49 (2 H, d, J 10.0 Hz); δ_H (-40°C) 1.22 (6 H, broad s), 1.88 (3 H, s), 3.23 (1 H, hept, J 7.0 Hz), 3.84 (1 H, d, J 13.0 Hz), 4.12 (1 H, d, J 13.0 Hz), 7.32 (2 H, d, J 10.0 Hz), 7.51 (2 H, d, J 10.0 Hz).

*O-Acetyl-N-2,4,5-trimethoxybenzyl-N-isopropylhydroxylamine (**116j**)*. Purified by chromatography using 1.5:1 hexane - ether mixture as eluent .White crystals, m.p 39-41°C (ether-hexane) (Found: C, 60.4; H, 7.8; N, 4.7. $C_{15}H_{23}NO_5$ requires C, 60.59; H, 7.80; N, 4.71%); ν_{max} (KBr) 2975, 2925, 2825, 1768, 1615, 1517, 1466, 1434, 1311, 1257,

1216, 1129, 1046, 989, 903, 861, 837, 810 and 751 cm^{-1}; δ_H ($CDCl_3$, +23°C) 1.21 (6 H, d, J 6.0 Hz), 1.88 (3 H, s), 3.22 (1 H, hept, J 6.0 Hz), 3.84 (3 H, s), 3.86 (3 H, s), 3.91 (3 H, s), 4.03 (2 H, s), 6.57 (1 H, s), 7.26 (1 H, s); δ_H (-53°C) 1.26 (6 H, t, J 7.0 Hz), 1.96 (3 H, s), 3.24 (1 H, hept, J 7.0 Hz), 3.89 (3 H, s, 1 H underneath), 3.92 (3 H, s), 3.97 (3 H, s), 4.02 (1 H, d, J 14.0 Hz), 6.60 (1 H, s), 7.01 (1 H, s).

*O-Acetyl-N-p-hydroxybenzyl-N-isopropylhydroxylamine (**116k**)*. Colourless crystals, m.p. 92-93°C (ether-hexane) (Found: C, 65.5; H, 7.7; N, 6.3. $C_{12}H_{17}NO_3$ requires C, 64.55; H, 7.68; N, 6.27); ν_{max} (KBr) 3346, 2956, 2942, 2895, 1752, 1614, 1519, 1366, 1248, 1232, 1177 and 811 cm^{-1}; δ_H ($CDCl_3$, +22°C) 1.21 (6 H, d, J 8.0 Hz), 1.87 (3 H, s), 3.22 (1 H, m), 3.96 (2 H, s), 6.79 (2 H, d, J 8.0 Hz), 7.28 (2 H, d, J 8.0 Hz), hydroxyl proton signal not observed; δ_H (-39°C) 1.24 (6 H, t, J 4.0 Hz), 1.94 (3 H, s), 3.29 (1 H, m), 3.84 (1 H, d, J 12.0 Hz), 4.11 (1 H, d, J 12.0 Hz), 6.77 (2 H, d, J 8.0 Hz), 7.27 (2 H, d, J 8.0 Hz), hydroxyl proton signal not observed.

*O-Acetyl-N-o-hydroxybenzyl-N-isopropylhydroxylamine (**116l**)*. Colourless plates, m.p. 53.0-54.0°C (ether-hexane) (Found: C, 65.6; H, 7.8; N, 6.2. $C_{12}H_{17}NO_3$ requires C, 64.55; H, 7.67; N, 6.28); ν_{max} (KBr) 3275, 3069, 2976, 2939, 2883, 1749, 1487, 1370, 1247, 1207, 999 and 763 cm^{-1}; δ_H ($CDCl_3$, +27°C) 1.12 (6 H, d, J 8.0 Hz), 2.07 (3 H, s), 3.13 (1 H, m), 4.16 (2 H, s), 6.79-7.33 (4 H, m), 9.33 (1 H, s); δ_H (-20°C) 1.11(6 H, q, J 8.0 Hz), 2.12 (3 H, s), 3.12 (1 H, m), 4.12 (1 H, d, J 14.0 Hz), 4.2 (1 H, d, J 14.0 Hz), 6.82-7.35 (4 H, m), 9.54 (1 H, s).

*O-Acetyl-N-o-methoxybenzyl-N-isopropylhydroxylamine (**116m**)*. Colourless liquid, $C_{13}H_{19}NO_3$ requires C, 65.80 ; H, 8.07; N, 5.90 ν_{max} (neat) 2976, 2939,1760, 1495, 1465, 1365, 1248, 1211 and 756 cm^{-1}; δ_H ($CDCl_3$,+18°C) 1.22 (6 H, d, J 6.0 Hz), 1.86 (3 H, s), 3.26 (1 H, m), 3.84 (3 H, s), 4.1 (2 H, s), 6.96-7.50 (4 H, m); δ_H (-49°C)

1.28 (6 H, t, J 8.0 Hz), 1.98 (3 H, s), 3.30 (1 H, m), 3.90 (3 H, s,), 3.98 (1 H, d, J 13.0 Hz), 4.34 (1 H, d, J 13.0 Hz), 6.94-7.48 (4 H, m).

O-Acetyl-N-o-hydroxybenzyl-N-^{t}butylhydroxylamine (117). White crystals, m.p. 87.5-89.5°C (decomp) (Found: C, 66.8 ; H, 8.2; N, 5.8. $C_{13}H_{19}NO_3$ requires C, 65.80; H, 8.07; N, 5.90); ν_{max} (KBr) 3342, 2974, 2930, 1737, 1604, 1505, 1456, 1370, 1327, 1264, 1249, 1225, 1207, 1179, 1105, 756 and 732 cm^{-1}; δ_H ($CDCl_3$, +24°C) 1.25 (9 H, s), 1.92 (3 H, s), 4.17 (2 H, broad), 6.75-7.41(4 H, m), 9.24 (1 H, s).

4.2.3 The Isoxazolidines *(123 and 124a)*

A mixture of the hydroxylamine **100** (10.0 mmol), paraformaldehyde (15 mmol) and ethyl vinyl ether (5 cm^3) in ethanol (5 cm^3) was heated in a closed vessel at 70°C for 2 h. The reaction mixture was taken up in H_2O (20 cm^3) and extracted with ether (2x20 cm^3). The organic layer was dried (Na_2SO_4) and concentrated by passing a gentle stream of nitrogen at 20°C. The residual liquid was purified by chromatography using ether as the eluent to give the isoxazolidines **123** as colourless liquid. In the preparation of the adduct (**123a**) N-methylhydroxylamine hydrochloride instead of the free base was used. One equivalent of KOH was added to the reaction mixture to liberate the free base. Care must be taken to isolate the isoxazolidines (**123a, b, c**) since these are found to be volatile.

2-Methyl-5-ethoxyisoxazolidine (123a). (55%); ν_{max} (neat) 3010, 2943, 2908, 1450, 1435, 1364, 1335, 1297, 1142, 1095, 995, and 926 cm^{-1}; δ_H ($CDCl_3$, -30°C) 1.25 (3 H, a major and minor overlapping triplets, J 7.0 Hz), 2.18 -3.10 (3 H, m), 2.76 (0.76 x 3 H, s), 2.90 (0.24 x 3 H, s), 3.44 (2 H, m) 3.90 (1 H, m), 5.20 (1 H, apparent dd, J 2.5, 6.0 Hz); δ_H (+50°C) displayed the signals of N-methyl at d 2.74 (s), OCH_2 at 3.47 (1 H, dq, J 7.0, 10.0 Hz) and 3.81 (1 H, dq, J 7.0, 10.0 Hz), C(5) H at 5.16 (1 H, d, J 5.0 Hz). In solvents CCl_4, pyridine-d_5, CD_3OD and CD_3CN at -30°C the N-methyl protons of the

major isomer appeared at δ 2.72, 2.83, 2.83, and 2.78 and the minor isomer at 2.55, 2.62, 2.66 and 2.60, respectively. The C(5) H appeared as a multiplet except in CD_3CN at δ5.12 (1 H, dd, J 2.5, 6.0 Hz). The C(5)H of the major and minor isomer apparently have same chemical shift values in all the solvents studied. *m/z* 131 (M^+ 5.4%)

*2-Isopropyl-5-ethoxyisoxazolidine (**123b**).* (61%); ν_{max} (neat) 3012, 2937, 2905, 1471, 1445, 1371, 1342, 1300, 1096, 1030, and 995 cm^{-1}; δ_H ($CDCl_3$, -30°C) 1.07 , 1.12 (3 H, two overlapping d, the minor appearing upfield, J 7.0 Hz); 1.26 (6 H, m), 2.12 - 3.06 (4 H, m), 3.28 -3.58 (2 H, m), 3.86 (1 H, m), 5.12 (1 H, m); In solvents pyridine-d_5, CD_3OD, and CD_3CN at -30°C the signal of one of the diastereotopic methyl of the *iso* propyl group appeared upfield for the minor isomer and downfield for the major isomer. The C(5) signal in pyridine and CD_3OD appeared as a multiplet and in CD_3CN as a dd (J 2.5, 6.5 Hz). The C(5)H of the major and minor isomer apparently have same chemical shift values in all the solvents studied. *m/z* 131 (M^+ 7.5%).

*2-tert-Butyl-5-ethoxyisoxazolidine (**123c**).* (65%); ν_{max} (neat) 3005, 2927, 2895, 1472, 1437, 1358, 1337, 1228, 1198, 1100, 1036, 1012, and 988 cm^{-1}; δ_H ($CDCl_3$, -30°C) 1.14 (9 H, s), 1.27 (3 H, t, J 7.0 Hz), 2.17 - 3.21 (4 H, m), 3.45 (2 H, m), 5.09 (0.42 x 1 H, d, J 4.5 Hz), and 5.15 (0.58 x 1 H, dd, J 2.3, 6.0 Hz). Spectrum at +50°C displayed the signals of OCH_2 at δ 3.50 (1 H, dq, J 7.0, 10.0 Hz) , 3.80 (1 H, dq, J 7.0, 10.0 Hz), and C(5) H at δ 5.11 (1 H, d, J 5.5 Hz). In solvents pyridine-d_5, CD_3OD and CD_3CN at -30°C the C(5)H of the major isomer appeared at d 5.04 (dd, J 3.0, 5.5 Hz), 5.18 (dd, J 2.0, 6.0 Hz), 5.05 (dd, J 2.5, 6.5 Hz), and for the minor isomer at 4.96 (d, J 4.5 Hz), 5.09 (d, J 4.0 Hz), and 4.98 (d, J 4.5 Hz), respectively.

*2-Phenyl-5-ethoxyisoxazolidine (**123d**).* (83%); (Found: C, 68.3; H, 7.7; N, 7.15. $C_{11}H_{15}NO_2$ requires C, 68.37; H, 7.82; N, 7.25%); ν_{max} (neat) 3010, 2935, 2900,

1601, 1488, 1449, 1438, 1366, 1337, 1280, 1184, 1090, 1017, 975, 732 and 671 cm^{-1}; δ_H ($CDCl_3$, 20°C) 1.18 (3 H, t, J 6.0 Hz), 2.36 (2 H , m), 3.37 (1 H, dt, J 5.5, 9.0 Hz), 3.56 (1 H, dq, J 7.0, 10.0 Hz), 3.68 (1 H, apparent q, J 7.5 Hz), 3.87 (1 H, dq, J 7.0, 10.0 Hz), 5.35 (1 H, dd, J 1.5, 5.5 Hz), and 6.90-7.40 (5 H, m). Identical spectrum at -30°C.

2-Benzyl-5-ethoxyisoxazolidine (124a). (93%); (Found: C, 69.4; H, 8.3; N, 6.6. $C_{12}H_{17}NO_2$ requires C, 69.53; H, 8.27; N, 6.76%); ν_{max} (neat) 3037, 2985, 2910, 2877, 1494, 1453, 1370, 1342, 1305, 1102, 1077, 1028, 982, 728, and 695 cm^{-1}; δ_H ($CDCl_3$, -30°C) 1.22, 1.27 (3 H, overlapping t, J 7.0 Hz, minor triplet appeared downfield), 2.08 - 2.72 (3 H, m), 2.98 - 3.60 (2 H, m), 3.85 (1 H, m), 3.98 (0.53 x 1 H, d, J 12.0 Hz), 4.05 (0.47 x 1 H, d, J 12.0 Hz), 4.12 (0.53 x 1 H, d, J 12.0 Hz), 4.31 (0.47 x1 H, d, J 12.0 Hz), 5.24 (1 H, m), and 7.42 (5 H, m). Spectrum at +50°C displayed the signals of OCH_2 at δ 3.48 (1 H, dq, J 7.0, 10.0 Hz) , 3.79 (1 H, dq, J 7.0, 10.0 Hz), and C(5) H at d 5.20 (1 H, dd, J 2.0, 5.5 Hz). In solvents CD_3OD and CD_3CN at -30°C the C(5)H appeared as multiplets and in pyridine-d_5 as a dd at δ 5.14 (J 2.5, 5.0 Hz). In all the solvents the minor triplets at δ~1.2 and a minor doublet at ~4.3 appeared downfield relative to the respective signals for the major isomer. *m/z* 207 (M^+ 15.5%).

4.2.4 The Isoxazolidines *(124b-124i)*

To a solution of the hydroxylamine (3.0 mmol) in CH_2Cl_2 (10 cm^3) at 0°C yellow HgO (2.60 g, 12 mmol) was added . The reaction mixture was stirred at 0°C until the formation of the nitrone and the disappearance of the hydroxylamine was complete (~1 h); as indicated by TLC experiment (silica, ether). After passing through a bed of $MgSO_4$ and washing the bed with CH_2Cl_2 the resultant nitrone solution was concentrated to ~10 cm^3 and ethyl vinyl ether was added to it. After stirring the mixture at 30°C for 48 h, the

solvent and excess alkane were removed and the residual mixture was chromatographed over silica gel using appropriate eluent as detailed below.

2-(p-Nitrobenzyl)-5-ethoxyisoxazolidine (**124b**). Purified by chromatography using 4:1 hexane - ether mixture as eluent. Colourless liquid (18% yield); (Found: C, 57.1; H, 6.3; N, 11.1. $C_{12}H_{16}N_2O_4$ requires C, 57.13; H, 6.39; N, 11.10%); ν_{max} (neat) 2971, 2906, 1520, 1350, 1106, 1101, 935, and 745 cm^{-1}; δ_H ($CDCl_3$, -30°C) 1.25 (0.60 x 3 H, t, J 7.0 Hz), 1.29 (0.40 x 3 H, t, J 7.0 Hz), 2.22-2.80 (2.60 x 1 H, m), 3.18-3.32 (0.40 x 1 H, m), 3.34-3.60 (2 H, m), 3.77 (1 H, dq, J 7.0 Hz, J 10.0 Hz), 4.05 (0.60 x 1 H, d, J 15.0 Hz), 4.17 (0.40 x 1 H, d, J 14.0 Hz), 4.25 (0.60 x 1 H, d, J 15.0 Hz), 4.41 (0.40 x 1 H, d, J 14.0 Hz), 5.28 (1 H, broad m), 7.69 (2 H, two overlapping doublets, J 9.0 Hz), 8.33 (2 H, two overlapping doublets, J 9.0 Hz); δ_H (+50°C) 1.22 (3 H, t, J 7.0 Hz), 2.44 (2 H, m), 3.0 (1 H, m), 3.27 (1 H, m), 3.50 (1 H, dq, J 7.0 Hz, J 10.0 Hz), 3.73 (1 H, dq, J 7.0 Hz, J 10.0 Hz), 4.07 (1 H, d, J 14.0 Hz), 4.27 (1 H, d, J 14.0 Hz), 5.24 (1 H, dd, J 2.3 Hz, J 5.75 Hz), 7.66 (2 H, d, J 10.0 Hz), 8.27 (2 H, d, J 10.0 Hz).

2-p-(Chlorobenzyl)-5-ethoxyisoxazolidine (**124c**). Purified by chromatography using 4:1 hexane - ether mixture as eluent. Colourless liquid (25% yield); (Found: C, 59.5; H, 6.7; N, 5.8. $C_{12}H_{16}NO_2Cl$ requires C, 59.62; H, 6.67; N, 5.79%); ν_{max} (neat) 2977, 2909, 1493, 1103, 1016, 933, and 811 cm^{-1}; δ_H ($CDCl_3$, -40°C) 1.24 (0.58 x 3 H, t, J 7.0 Hz), 1.29 (0.42 x 3 H, t, J 7.0 Hz), 2.17-2.71 (2.42 x 1 H, m), 3.11 (0.42 x 1 H, app.q J 8.0 Hz), 3.41 (2.16 x 1 H, m), 3.81 (1 H, m), 4.02 (0.58 x 2 H, AB, J 13.8 Hz), 4.05 (0.42 x 1 H, d, J 12.5 Hz), 4.25 (0.42 x 1 H, d, J 12.5 Hz), 5.25 (1 H, broad m), 7.38 (4 H, s); δ_H (+50 °C) 1.19 (3 H, t, J 7.0 Hz), 2.18-2.56 (2 H, m), 2.91 (1 H, m), 3.17 (1 H, m), 3.48 (1 H, dq, J 7.0 Hz, J 9.5 Hz), 3.75 (1 H, dq, J 7.0 Hz, J 9.5 Hz), 3.97 (1 H, d, J 14.0 Hz), 4.10 (1 H, d, J 14.0 Hz), 5.22 (1 H, dd, J 2.0 Hz, J 5.5 Hz), 7.36 (4 H, m); mass spectrum: m/z 243(M^+ 24)

2-(p-Methoxybenzyl)-5-ethoxyisoxazolidine **(124d)**. Purified by chromatography using 1:1 hexane - ether mixture as eluent . Colourless liquid (32% yield); (Found: C, 65.6; H, 8.05; N, 5.9. $C_{13}H_{19}NO_3$ requires C, 65.80; H, 8.07; N, 5.90%); ν_{max} (neat) 2977, 2909, 1517, 1249, 1103, 1034, 984, and 820 cm^{-1}; δ_H ($CDCl_3$, -30°C) 1.24 (0.60 x 3 H, t, J 7.0 Hz), 1.29 (0.40 x 3 H, t, J 7.0 Hz), 2.13-2.69 (2.40 x 1 H, m), 3.09 (0.40 x 1 H, app.q J 8.0 Hz), 3.21-3.59 (2.20 x 1 H, m), 3.81 (1 H, m), 3.85 (3 H, s), 3.91 (0.60 x 1 H, d, J 12.5 Hz), 4.01 (0.40 x 1 H, d, J 12.5 Hz), 4.09 (0.60 x 1 H, d, J 12.5 Hz), 4.24 (0.40 x 1 H, d, J 12.5 Hz), 5.25 (1 H, broad m), 6.95 (2 H, m), 7.37 (2 H, m); δ_H (+50°C) 1.22 (3 H, t, J 7.0 Hz), 2.15-2.51 (2 H, m), 2.89 (1 H, m), 3.13 (1 H, m), 3.49 (1 H, dq, J 7.0 Hz, J 10.0 Hz), 3.77 (1 H, m), 3.79 (3 H, s), 4.02 (2 H, broad s), 5.22 (1 H, dd, J 2.0 Hz, J 5.5 Hz), 6.90 (2 H, d, J 10.0 Hz), 7.34 (2 H, d, J 10.0 Hz); mass spectrum: *m/z* 237 (M^+ 9%)

2-(p-Methylbenzyl)-5-ethoxyisoxazolidine **(124e)**. Purified by chromatography using 4:1 hexane - ether mixture as eluent . Colourless liquid (33% yield); (Found: C, 70.6; H, 8.7; N, 6.5. $C_{13}H_{19}NO_2$ requires C, 70.56; H, 8.65; N, 6.33%); ν_{max} (neat) 2977, 2932, 1517, 1109, 1076, 1004. 935, and 802 cm^{-1}; δ_H ($CDCl_3$, -40°C) 1.26 (0.59 x 3 H, t, J 7.0 Hz), 1.31 (0.41 x 3 H, t, J 7.0 Hz), 2.12-2.72 (2.41 x 1 H, m), 2.39 (3 H, s), 3.18 (0.41 x 1 H, app.q J 8.0 Hz), 3.22-3.58 (2.18 x 1 H, m), 3.86 (1 H, m), 3.94 (0.59 x 1 H, d, J 13.5 Hz), 4.04 (0.41 x 1 H, d, J 12.5 Hz), 4.11 (0.59 x 1 H, d, J 13.5 Hz), 4.26 (0.41 x 1 H, d, J 12.5 Hz), 5.26 (1 H, broad m), 7.26 (2 H, m), 7.38(2 H, m). δ_H (+50°C) 1.22 (3 H, t, J 7.0 Hz), 2.16-2.52 (2 H, m), 2.34 (3 H, s), 2.92 (1 H, m), 3.14 (1 H, m), 3.50 (1 H, dq, J 7.0 Hz, J 10.0 Hz), 3.80 (1 H, dq, J 7.0 Hz, J 10.0 Hz), 4.05 (2 H, broad s), 5.22 (1 H, dd, J 2.0 Hz, J 5.25 Hz), 7.16 (2 H, d, J 8.0 Hz), 7.32 (2 H, d, J 8.0 Hz); mas spectrum: *m/z* 221(M+ 52%)

2-(p-N,N-dimethylbenzyl)-5-ethoxyisoxazolidine (**124f**). Purified by chromatography using 4:1 hexane - ether mixture as eluent. Colourless liquid (37% yield); (Found: C, 67.25; H, 8.8; N, 11.1.$C_{14}H_{22}N_2O_2$ requires C, 67.17; H, 8.86; N, 11.19); ν_{max} (neat) 2961, 2884, 1615, 1523, 1344, 1105, 1079, 1010, 984, 951, and 808 cm^{-1}; δ_H ($CDCl_3$, -40°C) 1.26 (0.62 x 3 H, t, J 7.0 Hz), 1.31(0.38 x 3 H, t, J 7.0 Hz), 2.12-2.71 (2.38 x 1 H, m), 2.94 (6 H, s), 3.06 (0.38 H, m), 3.27 (1.24 x H, m), 3.47 (1 H, m), 3.90 (1 H, m), 3.79 (0.62 x 1 H, d, J 12.5 Hz), 3.96 (0.38 x 1 H, d, J 12.5 Hz), 4.13 (0.62 x 1 H, d, J 12.5 Hz), 4.25 (0.38 x 1 H, d, J 12.5 Hz), 5.28 (1 H, broad m), 6.81 (2 H, m), 7.33 (2 H, m); δ_H (+50°C) 1.13 (3 H, t, J 7.0 Hz), 2.12-2.52 (2 H, m), 2.86 (1 H, s), 2.94 (6 H, s), 3.08 (1 H, m), 3.52 (1 H, dq, J 7.0 Hz, J 10.0 Hz), 3.84 (1 H, dq, J 7.0 Hz, J 10.0 Hz), 4.02 (2 H, broad s), 5.24 (1 H, dd, J 2.0 Hz, J 5.25 Hz), 7.11 (2 H, d, J 10.0 Hz), 7.65 (2 H, d, J 10.0 Hz).

2-(m-Nitrobenzyl)-5-ethoxyisoxazolidine (**124g**). Purified by chromatography using 4:1 hexane - ether mixture as eluent. Colourless liquid (12% yield); (Found: C, 57.0; H, 6.3; N, 11.2. $C_{12}H_{16}N_2O_4$ requires C, 57.13; H, 6.39; N, 11.10%); ν_{max} (neat) 2977, 2909, 1532, 1350, 1103, 1001, 948, 814, 730, and 677 cm^{-1}; δ_H ($CDCl_3$, -40°C) 1.29 (0.63 x 3 H, t, J 7.0 Hz), 1.33 (0.37 x 3 H, t, J 7.0 Hz), 2.23 -3.13 (2.37 x 1 H, m), 3.21 (0.37 x 1 H, app. q, J 8.0 Hz), 3.50 (2.26 x 1 H, m), 3.82 (1 H, m), 4.06 (0.63 x 1 H, d, J 15.5 Hz), 4.17 (0.37 x 1 H, d, J 13.8 Hz), 4.27 (0.63 x 1 H, d, J 15.5 Hz), 4.39 (0.37 x 1 H, d, J 13.8 Hz), 5.28 (1 H, broad m), 7.63 (1 H, m), 7.86 (1 H, m), 8.27 (1 H, m), 8.41(1 H, m); δ_H (+50 °C) 1.21 (3 H, t, J 7.0 Hz), 2.21-2.63 (2 H, m), 2.98 (1 H, m), 3.27 (1 H, m), 3.50 (1 H, dq, J 7.0 Hz, J 10.0 Hz), 3.76 (1 H, dq, J 7.0 Hz, J 10.0 Hz), 4.07 (1 H, d, J 15.5 Hz), 4.27 (1 H, d, J 15.5 Hz), 5.24 (1 H, dd, J 2.2 Hz, J 5.5 Hz), 7.55 (1 H, t, J 8.0 Hz), 7.81 (1 H, d, J 8.0 Hz), 8.19 (1 H, d, J 8.0 Hz), 8.36 (1 H, s); mass spectrum: *m/z* 252 (M^+ 54%)

2-(o-Hydroxybenzyl)-5-ethoxyisoxazolidine (**124h**). Purified by chromatography using 4:1 hexane - ether mixture as eluent . White crystal, m.p 47-49°C (ether-hexane) (27% yield); (Found: C, 64.6; H, 7.55; N, 6.3. $C_{12}H_{17}NO_3$ requires C, 64.56; H, 7.67; N, 6.27%); ν_{max} (KBr) 2975, 2913, 2875, 1592, 1490, 1266, 1258, 1099, 1076, 1040, 909, 948, and 760 cm^{-1}; δ_H ($CDCl_3$, -40°C) 1.25 (0.52 x 3 H, t, J 7.0 Hz), 1.29 (0.48 x 3 H, t, J 7.0 Hz), 2.23-2.77 (2.48 x 1 H, m), 3.18 (0.48 x 1 H, app. q J 8.0 Hz), 3.31-3.65 (2.04 x 1 H, m), 3.80 (1 H, m), 4.11 (0.52 x 1 H, d, J 14.7 Hz), 4.29 (0.48 x 1 H, d, J 14.2 Hz), 4.39 (0.52 x 1 H, d, J 14.7 Hz), 4.50 (0.48 x 1 H, d, J 14.2 Hz), 5.29 (1 H, m), 6.96 (2 H, m), 7.10 (1 H, m), 7.31 (1 H, m), 10.2 (1 H, s); δ_H (+50°C) 1.23 (3 H, t, J 7.0 Hz), 2.54 (2 H, m), 2.96-3.60 (3 H, m), 3.76 (1 H, dq, J 7.0 Hz, J 10.0 Hz), 4.08-4.56 (2 H, m), 5.26 (1 H, t, J 4.0 Hz), 6.81-7.15 (3 H, m), 7.27 (1 H, t, J 8.0 Hz), 9.84 (1 H, s).

2-(o-Methoxybenzyl)-5-ethoxyisoxazolidine (**124i**). Purified by chromatography using 4:1 hexane - ether mixture as eluent. Colourless liquid (26% yield); (Found: C, 65.8 ; H, 8.0 ; N, 5.8. $C_{13}H_{19}NO_3$ requires C, 65.80; H, 8.07; N, 5.90%); ν_{max} (neat) 2977, 2909, 1496, 1460, 1240, 1106, 1076, 1031, 1001, 945, and 757 cm^{-1}; δ_H ($CDCl_3$, -40°C) 1.61 (3 H, d, J 7.0 Hz), 2.29-2.71 (2 H, m), 2.76 (0.38 x 1 H, q, J 8.0 Hz), 3.16 (0.38 x 1 H, q , J 8.0 Hz), 3.29-3.63 (2.24 x 1 H, m), 3.89 (0.62 x 3 H, s), 3.92 (0.38 x 3 H, s), 3.96 (1 H, m), 4.11 (0.62 x 2 H, AB, J 15.0 Hz), 4.17 (0.38 x 1 H, d, J 13.0 Hz), 4.32 (0.38 x 1 H, d, J 13.0 Hz), 5.29 (1 H, broad m), 6.89-7.15 (2 H, m), 7.29 - 7.65 (2 H, m); δ_H (+50°C) 1.22 (3 H, t, J 7.0 Hz), 2.14-2.56 (2 H, m), 2.96 (1 H, m), 3.19 (1 H, m), 3.50 (1 H, dq, J 7.0 Hz, J 10.0 Hz), 3.83 (1 H, dq, J 7.0 Hz, J 10.0 Hz), 3.94 (3 H, s), 4.15 (2 H, s), 5.23 (1 H, dd, J 2.0 Hz, J 5.5 Hz), 6.90 (1 H, d, J 8.0 Hz), 6.98 (1 H, t, J 8.0 Hz), 7.28 (1 H, t, J 8.0 Hz), 7.53 (1 H, d, J 8.0 Hz); mass spectrum: *m/z* 237 (M^+ 35%)

4.2.5 The *tertiary* butyldimethylsilyl Derivatives *(112-114)*

To a solution of imidazole (6.0 mmol) in dry DMF (1.5 cm^3) *tertiary* butyl dimethylchlorosilane (2.0 mmol) at 0°C was added. To this mixture the corresponding hydroxylamine (1 mmol) was added. The mixture was stirred at 50°C for 2 h. The resulting mixture was taken up in ether (25 cm^3) and washed with H_2O (4 x 25 cm^3). The organic layer was dried (Na_2SO_4); excess solvent was removed by using a gentle stream of N_2. The residual liquid was chromatographed using hexane-ether mixture (90:10) as the eluent.

O-^{t}Butyldimethylsilyl-N-benzyl-N-methylhydroxylamine (112). Purified by chromatography using hexane as eluent. Colourless liquid, (Found: C, 67.0; H, 10.2; N, 5.8. $C_{14}H_{25}NOSi$ requires C, 66.88; H, 10.02; N, 5.57%); ν_{max} (neat) 2928, 2851, 1255, 1087, 954, 915, 885, 843, 784, 703, and 671 cm^{-1}; δ_H ($CDCl_3$, +20°C) -0.10 (3 H, broad s), 0.10 (3 H, broad s), 0.87 (9 H, s), 2.49 (3 H, s), 3.61 (1 H, d, J 13.0 Hz), 3.96 (1 H, d, J 13.0 Hz), 7.33 (5 H, m); δ_H (+50°C) 0.0 (6 H, s), 0.86 (9 H, s), 2.68 (3 H, s), 3.78 (2 H, broad s), 7.32 (5 H, m); mass spectrum: *m/z* 251 (M^+ 3%).

O-^{t}Butyldimethylsilyl-N-benzyl-N-isopropylhydroxylamine (113). Purified by chromatography using hexane as eluent. Colourless liquid, (Found: C, 68.6; H, 10.6; N, 5.0. $C_{16}H_{29}NOSi$ requires C, 68.76; H, 10.46; N, 5.01%); ν_{max} (neat) 2917, 2840, 1464, 1252, 939, 894, 840, 784, and 697 cm^{-1}; δ_H ($CDCl_3$, +20°C) -0.10 (6 H, broad), 0.84 (9 H, s), 1.08 (6 H, d, J 7.0 Hz), 2.99 (1 H, hept, J 7.0 Hz), 3.78 (2 H, s), 7.30 (5 H, m); δ_H (-50°C) -0.05 (6 H, s), 0.78 (9 H, s), 1.02 (3 H, d, J 7.0 Hz), 1.04 (3 H, d, J 7.0 Hz), 2.92 (1 H, hept, J 7.0 Hz), 3.64 (1 H, d, J 12.5 Hz), 3.77 (1 H, d, J 12.5 Hz), 7.32 (5 H, m); mass spectrum: *m/z* 279 (M^+ 16%)

O-^{t}Butyldimethylsilyl-N-benzyl-N-^{t}butylhydroxylamine (114). Purified by chromatography using hexane as eluent. Colourless liquid, (Found: C, 69.3; H, 10.7; N, 4.8 $C_{17}H_{31}NOSi$ requires C, 69.56; H, 10.65; N, 4.77%); ν_{max} (neat) 2954, 2931, 2841, 1359, 1258, 1207, 1025, 986, 867, 837, 808, 786, and 751 cm^{-1}; δ_H ($CDCl_3$, +20°C) -0.2 (6 H, broad s), 0.90 (9 H, s), 1.10 (9 H, s), 3.95 (2 H, broad s), 7.19-7.40 (5 H, m); δ_H (-50 °C) -0.60 (3 H, s), 0.10 (3 H, s), 0.83 (9 H, s), 1.17 (9 H, s), 3.70 (1 H, d, J 15.5 Hz), 4.17 (1 H, d, J 15.5 Hz), 7.35 (5 H, m); mass spectrum: *m/z* 293 (M^+ 30%)

4.2.6 The *tertiary* butyldimethylsilyl Derivatives *(118-120)*

To a solution of imidazole (408 mg, 6.0 mmol) in dry DMF (2.0 cm^3) was added *tertiary* butyldimethylchlorosilane (332 mg, 2.2 mmol) at 0°C. To this mixture was added the hydroxylamine **108h** (300 mg, 2.0 mmol) and then stirred at 50°C for 2 h. The resulting reaction mixture was taken up in ether (30 cm^3) and washed with H_2O (5 x 25 cm^3). The organic layer was dried (Na_2SO_4) evaporated and the residual liquid was chromatographed using hexane - ether mixture (95:5) as the eluent. The first compound isolated was compound **120** as a colourless liquid. Continued elution afforded a mixture of compound **119** and **120** and then the pure compound **119** as a colourless liquid. Further elution with hexane-ether (4:1) gave the compound **118** as colourless prisms.

N-o-^{t}butyldimethylsiloxybenzyl-N-methylhydroxylamine (118). Colourless Plates, m.p. 78-79.5°C (Found: C, 64.0; H, 9.6; N, 5.4. $C_{14}H_{25}NO_2Si$ requires C, 62.87; H, 9.42; N, 5.24); ν_{max} (KBr) 3219, 2957, 2855, 1802, 1493, 1280, 1266, 1115, 957, 933, 925, 837, 781 and 753 cm^{-1}; δ_H ($CDCl_3$, +24°C) 0.25 (6 H, s), 1.03 (9 H, s), 2.63 (3 H, s), 3.83 (2 H, s), 5.19 (1 H, broad), 6.82-7.50 (4 H, m).

O-^{t}Butyldimethylsilyl-N-o-hydroxybenzyl-N-methylhydroxylamine (119). Colourless liquid, (Found: C, 63.1; H, 9.5; N, 5.4. $C_{14}H_{25}NO_2Si$ requires C, 62.87; H, 9.42; N,

5.24); ν_{max} (neat) 2957, 2929, 2855, 1489, 1249, 883, 838, 782, and 754 cm^{-1}; δ_H ($CDCl_3$, +24°C) 0.17 (3 H, s), 0.25 (3 H, s), 0.93 (9 H, s), 2.58 (3 H, s), 3.90 (1 H, d, J 13.0 Hz), 4.29 (1 H, d, J 13.0 Hz), 6.80-7.52 (4 H, m), 9.10 (1 H, s); δ_H (+60°C) 0.14 (6 H, s), 0.92 (9 H, s), 2.56 (3 H, s), 4.04 (2 H, s), 6.87-7.46 (4 H, m), 8.86 (1 H, s).

*O-^{t}Butyldimethylsilyl-N-^{t}butyldimethylsiloxybenzyl-N-methylhydroxyl-amine(**120**).* Colourless liquid, (Found: C, 64.2; H, 10.8; N, 3.8. $C_{20}H_{39}NO_2Si_2$ requires C, 62.93; H, 10.30; N, 3.67); ν_{max} (neat) 2957, 2929, 2864, 1493, 1267, 1255, 923, 886, 837, and 780 cm^{-1}; δ_H ($CDCl_3$, +45°C) 0.08 (6 H, s), 0.31 (6 H, s), 0.93 (9 H, s), 1.53 (9 H, s), 2.61 (3 H, s), 3.92 (2 H, broad), 6.83-7.57 (4 H, m).

4.2.7 The Nitrones

Aldehyde (5.5 mmol) was added to a solution of the hydroxylamine (5.0 mmol) in ethanol (10 cm^3). The reaction mixture was stirred at 50-60°C for 5 h and TLC experiment (silica, ether) was used to determine the complete formation of the nitrone. After removal of the ethanol by a gentle stream of N_2 the nitrones were recrystallized by using hexane-ether mixture.

*α-(2-hydroxy)phenyl-N-isopropyl nitrone (**P1AH**).* (Found: C, 67.1, H, 7.3; N, 7.8. $C_{10}H_{13}NO_2$ requires C, 67.01; H, 7.31; N, 7.82%); ν_{max} (neat) 2990, 1590, 1480, 1420, 1284, 1144, 1062, 846 and 756 cm^{-1}; δ_H ($CDCl_3$, +19°C) 1.55 (6 H, d, J 7.0 Hz), 4.35 (1 H , hept), 6.90 (1 H, t, J 7.5 Hz), 7.02 (1 H, d, J 7.5 Hz), 7.15 (1 H, d, J 7.5 Hz), 7.44 (1 H, t, J 7.5 Hz), 7.71 (1 H, s), 12.5 (1 H, broad s).

*α-(2-hydroxy)phenyl-N-methyl nitrone (**P3AH**).* White crystals, m.p. 130-132°C (Found: C, 63.4; H, 6.1; N, 9.3. $C_8H_9NO_2$ requires C, 63.56; H, 6.00; N, 9.27%); ν_{max}

(KBr) 2557, 1586, 1462, 1398, 1270, 1152, 946, and 778 cm^{-1}; δ_H ($CDCl_3$, +19°C) 3.91 (3 H, s), 6.91 (1 H, t, J 8.0 Hz), 7.02 (1 H, d, J 8.0 Hz), 7.12 (1 H, d, J 8.0 Hz), 7.46 (1 H, t, J 8.0 Hz), 7.59 (1 H, s), 12.5 (1 H, broad s).

α-(2-hydroxy)phenyl-N-tertiary butylnitrone ***(P11AH)***. Pale yellow crystals, m.p. 83-84°C (Found: C, 68.3; H, 7.8; N, 7.2. $C_{11}H_{15}NO_2$ requires C, 68.37; H, 7.82; N, 7.25%); ν_{max} (KBr) 2972, 1580, 1456, 1362, 1286, 1006, and 762 cm^{-1}; δ_H ($CDCl_3$, +19°C) 1.65 (9 H, s), 6.90 (1 H, t, J 8.0 Hz), 7.03 (1 H, d, J 8.0 Hz), 7.15 (1 H, d, J 8.0 Hz), 7.43 (1 H, t, J 8.0 Hz), 7.77 (1 H, s), 12.4 (1 H, broad s).

α-(4-hydroxy)phenyl-N-isopropyl nitrone ***(P14AH)***. Pale yellow needles, 220-222°C (decomposed) (Found: C, 67.1; H, 7.3; N, 7.8. $C_{10}H_{13}NO_2$ requires C, 67.01; H, 7.31; N, 7.82%); ν_{max} (KBr) 2977, 1604, 1510, 1288, 1168, 1138, 1074, and 874 cm^{-1}; δ_H (CD_3OD, +19°C) 1.50 (6 H, d, J 7.0 Hz), 4.18 (1 H, hept), 4.95 (1 H, s), 6.96 (2 H, d, J 10.0 Hz), 7.88 (1 H, s), 8.09 (2 H, d, J 10.0 Hz).

α-(4-methyl)phenyl-N-isopropyl nitrone ***(P19AH)***. White plates, m.p. 43-45°C (Found: C, 74.6; H, 8.5; N, 7.9. $C_{11}H_{15}NO$ requires C, 74.54; H, 8.53; N, 7.90%); ν_{max} (KBr) 2977, 1570, 1446, 1308, 1150, 1084 and 836 cm^{-1}; δ_H ($CDCl_3$, +19°C) 1.55 (6 H, d, J 7.0 Hz), 2.42 (3 H, s), 4.26 (1 H, hept), 7.30 (2 H, d, J 8.0 Hz), 7.48 (1 H, s), 8.24 (2 H, d, J 8.0 Hz).

α-(4-dimethylamino)phenyl-N-isopropyl nitrone ***(P20AH)***.. White crystals, m.p. 120-121.5°C (Found: C, 69.7; H, 8.8; N, 13.6. $C_{12}H_{18}NO_2$ requires C, 69.65; H, 8.80; N, 13.58%); ν_{max} (KBr) 2978, 1060, 1522, 1366, 1304, 1166, 1084, 948, and 840 cm^{-1}; δ_H ($CDCl_3$, +19°C) 1.54 (6 H, d, J 7.0 Hz), 3.16 (6 H, s), 4.19 (1 H , hept), 6.76 (2 H, d, J 9.0 Hz), 7.35 (1 H, s), 8.26 (2 H, d, J 9.0 Hz).

*α-(3-Bromo)phenyl-N-isopropyl nitrone (**P22AH**).* White needles, m.p. 82-83°C (Found: C, 49.6; H, 5.1; N, 5.8. $C_{10}H_{12}NOBr$ requires C, 49.61; H, 5.00; N, 5.79%); ν_{max} (KBr) 2988, 1570, 1462, 1326, 1152, 1092, 826, 766, and 678 cm^{-1}; δ_H ($CDCl_3$, +19°C) 1.54 (6 H, d, J 7.0 Hz), 4.27 (1 H , hept), 7.34 (1 H, t, J 8.0 Hz), 7.48 (1 H, s), 7.70 (1 H, d, J 8.0 Hz), 8.11 (1 H, d, J 8.0 Hz), 8.68 (1 H, s).

*α-(4-Chloro)phenyl-N-isopropyl nitrone (**P27AH**).* White plates, m.p. 56-57.5°C (Found: C, 60.8; H, 6.0; N, 7.1. $C_{10}H_{12}NOCl$ requires C, 60.76; H, 6.12; N, 7.09%); ν_{max} (KBr) 2978, 1578, 1454, 1308, 1150, 1086, and 842 cm^{-1}; δ_H ($CDCl_3$, +19°C) 1.55 (6 H, d, J 7.0 Hz), 4.27 (1 H, hept), 7.45 (2 H, d, J 8.0 Hz), 7.49 (1 H, s), 8.30 (2 H, d, J 8.0 Hz).

*α-(4-Bromo)phenyl-N-isopropyl nitrone (**P28AH**).* White crystals, m.p. 53-55°C (Found: C, 49.6; H, 5.1; N, 5.8. $C_{10}H_{12}NOBr$ requires C, 49.61; H, 5.00; N, 5.79%); ν_{max} (KBr) 2958, 1578, 1458, 1320, 1154, 1092, and 832 cm^{-1}; δ_H ($CDCl_3$, +19°C) 1.55 (6 H, d, J 7.0 Hz), 4.28 (1 H , hept), 7.50 (1 H, s), 7.62 (2 H, d, J 8.0 Hz), 8.23 (2 H, d, J 8.0 Hz).

*α-(4-Nitro)phenyl-N-isopropyl nitrone (**P29AH**).* Yellow needles, m.p. 99-101°C (Found: C, 57.6; H, 5.8; N, 13.5. $C_{10}H_{12}N_2O_3$ requires C, 57.68; H, 5.81; N, 13.46%); ν_{max} (KBr) 2978, 1614, 1352, 1150, 1094, and 858 cm^{-1}; δ_H ($CDCl_3$, +19°C) 1.58 (6 H, d, J 7.0 Hz), 4.38 (1 H , hept), 7.50 (1 H, s), 7.62 (2 H, d, J 8.0 Hz), 8.23 (2 H, d, J 8.0 Hz).

*α-(3-Nitro)phenyl-N-isopropyl nitrone (**P37AH**).* Yellow needles, m.p. 134-136°C (Found: C, 57.7; H, 5.8; N, 13.5. $C_{10}H_{12}N_2O_3$ requires C, 57.68; H, 5.81; N,

13.46%); ν_{max} (KBr) 2978, 1524, 1322, 1070, and 678 cm^{-1}; δ_H ($CDCl_3$, +19°C) 1.58 (6 H, d, J 7.0 Hz), 4.37 (1 H, hept), 7.69 (1 H, s, 1 H, t, J 8.0 Hz), 8.33 (1 H, d, J 8.0 Hz), 8.74 (1 H, d, J 8.0 Hz), 9.18 (1 H, s).

*α-(2,4,5-tri methoxy)phenyl-N-isopropyl nitrone (**P40AH**).* Light brown crystals, m.p. 114-116°C (Found: C, 61.7; H, 7.6; N, 5.5. $C_{13}H_{19}NO_4$ requires C, 61.64; H, 7.56; N, 5.53%); ν_{max} (KBr) 2958, 1578, 1458, 1320, 1154, 1092, and 832 cm^{-1}; δ_H ($CDCl_3$, +19°C) 1.56 (6 H, d, J 7.0 Hz), 3.93 (3 H , s), 4.00 (6 H, s), 4.28 (1 H, s), 6.59 (1 H, s), 7.93 (1 H, s), 8.25 (1 H, s).

*α-(4-methoxy)phenyl-N-isopropyl nitrone (**P45AH**).* (Found: C, 68.3, H, 7.8; N, 7.2. $C_{11}H_{15}NO_2$ requires C, 68.37; H, 7.82; N, 7.25%); ν_{max} (neat) 2990, 1604, 1506, 1452, 1302, 1264, 1170, 1148, 1086, 1030, and 842 cm^{-1}; δ_H ($CDCl_3$, +19°C) 1.54 (6 H, d, J 7.0 Hz), 3.89 (3 H, s), 4.25 (1 H , hept), 7.00 (2 H, d, J 8.5 Hz), 7.46 (1 H, s), 8.34 (2 H, d, J 8.5 Hz).

*α-(2-methoxy)phenyl-N-isopropyl nitrone (**P46AH**)* (Found: C, 68.3, H, 7.8; N, 7.2. $C_{11}H_{15}NO_2$ requires C, 68.37; H, 7.82; N, 7.25%); ν_{max} (neat) 2980, 2943, 1594, 1560, 1466, 1436, 1308, 1284, 1246, 1150, 1026, and 766 cm^{-1}; δ_H ($CDCl_3$, +19°C) 1.54 (6 H, d, J 7.0 Hz), 3.89 (3 H, s), 4.29 (1 H , hept), 6.94 (1 H, d, J 8.0 Hz), 7.09 (1 H, t, J 8.0 Hz), 7.43 (1 H, t, J 8.0 Hz), 8.01 (1 H, s), 9.40 (1 H, d, J 8.0 Hz).

*α-(4-methyl)phenyl-N-methyl nitrone (**P72AH**).* White crystals, m.p. 117-119°C (Found: C, 71.3; H, 8.7; N, 9.3. $C_9H_{13}NO$ requires C, 71.49; H, 8.67; N, 9.27%); ν_{max} (KBr) 2931, 1586, 1414, 1168, 944 and 838 cm^{-1}; δ_H ($CDCl_3$, +19°C) 2.94 (3 H, s), 3.94 (3 H, s), 7.32 (2 H, d, J 8.0 Hz), 7.42 (1 H, s), 8.22 (2 H, d, J 8.0 Hz).

α-(4-dimethylamino)phenyl-N-methyl nitrone (P73AH). Yellow crystals, m.p. 133-135°C (Found: C, 67.4; H, 7.9; N, 15.7. $C_{10}H_{14}N_2O$ requires C, 67.38; H, 7.92; N, 15.72%); ν_{max} (KBr) 3359, 2889, 1612, 1528, 1374, 1188, 1146, 930, and 814 cm^{-1}; δ_H ($CDCl_3$, +19°C) 3.06 (3 H, s), 3.87 (6 H, s), 6.76 (2 H, d, J 8.5 Hz), 7.37 (1 H, s), 8.23 (2 H, d, J 8.5 Hz).

α-(3-Nitro)phenyl-N-methyl nitrone (P74AH). Yellow crystals, m.p. 111-112°C (Found: C, 53.3, H, 4.5; N, 15.5. $C_8H_8N_2O_3$ requires C, 53.33; H, 4.48; N, 15.55%); ν_{max} (KBr) 3113, 1586, 1522, 1416, 1354, 1174, 954, 910, and 826 cm^{-1}; δ_H ($CDCl_3$, +19 °C) 4.0 (3 H, s), 7.61 (1 H, s), 7.68 (1 H, t, J 8.0 Hz), 8.33 (1 H, d, J 8.0 Hz), 8.74 (1 H, d, J 8.0 Hz), 9.08 (1 H, s).

α-(2-methoxy)phenyl-N-methyl nitrone (P75AH). White crystals, m.p. 79-81°C (Found: C, 65.3, H, 6.7; N, 8.5. $C_9H_{11}NO_2$ requires C, 65.43; H, 6.71; N, 8.48%); ν_{max} (KBr) 2919, 1596, 1470, 1244, 1166, 1024, 946, 824, and 748 cm^{-1}; δ_H ($CDCl_3$, +19°C) 3.91 (3 H, s), 3.94 (3 H, s), 6.94 (1 H, d, J 8.0 Hz), 7.10 (1 H, t, J 8.0 Hz), 7.44 (1 H, t, J 8.0 Hz), 7.91 (1 H, s), 9.33 (1 H, d, J 8.0 Hz).

α-(4-Chloro)phenyl-N-methyl nitrone (P76AH). White crystals, m.p. 126-127°C (Found: C, 56.6, H, 4.7; N, 8.3. C_8H_8NOCl requires C, 56.65; H, 4.75; N, 8.26%); ν_{max} (KBr) 3075, 3026, 2929, 1592, 1484, 1424, 1182, 1166, 1090, 948, 854, and 706 cm^{-1}; δ_H ($CDCl_3$, +19°C) 3.95 (3 H, s), 7.45 (1 H, s), 7.48 (2 H, d, J 8.5 Hz), 8.28 (2 H, d, J 8.5 Hz).

α-phenyl-N-ethyl nitrone (P87AH). (Found: C, 72.3, H, 7.4; N, 9.4. $C_9H_{11}NO$ requires C, 72.45; H, 7.43; N, 9.39%); ν_{max} (neat) 2980, 1582, 1446, 1164, and 692

cm^{-1}; δ_H ($CDCl_3$, +19°C) 1.60 (3 H, t, J 8.0 Hz), 4.00 (1 H, d, J 8.0 Hz), 4.08 (1 H, d, J 8.0 Hz), 7.49 (5 H, s), 8.34 (1 H, broad s).

4.3 The Kinetic Study

4.3.1 HgO Oxidation of the Hydroxylamines

4.3.1.1 General Procedure

To a solution of the hydroxylamine $PhCH_2NOHR$ (0.15 mmol) and X-$C_6H_4CH_2NOHR$ (0.15 mmol) in $CDCl_3$ (2.0 cm^3) at 0°C was added yellow HgO (40.0 mg, 0.185 mmol) and the mixture was stirred for 30 min or until the mercury salt turned greyish. The solution was passed through a tightly packed glass wool in a pipette to remove the mercury salts. The ^1H NMR spectrum revealed the presence of starting materials along with product nitrones. Careful analysis of the spectrum helped to quantify each product and starting material by the integration of several proton signals. The N-alkyl protons of the nitrones and hydroxylamines are well separated and there are many other non overlapping signals of the starting materials and products. (^1H NMR data of the individual nitrones and hydroxylamines are described in the experimental section). Before the addition of the HgO, ^1H NMR spectra of the reaction mixture were taken in order to check the quantities of the starting materials by integration. After taking the spectra the content in the NMR tube was quantitatively transferred into the reaction flask. At the end of the oxidation and the quantification of the individual compounds, about 7 mg of the hydroxylamine $PhCH_2NOHR$ was mixed with the contents in the NMR tube. Peak enhancement of the unreacted $PhCH_2NOHR$ assured the assignment of the signals to the starting hydroxylamines. Using the rate equation of Ingold and Shaw [114] the relative rates were determined.

$$\frac{k_X}{k_H} = \frac{\log \frac{[X]_f}{[X]_i}}{\log \frac{[H]_f}{[H]_i}}$$

where,

$[H]_i$ = Initial concentration of unsubstituted hydroxylamine.

$[H]_f$ = Final concentration of unsubstituted hydroxylamine.

$[X]_i$ = Initial concentration of substituted hydroxylamine.

$[X]_f$ = Final concentration of substituted hydroxylamine.

k_X = Rate constant for the oxidation of substituted hydroxylamine.

k_H = Rate constant for the oxidation of unsubstituted hydroxylamine.

4.3.1.2 Relative Rates for the Oxidation Process

*Relative rates for the oxidation of **108a** and **108b**:*

Initial amounts = i (mmol)						
i:	**108a**	0.146;	**108b**	0.154;	HgO:	0.185
f:	**108a**	0.0348;	**108b**	0.0795;	nitrones:	0.173

$k_{p\text{-}NO2}/k_H = 0.461$

*Relative rates for the oxidation of **108a** and **108c**:*

i:	**108a**	0.146;	**108c**	0.146;	HgO:	0.185
f:	**108a**	0.0512;	**108c**	0.0568;	nitrones:	0.184

$k_{p\text{-}Cl}/k_H = 0.901$

*Relative rates for the oxidation of **108a** and **108d**:*

i:	**108a**	0.146;	**108d**	0.156;	HgO:	0.185
f:	**108a**	0.0665;	**108d**	0.0605;	nitrones:	0.175

$k_{p\text{-OMe}}/k_H = 1.21$

*Relative rates for the oxidation of **108a** and **108e**:*

i:	**108a**	0.150;	**108e**	0.150;	HgO:	0.171
f:	**108a**	0.0719;	**108e**	0.0631;	nitrones:	0.165

$k_{p\text{-Me}}/k_H = 1.18$

*Relative rates for the oxidation of **108a** and **108f**:*

i:	**108a**	0.146;	**108f**	0.150;	HgO:	0.185
f:	**108a**	0.0690;	**108f**	0.0450;	nitrones:	0.182

$k_{p\text{-NMe2}}/k_H = 1.61$

*Relative rates for the oxidation of **108a** and **108g**:*

i:	**108a**	0.146;	**108g**	0.148;	HgO:	0.185
f:	**108a**	0.0307;	**108g**	0.0778;	nitrones:	0.186

$k_{m\text{-NO2}}/k_H = 0.412$

*Relative rates for the oxidation of **108a** and **108h**:*

i:	**108a**	0.146;	**108h**	0.150;	HgO:	0.185
f:	**108a**	0.0536;	**108h**	0.0614;	nitrones:	0.181

$k_{o\text{-OH}}/k_H = 0.892$

*Relative rates for the oxidation of **108a** and **108i**:*

i:	**108a**	0.146;	**108i**	0.150;	HgO:	0.185
f:	**108a**	0.0612;	**108i**	0.0438;	nitrones:	0.191

$k_{o\text{-OMe}}/k_H = 1.42$

*Relative rates for the oxidation of **110a** and **110b**:*

i:	**110a**	0.150;	**110b**	0.150;	HgO:	0.150
f:	**110a**	0.0477;	**110b**	0.0745;	nitrones:	0.178

$k_{p\text{-NO2}}/k_H = 0.610$

*Relative rates for the oxidation of **110a** and **110c**:*

i:	**110a**	0.150;	**110c**	0.150;	HgO:	0.150
f:	**110a**	0.0587;	**110c**	0.0713;	nitrones:	0.170

$k_{p\text{-Cl}}/k_H = 0.794$

*Relative rates for the oxidation of **110a** and **110d**:*

i:	**110a**	0.150;	**110d**	0.150;	HgO:	0.150
f:	**110a**	0.0717;	**110d**	0.0633;	nitrones:	0.165

$k_{p\text{-OMe}}/k_H = 1.17$

*Relative rates for the oxidation of **110a** and **110e**:*

i:	**110a**	0.0500;	**110e**	0.0500;	HgO:	0.050
f:	**110a**	0.0233;	**110e**	0.0165;	nitrones:	0.0602

$k_{p\text{-Me}}/k_H = 1.45$

*Relative rates for the oxidation of **110a** and **110f**:*

i:	**110a**	0.100;	**110f**	0.0691;	HgO:	0.100
f:	**110a**	0.0138;	**110f**	0.0488;	nitrones:	0.106

$k_{p\text{-}NMe2}/k_H = 2.25$

*Relative rates for the oxidation of **110a** and **110g**:*

i:	**110a**	0.150;	**110g**	0.150;	HgO:	0.150
f:	**110a**	0.0505;	**110g**	0.0865;	nitrones:	0.163

$k_{m\text{-}NO2}/k_H = 0.505$

*Relative rates for the oxidation of **110a** and **110h**:*

i:	**110a**	0.150;	**110h**	0.150;	HgO:	0.150
f:	**110a**	0.0714;	**110h**	0.0851;	nitrones:	0.144

$k_{m\text{-}Br}/k_H = 0.767$

*Relative rates for the oxidation of **110a** and **110i**:*

i:	**110a**	0.150;	**110i**	0.150;	HgO:	0.150
f:	**10a**	0.0734;	**110i**	0.0766;	nitrones:	0.150

$k_{p\text{-}Br}/k_H = 0.942$

*Relative rates for the oxidation of **110a** and **110j**:*

i:	**110a**	0.150;	**110j**	0.150;	HgO:	0.150
f:	**110a**	0.0738;	**110j**	0.0602;	nitrones:	0.166

$k_{(OMe)3}/k_H = 1.29$

*Relative rates for the oxidation of **108a** and **109**:*

i:	**108a**	0.150;	**109**	0.126;	HgO:	0.150
f:	**108a**	0.0943;	**109**	0.053;	nitrones:	0.166

$k_{Et}/k_{Me} = 0.902$

*Relative rates for the oxidation of **108a** and **110**:*

i:	**108a**	0.150;	**110**	0.150;	HgO:	0.150
f:	**108a**	0.0732;	**110**	0.0548;	nitrones:	0.172

$k^{i}_{Pr}/k_{Me} = 1.40$

*Relative rates for the oxidation of **108a** and **111**:*

1st Trial:

i:	**108a**	0.150;	**111**	0.150;	HgO:	0.150
f:	**108a**	0.0597;	**111**	0.0923;	nitrones:	0.148

$k^{t}_{Bu}/k_{Me} = 0.528$

2nd Trial:

*Relative rates for the oxidation of **108a** and **109**:*

i:	**108a**	0.150;	**111**	0.150;	HgO:	0.150
f:	**108a**	0.0446;	**111**	0.0804;	nitrones:	0.175

$k^{t}_{Bu}/k_{Me} = 0.514$

4.3.2 *p*-Benzoquinone Oxidation of the Hydroxylamines

4.3.2.1 General Procedure

To a stirring solution of the hydroxylamine $PhCH_2NOHR$ (0.15 mmol) and X-$C_6H_4CH_2NOHR$ (0.15 mmol) in $CDCl_3$ (1.0 cm^3) at 20°C was added dropwise a solution of *p*-benzoquinone (0.15 mmol) in 1 cm^3 $CDCl_3$ over a period of 3-5 min. The solution immediately turned dark blue and after 10-20 min it became colourless with the separation of white crystals of hydroquinone. After passing through glass wool (tightly packed in a pipette) to remove the hydroquinone the reaction mixture was analysed by ^1H NMR and relative rates are determined as described above in the case of HgO oxidation.

4.3.2.2 Relative Rates for the Oxidation Process

*Relative rates for the oxidation of **108a** and **108b**:*

i:	**108a**	0.150;	**108b**	0.150;	*p*-Benzoquinone:	0.173
f:	**108a**	0.0429;	**108b**	0.0881;	nitrones:	0.169

$k_{p\text{-}NO2}/k_H = 0.425$

*Relative rates for the oxidation of **108a** and **108c**:*

i:	**108a**	0.150;	**108c**	0.150;	*p*-Benzoquinone:	0.150
f:	**108a**	0.0734;	**108c**	0.0826;	nitrones:	0.144

$k_{p\text{-}Cl}/k_H = 0.835$

*Relative rates for the oxidation of **108a** and **108d**:*

i:	**108a**	0.150;	**108d**	0.150;	*p*-Benzoquinone:	0.150
f:	**108a**	0.0885;	**108d**	0.0705 ;	nitrones:	0.141

$k_{p\text{-}OMe}/k_H = 1.43$

*Relative rates for the oxidation of **108a** and **108e**:*

i:	**108a**	0.150;	**108e**	0.150;	*p*-Benzoquinone:	0.150
f:	**108a**	0.0792;	**108e**	0.0718;	nitrones:	0.149

$k_{p\text{-Me}}/k_H = 1.16$

*Relative rates for the oxidation of **108a** and **108f**:*

i:	**108a**	0.150;	**108f**	0.150;	*p*-Benzoquinone:	0.150
f:	**108a**	0.0896;	**108f**	0.0584;	nitrones:	0.152

$k_{p\text{-NMe2}}/k_H = 1.83$

*Relative rates for the oxidation of **108a** and **108g**:*

i:	**108a**	0.150;	**108g**	0.150;	*p*-Benzoquinone:	0.150
f:	**108a**	0.0623;	**108g**	0.107;	nitrones:	0.131

$k_{m\text{-NO2}}/k_H = 0.387$

*Relative rates for the oxidation of **108a** and **108h**:*

i:	**108a**	0.150;	**108h**	0.150;	*p*-Benzoquinone:	0.150
f:	**108a**	0.0749;	**108h**	0.103;	nitrones:	0.122

$k_{o\text{-OH}}/k_H = 0.540$

*Relative rates for the oxidation of **108a** and **108i**:*

i:	**108a**	0.150;	**108i**	0.150;	*p*-Benzoquinone:	0.150
f:	**108a**	0.0938;	**108i**	0.0563;	nitrones:	0.150

$k_{o\text{-OMe}}/k_H = 2.09$

*Relative rates for the oxidation of **110a** and **110b**:*

i: **110a** 0.150; **110b** 0.150; *p*-Benzoquinone: 0.150

f: **110a** 0.0630; **110b** 0.0870; nitrones: 0.150

$k_{p\text{-}NO2}/k_H = 0.202$

*Relative rates for the oxidation of **110a** and **110c**:*

i: **110a** 0.150; **110c** 0.150; *p*-Benzoquinone: 0.150

f: **110a** 0.0799; **110c** 0.0851; nitrones: 0.135

$k_{p\text{-}Cl}/k_H = 0.901$

*Relative rates for the oxidation of **110a** and **110d**:*

i: **110a** 0.100; **110d** 0.100; *p*-Benzoquinone: 0.100

f: **110a** 0.0505; **110d** 0.0435; nitrones: 0.106

$k_{p\text{-}OMe}/k_H = 1.22$

*Relative rates for the oxidation of **110a** and **110e**:*

i: **110a** 0.0500; **110e** 0.0500; *p*-Benzoquinone: 0.0500

f: **110a** 0.0307; **110e** 0.0243; nitrones: 0.0450

$k_{p\text{-}Me}/k_H = 1.48$

*Relative rates for the oxidation of **110a** and **110f**:*

i: **11a** 0.100; **110f** 0.0786; *p*-Benzoquinone: 0.150

f: **110a** 0.0516; **110f** 0.0181; nitrones: 0.1089

$k_{p\text{-}NMe2}/k_H = 2.22$

*Relative rates for the oxidation of **110a** and **110g**:*

i:	**110a**	0.150;	**110g**	0.150;	*p*-Benzoquinone:	0.150
f:	**110a**	0.0476;	**110g**	0.0904;	nitrones:	0.162

$k_{m\text{-}NO2}/k_H = 0.442$

*Relative rates for the oxidation of **110a** and **110h**:*

i:	**110a**	0.150;	**110h**	0.150;	*p*-Benzoquinone:	0.150
f:	**110a**	0.0692;	**110h**	0.0918;	nitrones:	0.139

$k_{m\text{-}Br}/k_H = 0.634$

*Relative rates for the oxidation of **110a** and **110i**:*

i:	**110a**	0.150;	**110i**	0.150;	*p*-Benzoquinone:	0.150
f:	**110a**	0.0750;	**110i**	0.0880;	nitrones:	0.137

$k_{p\text{-}Br}/k_H = 0.770$

*Relative rates for the oxidation of **110a** and **110j**:*

i:	**110a**	0.150;	**110j**	0.150;	*p*-Benzoquinone:	0.150
f:	**110a**	0.0943;	**110j**	0.0657;	nitrones:	0.140

$k_{(OMe)3}/k_H = 1.77$

*Relative rates for the oxidation of **108a** and **109**:*

i:	**108a**	0.100;	**109**	0.105;	*p*-Benzoquinone:	0.100
f:	**108a**	0.0618;	**109**	0.0547;	nitrones:	0.189

$k_{Et}/k_{Me} = 1.35$

*Relative rates for the oxidation of **108a** and **110**:*

i:	**108a**	0.150;	**110**	0.150;	*p*-Benzoquinone: 0.150
f:	**108a**	0.0854;	**110**	0.0406;	nitrones: 0.174

$k^{i}_{Pr}/k_{Me} = 2.32$

*Relative rates for the oxidation of **110a** and **111**:*

i:	**108a**	0.150;	**111**	0.150;	*p*-Benzoquinone: 0.150
f:	**108a**	0.0863;	**111**	0.0777;	nitrones: 0.136

$k^{t}_{Bu}/k_{H} = 1.20$

4.4 The *E* -*Z* Isomerization

4.4.1 ^{1}H NMR Chemical Shifts of the *E* & *Z* Nitrones

*Z-α-phenyl-N-methyl nitrone (**Z-101a**).* δ_H ($CDCl_3$, -10°C) 3.93 (3 H, d, J 0.5 Hz), 7.50 (4 H, m), 8.30 (2 H, m).

*E-α-phenyl-N-methyl nitrone (**E-101a**).* δ_H ($CDCl_3$, -10°C) 3.89 (3 H, d, J 1.0 Hz), 7.50 (5 H, m), 8.04 (1 H, s).

*Z-α-(4-nitro)phenyl-N-methyl nitrone (**Z-101b**).* δ_H ($CDCl_3$, -10°C) 3.99 (3 H, s), 7.63 (1 H, s), 8.34 (2 H, d, J 9.0 Hz), 8.46 (2 H, d, J 9.0 Hz).

*E-α-(4-nitro)phenyl-N-methyl nitrone (**E-101a**).* δ_H ($CDCl_3$, -10°C) 3.95 (3 H, s), 7.72 (2 H, d, J 8.0 Hz), 8.05 (1 H, s), 8.35 (2 H, d, J 8.0 Hz).

Z-α-(4-Chloro)phenyl-N-methyl nitrone ***(Z-101c)***. δ_H ($CDCl_3$, -10°C) 3.92 (3 H, s), 7.44 (2 H, d, J 9.0 Hz), 7.44 (1 H, overlapping s), 8.26 (2 H, d, J 9.0 Hz)

E-α-(4-Chloro)phenyl-N-methyl nitrone ***(E-101c)***. δ_H ($CDCl_3$, -10°C) 3.87 (3 H, d, J 1.0 Hz), 7.33 (2 H, d, J 9.0 Hz), 7.50 (2 H, d, J 9.0 Hz), 7.98 (1 H, s).

Z-α-(4-methoxy)phenyl-N-methyl nitrone ***(Z-101d)***. δ_H ($CDCl_3$, -10°C) 3.87 (6 H, s), 6.98 (2 H, d, J 9.0 Hz), 7.37 (1 H, s), 8.28 (2 H, d, J 9.0 Hz).

E-α-(4-methoxy)phenyl-N-methyl nitrone ***(E-101d)***. δ_H ($CDCl_3$, -10°C) 3.84 (6 H, s), 7.02 (2 H, d, J 9.0 Hz), 7.28 (2 H, d, J 9.0 Hz), 7.96 (1 H, s).

Z-α-(4-methyl)phenyl-N-methyl nitrone ***(Z-101e)***. δ_H ($CDCl_3$, -10°C) 2.41 (3 H, s), 3.90 (3 H, s), 7.28 (2 H, d, J 8.5 Hz), 7.42 (1 H, s), 8.20 (2 H, d, J 8.5 Hz)

E-α-(4-methyl)phenyl-N-methyl nitrone ***(E-101e)***. δ_H ($CDCl_3$, -10°C) 2.41 (3 H, s), 3.87 (3 H, s), 7.30 (4 H, underneath other signals), 8.00 (1 H, s)

Z-α-(4-dimethylamino)phenyl-N-methyl nitrone ***(Z-101f)***. δ_H ($CDCl_3$, -10°C) 3.02 (6 H, s), 3.84 (3 H, s), 6.74 (2 H, d, J 9.5 Hz), 7.27 (1 H, s), 8.22 (2 H, d, J 8.5 Hz)

E-α-(4-dimethylamino)phenyl-N-methyl nitrone ***(E-101f)***. δ_H ($CDCl_3$, -10°C) 2.99 (6 H, s), 3.89 (3 H, d, J 1.0 Hz), 6.74 (2 H, overlapping doublet), 7.92 (1 H, s).

Z-α-(3-nitro)phenyl-N-methyl nitrone ***(Z-101g)***. δ_H ($CDCl_3$, -10°C) 4.04 (3 H, s), 7.79 (1 H, s), 8.72 (1 H, d, J 8.0 Hz), 9.18 (1 H, s).

Z-α-(2-hydroxy)phenyl-N-methyl nitrone ***(Z-101h)***. δ_H ($CDCl_3$, -10°C) 3.94 (3 H, s), 6.88-7.58 (4 H, m), 7.66 (1 H, s), 12.40 (1 H, s).

E-α-(2-hydroxy)phenyl-N-methyl nitrone ***(E-101h)***. We couldn't detect the presence of E isomer.

Z-α-(2-methoxy)phenyl-N-methyl nitrone (Z-101i). δ_H ($CDCl_3$, -10°C) 3.87 (3 H, s), 3.92 (3 H, s), 6.94 (1 H, d, J 8.0 Hz), 7.08 (1 H, t, J 8.0 Hz), 7.45 (1 H, t, J 8.0 Hz), 7.92 (1 H, s), 9.30 (1 H, d, J 8.0 Hz).

E-α-(2-methoxy)phenyl-N-methyl nitrone (E-101i) δ_H ($CDCl_3$, -10°C) 3.87 (6 H, s), overlapping signals at δ 6.92-7.12 and 7.45 (3 H), 7.28 (1 H, d, J 8.0 Hz), 8.02 (1 H,s).

Z-α-phenyl-N-ethyl nitrone (Z-103). δ_H ($CDCl_3$, +10°C) 1.58 (3 H, t, J 7.0 Hz), 4.00 (2 H, q, J 7.0 Hz), 7.45 (3 H, m), 7.49 (1 H, s), 8.30 (2 H, m)

E-α-phenyl-N-ethyl nitrone (E-103). δ_H ($CDCl_3$, +10°C) 1.56 (3 H, t , J 7.0 Hz), 4.05 (2 H, q, J 7.0 Hz), 7.26-7.58 (5 H, m), 7.97 (1 H, s)

Z-α-phenyl-N-isopropyl nitrone (Z-105). δ_H ($CDCl_3$, +10°C) 1.51 (6 H, d, J 7.0 Hz), 4.23 (1 H, hept, J 7.0 Hz) 7.50 (1 H, s), 7.45 (3 H, m), 8.28 (2 H, m)

E-α-phenyl-N-isopropyl nitrone (E-105). δ_H ($CDCl_3$, +10°C) 1.44 (6 H, d, J 7.0 Hz), 4.72 (1 H, hept, J 7.0 Hz) 7.32 (1 H, s), 7.45 (3 H, m), 7.90 (1 H, s)

Z-α-phenyl-N-tertiarybutylnitrone (Z-107). δ_H ($CDCl_3$, +25°C) 1.60 (9 H, s), 7.43 (3 H, m), 7.58 (1 H, s), 8.33 (2 H, m).

4.4.2 ^{1}H NMR Chemical Shifts of the Non Conjugated Nitrones

α-methenyl-N-benzyl nitrone (102a). δ_H ($CDCl_3$, -10°C) 4.98 (2 H, s), 6.32 (1 H, d, J 8.0 Hz), 6.64 (1 H, d, J 8.0 Hz), 7.5 (5 H, m).

α-methenyl-N-(4-nitro)benzyl nitrone (102b). δ_H ($CDCl_3$, -10°C) 5.10 (2 H, s), 6.56 (1 H, d, J 7.0 Hz), 6.68 (1 H, d, J 7.0 Hz), 7.60 (1 H, d, J 8.0 Hz), overlapping signal at δ.8.34 (2 H).

*α-methenyl-N-(4-Chloro)benzyl nitrone (**102c**)*. δ_H ($CDCl_3$, -10°C) 4.94 (2 H, s), 6.38 (1 H, d, J 7.0 Hz), 6.62 (1 H, d, J 7.0 Hz), 7.44 (4 H, overlapping AB).

*α-methenyl-N-(4-methoxy)benzyl nitrone (**102d**)*. δ_H ($CDCl_3$, -10°C) 3.84 (3 H, s), 4.88 (2 H, s), 6.24 (1 H, d, J 8.0 Hz), 6.58 (1 H, d, J 8.0 Hz), 6.98 (2 H, d, J 9.0 Hz).7.39 (2 H, d, J 9.0 Hz).

*α-methenyl-N-(4-methyl)benzyl nitrone (**102e**)*. δ_H ($CDCl_3$, -10°C) 2.39 (3 H, s), 4.94 (2 H, s), 6.26 (1 H, d, J 8.0 Hz), 6.60 (1 H, d, J 8.0 Hz), 7.30 (4 H, underneath other signals).

*α-methenyl-N-(4-dimethylamino)benzyl nitrone (**102f**)*. δ_H ($CDCl_3$, -10°C) 2.99 (6 H, s, underneath other signals), 4.85 (2 H, s), 6.19 (1 H, d, J 8.0 Hz), 6.60 (1 H, d, J 8.0 Hz),6.76 (2 H, d, J 9.0 Hz, underneath other signals), 7.30 (2 H, d, J 9.0 Hz, underneath other signals).

*α-methenyl-N-(3-nitro)benzyl nitrone (**102g**)*. δ_H ($CDCl_3$, -10°C) 5.14 (2 H, s), 6.67 (2 H, s),

*α-methenyl-N-(2-hydroxy)benzyl nitrone (**102h**)*. δ_H ($CDCl_3$, -10°C) 5.10 (2 H, s), 6.70 (2 H, s), 6.68 -7.58 (4 H, m).

*α-methenyl-N-(2-methoxy)benzyl nitrone (**102i**)*. δ_H ($CDCl_3$, -10°C) 3.87 (3 H, s), 5.00 (2 H, s), 6.27 (1 H, d, J 8.0 Hz), 6.60 (1 H, d, J 8.0 Hz), overlapping signals at δ 6.92-7.12 and 7.45 (4 H).

α-ethenyl-N-benzyl nitrone (104). δ_H ($CDCl_3$, +10°C) 2.02 (3 H, d, J 6.0 Hz), 4.92 (2 H, s) 6.77 (1 H, q, J 6.0 Hz), 7.50 (5 H, m)

α-isopropenyl-N-benzyl nitrone (106). δ_H ($CDCl_3$, +25°C) 2.14 (3 H, s), 2.19 (3 H, s), 5.09 (2 H, s), 7.45 (5 H, s).

5

RESULTS AND DISCUSSION

5.1 Rotation Inversion Dichotomy

In acylic hydroxylamines **98** the diastereotopic methylene hydrogens appear as a AB quartet in the ^{1}H NMR spectrum at low temperatures. At higher temperature the chiral amine **98A** (the most stable conformer with bonds and lone pairs formally eclipsed) would undergo stereomutation to the enantiomer **98A*** (Scheme 5.1) and when the rate process

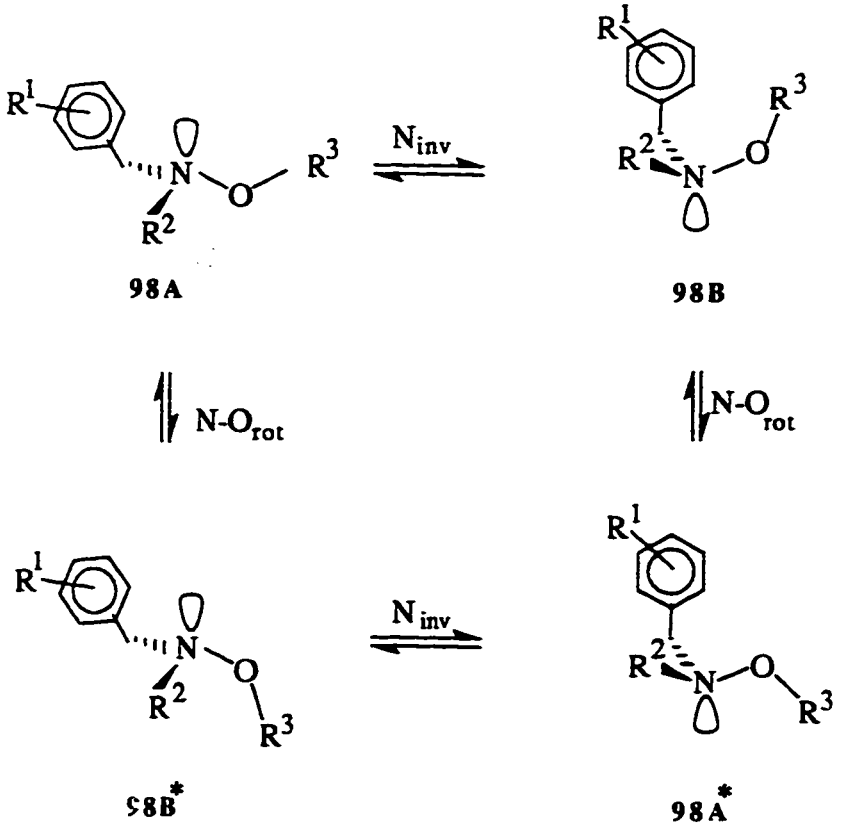

Scheme 5.1: Stereomutation in acyclic hydroxylamines.

becomes faster in the NMR time scale the methylene AB quartet coalesces and then appears as a singlet [45].

Such a stereomutation requires two steps: nitrogen inversion and N-O bond rotation, both of which have considerable and comparable energy barriers. As a consequence there has been considerable discussion (and controversy) as to whether nitrogen inversion [30] or N-O rotation [32,116] or even a complex composite of both (in an energy saving pathway) is the rate limiting step [60]. While solvent study provided conflicting conclusion, numerous experimental evidences point out that steric acceleration and deceleration of the rate is an indication of inversion and rotation controlled rate limiting process respectively. Steric crowding raises the energy of the pyramidal ground state whereas in the planar transition state for the inversion with extended CNC angle (120°C) such crowding is relieved and as a consequence energy barrier decreases. Steric crowding on the other hand would obviously raise the energy barrier for the rotational process [60].

It is well known that electronegative substitutents (O, N, halogens) on nitrogen raises the inversion barrier by their σ inductive electron withdrawing ability and π repulsive character due to the lone pairs. Both electronegativity and maximized lone pair repulsion destablizes the planar transition state. The relative contribution of these two effects (which are the origins of 'hetero effect') still remains a long-standing question which many most researchers including theoreticians have been unable to answer [55b].

In order to study the substituent effects on the inversion and rotational behaviour a multitude of hydroxylamine derivatives **108-117** and isoxazolidines **123, 124** have been synthesized (Scheme 5.2). By locking at the N-O bond in the ring skeleton of 5-membered ring **123, 124** the rotational aspect will be precluded. Presence of ethoxy group at C5 in isoxazolidines **123, 124** would also enable to study anomeric effect in 5 membered ring system.

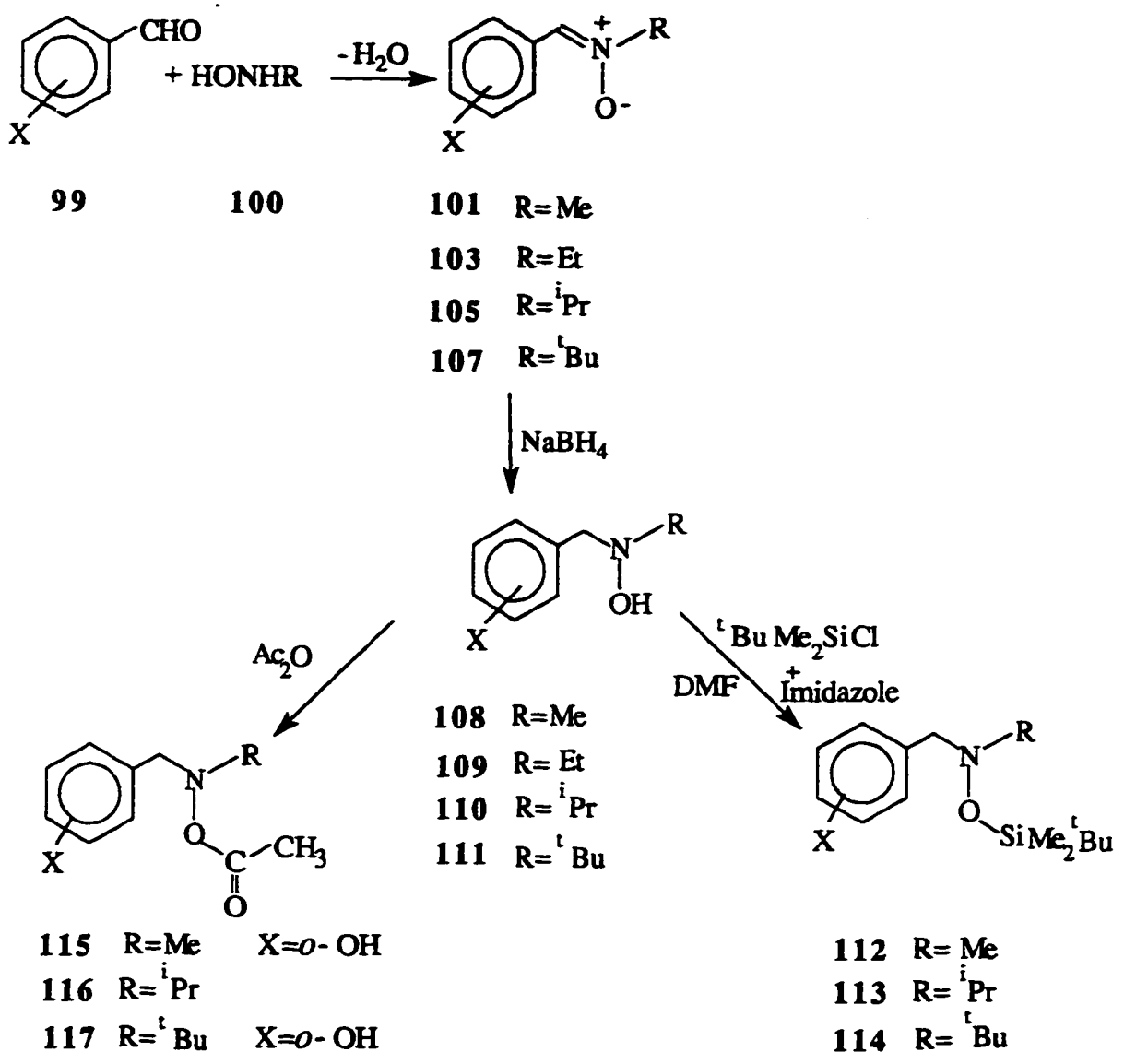

Scheme 5.2: Synthetic routes to various hydroxylamine derivatives.

Nitrones **101,103,105,107** with a variety of alkyl (R) groups and substituents X were prepared by condensation reaction of the corresponding aromatic aldehydes **99** and hydroxylamines **100**. The nitrones on reduction with sodium borohydride afforded the hydroxylamines **108-111** required for the study of inversion and rotational energy

barriers. A series of N-acetoxy derivatives **115,116,117** were obtained by treating the hydroxylamines with acetic anhydride (Scheme 5.2).

The hydroxylamines **108a, 110a** and **111a** were silylated with *tertiary* butyldimethylchlorosilane in the presence of imidazole to give the compounds **112, 113** and **114** respectively. The various compounds studied are included in Table 5.1-5.3.

With a series of di- and tri- substituted hydroxylamines in hand a study of the inversion /rotation process by ^{1}H NMR spectroscopy. At ambient temperature benzylic protons in most of the compounds appeared as broad singlets which on lowering the temperature became AB quartets. The complete bandshape analysis yielded the rate constants and the free energy of activation ($\Delta G^{\#}$) calculated using transition state theory:

$$k=(k_BT/h)\exp(-\Delta G^{\#}/RT) \qquad 3.10$$

The activation parameters $\Delta H^{\#}$ and $\Delta S^{\#}$ were calculated from the plots of ln (k/T) vs 1/T. It is well known [114] that NMR bandshape fitting frequently gives mutually compensating systematic errors in $\Delta H^{\#}$ and $\Delta S^{\#}$ ($\pm$0.8 kJ mol^{-1} and $\pm$4 J mol^{-1} K^{-1} respectively) and are not reported here. However, the bandshape fitting is viewed as a method of getting rather accurate values (probably to within $\pm$ 0.5 kJ mol^{-1}) for $\Delta G^{\#}$ in the vicinity of the coalescence temperature (see Appendix). The $\Delta G^{\#}$ values calculated at 0°C are reported in Table 5.1- 5.3.

For the hydroxylamines **109, 110a** and **111a** (Table 5.1) the barriers obtained fits best with the nitrogen inversion as the rate determining step. The compound **111a** with the most crowded *tertiary* butyl group has the lowest energy barrier as a consequence of the steric acceleration of the rate of inversion. However increased steric crowding in the silylated derivatives **112, 113** and **114** caused steric deceleration of the rate of inversion in comparison to their corresponding hydroxylamines (cf. **110a** and **113**; **111a** and **114**). Incorporation of the silyl group increases the barrier by almost 8 kJ/mol and the barriers observed fit best with the N-O rotation as the rate limiting process. Involvement of

Table 5.1: Compounds studied and their nitrogen inversion barriers in $CDCl_3$

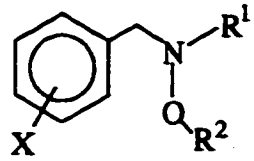

Compound No	X	R1	R2	$\Delta G^{\#}$ (273K) kJ/mol
108a	H	Me	H	55.8[a]
112	H	Me	$SiMe_2{}^tBu$	57.8
109	H	Et	H	55.3
110a	H	^iPr	H	51.6
113	H	^iPr	$SiMe_2{}^tBu$	59.2
111	H	^tBu	H	49.2
114	H	^tBu	$SiMe_2{}^tBu$	56.1
108b	*p*- NO_2	Me	H	52.3
108c	*p* - Cl	Me	H	-
108d	*p* - OMe	Me	H	-
108e	*p* - Me	Me	H	56.6
108f	*p* - NMe_2	Me	H	57.7
108g	*m* - NO_2	Me	H	54.1
108i	*o*- OMe	Me	H	56.2

[a] Extrapolated from the Hammett plot (Figure 5.1).

Table 5.2: Energy barriers of various N-*iso*propyl hydroxylamine derivatives in $CDCl_3$.

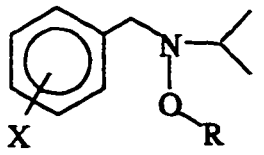

Compound No.	X	R	$\Delta G^{\#}_{(273K)}$ kJ/mol
110a	H	H	51.6
116a	H	Ac	50.2
110b	*p*-NO2	H	49.5
116b	*p*-NO_2	Ac	48.7
110c	*p*-Cl	H	51.0
116c	*p*-Cl	Ac	50.2
110d	*p*-OMe	H	52.0
116d	*p*-OMe	Ac	50.7
110e	*p*-Me	H	51.3
116e	*p*-Me	Ac	50.7
110f	*p*-NMe_2	H	52.1
116f	*p*-NMe_2	Ac	51.2
110g	*m*-NO_2	H	50.4
116g	*m*-NO_2	Ac	49.0
110h	*m*-Br	H	50.7
116h	*m*-Br	Ac	49.9
110i	*p*-Br	H	51.2
116i	*p*-Br	Ac	50.2
110j	2,4,5-$(OMe)_3$	H	54.3
116j	2,4,5-$(OMe)_3$	Ac	53.9
110k	*p*-OH	H	52.2
116k	*p*-OH	Ac	51.9

Table 5.3 Compounds studied and their nitrogen inversion barriers in $CDCl_3$

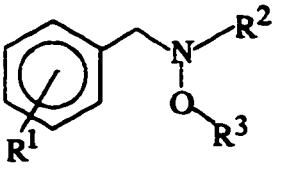

Compound	R^1	R^2	R^3	$\Delta G^{\#}$(273 K) kJ/mol	
108h	*o*-OH	CH_3	H	61.2	
115	*o*-OH	CH_3	Ac	57.8	
110l	*o*-OH	^{i}Pr	H	59.8	(53.5)[b]
116l	*o*-OH	^{i}Pr	Ac	60.6	
111b	*o*-OH	^{t}Bu	H	58.8	
117	*o*-OH	^{t}Bu	Ac	59.2	
110k	*p*-OH	^{i}Pr	H	52.2	(51.7)[b]
116k	*p*-OH	^{i}Pr	Ac	51.9	
110m	*o*-OCH_3	^{i}Pr	H	51.0	
116m	*o*-OCH_3	^{i}Pr	Ac	49.2	
110a	H	^{i}Pr	H	51.6	
116a	H	^{i}Pr	Ac	50.2	
118	*o*-$OSi(CH)_3{}^{t}Bu$	CH_3	H	54.9	
119	*o*-OH	CH_3	$Si(CH)_3{}^{t}Bu$	66.8	
120	*o*-$OSi(CH)_3{}^{t}Bu$	CH_3	$Si(CH)_3{}^{t}Bu$	62.8	

[a] Ac=CH_3CO ^{i}Pr=$(CH_3)_2CH$ ^{t}Bu=$(CH_3)_3C$ [b] in CD_3OD

vacant d orbitals in silicon in bonding with the oxygen lone pair should decrease the barriers for both the inversion and rotational processes in so far as the destabilization of the transition state by lone pair repulsion is concerned. However steric encumbrance of the silyl group forces the rotational process to play a dominant part in the overall process. In the series **112, 113** and **114** changing the R' group from methyl to *iso*propyl causes an increase in the energy barrier in line with the rate limiting rotational process. However changing to *tertiary* butyl groups (compound **114**) makes the barrier lower than the *iso* propyl **113** or even methyl derivative **112.** Lowest energy pathway leading to inversion follows sequential rotation [39] and inversion process as predicted by molecular orbital calculations [44] on simpler related model compounds. However it is suggested in a recent study that complex composite of the two processes with an energy saving pathway may constitute a single process. It is tempting to contemplate that near or at the transition state for the nitrogen inversion, the rotation around the extended C-N-C bond (with bond angle of 120°) would be easier than when it is pyramidal. In such a complex process, however, the substituent effects will also be complex.

In order to assess the importance of substituents on the nitrogen inversion process we measured the energy barrier for hydroxylamines **108b, 108e-108g, 108i** (Table 5.1). For compounds with X = H (**108a**), *p* -Cl (**108c**) and *p* -OMe (**108d**) we did not observe the usual AB quartet for the benzyl methylene protons at -40°C which is well below the coalescence temperature of the other compounds in this series. This could be attributed to accidental rather than real equivalence of the methylene protons. However, at around -90°C the methylene proton signals of **108a** did indeed split into an AB quartet (δ_A 3.51 ppm, 1 H, J 12.0 Hz; δ_B 3.66 ppm, 1 H, J 12.0 Hz). Increasing the temperature did not broaden the line width as is observed in the usual exchange process. However, the chemical shift difference between the methylene protons decreases and finally it becomes a singlet at around -40°C. At -90°C the separation of the inner peaks was 15.0 Hz. However

at -70, -50 and -40°C this separation became 4.76, 2.5 and 0 Hz respectively. The similar observation was made for the *p* -Cl (**108c**) and *p* -OMe (**108d**) derivatives. This is actually a temperature dependence of chemical shifts rather than an exchange phenomena. Hammett plot of free energy of activation against substituent constant σ (Figure 5.1) and using the free-energy form of the Hammett equation,

$$\Delta G^{\#} = -2.3\ RT\rho\sigma + \Delta G_o^{\#}$$

a value of +0.648 for the reaction constant, ρ, is obtained. Transition state for the inversion process is, thus, richer in electron density and perhaps through -space' conjugate with the aromatic ring or the inductive effect stabilizes the planar transition state.

Free energy of activation for the exchange process in the N-hydroxy and N-acetoxy compounds in the *iso*propyl series **110** and **116** are included in Table 5.2 and the Hammett plots are shown in Figures 5.2 and 5.3. The acetyl derivatives have barriers approximately 1 kJ/mol lower than their parent hydroxylamines. While the acetoxy group by virtue of being more electronegative than OH group should increase the inversion barrier, depletion of the lone pair density in oxygen by delocalization into the acyl group decreases the activation energy. However such a small lowering of activation energy, presumably, reflects lesser dominance of nitrogen inversion; increase in the steric bulk owing to the incorporation of acyl group moves the process more towards N-O rotation-controlled process. Positive ρ values of 0.33 and 0.35 for the hydroxy **110** and acetoxy **116** series, respectively, again demonstrates the increased electron density in the planar transition state.

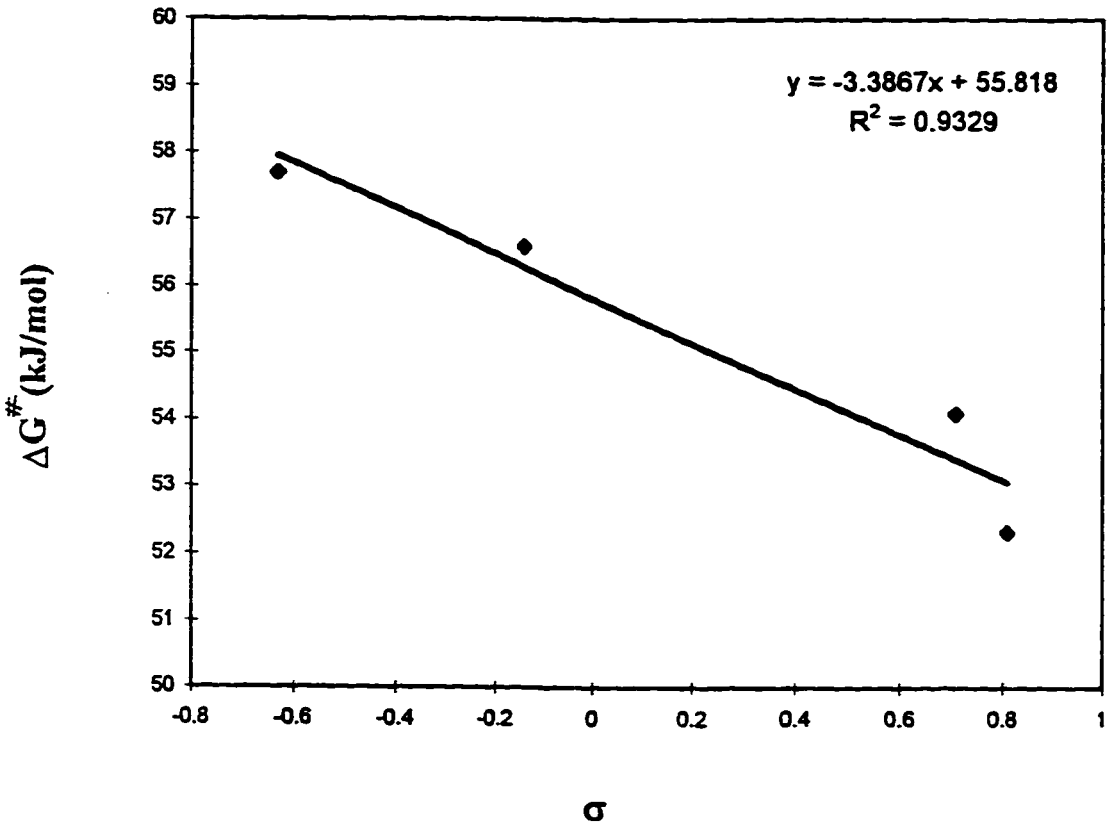

Figure 5.1 Hammett plot for the nitrogen inversion barrier in N-aryl-N-methyl hydroxylamines (108).

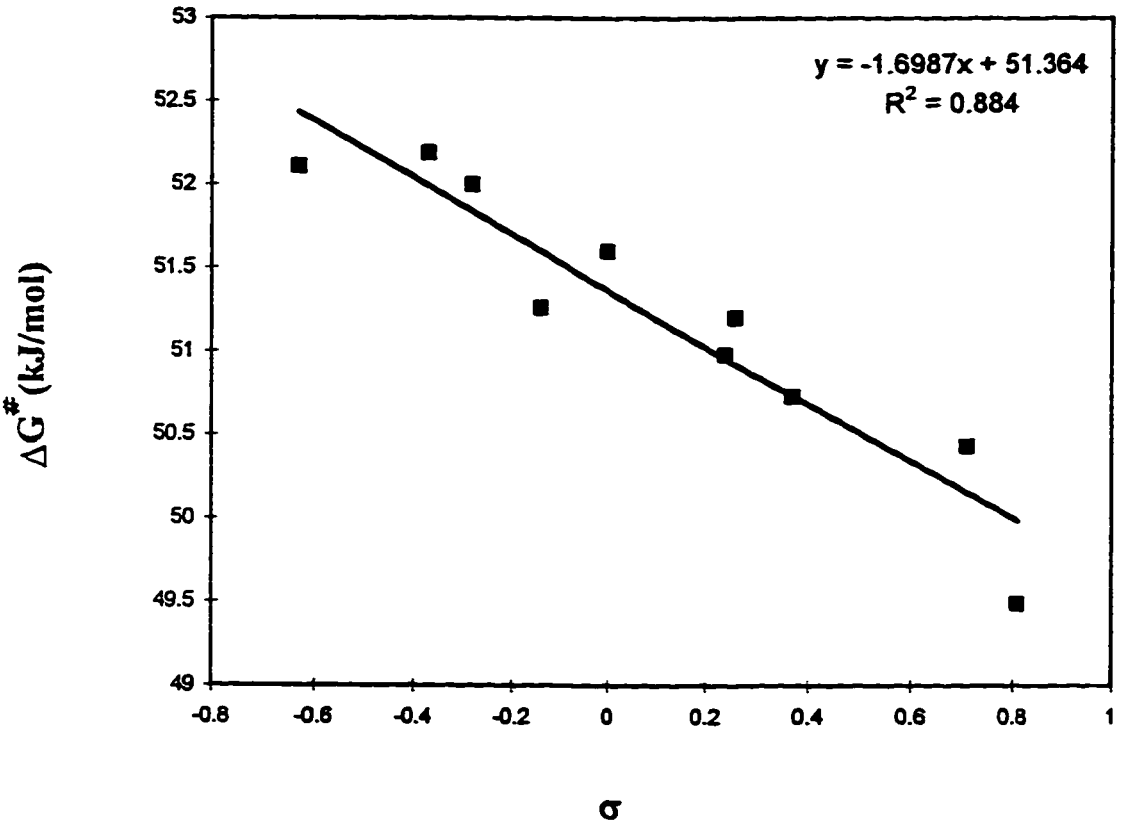

Figure 5.2 Hammett plot for the nitrogen inversion barrier in N-aryl-N-isopropyl hydroxylamines (110).

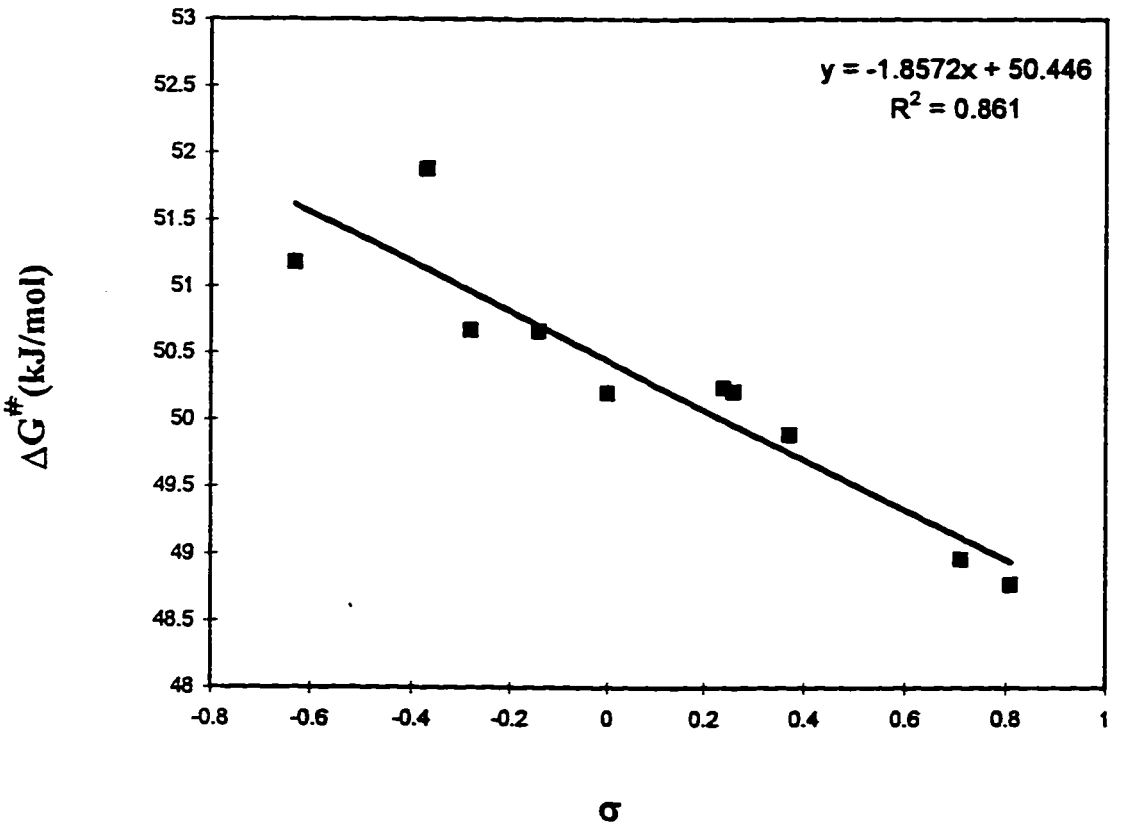

Figure 5.3 Hammett plot for the nitrogen inversion barrier in N-aryl-N-isopropyl-O-acetyl hydroxylamines (116).

5.2 Effect of Hydrogen Bonding.

Hydroxylamines, owing to their unique conformational properties, have etched an important place in the field of conformation analysis. [45] Both theoretical calculations [25] and experimental discoveries [27] have surprised the chemists by the finding that the most stable conformation **28a**, in complete contrast to its organic counterparts (ethane, methanol, methylamine), has the lone pairs and bonds formally eclipsed and N-O bond rotation has to traverse a pathway leading to the less stable staggered conformation **28d**, with a very high barrier of ~50 kJ mol^{-1}. The sp^3 hybridized nitrogen atom in hydroxylamines with a

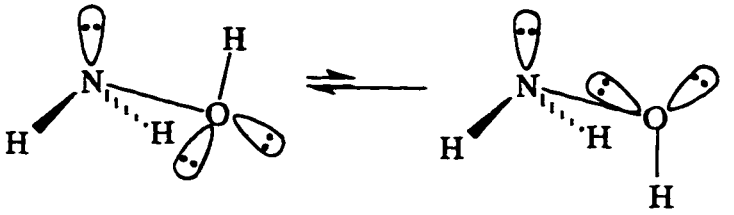

28a **28d**

pyramidal geometry is also capable of changing its conformation by inversion of its configuration *via* sp^2 hybridized planar transition state. The σ inductive effect of electronegative oxygen attached to nitrogen and π repulsive effect in the transition state, quite interestingly, raises the barrier to nitrogen inversion to the similar magnitude as in the rotational process [55].

Inability of the chiral hydroxylamine derivative **98** to sustain optical activity can be attributed to the nitrogen inversion and N-O bond rotation [31] leading to the enantiomer A*(Scheme 5.3). The benzylic protons in **98** are diastereotopic in either structure but become non-equivalent when either nitrogen inversion or bond rotation or both become slow on the NMR time scale [45]. Thus the NMR spectra of these compounds show temperature dependence and the methylene proton resonances, at lower temperatures appear as AB quartets, which coalesce and become a singlet with the increase in the temperature.

Whether bond rotation [32, 116] or nitrogen inversion [30] or a complex composite of both is the rate determining step (in the total inversion pathway as shown in Scheme 5.3) still

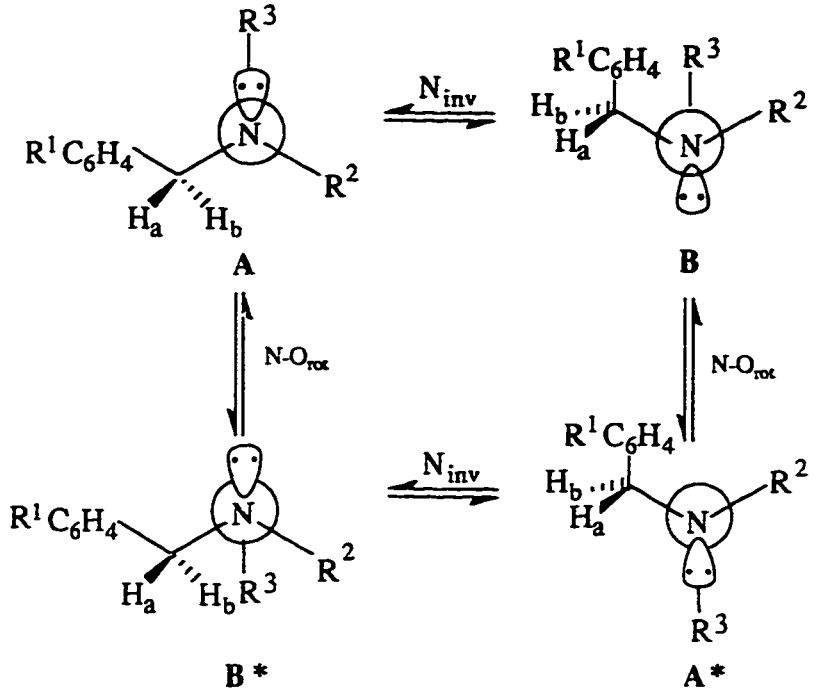

98

Scheme 5.3: Interconversion of diastereomers.

remains a matter of controversy and speculation [12]. Usually polar solvents and steric crowding in the pyramidal ground state accelerate the nitrogen inversion process. The transition state, which has a higher dipole moment than the ground state, is stabilized by polar solvents thereby lowering the inversion barrier. On the other hand, steric crowding in the ground state raises the energy of the ground state and hence lowers the barrier. The transition state has more space with extended CNC and ONC angles (120°) to make room for the bulky substituents [30]. However, steric deceleration and solvent independency would point toward bond rotation as the rate-limiting process in the total inversion pathway [60].

While hydrogen bonding in solvents like methanol raise the nitrogen inversion barrier in trialkylamines [117-119] by 4-8 kJ mol^{-1} by stabilizing the staggered ground state

conformers, protic solvent in contrast, lowers the barrier in acyclic dialkyl- and trialkylhydroxylamines [32,120,121] but increases the barrier in cyclic trialkylhydroxyl. amines [61] (in which N-O bond is a part of ring skeleton). In acyclic system, however, solvent interaction with lone pairs destabilizes the eclipsed ground state and hence lowers both the nitrogen inversion and bond rotation barriers. In cyclic system, however, geometric constraints do not permit N-O bond rotation or lone pair eclipsing with bonds and the hydrogen bonding thus stabilizes the ground state. Site of hydrogen bonding (at N or O) may also vary from compound to compound and as such the study of solvent effects does not really add much to the knowledge of distinguishing inversion from rotation process. [60]

Condensation of aromatic aldehydes **99** with hydroxylamines **100** gave the nitrones **101-107** which on reduction with sodiumborohydride afforded the hydroxylamines **108, 110, 111** in good overall yield (Scheme 5.2). The hydroxylamines on treatment with 1.1 equivalent of acetic anhydride led to the formation of monoacetyl derivatives **115, 116, 117** selectively (Scheme 5.2, Table 5.3). Phenolic hydroxyl group was found to be unreactive towards acetic anhydride under the reaction conditions. Quite interestingly this was found not to be the case in the reaction with 1.1 equivalent of *tertiary*-butyldimethylchlorosilane. Thus, the hydroxylamine **108h** afforded a mixture of mono- (**118, 119**) and di-silylated derivatives **120** (Scheme 5.4). The difference in the selectivity of the two hydroxyl groups towards acetic anhydride and the silylating agent could be attributed to the differences in the nucleophilicity of the oxygens in phenolic OH and N-OH. While oxygen attached to the nitrogen is more nucleophilic due to the lone pair repulsion, the lone pair in phenolic hydroxyl group is appreciably delocalized. However, in the presence of imidazole, presumably, the conjugate base (obtained by abstraction of the more acidic phenolic proton) in equilibrium with the hydroxylamine **108h** can effectively compete with the N-OH to give a mixture of compounds **118-120**.

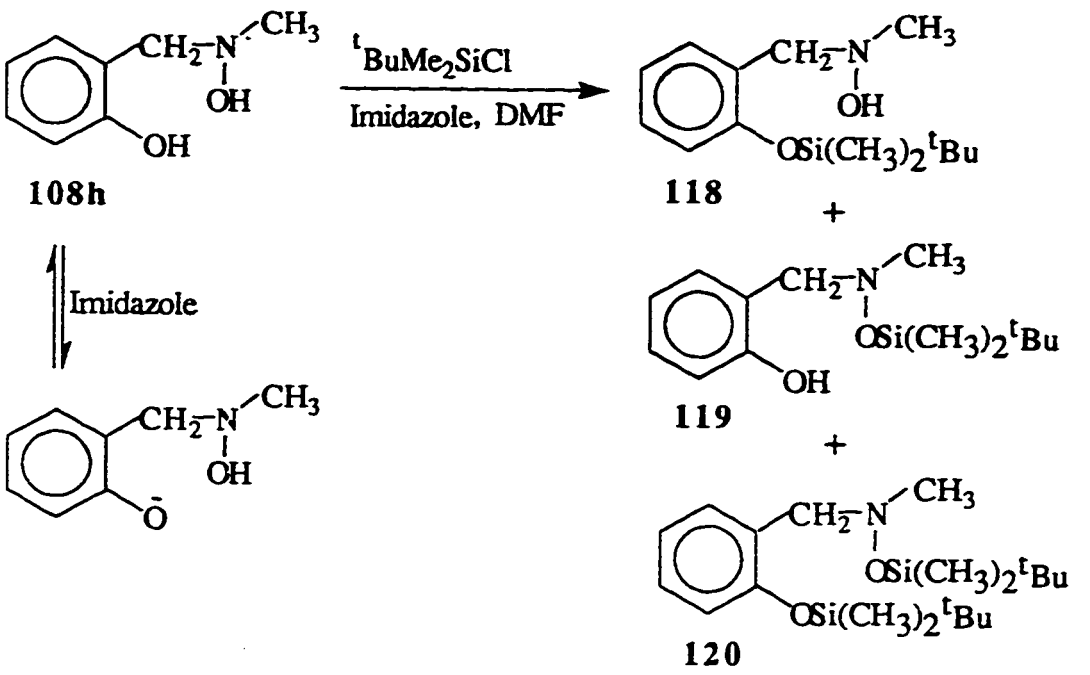

Scheme 5.4: Synthetic route to silyl derivatives.

For the hydroxylamines (**110, 116**) **a, k, m** the barriers obtained (Table 5.3) fits best with nitrogen inversion as the rate determining step. The acetyl derivatives **116 a, k,** m have lower barriers than their corresponding N-OH compounds **110 a, k, m.** Acetyl ($CH_3C{=}O$) group with a strong conjugative interaction with the oxygen lone pair reduces the lone pair repulsion in the transition state for the inversion process thus results in the decrease in the barriers. Acetyl being bulkier than hydrogen also helps the inversion process. A dominant contribution from N-O bond rotation would have resulted in an increased barriers for the acetyl derivatives.

The compounds discussed so far have substantially lower barriers than the barriers observed for the rest of the hydroxylamines in the table. Sterically, the pair **110m, 116m** is not much different from the pair **110l, 116l**; however an increase of ~ 10 kJ mol^{-1} in the barrier is observed for the latter. This could be attributed to the presence of intramolecular hydrogen bonding which stabilizes the ground pyramidal state, and an

additional amount of energy must be supplied to break the hydrogen bond in the inversion pathway. In the series **108h**, **110l** and **111b** changing the R^2 from methyl to *iso* propyl to *tertiary* butyl group, a gradual decrease in the barrier reflects the dominance of inversion rather than N-O bond rotation. In the acetyl derivatives **115**, **116l** and **117** no clear trend is observed. Both *iso* propyl and *tertiary* butyl derivatives **116l** and **117** only have higher barriers than their corresponding N-OH compounds **110l** and **111b** and the acetyl derivative **115**. Repulsion between oxygen and nitrogen lone pairs in the transition state, is reduced by electron withdrawing conjugating substituent acyl on the oxygen and as such this electronic effect should lower both nitrogen inversion and rotational barriers. However steric effect raises the rotational barriers but lowers the inversion barrier. In compound **116l** and **117** the dominant rotational contribution due to steric crowding of *iso*propyl */tertiary* butyl and acetyl groups increase the overall barrier of the inversion pathway. Dominant rotational contribution should have imparted greater destabilization of the transition state for the *tertiary* butyl derivative **111b** than its *iso* propyl counterpart **110l**. However, this was found to be not the case. Steric and electronic effects give different contributions to the barriers to inversion and rotation. Comparing the energy barriers in compounds (**110**, **116**) **a**, **l**, **m** it is evident that the breaking of hydrogen bond contributes an additional ~10 kJ/mol of energy to the barrier.

Among the compounds presented in the Table 5.3 the monosilyl derivative **119** was found to have the highest barrier of 66.8 kJ mol^{-1}. Involvement of vacant d orbitals in silicon in bonding with the oxygen lone pair should decrease the barriers for both the inversion and rotational processes in so far as the destabilization of the transition state by lone pair repulsion is concerned. However steric encumbrance of the silyl group forces the rotational process to play a dominant part in the overall process. Among the compounds **108h**, **118-120** the disilylated derivative **120** is the most crowded around the N-O bond, yet steric acceleration of the process is not observed. The compound **120** even has higher barrier than that of **108h** indicating that the additional difficulty in N-O bond rotation in the

former is more than the difficulty in the nitrogen inversion due to hydrogen bonding in the latter. While the nitrogen inversion is the rate controlling step in the monosilyl compound **118**, the N-O bond rotation dictates the barrier in mono **119** and disilylated derivative **120**.

While in methanol the inversion barrier is decreased noticeably for the *ortho*-hydroxy compound **110l** by an amount of 6.3 kJ/mol, the barrier remained virtually similar for the *para*- hydroxy derivative **110k**. This strongly suggests the involvement of intramolecular hydrogen bonding in **110l** in $CDCl_3$ but not in methanol which effectively competes with the *ortho* - hydroxy substituent for hydrogen- bonding with the nitrogen lone pair.

Intramolecular hydrogen bonding can be confirmed somewhat from the crystal structure of the compound **116l**. As is evident from the ORTEP diagram (Figure 5.4) the N1-O4 distance of 2.748A° indicates the presence of intramolecular hydrogen bonding. The dihedral angles of C5-N1-O2-C15 and C12-N1-O2-C15 were found to be 105.97° and 129.46°, respectively. Assuming the nitrogen lone pair symmetrically located with respect to the dialkyl substituents on nitrogen, the oxygen substituent is thus found to be within 12° of eclipsing the nitrogen lone pair. The ORTEP diagram also demonstrates the expected *cis* planar arrangement of the O-N and C=O bonds [122] (the N1-O2-C15-O3 dihedral angle was found to be 4.21°).

To the best of our knowledge, this study demonstrates for the first time the effect of intramolecular hydrogen bonding (involving phenolic hydroxyl group) in nitrogen inversion barrier in acyclic hydroxylamines. Increasing the bulk around the N-O bond, the rate controlling step of the overall inversion pathway switches from nitrogen inversion to N-O bond rotation. The X-ray structure substantiates the finding that the more stable form has the eclipsed conformation.

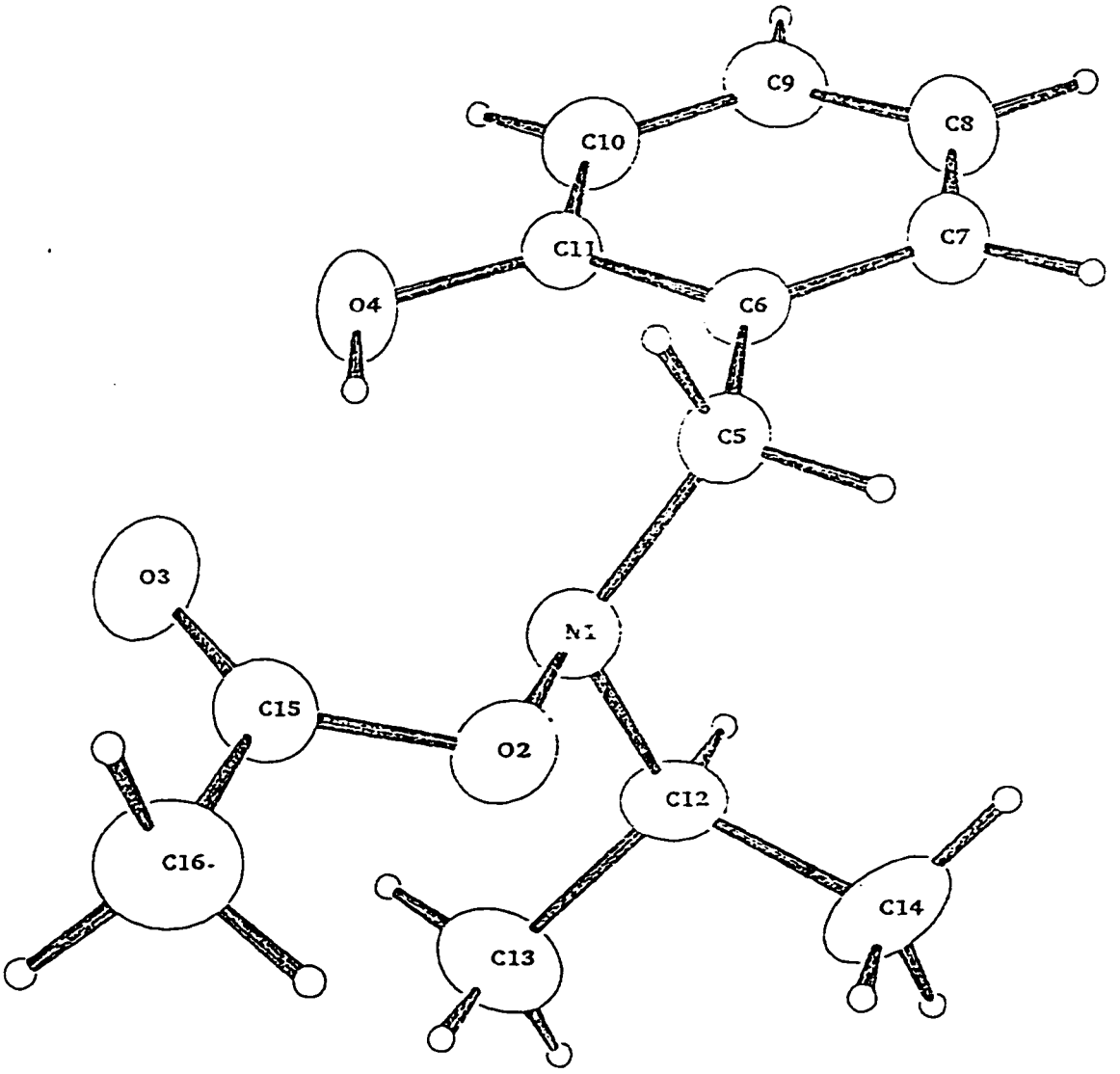

Figure 5.4 ORTEP diagram of the compound **116l**.

5.3 Anomeric Effect and Nitrogen Inversion in Isoxazolidines

While the use of ^1H NMR coupling constants using Karplus equation is highly successful in assigning configuration in six-membered rings, such applications often do not work well with five-membered ring systems. This is not surprising in view of the fact that the five-membered ring does not have a well-defined conformation as in six-membered systems.[123] Isoxazolidines, an important five-membered ring system, have been extensively used as key intermediates in the synthesis of various natural products [124]. Most of the NMR studies on isoxazoldines centre around conformationally rigid compounds having alkoxy group at either N or at C-5 position, where substituents by virtue of exerting strong anomeric effect fixes the geometry with axially oriented alkoxy substituent [24]. In one such study [125] it has been shown that the trisubstituted isoxazolidine **121** in solution adopts the conformation **A** with two substituents in an unfavourable 1,3-dipseudoaxial orientation. Absence of the conformer **B** was attributed [125] to the unfavourable electronic interaction arising out of the antiperiplanar arrangement of the lone pairs on the ring heteroatoms. It was argued [126] that the invertomer **A** like the hydrazine, hydroxlamines and hydroperoxides

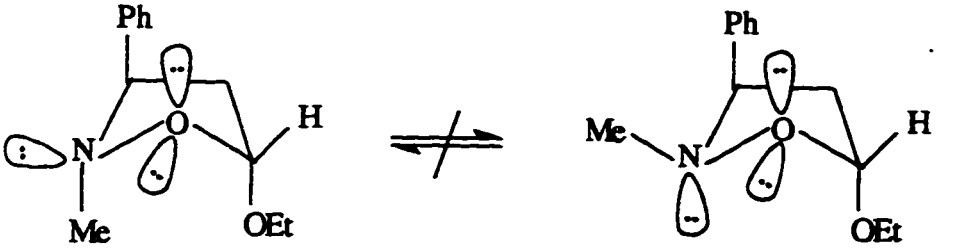

121-A **121-B**

Figure 5.5. The two conformations of the trisubtituted isoxazolidine **121.**

enjoys the favourable *gauche* relationship between the lone pairs on the adjacent heteroatoms. However, the authors in justifying the adaptation of the conformer **A**

overlooked the steric factors which destabilizes and thus excludes the presence of the invertomer **B** with *cis* disposition of the 2,3-substituents. *Trans* -1,2- Dimethylcyclopentane is more stable than its *cis* counterpart by an enthalpy difference of 7.2 - 8.7 kJ/mol. [123] Effects of substituents larger than methyl and shorter bond lengths due to presence of heteroatoms in the ring skeleton are expected to increase the enthalpy difference to such an extent that the invertomer **B** with *cis* disposition of the 2,3-substituents cannot be detected by NMR. One has to consider the effects of three factors involved in the selection of the favoured configuration. While the *gauche* orientation of the lone pair and the *trans* disposition of the 2,3- substituents favours the invertomer A, the diaxial orientation of 2,5-substituents is likely to disfavour it. It would be interesting to find out whether, in the absence of any substituents at C-3, the *gauche* orientation of the lone pairs may alone impart enough stability to make the invertomer of the type A as the sole isomer.

With this in mind, a series of isoxazolidines **123**, which are devoid of any substituent at C-3, were prepared to study the configurational and conformational aspects as well as nitrogen inversion process by NMR spectroscopy.

Dipolar cycloaddition of nitrone **122** and ethyl vinyl ether at 70°C for 1.5 h resulted in regiospecific formation of the isoxazolidines **123**. The NMR spectra of the crude and purified adducts failed to detect the presence of regioisomeric adduct with ethoxy group at the C-4 position. Similar regiospecificity was observed in various cycloaddition reactions with vinyl ethers [24,127]. The spectra of the adducts when measured in $CDCl_3$ at 50°C displayed either a doublet (J = ~5 Hz) or a doublet of doublets (J =~1.5, 5.5 Hz) at around

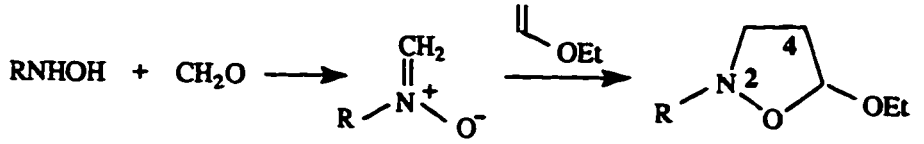

100 **122** **123**

δ 5.2 assigned to the C-5 proton. The isoxazolidines **123** can, in principle, exist in several puckered conformations with geometry of envelope and half-chair forms. Ring puckering would lead to the relief of bond eclipsing strain and maximum puckering should occur at such part of the ring so as to give the substituents favourable pseudoequatorial orientation. *Cis*-1,3-Dimethlcyclopentane is presumed to take diequatorially substituted envelope form with the C-2 at the tip of the envelope [123]. Nitrogen inversion process is expected to allow the isoxazolidines **123** to remain either as *cis*- or *trans*- isomer or as a mixture of both with the relative proportions depending on their thermodynamic stability. The pseudo-equatorial -axial substituted *trans*-isoxazolidine is expected to exist in two forms **B** and **C** which are in equilibrium by fast pseudorotation (Scheme 5.5).

Relatively slow nitrogen inversion (N_i) would transform the *cis* isomer **A** into the *trans* isomer **B** which on pseudorotation (P_r) goes to conformer **C**. Nitrogen inversion of **C** into **D** followed by pseudorotation to **A** completes the dynamic cycle of these conformers /isomers. Small coupling constants of 0-1.5 Hz indicate that the isoxazolidines **123** at high temperature (50°C) exist in an average conformation where the dihedral angle between the C-5 proton and one of the C-4 protons is ~90°. Inspection of the Dreiding models indicated that a dihedral angle of 90° is possible between H_a and H_c in conformations **A** and **B** with pseudoaxially oriented ethoxy group. Presence of the conformers **C** and **D** with pseudoequatorially oriented ethoxy group, is excluded since the dihedral angles between H_a/H_b and H_a/H_c being nearly 0 and 180° would lead to much larger coupling constants. On steric grounds the conformation **B** is expected to be more stable than the 2,5-dipseudoaxially substituted isomer **A**. However, the isomer **A** has the advantage of having the lone pairs in gauche relationship. Both *cis* and *trans* isomers adopt the pseudoaxial orientation of ethoxy group in **A** and **B** to take advantage of the stabilization of an anomeric effect between the axially oriented lone pair on the ring oxygen and the ethoxy group.

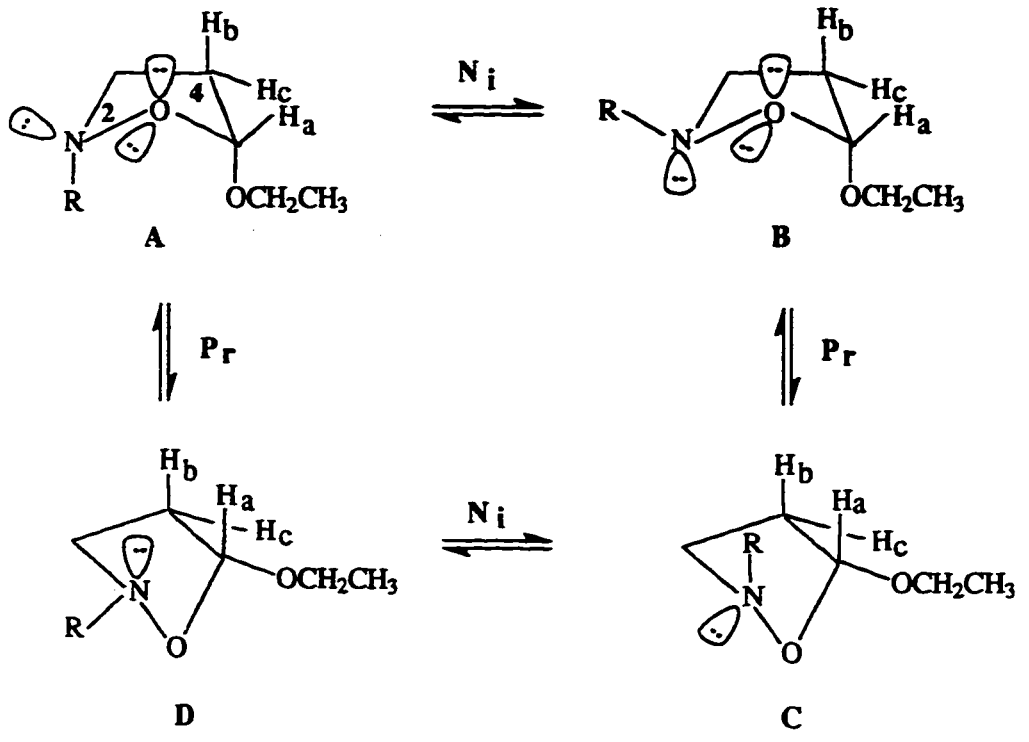

Scheme 5.5: Nitrogen inversion and pseudorotation in isoxazolidines.

Relatively slow nitrogen inversion is observed in these isoxazolidines to give broadened peaks in ^{1}H and ^{13}C NMR spectra recorded at ambient temperature. On lowering the temperature the spectral lines become sharper and show two distinct forms of the compounds. The ^{13}C NMR chemical shifts were assigned on the basis of general chemical shifts arguments and consideration of substituent effects, and are given in Table 5.4. The detailed ^{1}H chemical shift values are incorporated in the Experimental section.

Around -10°C, the ^{13}C NMR spectra of these compounds show well separated signals for the two isomers. Integration of the relevant peaks gives the population trends in these systems. The calculated equilibrium constant K for the major <=> minor equilibrium are given in Table 5.5. The ^{13}C integration were found to be satisfactory when compared with ^{1}H integration for the nonoverlapping proton signals of the two isomers.

The nitrogen inversion barrier is expected to be high where an oxygen atom is directly attached to the nitrogen as in isoxazolidine [24,61,62]. As the nitrogen substituents is

changed from methyl (in **123a**) to *iso* propyl (in **123b**) and *tertiary* butyl (in **123c**), the inversion barrier is decreased from 65.6 to 59.3 kJ/mol. In line with the earlier studies [24,61] the bulky *tertiary* butyl group in sp^3 hybridized nitrogen increases the ground state energy in **123c** and the sp^2 hybridized transition state (through which the nitrogen inversion occurs) enjoys the relief of steric congestion and as such the activation barrier is less than that in methyl and *iso* propyl substituted nitrogen. At high, ambient, or lower temperature (-60°C) the adduct **123d** showed virtually identical spectra with sharp and well defined spectral

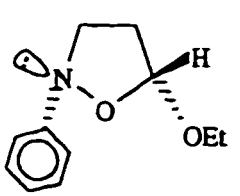

123d-A

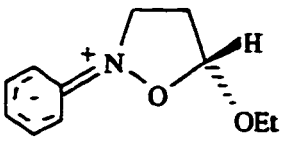

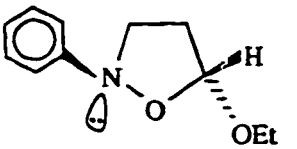

123d-B

lines. This could be attributed to the delocalization of the nitrogen lone pair into the phenyl ring and the nitrogen with substantial sp^2 character will be very close to the transition state and as such the lone pair inversion will have a very low energy barrier and we observe only the average spectrum of the fast equilibrating isomers **A** and **B** even at -60°C. Here the coupling constants of 1.5 and 5.5 Hz for the C-5 proton indicates the pseudoaxial orientation of the ethoxy group due to anomeric effect.

The isoxazolidines **123 a-c, 124a** all showed the presence of two isomers in unequal proportions. Unfortunately, the C-5 proton signals of the major and minor isomers in various solvents (CCl_4, $CDCl_3$, Pyridine-d_5, CD_3OD, and CD_3CN) appeared at the same chemical shifts (δ ~5.1) except in the case of **123c** which displayed a major doublet of doublets at δ~5.15 (J = 2.3, 6.0 Hz) and a minor doublet at δ~5.09 (J =4.5 Hz). Even though the C-5 H chemicals shifts for the *cis* and *trans* isomers of **123a**, **123b**, and **124a** are identical in each case, the line widths of ~10-12 Hz at half heights indicate the small coupling constant associated with the pseudoequatorial orientation of the C-5 proton.

Table 5.4: ^{13}C NMR chemical Shifts [a] in $CDCl_3$ at -40°C

Compound	R		C-3	C-4	C-5	OCH_2	CH_3	other(R)
123a	Me	major	56.19	36.66	101.33	63.45	14.86	45.10
		minor	54.33	36.38	102.57	62.62	14.96	48.43
123b	^{i}Pr	major	52.72	36.54	100.54	63.42	15.06	57.91
		minor	50.71	36.54	101.00	62.50	15.15	59.93
								}20.12, 21.49- ^{i}Pr
123c	^{t}Bu	major	45.65	36.34	100.01	63.13	14.95	56.35, 24.94
		minor	44.35	36.34	99.61	62.09	14.70	57.67, 25.16
123d	Ph		51.92	35.39	101.26	63.48	14.85	*i* -151.36, *o* -114.86, *p* -121.40, *m* -128.39
124a	Bz	major	53.38	36.35	101.15	63.30	14.90	62.97
		minor	52.12	36.25	102.85	62.10	14.98	64.74
								}N-CH_2 *p* -127.58, *o* -128.43 *m* -128.60, *i* -138.61

[a] in ppm relative to internal TMS

Table 5.5: Free Energy of activation($\Delta G^{\#}$) for nitrogen inversion, Equilibrium Constant (K) and Standard Free Energy Change (ΔG^{o}) for major <==> minor isomerization in $CDCl_3$.

Compound	R	$\Delta G^{\#}$ /(kJ/mol)[a]	K[b]	ΔG^{o}(kJ/mol)[b]
123a	Me	65.6	0.32	2.6
123b	^{i}Pr	63.5	0.47	1.7
123c	^{t}Bu	59.3	0.72	0.75
123d	Ph	-	0.00	
124a	Bz	61.5	0.89	0.26

[a] at 298 K; [b] at 273 K

In some solvents the major isomers of **123 a-c** displayed C-5 H as a doublet of doublets with similar coupling constants as in the *tertiary* butyl compound.

The ratio of the major and minor isomers does not seem to vary to a meaningful degree with the dielectric constants of the solvents (Table 5.6). The data indicate that both major and minor isomers have the ethoxy group in the pseudoaxial orientation. Isomer with pseudoequatorial ethoxy group as in (C) and (D) is expected to have higher dipole moment and as such should be favoured in solvents with higher dielectric constants. Virtually unchanged isomer ratio in several solvents indicates that both the isomers have similar dipole moment and thus a fixed axial orientation of the C-5 ethoxy group.

Now the problem remains in assigning the configuration of the major and minor isomers. Assignment of conformation/configuration of the major and minor isomer of the disubstitued isoxazolidines **123**, a simple system as it may seem, is indeed a formidable task [123]. The ^{13}C NMR spectra reveals almost similar trend in the chemical shifts between the corresponding carbons of the major and minor isomers. While the C-3 carbon signal of all the major isomers of the isoxazolidines **123** appeared downfield, the C-5 carbon appeared upfield (except in the case of **123c**). Similar trends are observed for the -OCH_2- carbon and the substituent carbon attached to the nitrogen. The ^1H NMR spectra revealed the C(5)H for all the major isomers as a doublet of doublets and as a doublet for the minor isomer of **123c**. The spectral data thus point towards similar configuration of all the major isomers which was presumed to be the *cis* isomers from the following evidence. As the size of the nitrogen substituent increases from methyl to *iso* propyl to *tertiary* butyl the relative proportion of the minor isomer increases. For instance the major and minor isomers of **123 a**, **123b**, and **123c** in $CDCl_3$ at -30°C are found to be in the ratio of 3.2:1, 2.1:1, and 1.4:1, respectively. Due to anomeric effect the *cis* forms will have dipseudoaxial orientation of the substituents in the envelope form and as such any increase in the steric encumbrance should destabilize and hence decrease its relative preference. Still the question remains: why

Table 5.6. Composition of isoxazolidines (**123**) in various solvents at -30°C.

Solvent	Composition of major and minor isomers			
	(123a)	**(123b)**	**(123c)**	**(124a)**
$CDCl_3$	76 : 24[a]	68 : 32	58 : 42	53 : 47
Pyridine-d_5	72 : 28	65 : 35	66 : 34	62 : 38
CD_3OD	70 : 30	58 : 42	61 : 39	58 : 42
CD_3CN	77 : 23	70 : 30	58 : 42	60 : 40

[a] 66 : 34 in CCl_4 at -30°C

should the *cis* form with diaxially oriented substituents should prevail over pseudo -equatorial , -axial substituted *trans* form in isomeric abundance? Presumably the *cis* form has the advantage of having lone pairs in gauche orientation. We had anticipated, at least in the case of isoxazolidine **123c** the exclusive presence of the *trans* isomer since it is energetically inconceivable to have pseudoaxially oriented *tertiary* butyl group in the *cis* form let alone the disturbing 2,5-diaxial interactions. However inspection of Dreiding models reveals that the *cis* isomer may exist in half-chair conformation in which the strong anomeric effect (with one lone pair in ring oxygen and axial ethoxy group in antiperiplanar arrangement) as well as H_a/H_c dihedral angle of ~90° can be maintained and at the same time the nitrogen substituent is removed away from the C(5) ethoxy group as depicted below, (Figure 5.6) to minimize steric congestion.

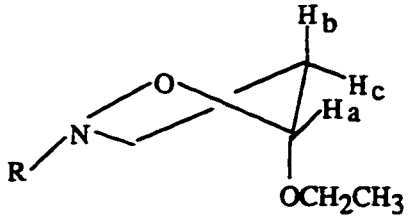

Figure 5.6: Half chair conformation of the *cis* isomer.

The presence of two invertomers complicates the ^1H spectra due to signal overlap and the pseudorotation process in the ring does not give a rigid structure and as such NOE studies failed to shed light on the configuration or conformation of the isoxazolidines studied.

While C(5) ethoxy group in the *trans* conformer **B** will occupy axial orientation in its true sense, in the *cis* form **A** the group will move outside to the extent that it would not seriously jeopardize the anomeric advantage. Coupling constants reflects this trend - the C(5)H appeared as dd (J 3, 6 Hz) and the minor trans isomer as a doublet (J 4.5 Hz). Thus Ha/Hc dihedral angle is greater than 90° indicates less staggering of C4-C5 in the major *cis*

isomer. The *trans* isomer **B** with axial orientation of ethoxy group is expected to shield the C(3) due to the g-gauche interaction. Such a g-gauche interaction will be less in the *cis* conformer **A** or **D** since the C(5) ethoxy group has moved outside from its actual axial position. Carbons in "R" attached to nitrogen, and in OEt attached to oxygen, being in a crowded environment in the *cis* isomer appear upfield as would be expected. The chemical shift differences between the isomers for C-4 and C-5 is very small, indeed zero in many cases. This is not surprising in view of the fact that the substituents attached to nitrogen in the *trans* as well as the half chair *cis* form does not give gauche interaction with C-4 or C-5. It is thus found that the absence of C-3 substituent makes the isoxazolidines mobile and the *gauche* interaction of the lone pairs favours the *cis* isomer.

A series of isoxazolidines with C(5) ethoxy substituent and several *o* -, *m* - and *p* - substituted benzyl groups at N are prepared as shown in the Scheme 5.6.

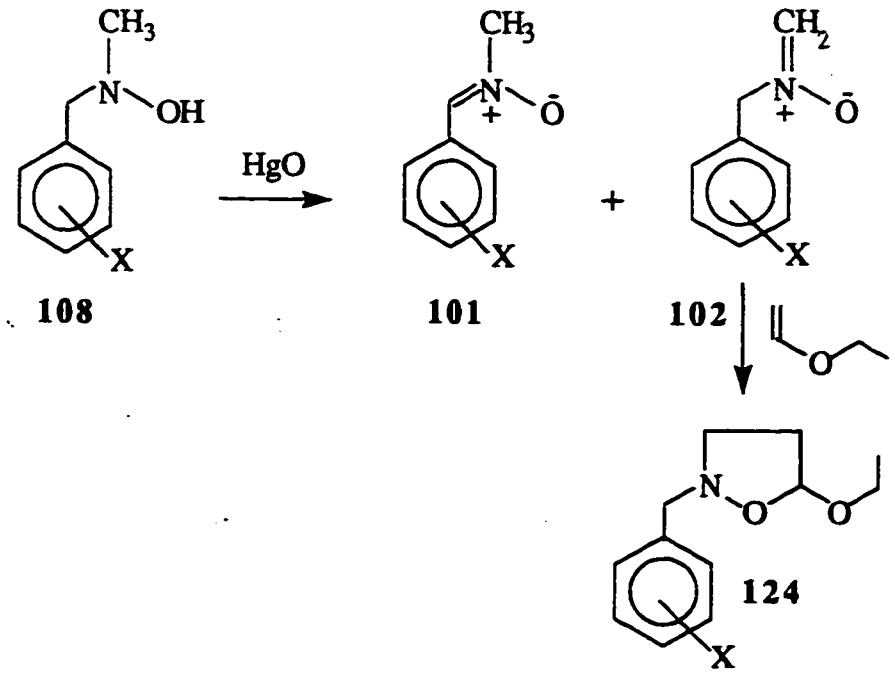

Scheme 5.6: Synthetic route to isoxazolidines **124**

The mercury (II) oxide oxidation of the hydroxylamines **108** afforded a mixture of the nitrones **101** and **102**. The monosubstituted mixture **102** is anticipated to be more reactive than **101** towards dienophile. This is attributed to the steric encumbrance in disubstituted nitrone **101**. The mixture of the nitrones **101** and **102** on treatment with ethyl vinyl ether at 30°C gave the cyclo adduct **124** regiospecifically. The nitrone **101** was found to be unreactive under the reaction conditions.

^1H proton spectra of all these isoxazolidines show the broadened signals as the temperature is lowered below the ambient temperature and then distinct signals for two different isomers (*cis* and *trans*) are displayed in the spectrum. The benzyl methylene protons chemical shift for the major and minor isomers along with their ratios are listed in the Table 5.7. Invariably the signals (AB or two dd) for the major isomers appear upfield in all the derivatives. Further evidence that the major isomer in all these derivatives have the same configuration come from the signal of the $-CH_3$ protons. In almost all the cases the major triplet appeared upfield. Unfortunately the signals for the C(5) H_e of the two isomers appeared at the same chemical shifts (i.e. chemical shift equivalence) in all the derivatives at around δ 5.24-5.29 ppm as multiplets (at -40°C). The NMR spectra at +50°C revealed the signal of the C(5) H as a dd in all the compound (with coupling constant, J~ 2.0, ~5.5) at δ 5.22-5.26. The magnitude of coupling constants are indicative of the pseudo axial orientation of the C(5) ethoxy group in both the isomers. The ratio of the isomers was found to be 60:40 in all the cases except for X = *o* -OH where the ratio was found to be almost 50:50. It is to be noted that the CH_3 protons of the major isomer in (R= CH_3) also appeared upfield.

Nitrogen inversion barrier $\Delta G^{\#}$(273K) is given for isoxazolidines **124** in Table 5.8. Hammett plot for the nitrogen inversion barrier for the isoxazolidines **124** is given in Figure 5.7. The N-O bond is locked in the ring skeleton of the five membered ring, hence the question of rotation around the bond does not arise. It is now purely a matter of nitrogen inversion. Electronegative substituent X accelerate the rate of inversion by

Table 5.7: The ^1H NMR chemical shifts of benzyl methylene protons in $CDCl_3$.

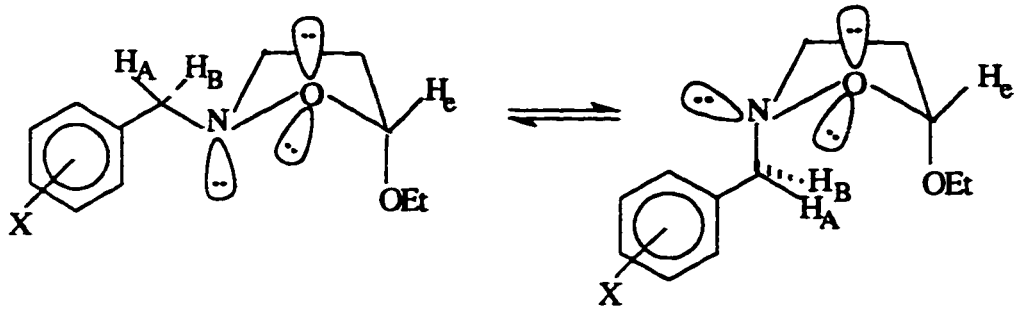

Compound		Temp °C	Major		Minor		Major/Minor
			δH_A	δH_B	$\delta H'_A$	$\delta H'_B$	ratio
124a	H	-30°C	3.98	4.12	4.05	4.31	53:47
124b	*p*-NO_2	-30°C	4.05	4.25	4.17	4.41	60:40
124c	*p*-Cl	-40°C	4.02		4.05	4.25	58:42
124d	*p*-OMe	-30°C	3.91	4.09	4.01	4.24	60:40
124e	*p*-Me	-40°C	3.94	4.11	4.04	4.26	59:41
124f	*p*-NMe_2	-40°C	3.79	4.13	3.96	4.25	62:38
124g	*m*-NO_2	-40°C	4.06	4.27	4.17	4.39	63:37
124h	*o*-OH	-40°C	4.11	4.39	4.29	4.50	52:48
124i	*o*-OMe	-40°C	4.11		4.17	4.32	62:38

Table 5.8: Nitrogen inversion barriers of various Isoxazolidines.

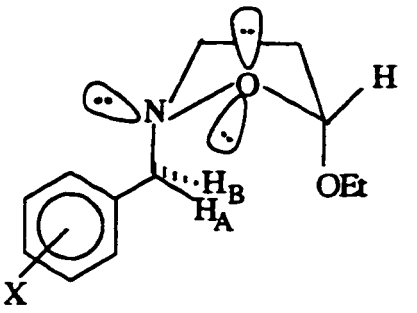

Compound No.	X	$\Delta G^{\#}$ (273K) kJ/mol
124a	H	59.6
124b	*p* -NO_2	57.4
124c	*p* -Cl	58.8
124d	*p* -OMe	60.4
124e	*p* -CH_3	60.0
124f	*p* -NMe_2	61.6
124g	*m* -NO_2	57.2
124h	*o* -OH	66.3
124i	*o* -OMe	59.4

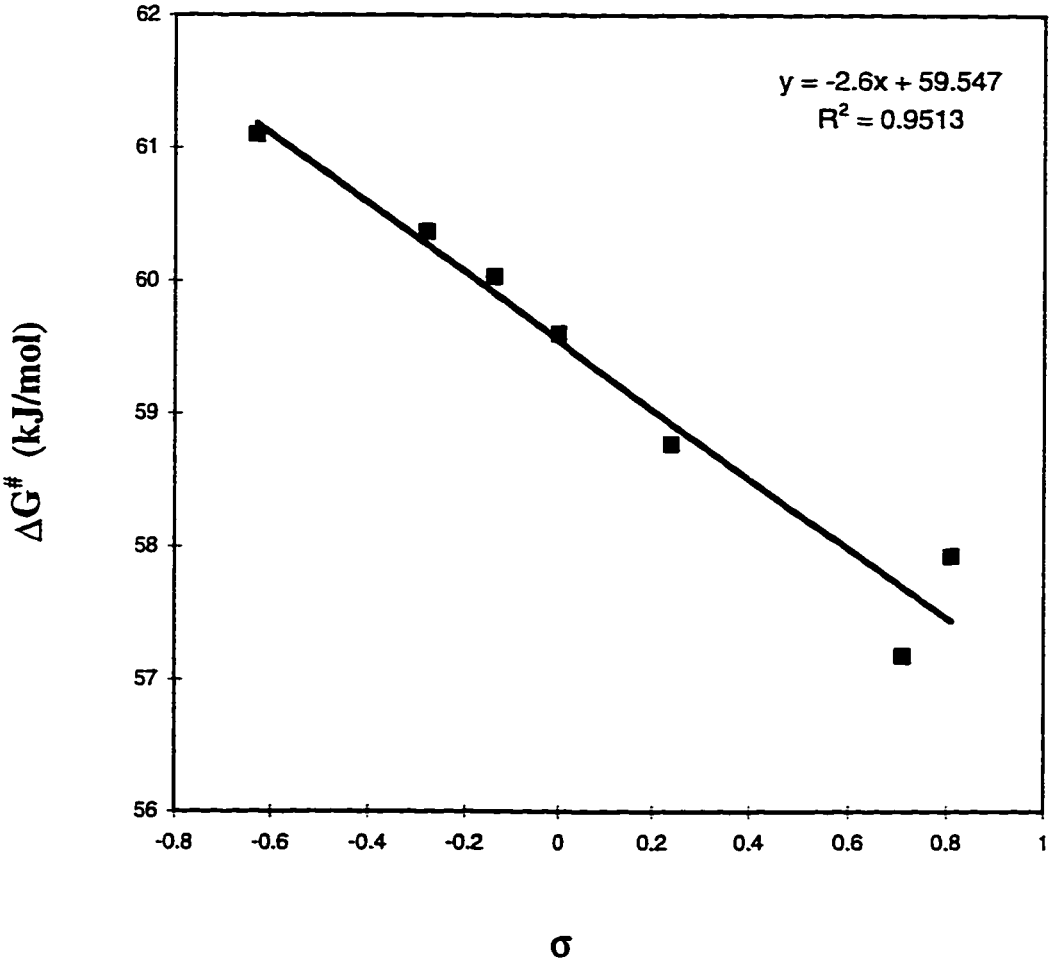

Figure 5.7 Hammett plot for the nitrogen inversion barrier in isoxazolidines **(124)**.

stabilizing the transition state which has higher electron density than the ground state as indicated by a ρ value of + 0.497.

In all the isoxazolidines studied a strong anomeric effect is demonstrated since the ^{1}H NMR spectra did not reveal the presence of the isomers with equatorially oriented C(5) ethoxy substituent. The effect of H-bonding is amply demonstrated in the inversion barrier of the compound **124h** with *o* -hydroxy substituent. The barrier is found to be 7 kJ/mol higher than the barrier found for the corresponding *o* -methoxy derivative **124i**. The nitrogen inversion require prior breaking of the H-bond. H-bonding is demonstrated by the appearance of the proton signal at down field (δ 10.2 ppm) as a singlet.

5.4 Oxidation of Hydroxylamines. A Mechanistic Study

5.4.1 Ease of Oxidation

The ease of oxidation of hydroxylamine **108-111** to the nitrones **101, 107** should reflect the ease of nitrogen inversion provided the oxidation process like nitrogen

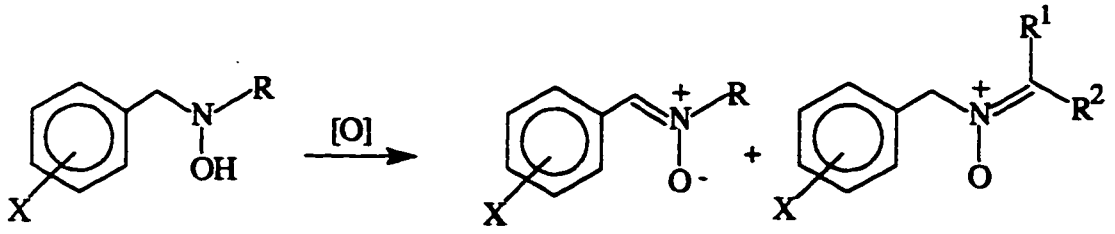

108a	X=H	R=Me	**101a**	R=Me	**102a**	X=H	$R^1=R^2=H$
109a	X=H	R=Et	**103a**	R=Et	**104a**	X=H	$R^1=H$ $R^2=Me$
110a	X=H	R=^{i}Pr	**105a**	R=^{i}Pr	**106a**	X=H	$R^1=R^2=Me$
111a	X=H	R=^{t}Bu	**107a**	R=^{t}Bu			

Scheme 5.7: Oxidation of hydroxylamine derivatives to nitrones.

inversion, involves planar transition state of the rate determining step (RDS) with sp^2 character of nitrogen orbitals. Any crowding in the pyramidal ground state would be relieved in the transition state with extended CNC bond angle (120°). The relative rates of oxidation of the hydroxylamines **108-111** by HgO and *p* -benzoquinone (*p* -BQ) along with the energy barrier for the nitrogen inversion process are listed in Table 5.9.

Relative rates of the oxidation were determined by reacting a solution of **108a** (0.150 mmol) and another hydroxylamine **109a** or **110a** or **111a** (0.150 mmol) in $CDCl_3$ with 0.150 mmol of the oxidant. Using rate equation of Ingold and Shaw [115] the relative rates are determined as described in the experimental section. In case of oxidation with

Table 5.9: Relative rates of oxidation of various hydroxylamines using *p*- BQ and HgO.

Compound		$\Delta G^{\#}_{273K}$ kJ/mol	Relative rate of oxidation using *p* -Benzoquinone[a]	HgO[b]
108a	Me	55.8	1.00	1.00
109a	Et	55.3	1.35	0.902
110a	^{i}Pr	51.6	2.32	1.40
111a	^{t}Bu	49.2	1.20	0.528

a at 20°C b at 0°C

p - benzoquinone the reaction mixture turned deep blue within minutes, probably indicating the formation of free radicals. It is evident from the table, that the rate of oxidation of **108a** or **109a** or **110a** using *p* -benzoquinone parallels the rate of nitrogen inversion. However, while the rate of oxidation of the *tertiary* butyl derivative **111a** is still higher than the methyl derivative **108a**, it is considerably lower than the *iso*propyl hydroxylamine **110a** reflecting the complex interplay of the steric encounter in the approach of the oxidant toward **111a** and its desire to relieve steric compression in the planar transition state. In the

oxidation using HgO, the *tertiary* butylhydroxylamine **111a** undergoes oxidation at slower rate in comparison to both the methyl **108a** and *iso* propyl derivative **110a**.

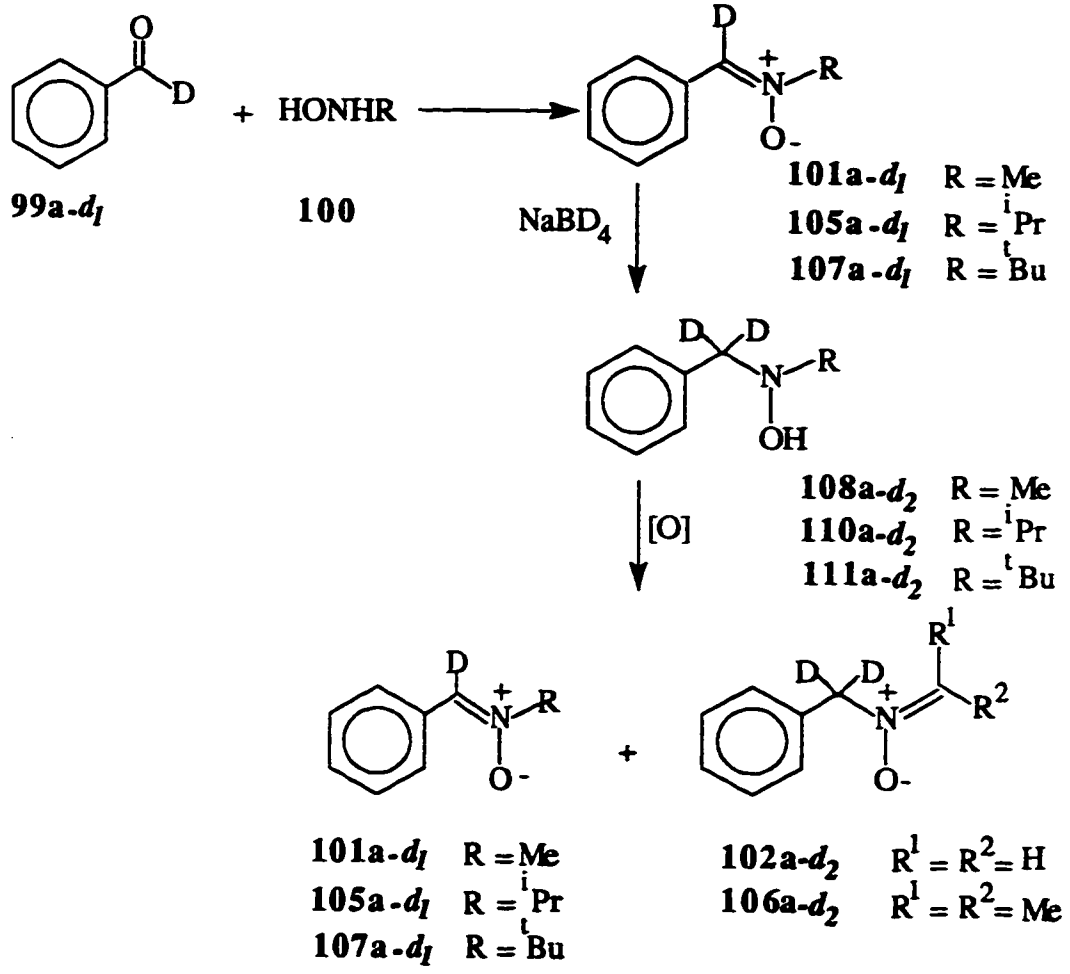

Scheme 5.8: Synthetic route to deuteriated hydroxylamine.

To shed more light on the oxidation process, the hydroxylamine deuteriated at the benzyl position was prepared as shown in the scheme 5.8. Condensation of hydroxylamine **100** with PhCDO afforded the nitrone **101a-d_1** , **105a-d_1** , **107a-d_1** which on reduction with $NaBD_4$ gave the hydroxylamine **108a-d_2** , **110a-d_2** , **111a-d_2** with benzyl position dideuteriated. While the hydroxylamine **108a-d_2** on oxidation with HgO and *p* - benzoquinone gave a mixture of the nitrones **101a** and **102a** in a ratio of 57:43 and 65:35 respectively (Table 5.10), with either oxidant the regiochemistry of the oxidation is

Table 5.10 : Regiochemistry and reactivity of hydroxylamines in oxidation using HgO (0°C) and *p* - benzoquinone (20°C) in $CDCl_3$.

Hydroxylamine	Oxidant	% Composition of nitrones				Rate ratio using	
						HgO	*p*-BQ
$PhCH_2N(OH)CH_3$	HgO	**101a**	57	**102a**	43	k **108a**/k**108a**-d_2	
108a	*p*-BQ	**101a**	65	**102a**	35	1.34	1.15
$PhCD_2N(OH)CH_3$	HgO	**101a**-d_1	17	**102a**-d_2	83		
108a-d_2	*p*-BQ	**101a**-d_1	33	**102a**-d_2	67		
$PhCH_2N(OH)CH_2CH_3$	HgO	**103**	50	**104**	50		
109	*p*-BQ	**103**	46	**104**	54		
$PhCH_2N(OH)CH(CH_3)_2$	HgO	**105a**	93	**106a**	7	k **110a**/k**110a**-d_2	
110a	*p*-BQ	**105a**	93	**106a**	7	3.35	4.39
$PhCD_2N(OH)CH(CH_3)_2$	HgO	**105a**-d_1	68	**106a**-d_2	32		
110a-d_2	*p*-BQ	**105a**-d_1	63	**106a**-d_2	37		
$PhCH_2N(OH)C(CH_3)_3$	HgO	**107**	100	-		k **111**/k**111**-d_2	
111						7.0	7.5
$PhCD_2N(OH)C(CH_3)_3$	HgO	**107**-d_1	100	-			
111-d_2							

reversed providing the nitrones **101a-d_1** , and **102a-d_2** in a respective ratio of 17:83. Such isotope effect is also observed in the oxidation of **110a** and **110a-d_2** . While **110a** gave a mixture of the nitrones **105a** and **106a** in a ratio of 93:7 respectively, the corresponding ratio from the oxidation of the dideuteriated derivative **110a-d_2** becomes 68:32. The most interesting regiochemistry is observed in the oxidation of the hydroxylamine **109** which afforded the conjugated and nonconjugated nitrones **103** and **104** in a ratio of 1:1. Much high acidity of the benzylic protons in **109** is not reflected in the formation of the conjugated nitrone **103**. The isotope effect observed in these oxidations does not confirm the involvement of C-H(D) bond breaking in the transition state of the rate determining step. In a stepwise pathway isotope effect should be manifested even if the C-H(D) bond breaking takes place in a fast step since we are talking about breaking of C-H versus C-D bond breaking within the same molecule. To confirm whether the C-H(D) bond breaking is happening in the rate determining step or not, a 1:1:1 mixture of **108a**, **108a-d_2** and the oxidant was allowed to undergo reaction.

Analysis of the ^1H spectrum allowed to quantify the amounts of unreacted hydroxylamines; and using rate equations of Ingold and Shaw [115] the following rate ratios were obtained: k(**108a**)/k(**108a-d_2**) = 1.34 (using HgO), 1.15 (using *p* -Benzoquinone); k(**110a**) / k(**110a-d_2**) = 3.35 (using HgO), 4.39 (using *p* -Benzoquinone) and k(**111**) /k(**111-d_2**) = 7.0 (using HgO), 7.5 (using *p* -Benzoquinone). Considerable isotope effect in all three cases reveals the involvement of C-H bond breaking in the rate determining step. The rate ratio decreases as the *tertiary* butyl group is switched to *iso* propyl **110a** and then to the methyl **108a** group. This is expected since unlike the hydroxylamine (**111**) the latter two hydroxylamines (**108a**) and **110a** have terminal other than the $PhCH_2(D_2)$ from where the hydrogen can be abstracted. So the magnitude of the isotope effect can be realized when the rate constants for the abstraction of benzylic H (and D) alone are considered. For the hydroxylamine **110a**, the formation of the conjugate **105a** and nonconjugates nitrones **106a** in a respective ratio of 93:7 reveals the rate ratio for the

formation of conjugated and nonconjugated nitrones k(**105a**)/k(**106a**) to be approximately 93:7, whereas the corresponding rate ratio k(**105a**-d_1)/k(**106a**-d_2) for the oxidation of hydroxylamine **110a**-d_2 was found to be 68:32. Since the formation of the non-conjugated nitrones **106a** and **106a**-d_2 involves abstraction of hydrogen isotope in both

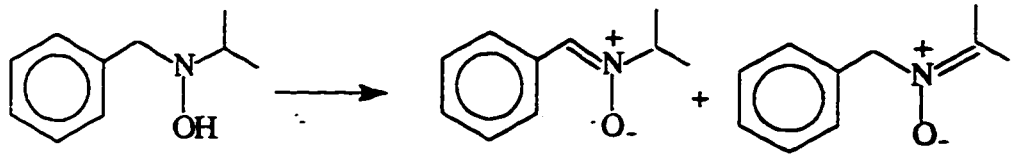

110a **105a** **106a**

$$\frac{k_{105a}}{k_{106a}} = \frac{93}{7}$$

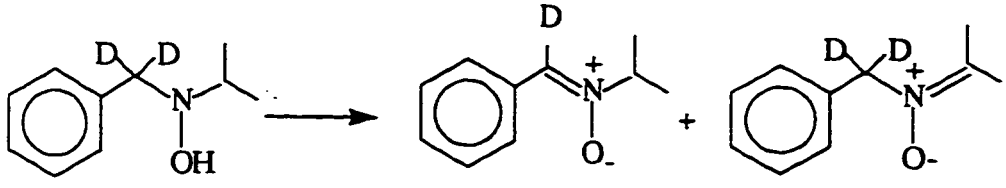

110a-d_2 **105a**-d_1 **106a**-d_2

$$\frac{k_{105a\text{-}d_1}}{k_{106a\text{-}d_2}} = \frac{68}{32} = \frac{68 \times \frac{7}{32}}{32 \times \frac{7}{32}} = \frac{14.9}{7}$$

$$\frac{k_{105a}}{k_{106a}} \times \frac{k_{106a\text{-}d_2}}{k_{105a\text{-}d_1}} = \frac{93}{7} \times \frac{7}{14.9} = 6.24$$

$$\frac{k_{105a} + k_{106a}}{k_{105a\text{-}d_1} + k_{106a\text{-}d_2}} = \frac{100}{14.9 + 7.0} = 4.6$$

cases, the rate constant k(**106a**) and k(**106a**-d_2) should sense that secondary isotope effect in the formation of **106a** versus **106a**-d_2 is not considered. The simple arithmetic

leads to the rate ratio k(**105a**)/k(**105a-d_1**) i.e. isotope effect of 6.24. If C-H(D) bond breaking is indeed involved in the rate determining step then the rate ratio [k(**105a**)+k(**106a**)]/[k(**105a-d_1**)+k(**106a-d_2**) should be equal to 4.6. The observed rate ratio of 3.35 and 4.39 in the oxidation using HgO and *p*-benzoquinone respectively certifies the involvement of C-H(D) bond breaking in the rate determining step. Similar calculation in the oxidation of hydroxylamine **108a** and **108a-d_2** using HgO and *p*-benzoquinone led to the isotope effect of 6.5 and 7.4 respectively. This should translate into a ratio k(**108a**)/k(**108a-d_2**) of 1.93 and 2.29. The observed rate ratio of 1.34 and 1.15 in HgO and *p* -benzoquinone oxidation respectively is somewhat less indicating that C-H(D) bond breaking is involved in the rate determining step but not to the same extent as in the oxidation of *iso*propyl (**110a**) and *tertiary* butyl derivative (**111**).

Next, attention was focused on the oxidation **108** and **110** with various substituents in the aromatic ring. The compound studied and their relative rate (k_X/k_H) of oxidation using HgO and *p* -BQ are listed in Tables 5.11-5.14. As is evident from the tables, the rate of oxidation increases with the electron donating ability of the substituents

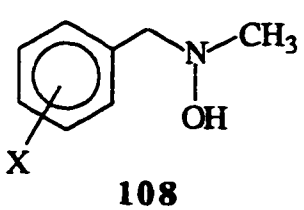

108

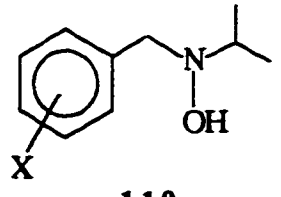

110

X. In the methyl series **108** the hydroxylamine **108f** (X= *p* -NMe_2) is found to be more reactive than **108g** (X= *m*-NO_2) by factors of 3.86 and 4.73 using HgO and *p*-benzoquinone respectively (Tables 5.11, 5.12). Similar rate enhancement is also observed in the *iso*propyl series (Tables 5.13, 5.14). Thus **110f** (X= *p* -NMe_2) is more reactive than **110g** (X=*m*- NO_2) by a factor of 4.45 using HgO and 5.02 using *p*- benzoquinone. Hammett plot for the oxidation of **108** and **110** are shown in Figures 5.8-5.11. A good linear free energy relationship is obtained in all the cases with reaction constant ρ values of

Table 5.11: Relative rates of oxidation of N-methyl hydroxylamine by HgO

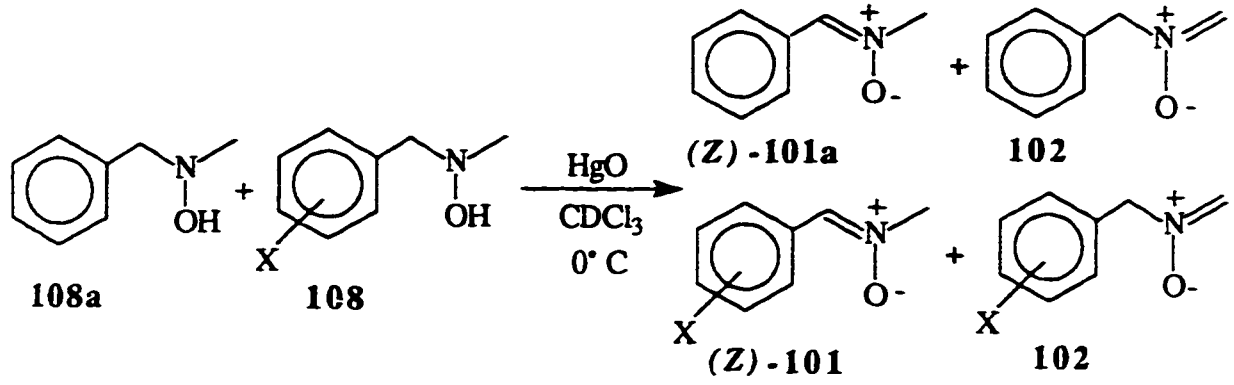

Hydroxylamine	k_X/k_H	log (k_X/k_H)
108b *p*-NO_2	0.461	-0.336
108c *p* -Cl	0.901	-0.0452
108d *p* -OMe	1.21	0.0811
108e *p* -Me	1.18	0.0714
108f *p*-NMe_2	1.61	0.207
108g *m* -NO_2	0.412	-0.358
108h *o* -OH	0.892	-0.0496
108i *o* -OMe	1.415	0.151

Table 5.12: Relative rates of oxidation of N-methyl hydroxylamine by *p* -benzoquinone

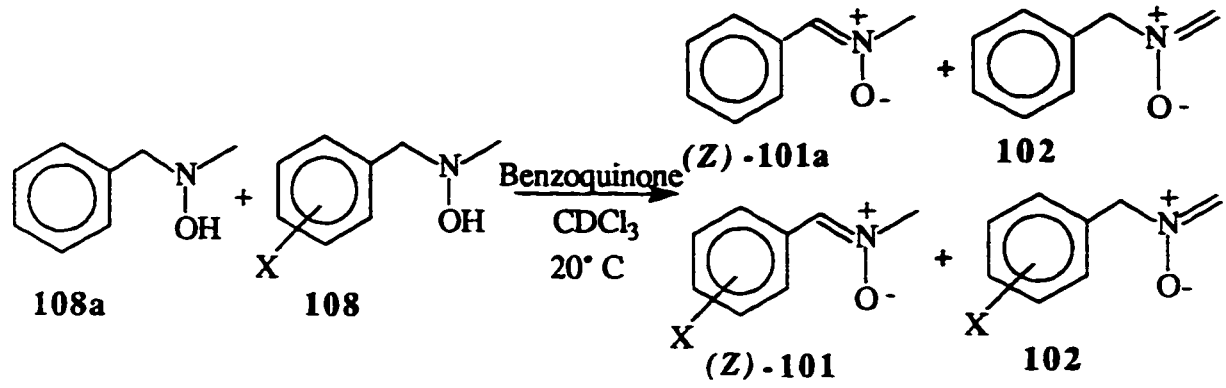

Hydroxylamine	k_X/k_H	log (k_X/k_H)
108b *p*-NO2	.425	-0.372
108c *p* -Cl	0.835	-0.0781
108d *p* -OMe	1.43	0.156
108e *p* -Me	1.155	0.0627
108f *p*-NMe_2	1.83	0.263
108g *m* -NO_2	0.387	-0.412
108h *o* -OH	0.540	-0.267
108i *o* -OMe	0.479	0.320

Table 5.13: Relative rates of oxidation of N-*iso*propyl hydroxylamine by HgO.

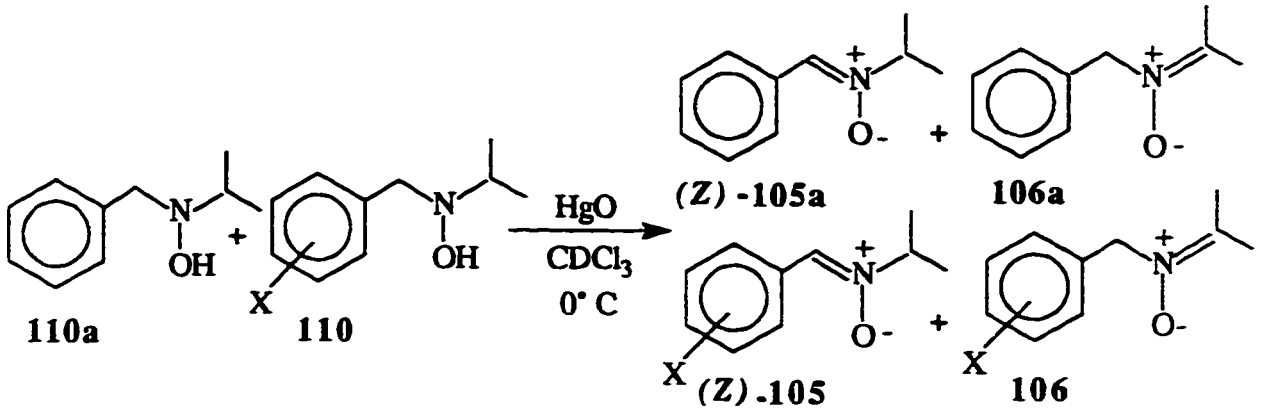

110a 110 (Z) -105a 106a (Z) -105 106

Hydroxylamine	k_X/k_H	log (k_X/k_H)
110b *p*-NO_2	0.610	-0.214
110c *p* -Cl	0.794	-0.100
110d *p* -OMe	1.165	0.0653
110e *p* -Me	1.448	0.161
110f *p*-NMe2	2.245	0.351
110g *m* -NO_2	0.505	-0.296
110h *m*-Br	0.767	-0.115
110i *p*-Br	0.942	-0.026
110j 2,4,5-$(OMe)_3$	1.29	0.111

Table 5.14: Relative rates of oxidation of N-*iso*propyl hydroxylamine by *p* -benzoquinone.

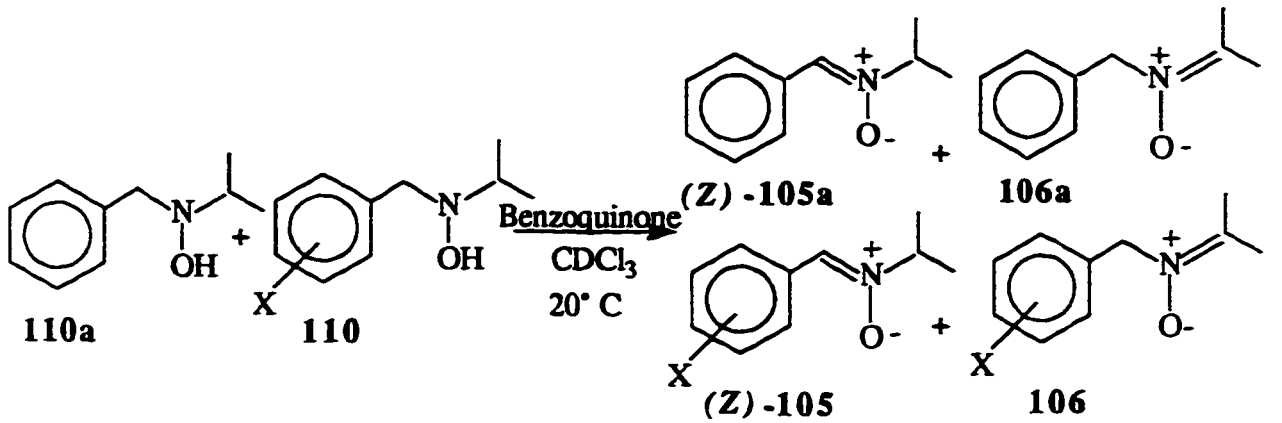

Hydroxylamine	kx/kH	log (kx/kH)
110b *p*-NO_2	0.629	-0.202
110c *p* -Cl	0.901	-0.0451
110d *p* -OMe	1.22	0.0859
110e *p* -Me	1.476	0.169
110f *p*-NMe_2	2.22	0.347
110g *m* -NO_2	0.442	-0.355
110h *m*-Br	0.634	-0.198
110i *p*-Br	0.770	-0.113
110j 2,4,5-$(OMe)_3$	1.772	0.248

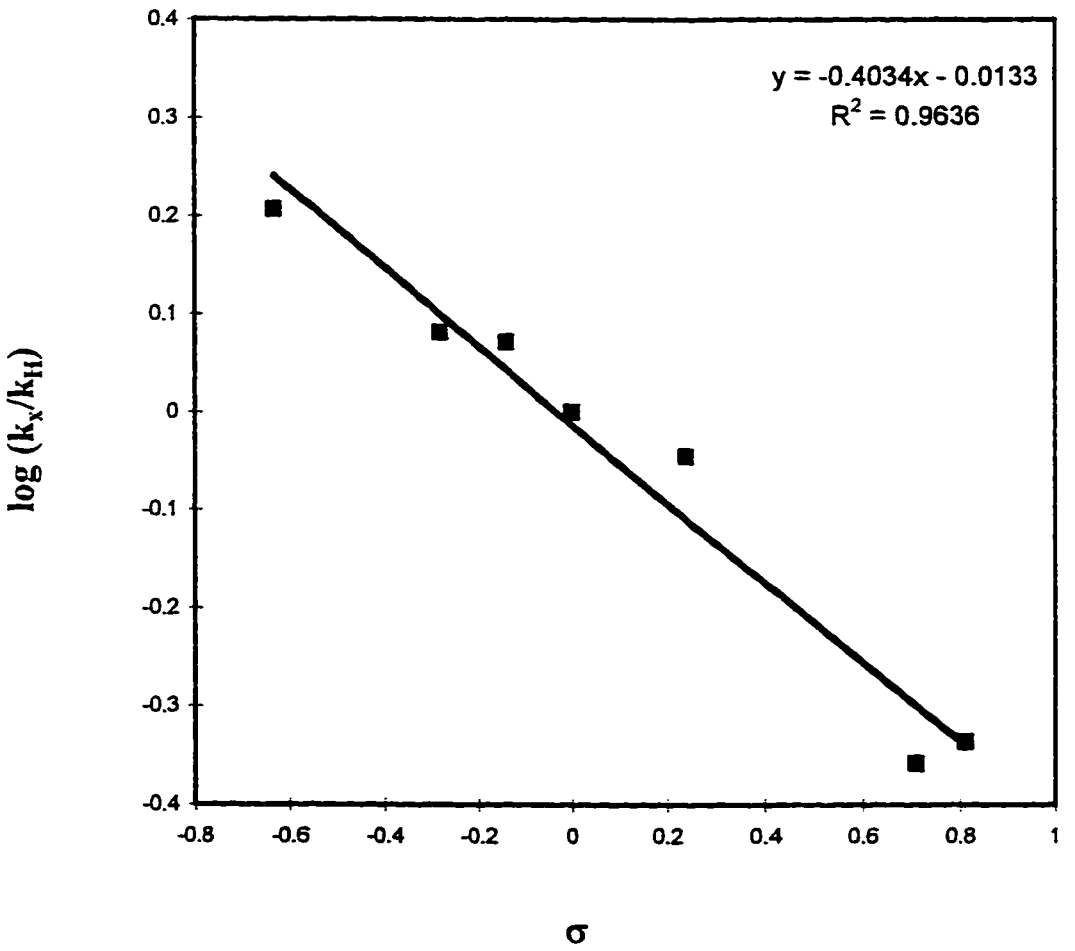

Figure 5.8 Hammett plot for the HgO oxidation of N-aryl-N-methyl hydroxylamines (**108**).

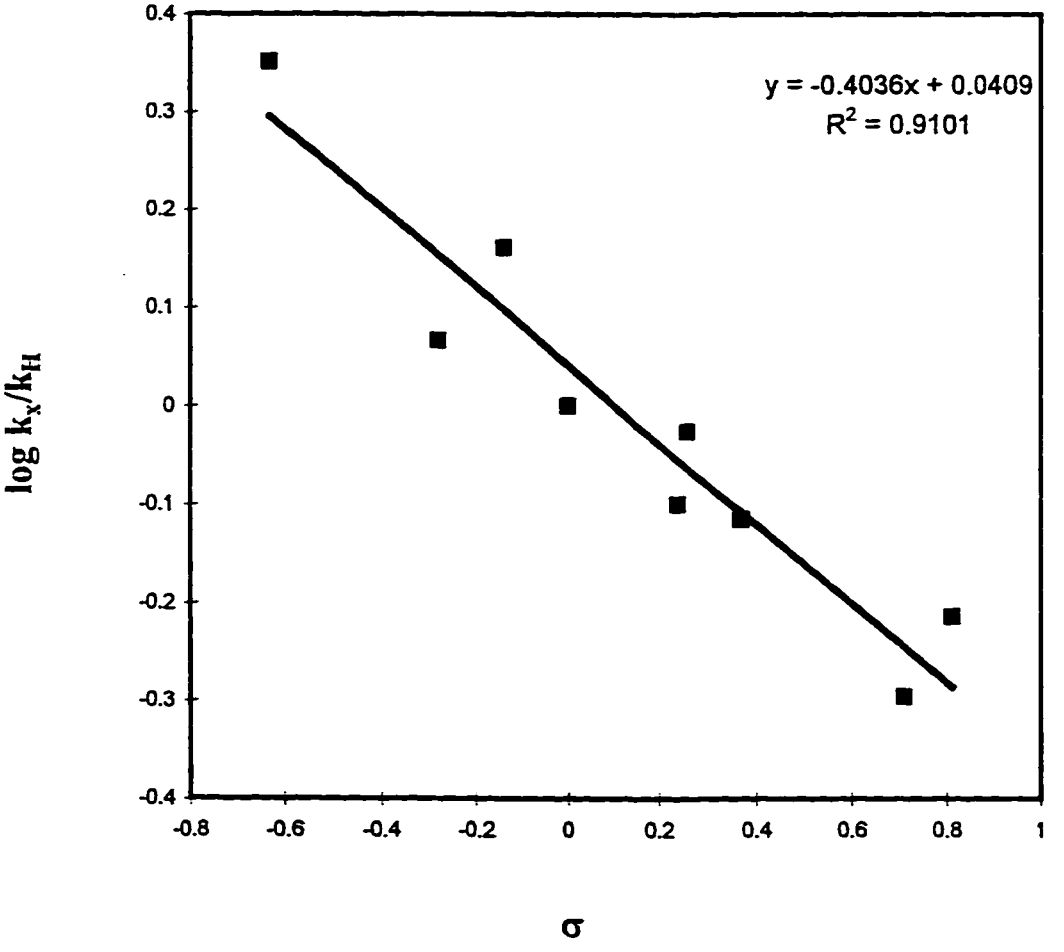

Figure 5.9 Hammett plot for the HgO oxidation of N-aryl-N-isopropyl hydroxylamines (110).

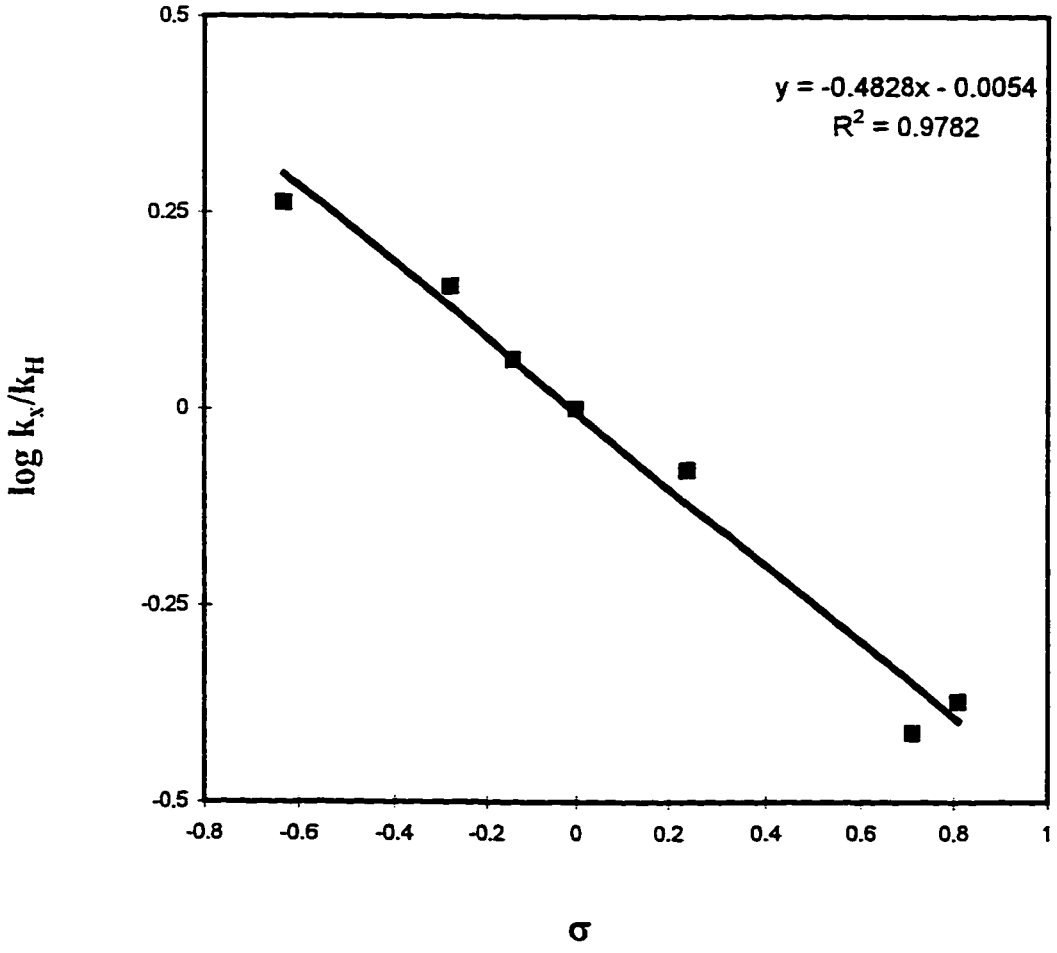

Figure 5.10 Hammett plot for the benzoquine oxidation of N-aryl-N-methyl hydroxylamines (**108**).

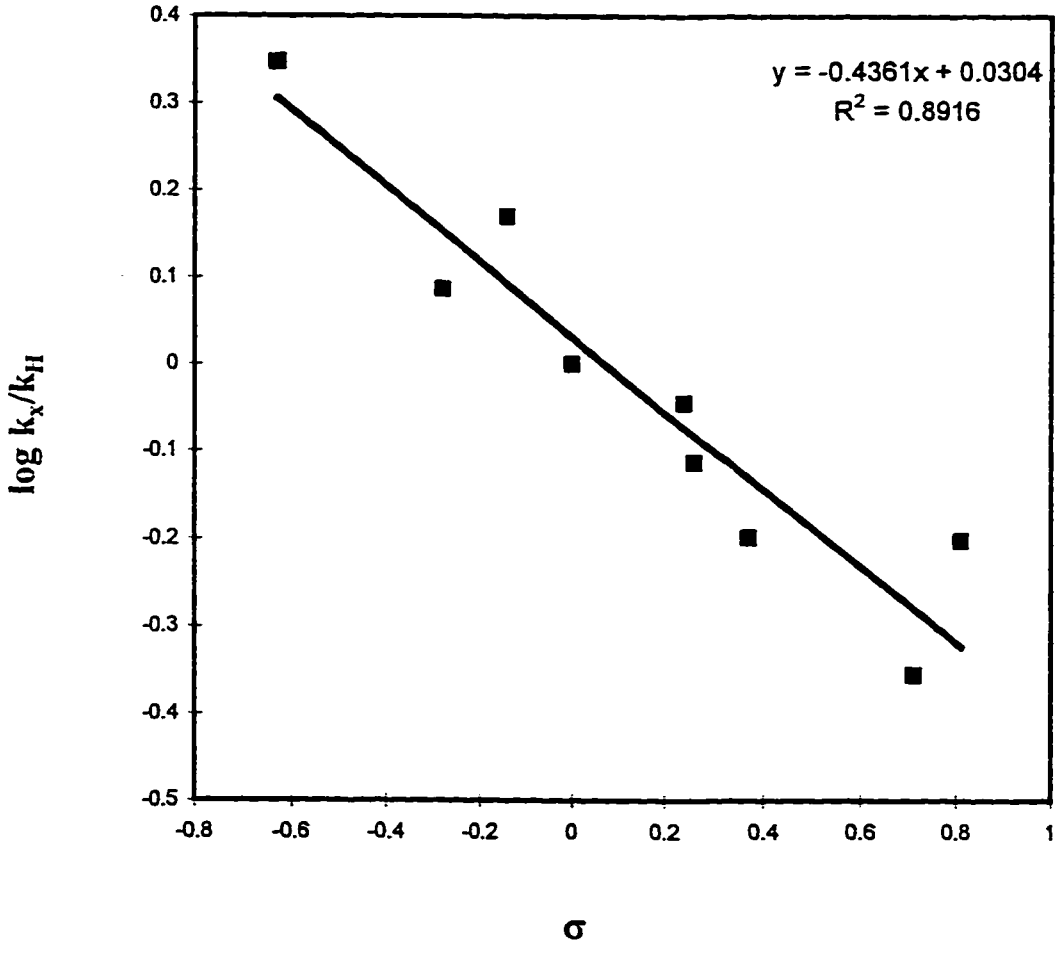

Figure 5.11 Hammett plot for the benzoquinone oxidation of N-aryl-N-isopropyl hydroxylamines (**110**).

-0.403, -0.483 for the oxidation of hydroxylamine **108** using HgO and *p*-BQ, respectively. The corresponding ρ values in the **110** series were found to be -0.404 and -0.436. The negative ρ values indicate the development of positive charge in the transition states. Within each series the steric factor doesn't play a part in determining the energy of activation since all the substituents are in the *meta* or *para* position. It is to be noted that the hydroxylamine **108h** with hydroxy substituent at the *ortho* position undergoes oxidation with HgO and *p* -BQ slower than the unsubstituted hydroxylamine **108a** by a factor of 0.892 and 0.540, respectively. The slower rate indicates the difficulty in donation of the nitrogen non-bonding electron to the oxidant since it requires additional energy to break the intermolecular H-bonding prior to electron donation.

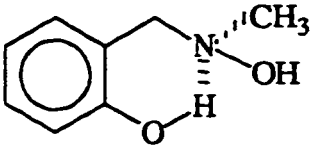

108h

In order to shed more light on the mechanistic pathway the oxidation process traverses; the product regiochemistry of the oxidation of the hydroxylamine **108** was analysed. It was anticipated that if C-H bond breaking is indeed involved in the rate determining step, then the hydroxylamine **108b** (X=*p*-NO_2) and **108g** (X=*m*-NO_2) should undergo oxidation faster than the hydroxylamine with electron donating substituent in the aromatic ring. The former compounds should facilitate the H abstraction from the benzylic position by stabilizing the transition state provided the H abstraction leads to radical or anionic character at the benzylic position. However this was found not to be the case; as the electron withdrawing ability of the substituent (X) increases the rate of oxidation decreases. Regiochemistry of the oxidation process is included in Table 5.15.

As is evident from the table the composition of the nitrones depends on the nature of the substituent X. As the electron withdrawing ability of the substituent increases, the percentage of the conjugated nitrones also increases indicating either free radical or

Table 5.15: Composition of nitrones in the oxidation of hydroxylamine **108** with HgO at -20°C and *p*- benzoquinone at + 20°C.

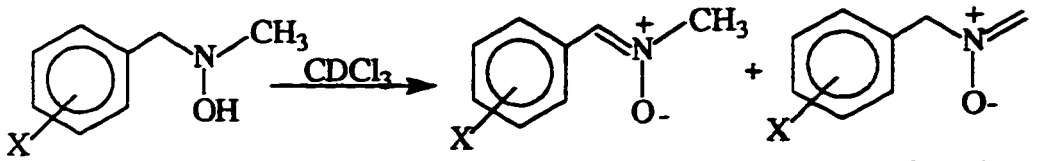

108 **(Z) - 101** **102(*Mono*)**

Hydroxylamine	Composition of the nitrones	
	using *p*-benzoquinone	using HgO
108a (X=H)	65:35	60:40
108b (X=*p* -NO_2)	88:12	80:20
108c (X=*p* -Cl)	77:23	68:32
108d (X=*p* -OMe)	60:40	54:46
108e (X=*p* -Me)	60:40	59:41
108f (X=*p* -NMe_2)	53:47	59:41
108g (X=*m* -NO_2)	90:10	83:17
108h (X=*o* -OH)	68:32	60:40
108i (X=*o* -OMe)	30:70	44:56

carboanion character at the benzylic position during H abstraction. Hydride abstraction would have placed positive charge on the benzylic position in which case electron donating group (X) would have preferred that situation to give nitrones with increased percentage of the conjugated nitrone **101**. To summarize the results presented so far the following points are to be noted.

1. Steric crowding in the ground state facilitates the oxidation process upto a point. As seen in the Table 5.9 the *iso*propyl hydroxylamine **110a** reacts faster than the oxidation of the methyl or ethyl hydroxylamine.

2. Rate study with deuteriated hydroxylamine derivatives **108a-d_2**, **110a-d_2** and **111-d_2** clearly demonstrates primary isotope effect indicating involvement of C-H(D) bond breaking in the transition state (Table 5.10).

3. Rate of oxidation of a multitude of hydroxylamines **108** and **110** having a variety of substituents in the aromatic ring (Table 5.11-5.14) provided negative ρ values indicating positive charge development in the transition state. Electron donating substituents in aromatic ring increases electron density on the nitrogen thus making the reductant a better electron donor to the oxidant molecule.

4. Hydrogen abstraction is very much controlled by the kinetic factor. Surprisingly regiochemical data for the oxidation of N-benzyl-N-ethyl hydroxylamine **109** (Table 5.10) clearly demonstrates the indifference of the thermodynamic acidity of the benzylic protons. Rate of hydrogen abstraction is dictated by the steric factor as indicated in the oxidation of the *iso* propyl hydroxylamine **110a** (Table 5.10). One could also see the importance of the steric factor in the oxidation of *p*-methoxy **108d**, and *o*-methoxybenzyl-N-methylhydroxylamine **108i**. Steric crowding decelerates the hydrogen abstraction from the benzylic position of the *ortho* derivative thus giving nonconjugated nitrone **102i** as the major product (Table 5.15).

5. Thermodynamic acidity does however play a part (albeit minor) in the abstraction of hydrogen. In a series of hydroxylamines **108** (Table 5.15) with *meta* or *para* substituents the steric requirements at the benzylic and methyl terminal are kept fixed. The data in Table 5.15 demonstrates that electron withdrawing groups in the aromatic ring (X= *para* or *meta* NO_2) give conjugated nitrones **101** in higher ratios than the electron donating substituents (X= Me, NMe_2, OMe). This is in line with the higher acidity of the benzylic protons in case of the electron withdrawing substituents.

Oxidation process can follow a pathway of single electron transfer (SET) or polar (SN_2) mechanism. However in order to accommodate our experimental findings we envisaged a rate determined by more than one step.

Accumulated evidence could led to the depiction of probable mechanistic pathway this reaction traverses. As presented in Scheme 5.9 the hydroxylamine could have two stable conformers **A** and **B** with gauche interaction between phenyl-methyl and phenyl-hydroxyl respectively. In both conformers the O-H bond is shown to be eclipsed with the nitrogen lone pair. Approach of the oxidant towards the nitrogen lone pair would occur from the least hindered side. The encounter complex formation will be favoured in the conformer **A**. Some kind of hydrogen bonding would increase the effective size of the hydroxyl group and as such the conformer **A** with the disposition of phenyl ring in the anti position would facilitate such approach of the oxidant. A single electron transfer from the nitrogen non bonding electrons would led to the formation of cationic **C** and anionic radicals. Kinetic abstraction of hydrogen atom would lead to the formation of the unstable nitrone ***(E)*-101** and the monosubstituted nitrone **102**. The corresponding cation radical **D** would lead to the formation of the nitrones ***(Z)*-101** and **102**. HgO oxidation of the conformer **A** is shown in Scheme 5.10. Formation of the cationic radical is demonstrated by the negative ρ values obtained in the Hammett plots (Figure 5.8-5.9).

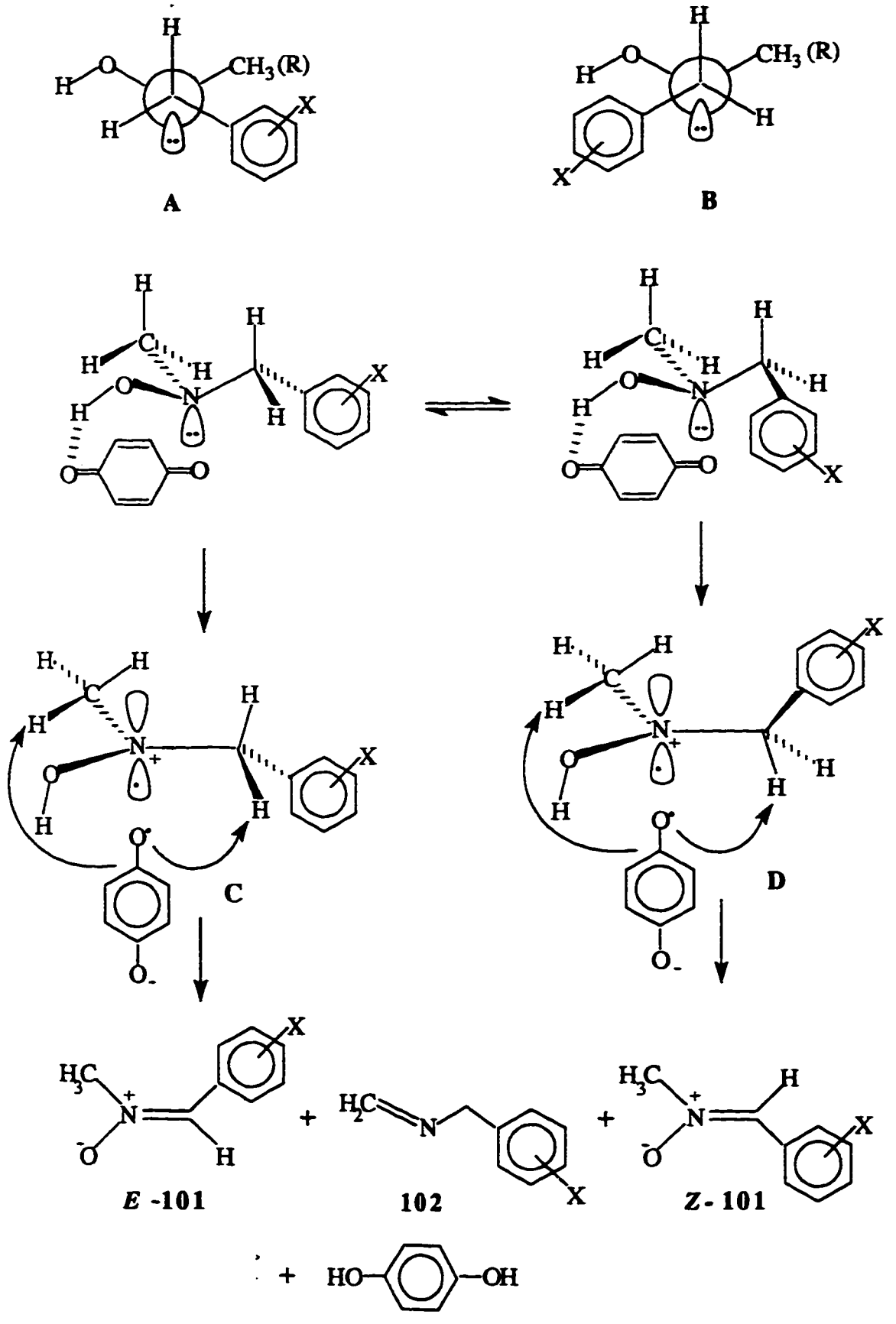

Scheme 5.9: Mechanistic pathway of the oxidation process.

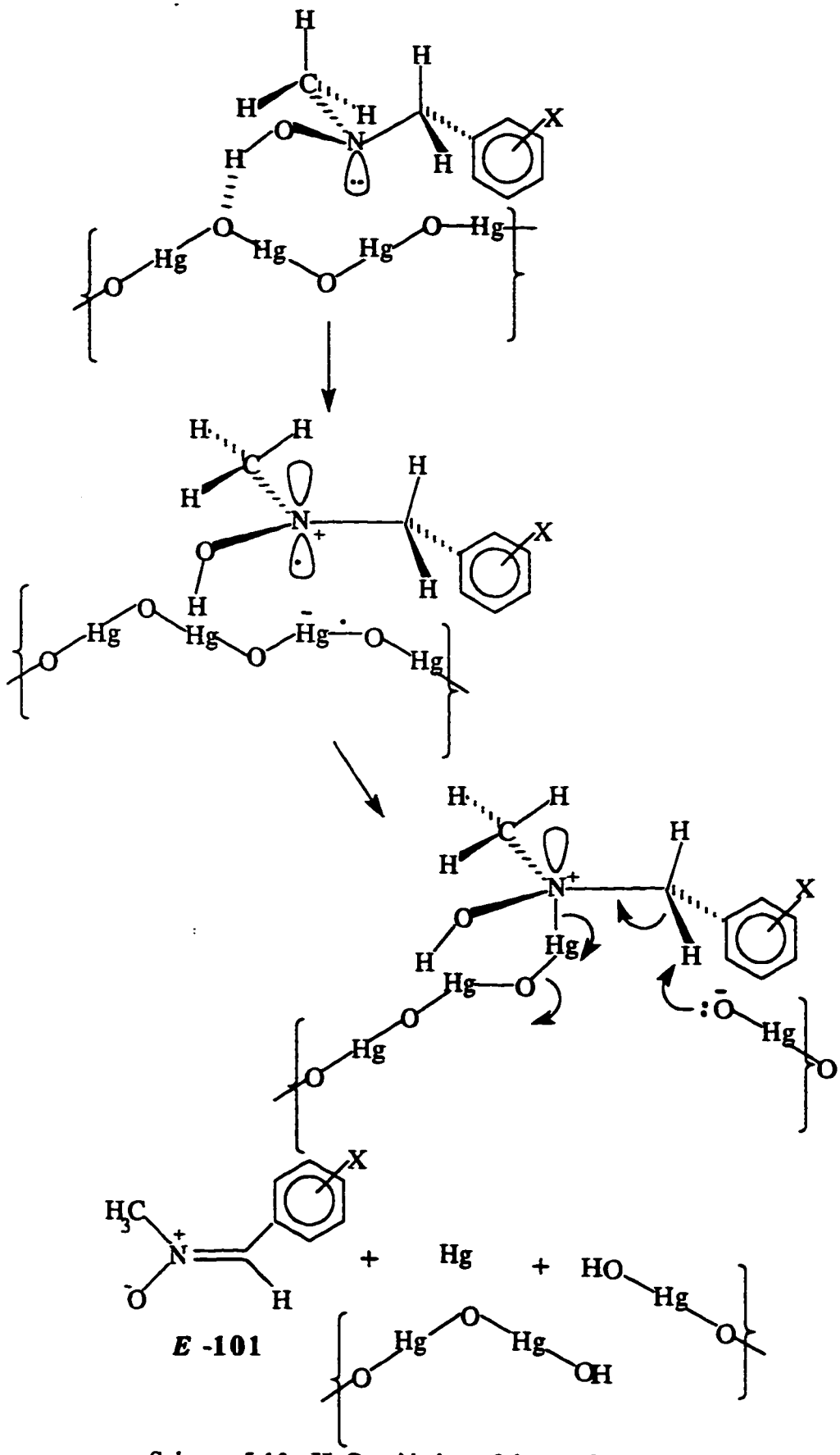

Scheme 5.10: HgO oxidation of the conformer **A**.

The magnitude of the ρ values are small but it is expected since the cationic centre is removed from the aromatic ring by intervening two σ bonds. Changing the N-alkyl group from methyl to ethyl, *iso* propyl or *tertiary* butyl group would lead to the increased stability of the conformer **B** with the anti disposition of phenyl and alkyl groups. However approach of the oxidant is favoured in case of the conformer **A**. The steric influence of phenyl ring is dependent on its orientation and presumably can tolerate the gauche interaction in **A** upto the *iso* propyl groups which still has a hydrogen attached to the carbon bonded to nitrogen.

To minimize steric crowding the benzene ring can orient itself in order to face the hydrogen. Once the remaining H is removed as in the *tertiary* butyl derivative the conformer **B** must definitely be the stable conformer. The planar transition state with extended C-N-C angle would enjoy relief of steric strain present in the pyramidal ground state. A rate ratio of 1:1.35:2.32:1.20 for the oxidation of **108a** (N-Me), **109a** (N-Et), **110a** (N-^{i}Pr), **111**(N-^{t}Bu) demonstrate the inportance of steric assistance in the rate enhancement. Less than expected rate enhancement for the *tertiary* butyl derivative could be attributed to the difficulty of the oxidant to reach the crowded hydroxylamine which prefers conformer **B**.

If one envisages the formation of radicals **C** and hydrogen abstraction as two discrete irreversible steps, with two transition states, then the oxidation rate ratio for the pair **108a/108a-d_2** or **110a/110a-d_2** or **111/111-d_2** should not be able to demonstrate primary isotope effect in the present experimental set up as described. The rate of formation of cation radical **C** should be approximately equal in each pair (there will be some difference due to secondary isotope effect). Abstraction of H or D in the second step would of course have different energy requirements. For a two step process (Figure 5.12) reversible formation of **C** in the first step would be able to demonstrate primary isotope effect. Formation of blue-coloured solution in the oxidation using *p*-benzoquinone

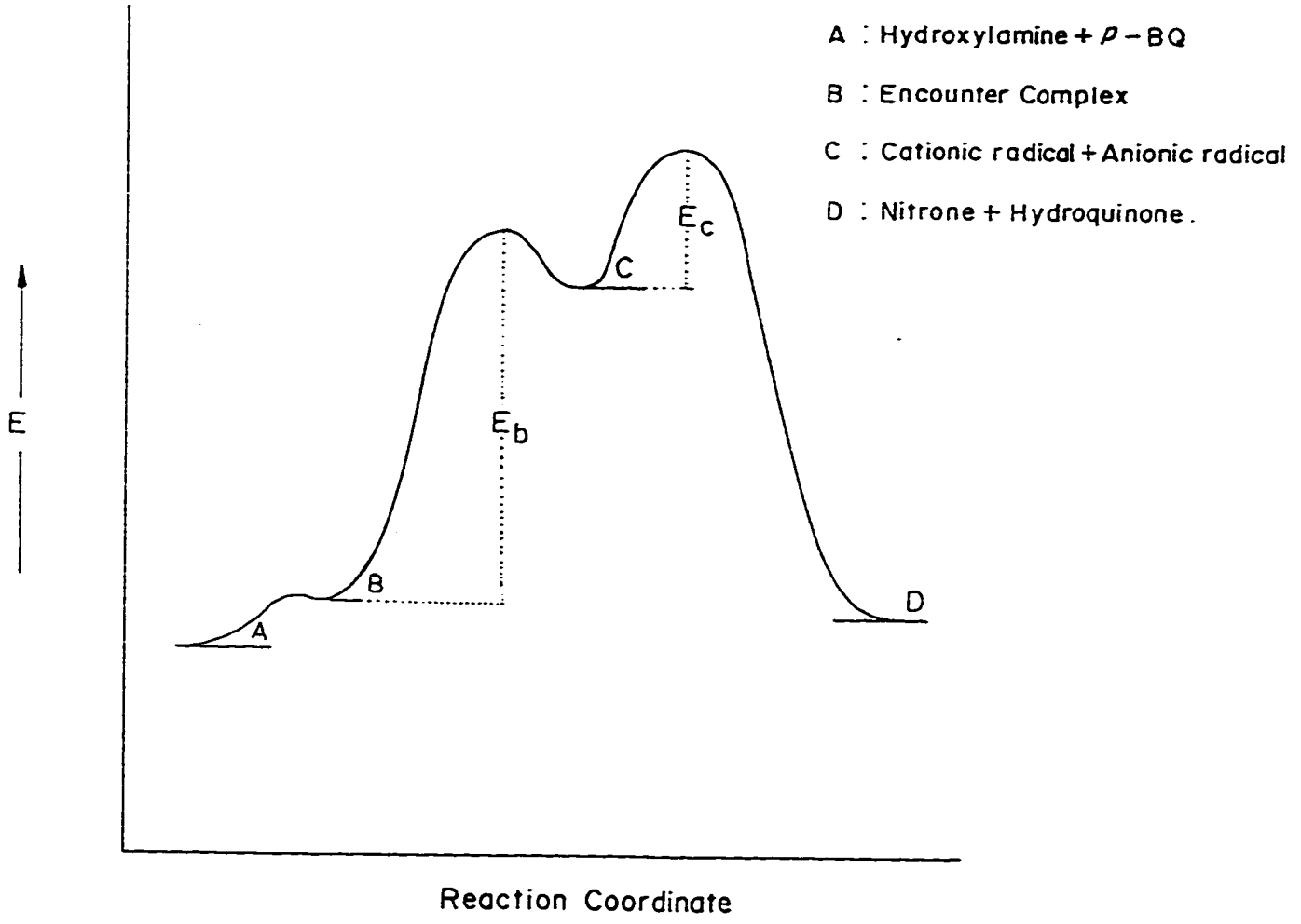

Figure 5.12 Energy diagram for the isomerization process.

indicated the formation of the free radicals. In the SET and polar pathway mechanistic spectrum, this oxidation lies more towards the SET terminal. To a great extent the abstraction of H is determined by the steric factor around the H to be abstracted. The barrier height E_b is determined by the relief of steric strain in planar transition state whereas E_c is determined by the steric encounter in the H abstraction. The relative height of the barrier is expected to be different for different N-alkyl groups since the benzyl group is the same in the hydroxylamines **108a -111**. In the HgO oxidation, the relative increase in the barrier E_c for oxidation of **111** is more than the decrease in E_b. However the *tertiary* butyl derivative reacts more slowly than other hydroxylamines.

5.4.2 E - Z Isomerization

During the course of the kinetic investigation of the oxidation of hydroxylamines the formation of a considerable proportion of the unstable *E* nitrones which isomerizes to the *Z* isomers readily, was observed (Scheme 5.11). Both HgO and *p*-BQ oxidation afforded a variable proportion of the *E* and *Z* isomers.

Since *p*- BQ oxidation was done at 20°C, most of the *E* -*Z* isomerization takes place before the NMR is taken. Previous workers, probably, did not notice the formation of *E* isomer in the HgO oxidation (0°C) because of the time lapse between the completion of the reaction and NMR recording (at room temperature). Table 5.16-5.17 display the *E*, *Z* regioisomeric distribution of HgO oxidation of several hydroxylamines carried out at -20°C. As is evident from the Table 5.16 20 -60 % of the nitrone **101** is formed as the unstable *E* isomer . In the oxidation of hydroxylamines **108f** it is the *E* isomer which predominates. This may also be the case with other hydroxylamines in this series, but the *E* nitrones might be isomerizing at a faster rate than in the case of **108f** (X=*p* -NMe_2) before the NMR spectra were recorded. It is to be noted that aromatic ring with electron withdrawing substituents tend to give lesser amount of unstable *E* isomer. This could be

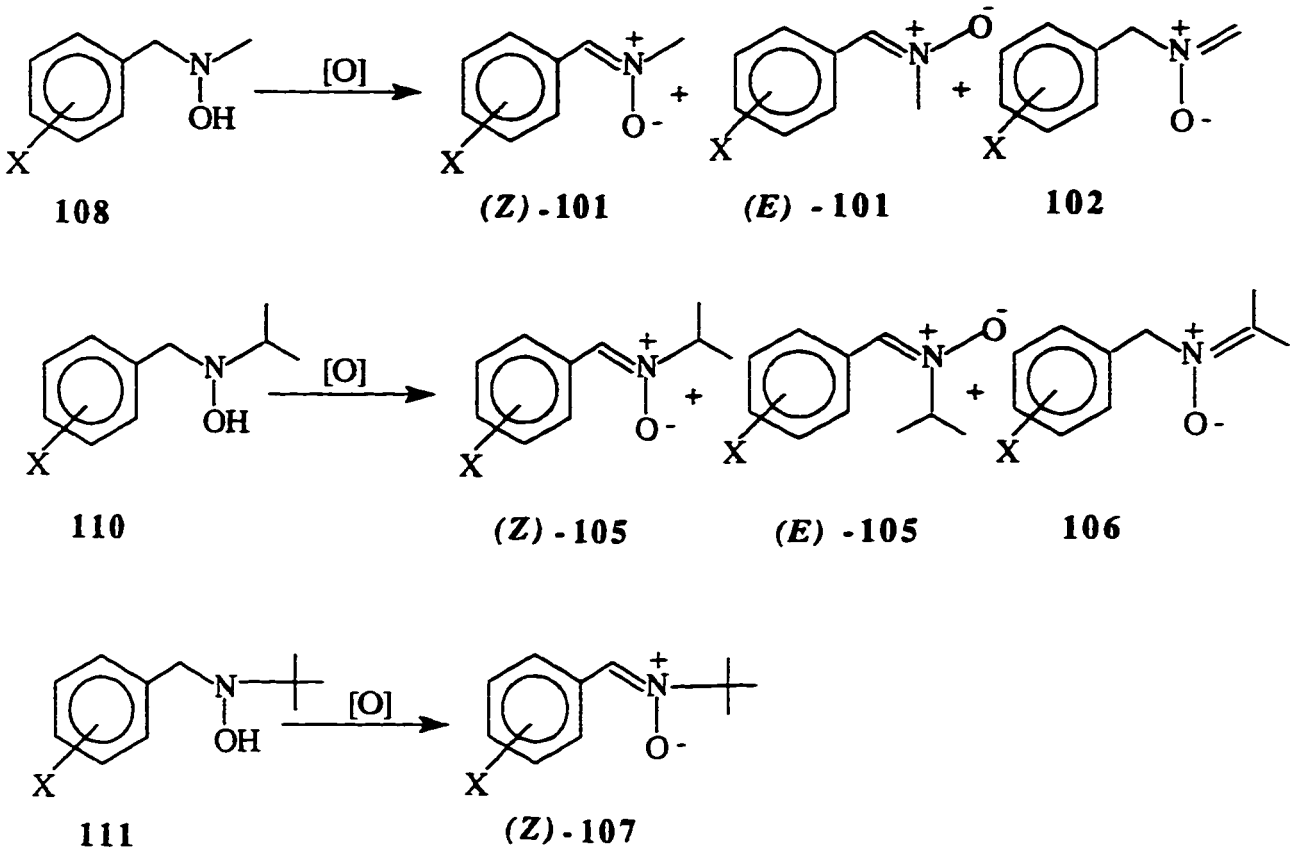

Scheme 5.11: Oxidation of the Hydroxylamines.

either attributed to the faster rate of *E* -*Z* isomerization or it is the inherent fact of the oxidation process which would give lesser amount of the unstable *E* nitrones. As the N-alkyl group is changed from methyl to ethyl or *iso* propyl the amount of the *E* isomer increases and become the major isomer, in the *iso* propyl series (Table 5.17). This could be understood in terms of the approach of the oxidant from the less hindered side of the conformer **A** and the subsequent formation of the *E* nitrone. For the *tertiary* butyl derivative the replacement cf the last hydrogen from the carbon attached to the nitrogen makes the conformer **B** the overwhelming preferred isomer since phenyl ring in conformer **A** cannot escape the steric encumbrance of the *tertiary* butyl group. We did not detect any formation of the *E* nitrone **107** in the oxidation of the hydroxylamine **111**. Transition state as well as the product ***E*** **107** would experience intolerable steric crowding between the phenyl

Table 5.16 : Composition of the nitrones in the oxidation of N-methylhydroxylamine with HgO in $CDCl_3$ at -20°C.

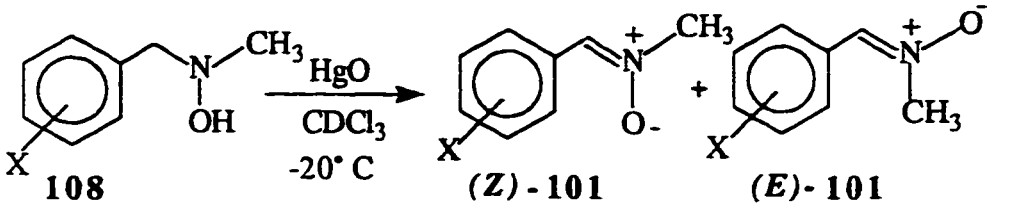

Hydroxylamine	Z:E [a]	Z:E [b]
108a H	70:30	55:45
108b *p*- NO_2	85:15	80:20
108c *p* -Cl	67:33	63:37
108d *p* - OMe	56:44	50:50
108e *p* -Me	68:32	53:47
108f *p*- NMe_2	58:42	40:60
108i *o* -OMe	68:32	50:50

a: Ratio of E/Z isomers at -20°C at the end of the reaction (2h).

b: In situ experiment in the NMR probe at -20°C.

Table 5.17 Composition of the nitrones in the HgO oxidation of hydroxylamines at -20°C.

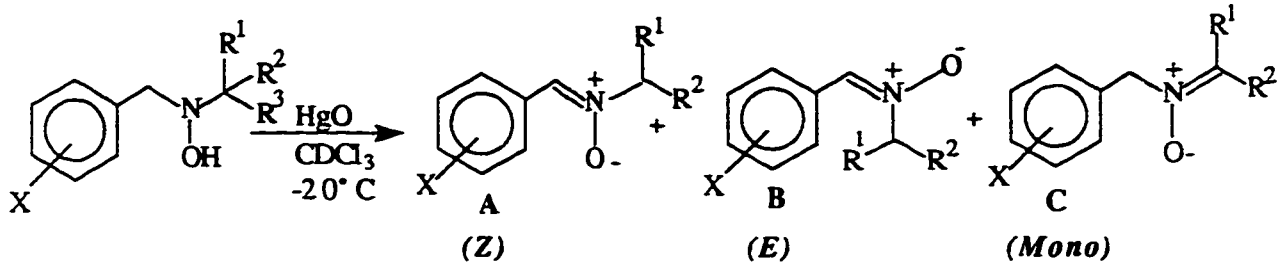

Hydroxylamine	R^1	R^2	R^3	(%) composition of Nitrones					
				A		B		C	
108a	H	H	H	***(Z)*-101a**	37	***(E)*-101a**	16	**102a**	47
109a	Me	H	H	***(Z)*-103**	31	***(E)*-103**	19	**104**	50
110a	Me	Me	H	***(Z)*-105a**	40	***(E)*-105a**	54	**106**	6
111a	Me	Me	Me	***(Z)*-107**	100	***(E)*-107**	~0	-	

and *tertiary* butyl groups. Such crowding in the *iso* propyl series can be relieved by orientation of the phenyl ring facing the α- hydrogen. The hydroxylamine **110** failed to produce the nonconjugated *E* nitrone **106** indicating more severe steric crowding between the *tertiary* butyl and phenyl group as compared to methyl versus phenyl group. Steric influence of phenyl ring is orientation dependent and its effective size for a particular orientation could be much smaller than the alkyl groups.

The *E* isomer equilibrates completely to the *Z* isomer. So we are not able to determine the equlibrium constant. An energy difference of 13-17 kJ/mol would correspond to an eqilibrium concentration of the *E* isomer of < 1%; which would be less than the NMR detection limit. The free energy difference between the *E* and *Z* isomers may well be higher than 13-17 kJ/mol. For all practical purposes the isomerization process seems to be irreversible. In any case stable *Z* isomers to the unstable *E* isomer will be very much energetically unfavourable. Proton NMR signals of various *E* and *Z* isomers are given in Tables 5.18 and 5.19. The aromatic *ortho* protons of *E* nitrones appear almost δ 1ppm higher field than the corresponding *Z* nitrones. The downfield shift for the *ortho* proton in *Z*, thus indicates the conjugation of the nitrone functionality with the aromatic ring, whereas in the *E* nitrone such conjugative deshielding is absent. The methine hydrogen (CH=N) in the *E* isomers is shifted downfield by 0.5-0.6 ppm (in comparision to the *Z* nitrones) indicating the *cis* relationship between the H and O. The *cis* desposition of H and negatively charged O are known to deshield the proton. Based on the proton chemical shifts the conformation and configuration of the *E* and *Z* nitrones can be drawn as shown in Figure 5.13. The *E* nitrone have the aromatic plane perpendicular to the plane of the nitrone functionality whereas they are coplanar in the *Z* nitrones. In order to avoid steric congestion between the aromatic *ortho* protons and the alkyl (R) group the *E* isomer adopts the perpendicular conformation. This is, to our knowledge the first comprehensive

Table 5.18: ^1H chemical shifts of *E* and *Z* nitrones of various derivatives of hydroxylamine **101**.

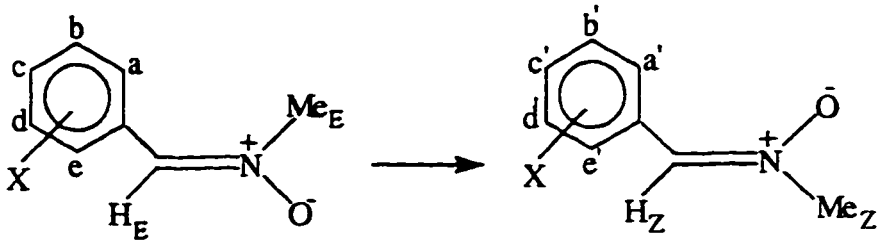

(E) - **101** *(Z)* - **101**

Nitrones	*E* (ppm)			*Z* (ppm)		
101	Aromatic protons	H_E	Me_E	Aromatic protons	H_Z	Me_Z
a X=H	7.5 (a-e)	8.04	3.89	8.30 (a', e')	7.50	3.93
				7.50 (b', d')		
b X=*p* -NO_2	7.72 (a, e)	8.05	3.95	8.46 (a', e')	7.63	3.99
	8.35 (b, d)			8.34 (b', d')		
c X=*p* -Cl	7.33 (a, e)	7.98	3.87	8.26 (a', e')	7.44	3.92
	7.50 (b, d)			7.44 (b', d')		
d X=*p* -OMe	7.28 (a, e)	7.96	3.84	8.28 (a', e')	7.37	3.87
	7.02 (b, d)			6.98 (b', d')		
e X=*p* -Me	7.30 (a, b, d, e)	8.00	3.87	8.20 (a', e')	7.42	3.90
				7.28 (b', d')		
f X=*p*-NMe_2	7.26 (a, e)	7.92	3.89	8.22 (a', e')	7.27	3.84
	6.74 (b, d)			6.74 (b', d')		
g X=*m* -NO_2	-	-	-		7.79	4.04
i X=*o* - OMe	~7 (b, c)7.28 (d)	8.02	3.87	9.30 (a') 7.45 (c')	7.92	3.92
	7.45 (a)			7.08 (b') 6.94 (d')		

Table 5.19: ^1H chemical shifts of E and Z nitrones of various hydroxylamines.

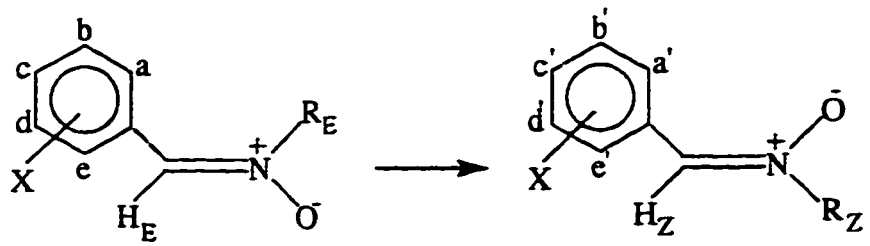

(E) *(Z)*

Nitrones	*E* (ppm)			*Z* (ppm)		
	Aromatic protons	H_E	R_E	Aromatic protons	H_Z	R_Z
103 X=H	7.3-7.6 (a-e)	7.97	1.56,	8.30 (a', e')	7.49	1.58
R=Et			4.05	7.45 (b', d')		4.00
105a X=H	7.3- 7.5 (a - e)	7.90	1.44	8.28 (a', e')	7.50	1.51
R=^{i}Pr			4.72	7.45 (b', d')		4.23
107 X=H	-	-	-	8.33 (a', c')	7.58	1.60
R=^{t}Bu				7.43 (b'- d')		

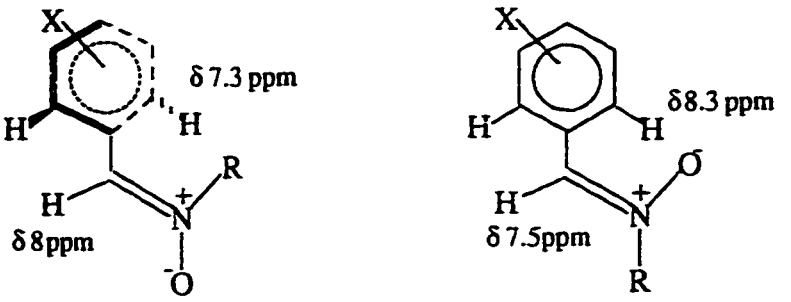

E *Z*

Figure 5.13: The conformation and configuration of *E* and *Z* nitrone

study of *E*, *Z* isomeric nitrones where the aromatic *ortho* (2, 6) positions are not substituted. Previous studies dealt with nitrones which remained in perpendicular conformation in both *E* and *Z* isomer due to the presence of substituents. The *Z* nitrones in those cases also adopts the perpendicular conformation in order to avoid crowding between the methine H and the *ortho* substituents. The present study provided the opportunity to compare the NMR chemical shifts between noncoplanar *E* and coplanar *Z* and also to study the kinetics of E - Z isomerization.

The difference (0.04 ppm) between the chemical shifts of N-R proton signals of the *E* and *Z* nitrones are found to be less than the difference (0.5 ppm) found in the study involving noncoplanar *E*, *Z* nitrones. Shielding effect of the aromatic π - cloud in the noncoplanar *E* nitrones are supposed to induce an upfield shift of the N-R signals. However in the present study this upfield shift was found to be a meager 0.04 ppm. In case of the nitrone **101f** ($X=NMe_2$) this upfield trend of the N-methyl signal is even reversed. Aromatic π cloud with increased π density due to electron donation by NMe_2 group even caused the N-methyl signal in the E-isomer to appear downfield (increased electron density should have shielded the N-methyl protons). In *iso* propyl series while the methyl protons

appeared slightly upfield in the *E* nitrones, the CH proton of the *iso* propyl group unexpectedly experiences a downfield shift of 0.5 ppm. At this stage an explanation for this apparent anomaly cannot be offered.

Semiemperical molecular orbital calculation on the nitrone **101a** predicted that the *Z*- isomer with coplanar arrangement is more stable than the *E* isomer with orthogonal geometry by 13-17 kJ/mol. Our experimental findings of non detectable amount of *E* isomer after equilibration supports the calculation. It was calculated that the planar arrangement in *E* isomer is destabilized by c.a 126 kJ/mol with the orthogonal geometry.

Formation of considerable amount of *E* isomer in the oxidation of hydroxylamines provided us with the opportunity to study the kinetics of E=Z isomerization. Unlike other

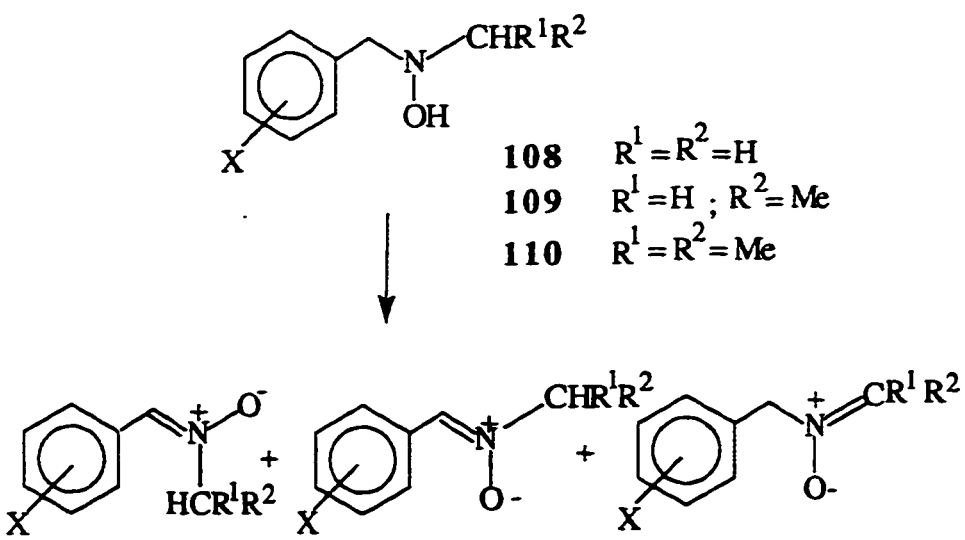

(E) **-101**	***(Z)*** **-101**	**102**
(E) **- 103**	***(Z)*** **-103**	**104**
(E) **- 105**	***(Z)*** **-105**	**106**

Scheme 5.12: Formation of three kinds of nitrones during the oxidation process.

studies involving the kinetics of nitrone E-Z isomerization, we cannot in our study obtain the *E* isomers in its pure isolated form. The HgO oxidation of a 0.2 M solution of the hydroxylamines **108-110** in $CDCl_3$ (at -15 to -20 °C, 2h), afforded a mixture of the *E* and *Z* nitrones **101, 103,** and **105** and the regioisomeric nitrones **102, 104,** and **106** alongwith the unreacted starting hydroxylamines (5-15%). In order to ensure the complete consumption of the hydroxylamines the oxidation process needed to be run for longer duration which would jeoperdize the appreciable presence of the *E* nitrone required for the kinetic runs. As soon as the nitrones are formed, the E-Z isomerization would occur in the reaction flask. Kinetic runs were run in base (NH_3) washed NMR tubes, by NMR technique. Change of intensity of N-CH_3, N-CH_2-, N-CH-, CH=N, aromatic *ortho* protons were monitored and the first order rate constant for E=Z isomerization process were detrmined by the linear regression analysis. Excellent correlation coefficients were obtained in all the cases. Rate constants along with activation parameters are included in the Table 5.20. Low values of E_a and $\Delta G^{\#}$ and very large negative values of entropy of activation cast doubt on the validity of the assumption that the isomerization is a unimolecular process. In any unimolecular process the entropy of activation should be close to zero. The rate constants are not reproducible. Higher rate constants for the isomerization of N-methyl nitrone ***(E)*-101** than the N-*iso* propyl derivative ***(E)*-105** is also unexpected, since the severe crowding in the later should lead to easier isomerization.

In a series of experiments with a mixture of ***(E)* -101** and ***(E)* -101f** in the same NMR tube the rate constants for the individual isomerization were measured. This was done in order to determine the relative rates of isomerization. The presence of two nitrones in the same NMR tube would experience the same effects (whatever those effects may be). As presented in Table 5.21 the rate constants for the isomerisation of ***(E)* -101f** varies from 4.70×10^{-5} s^{-1} to 25.0×10^{-5} s^{-1}. The rate constants are not reproducible. However one thing is clear. The rate constant for the isomerization of ***(E)*-101f** is found to be always slower than that of its counterpart with different substituent X.

Table 5.20: Rate constants and Thermodynamic parameters obtained for isomerization process.

Z	Temp °C	k *10-5 s^{-1}	E_a kJ/mol	$\Delta H^{\#}$ kJ/mol	$\Delta G^{\#}$ 273K kJ/mol	$\Delta S^{\#}$ J/mol K
101a	-31.2	2.25				
	-20	11.6	66.1	64.0	81.9	-65.6
	-10.5	61.2 [a]				
	0.5	93.7				
101a	-10	9.46				
	0	16.8	40.0	37.8	86.2	-177
	9.8	35.7				
101f	-20	6.60				
	-10	16.4	46.3	44.2	84.7	-148
	0	35.6				
101f	-20	6.16				
	-10	9.45 [b]	34.5	32.3	86.0	-196
	0	21.8				
103	0.2	31.5	66.7	64.4	85.0	-75.4
	10.4	94.4				
105a	10	3.83				
	19.7	7.56	48.5	46.1	91.5	-166
	29.8	15.4				

[a] 21.0 [b] 19.8

Table 5.21: Individual rate constant (k) for the isomerization of a mixture of*(E)* **-101** and *(E)* **-101f** at -10°C in $CDCl_3$.

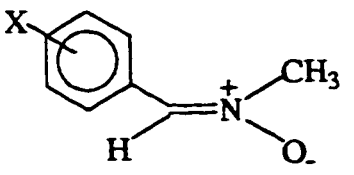

(E) **-101**

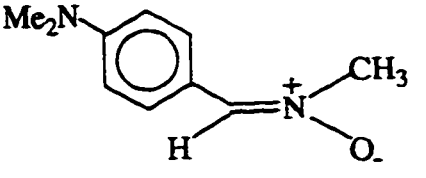

(E) **-101f**

Entry	X	$k_X \times 10^5$ s^{-1}	$k_{NMe2} \times 10^5 s^{-1}$
1	X= H	41.5	25.0
2	X= H	35.4	14.7
3	X= *p* -Me	14.9	8.54
4	X= *p* -Cl	26.9	13.1
5	X= *p* -Cl	33.7	17.2
6	X=*p* -OMe	47.6	25.0
7	X=*p* -OMe	41.6	16.1
8	X=*o* -OMe	28.8	6.17
9	X= *p* -NO_2	40.9	4.70

Evidence presented so far indicate the isomerization to be a bimolecular process. Nucleophilic addition to the *E* nitrone would lead to the reversible formation of the tetrahedral addition product **A** which could either go back to the starting *E* nitrone or

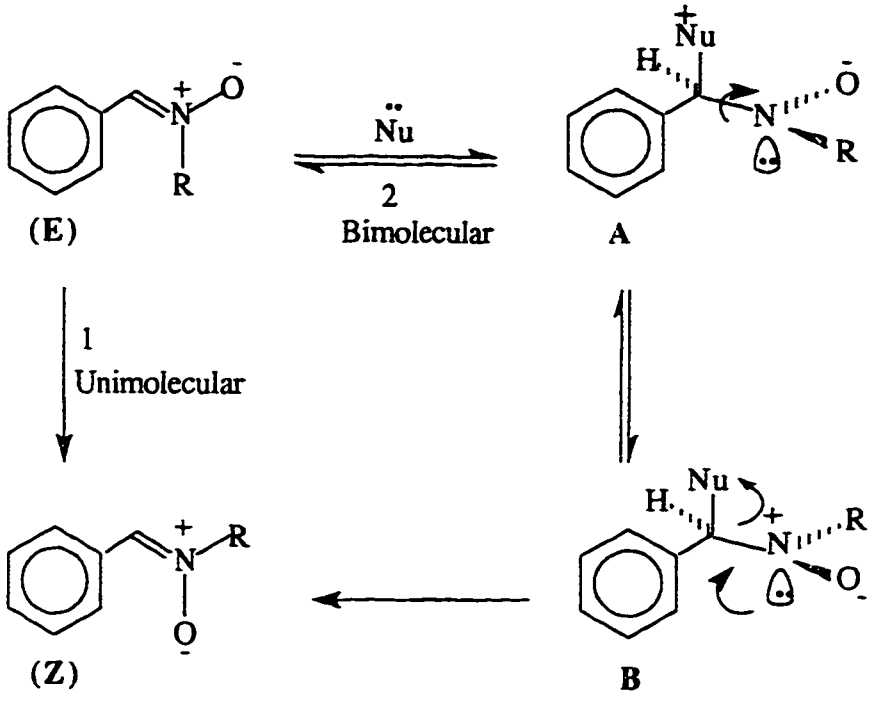

Scheme 5.13: The mechanistic pathway of the E-Z isomerization process.

to the stable nitrone *Z* via the conformer **B** (obtained from **A** by C-N rotation). This isomerization scheme clarifies various points. Bimolecular process would lead to a large negative entropy of activation. Because of steric reason addition of nucleophile to the N-*iso* propyl nitrone ***(E)*-105** would be slower as observed. Addition of nucleophile to the electron rich ***(E)*-101f** is expected to be slower. As regards to the nature of the nucleophilic species it could be the unreacted hydroxylamine, the nitrone itself or any basic entity present during the oxidation with HgO.

REFERENCES

1. O. Finn, J. Meisenheimer, C. Angerman and E. Vieweg, *Ber.*, **57**, 1745, (1924).
2. E. F. Barker, *Phys. Rev.*, **33**, 684, (1929).
3. D. M. Dennison and J. D. Hardy, *Phys. Rev.*, **39**, 938, (1932).
4. J. B. Lambert, *Top. Stereochem.*, **6**, 19, (1971).
5. H. Kessel :r, *Angew. Chem. Int. Ed. Engl.*, **9**, 219, (1970).
6. K. Mislow, A. Rauk, and L. C. Allen, *Angew. Chem. Int. Ed. Engl.*, **9**, 400, (1970).
7. J. M. Lehı., *Fortschr. Chem. Forsch.*, **15**, 311, (1971).
8. (a) G. C. Levin, *J. Am. Chem. Soc.*, **97**, 5649, (1975).
   (b) W. Cherry and N. Epiotis, *J. Am. Chem. Soc.*, **98**, 1135, (1976).
9. H. S. Gutowsky, *J. Chem. Phys.*, **37**, 2196, (1962).
10. M. Saunders and F. Yamada, *J. Am. Chem. Soc.*, **85**, 1882, (1963).
11. W. Gordy, W. V. Smith and R. F. Trambarulo, "*Microwave Spectroscopy*", Wiley, Ne w York, (1953).
12. J. B. Lam ɔert and W. L. Oliver, *J. Am. Chem. Soc.*, **91**, 7774, (1969).
13. F. A. L. Anet and J. M. Osyany, *J. Am. Chem. Soc.*, **89**, 352, (1967).
14. S. J. Brois, *J. Am. Chem. Soc.*, **90**, 506, (1968).
15. K. Muller and Escheumoser, *Helv. Chim. Acta.*, **52**, 1823, (1969).

16. R. Annunziata, R. Fornasier and F. Montanari, *Chem. Commun.*, 1133, (1972).

17. A. Rauk, L. C. Allew, and K. Mislow, *Angew. Chem., Int. Ed. Engl.*, **9**, 400, (1970).

18. M. Raban and D. Kost, *J. Am. Chem. Soc.*, **94**, 3234, (1972).

19. R. D. Baechler and K. Mislow, *J. Am. Chem. Soc.*, **93**, 773, (1971).

20. O. J. Scherer and R. Mergner, *J. Organometal Chem.*, **40**, C64, (1972).

21. R. H. Bowman and K. Mislow, *J. Am. Chem. Soc.*, **94**, 2861, (1972).

22. J. B. Lambert and D. H. Johnson, *J. Am. Chem. Soc.*, **90**, 1349, (1968).

23. (a) A. J. Gordon and J. P. Gallagher, *Tetrahedron Lett.*, 2541, (1970).
(b) D. L. Griffith, J. E. Anderson and J. D. Roberts, *J. Am. Chem. Soc.* **91**, 6371, (1969).

24. M. Raban, F. B. Jones, Jr., E. H. Carlson, E. Bannuci, and N. A. LeBel, *J. Org. Chem.*, **35**, 1496, (1970).

25. (a) L. Pedersen and K. Morukama, *J. Chem. Phys.*, **46**, 3941, (1967).
(b) W. H. Fink, D. C. Pan and L. C. Allen, *J. Chem. Phys.*, **47**, 895, (1967).

26. L. Radom, W. J. Hehre and J. A. Pople, *J. Am. Chem. Soc.*, **94**, 2371, (1972).

27. (a) P. A. Giguere and I. D. Liu, *Can. J. Chem.*, **30**, 948, (1952).
(b) Tsunekawa, *J. Phys. Soc. Japan.*, **33**, 167, (1972).

28. R. A. Y. Jones, A. R. Katritzky, S. Saba and A. J. Sparrow, *J. Chem. Soc. Perkin Trans 2.*, 1154, (1974).

29. F. G. Riddel, E. S. Turner, D. W. H. Rankin and M. R. Todd, *J. Chem. Soc. Chem. Commun.*, 72, (1979).

30. D. L. Grifith and J. D. Roberts, *J. Am. Chem. Soc.*, **87**, 4089, (1965).

31. (a) M. Raban and G. W. J. Kenney, *Tetrahedron Letters.*, 1295, (1969).
(b) W. Walter and E. Schaumann, *Liebigs Ann.*, **747**, 191, (1971).

32. J. R. Fletcher and I. O. Sutherland, *Chem. Comm.*, 687, (1970).

33. T. B. Posner, D. A. Crouch and C. D. Hall, *J. Chem. Soc. Perkin Trans 2.*, 450, (1978).

34. (a) B. J. Price, and I. O. Sutherland, *Chem. Comm.*, 1070, (1967).
(b) M. Raban and D. Kost, *J. Org. Chem.*, **37**, 449, (1972).

35. F. Montanri, I. Moretti and G. Torre, *Chem. Comm.*, 1086, (1969).

36. J. Lee and K. G. Orrell, *Trans. Faraday Soc.*, **61**, 2342, (1965).

37. F. G. Riddell, J. M. Lehn and J. Wagner, *Chem. Comm.*, 1043, (1968).

38. D. L. Griffith and B. L. Olson, *Chem. Comm.*, 1682, (1968).

39. M. Raban and D. Kost, *Tetrahedron.*, **40**, 3345, (1984).

40. H. Hirschman and K. R. Hanson, *Tetrahedron.*, **30**, 3649, (1974).

41. M. Raban, G. W. J. Kenney, Jr. and F. B. Jones, Jr., *J. Am. Chem. Soc.*, **91**, 6677, (1969).

42. W. G. Stewart and T. H. Spidall III, *Chem. Rev.*, **70**, 517, (1970).

43. G. Binsch, E. L. Eliel and H. Kessler, *Angew. Chem. Int. Ed.*, **10**, 570, (1971).

44. F. Bernardi, I. G. Csizmadia, A. Mangini, H. B. Schelgel, M. H. Whangbo and S, Wolfe, *J. Am. Chem. Soc.*, **97**, 2209, (1975).

45. F. G. Riddel, *Tetrahedron.*, **37**, 849, (1981).

46. (a) D. Kost and E. Berman, *Tetrahedron Letters.*, **21**, 1065, (1980).
(b) M. D. Raban and D. Kost, *J. Org. Chem.*, **37**, 499, (1972).
(c) F. G. Riddel and E. S. Turner, *J. Chem. Soc., Perkin Trans 2.*, 707, (1978).

47. (a) F. Montanari, I. Moretti and G. Torre, *Chem. Commun.*, 1086, (1969).
(b) J. Lee and K. G. Orrell, *Trans. Faraday Soc.*, **61**, 2342, (1965).
(c) K. Muller, and A. Eschemmoser, *Helv. Chim. Acta.*, **52**, 1823, (1969).

48. M. Raban, F. B. Jones, Jr., E. H. Carlson, E. Banuci, and N. A. LeBel, *J. Org. Chem.*, **35**, 1496, (1970).

49. G. S. Denisov, V. A. Gindin, N. S. Golubev, A. I. Koltsov, S. N. Smirnov, M. Rospenk, A. Koll and L. Sobczyk, *Mag. Reson. Chem.*, **31**, 1034, (1993).

50. S. F. Nelson, P. A. Petillo, H. Chang, T. B. Frigo, D. A. Dougherty and M. Kaftory, *J. Org. Chem.*, **56**, 613, (1991).

51. S. F. Nelson, P. A. Petillo and D. T. Rumack, *J. Am. Chem. Soc.*, **112**, 7144, (1990).

52. W. B. Jennings and S. P. Watson, *Tetrahedron Letters.*, **30**, 235, (1989).

53. W. B. Jennings, S. P. Watson and M. S. Tolley, *J. Am. Chem. Soc.*, **109**, 8099, (1987).

54. S. F. Nelson, T. B. Frigo, Y. Kim and J. A. Thomson-Colon, *J. Am. Chem. Soc.*, **108**, 7926, (1986).

55. (a). R. D. Bach and J. C. Evans, *J. Am. Chem. Soc.*, **108**, 1374, (1986).
(b). C. L. Perrin, J. D. Thoburn and S. Elsheimer, *J. Org. Chem.*, **56**, 7034, (1991).

56. (a). S. Wolfe, D. J. Mitchel and H. B. Schelegel, *Can. J. Chem.*, **60**, 1291, (1982).
(b). S. F. Nelson, P. A. Petillo and D. T. Rumack, *J. Am. Chem. Soc.*, **112**, 7144, (1990).

57. A. M. Brower and B. Krijnen, *J. Org. Chem.*, **60**, 32, (1995).

58. J. C. Wilson, S. L. A. Munro and D. J. Craik, *Mag. Reson. Chem.*, **33**, 367, (1995).

59. C. H. Bushweller, J. H. Brown, and C. M. Dimeglio, *J. Org.Chem.*, **60**, 268, (1995).

60. J. E. Anderson and J. E. T. Corrie, *J. Chem. Soc., Perkin Trans.* 2., 1027, (1992).

61. M. I. M. Wazeer and Sk. A. Ali, *Can. J. Appl. Spectro.*, **40**, 53, (1995).

62. M. I. M. Wazeer and Sk. A. Ali, *Mag. Reson. Chem.*, **31**, 12, (1993).

63. M. I. M. Wazeer, H. A. Al. Muallem and Sk. A. Ali, *J. Phys. Org. Chem.*, **6**, 326, (1993).

64. M. I. M. Wazeer and Sk. A. Ali, *Can. J. Appl. Spectro.*, **38**, 22, (1993).

65. (a) Sk. A. Ali and M. I. M. Wazeer, *Tetrahedron Letters.*, **34**, 137, (1993).
(b) Sk. A. Ali and M. I. M. Wazeer, *Tetrahedron Letters.*, **33**, 3219, (1992).

66. R. U. Lemieux, *Pure. Appl. Chem.*, **25**, 527, (1971).

67. W. A. Bonner, *J. Am. Chem. Soc.*, **73**, 2659, (1951).

68. E. L. Eliel and C. A. Giza, *J. Org. Chem.*, **33**, 3754, (1968).

69. C. B. Anderson and D. T. Sepp, *J. Org. Chem.*, **32**, 607, (1967).

70. C. V. Holland, D. Horton, J. S. Jewell, *J. Org. Chem.*, **32**, 1818, (1967).

71. F. A. Van-Catledge, *J. Am. Chem. Soc.*, **96**, 5693, (1974).

72. S. Wolfe, M. H. Whangbo and D. J. Mitchell, *Carbodhydr. Res.*, **69**, 1, (1979).

73. E. L. Eliel, D. K. Harograve, K. M. Dietrusoewicz and M. Manoharan, *J. Am. Chem. Soc.*, **104**, 3635, (1982).

74. I. Tvaroska and T. Bleha, *Advances in Carbohydrate Chemistry and Biochemistry*, D. Harton (Eds.) Academic Press, Sandiego, (1989), p45, and references cited therein.

75. (a) A. J. Kirby, *The Anomeric Effect and related Stereoelectric Effects at Oxygen* , Springer Verlag, Berlin, (1983).
(b) E. Juaristi and G. Cuevas, *Recent Studies of the Anomeric Effect, Tetrahedron* Report No. 315, Tetrahedron., **48**, 5019, (1992).

76. (a) E. L. Eliel and M. C. Knoeber, *J. Am. Chem. Soc.*, **90**, 3444, (1968).
(b) E. Juaristi, *Introduction to Stereochemistry and Conformational Analysis*, Wiley, N.Y., Chap. 16, (1991).

77. E. L. Eliel and C. A. Giza, *J. Org. Chem.*, **33**, 3754, (1968).

78. (a) I. Tvaroska and T. Kozar, *Int. J. Quantum Chem.*, **23**, 765, (1983).
(b) C. J. Kramer, *J. Org. Chem.*, **57**, 7034, (1992).

79. J. T. Edward, *J. Chem. Ind. London.*, 1102, (1955).

80. N. D. Epiotis, R. L. Yates, F. Bernardi and S. Wolfe, *J. Am. Chem. Soc.*, **98**, 5435, (1976).

81. A. J. Kirby, *The Anomeric Effect and Related Stereoelect.ronic Effects of Oxygen*, Springer Verlag Berlin, (1983).

82. M. Liang, *J. Chem. Edu.*, **64**, 124, (1987).

83. A. Cosse-Barbi and J. E. Dubois, *J. Am. Chem. Soc.*, **109**, 1503, (1987).

84. A. Cosse-Barbi, D. J. Watson and J. E. Dubois, *Tertrahedron Lett.*, **30**, 163, (1968).

85. H. Booth, K. A. Khedhair and S. A. Readshaw, *Tetrahedron.*, **43**, 4699, (1987).

86. J. P. Praly and R. U. Lemieux, *Can. J. Chem.*, **65**, 213, (1987).

87. H. Booth, T. B. Grindley and K. A. Khedhair, *J. Chem. Soc. Chem. Commun.*, 1047, (1982).

88. B. M. Pinto, B. D. Johnson and R. Nagelkarke, *J. Org. Chem.*, **53**, 5668, (1988).

89. R. U. Lemieux, *Explorations with Sugars - How Sweet it was, in Profiles, Pathways and Dreams.*, (J. I. Seeman, Ed.) *Am. Chem. Soc.* Washington DC, (1990).

90. M. L. Sinnot, *Adv. Phy. Org. Chem.*, **24**, 113, (1988).

91. V. G. S. Box, *Heterocylces.*, **31**, 157, (1990).

92. J. Bjorgo, D. R. Boyd, C. G. Watson, W. B. Jennings and D. M. Jerina, *J. Chem. Soc. Perkin Trans* 2., 1081, (1974), and references cited therein.

93. W. B. Jennings and D. R. Boyd, *J. Am. Chem. Soc.*, **94**, 7187, (1972).

94. (a) J. Bjorgo, D. R. Boyd and D. C. Neill, *J. Chem. Soc. Chem. Comm.*, 478, (1974).

(b) J. Bjorgo, D. R. Boyd, D. C. Neill and W. B. Jennings, *J. Chem. Soc. Perkin Trans 1.*, 254, (1977).

95. L. W. Boyle, M. J. Peagram and G. H. Whitham, *J. Chem. Soc. (B).*, 1728, (1971).

96. K. Koyano and I. Tanaka, *J. Phys. Chem.*, **69**, 2545, (1965).

97. (a) G. B. Kistiakowsky and W. R. Smith, *J. Am. Chem. Soc.*, **56**, 638, (1973).

(b) J. E. Douglas, B. S. Rabinavitch and F. S. Looney, *J. Chem. Phys.*, **23**, 315, (1955).

98. W. B. Jennings and D. R. Boyd, *J. Am. Chem. Soc.*, **94**, 7187, (1972).

99. W.B. Jennings, D. R. Boyd, L. C. Wearing, *J. Chem. Soc. Perkin Trans 2.*, 610, (1976).

100. W. B. Jennings, S. Al-Showiman, M. S. Tolley, D. R. Boyd, *J. Chem. Soc. Perkin Trans. 2.*, 1535, (1975).

101. (a) H. O. Kalinowski and H. Kessler, *Topics Setreochem.*, **7**, 295, (1973).

(b) H. Kessler, *Tetrahedron.*, **30**, 1861, (1974).

102. J. Bjorgo, D. R. Boyd, *J. Chem. Soc. Perkin Trans 2.*, 1575, (1973).

103. M. Raban, *Chem. Commun.*, 1415, (1970).

104. T. S. Dobashi, M. H. Goodrow and E. J. Grubbs, *J. Org. Chem.*, **38**, 4440, (1973).

105. E. L. Hahn and D. E. Maxwell, *Phys. Rev.*, **88**, 1070, (1952).

106. H. M. McConnell, *J. Chem. Phys.*, **28**, 430, (1958).

107. H. Shanan-Atidi and K. H. Bar-Eli, *J. Phys. Chem.*, **74**, 961, (1970).

108. C. S. Johnson, *Adv. in Mag. Res.*, **1**, 33, (1965).

109. R. M. Lynden-Bell, *Prog. NMR Spectry.*, **2**, 163, (1967).

110. The NMR Program Library, Science and Engineering Research Council, Daresbury, U.K. (1975).

111. S. W. Benson, *The Foundations of Chemical Kinetics*, McGraw-Hill, (1960).

112. W. Walter, E. Schaumann and J. Voss, *Org. Mag. Res.*, **3**, 733, (1971).

113. R. K. Harris, *Specialists Periodical Reports, NMR*, **2**, 220, (1973).

114. J. Sandstrom, *"Dynamic NMR Spectroscopy"*. Academic Press, London, (1982).

115. C. K. Ingold and F. R. Shaw, *J. Chem. Soc.*, 2918, (1927).

116. D. L. Griffith, B. L. Olson and J. D. Roberts, *J. Am. Chem. Soc.*, 1648, **93**, (1971).

117. A. T. Bottini and J. D. Roberts, *J. Am. Chem. Soc.*, **80**, 5203, (1958).

118. J. E. Anderson and J. M. Lehn, *J. Am. Chem. Soc.*, **89**, 81, (1967).

119. J. E. Anderson and A. C. Oehlschlager, *J. Chem. Soc. Chem. Commun.*, 284, (1968).

120. W. K. Busfield, I. D. Jenkins, S. H. Thang, G. Moad, E. Rizzardo and D. H. Solomon, *J. Chem. Soc. Chem. Commun.*, 1249, (1985).

121. M. I. M. Wazeer, H. A. Al. Muallem, S. S. Fayyaz and Sk. A. Ali, *Canadian J. App. Spectro.*, **40**, 27, (1995).

122. T. B. Grindley, *Tetrahedron Lett.*, 1757, (1982).

123. E. L. Eliel, and S. H. Wilen, *"Stereochemistry of Organic Compounds"*, John Wiley & Sons, Inc., p.758, (1994).

124. P. N. Confalone and E. M. Huie, *Organic Reactions.*, **36**, 1, (1988).

125. P. Deshong, C. M. Dicken, R. R. Staib, A. J. Freyer, and S. M. Weinreb, *J. Org.Chem.*, **47**, 4397, (1982).

126. F. G. Riddel, *"The Conformational Analysis of Heterocyclic Compounds"*, Academic Press, London, (1980), and references cited therein.

127. Sk. A. Ali and M. I. M. Wazeer, *J. Chem. Soc. Perkin Trans 2.*, 1789, (1986).

APPENDIX

BANDSHAPES OF FEW COMPOUNDS

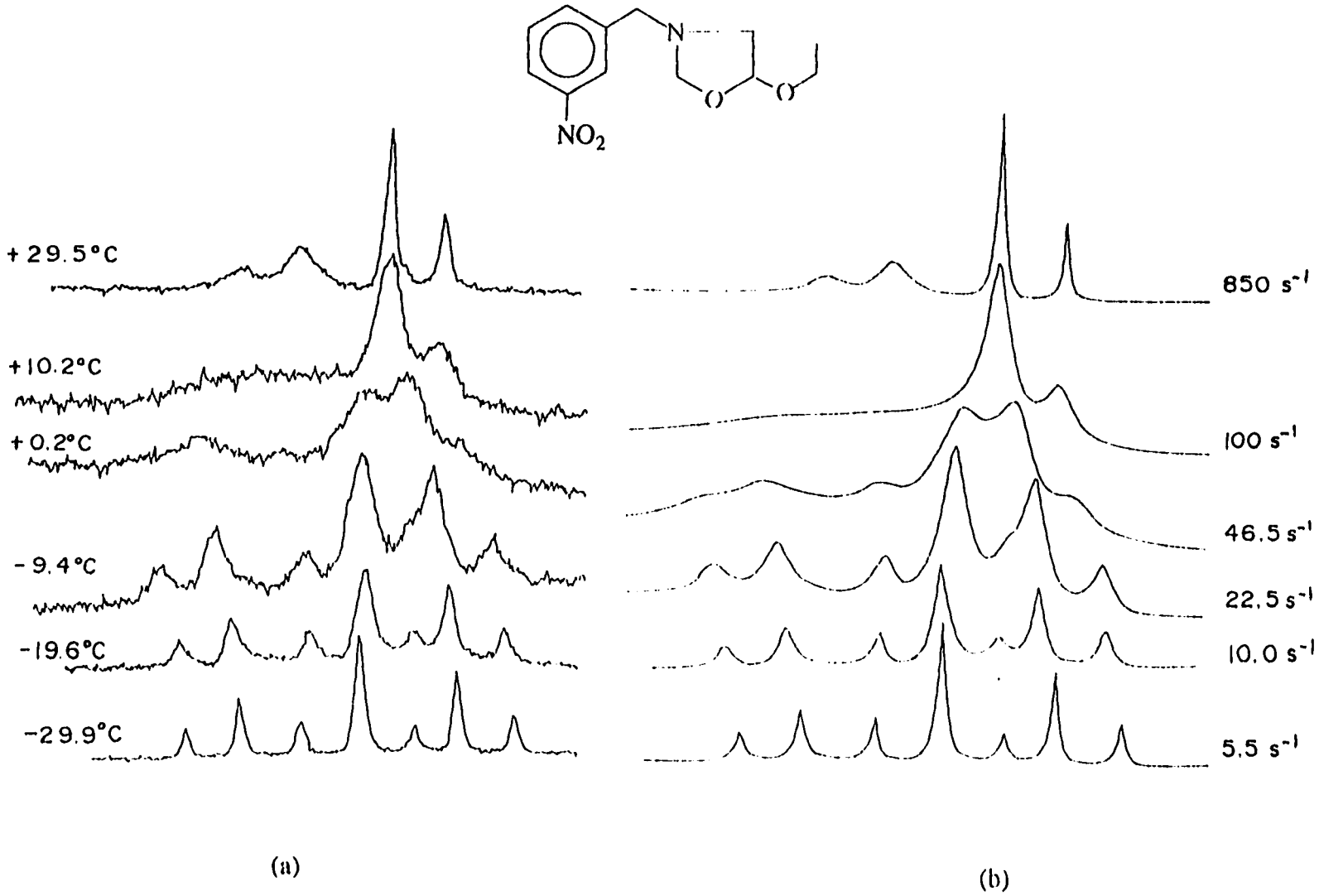

Figure A.1 ^{1}H spectrum of **124b**. (a) Observed (b) Calculated.

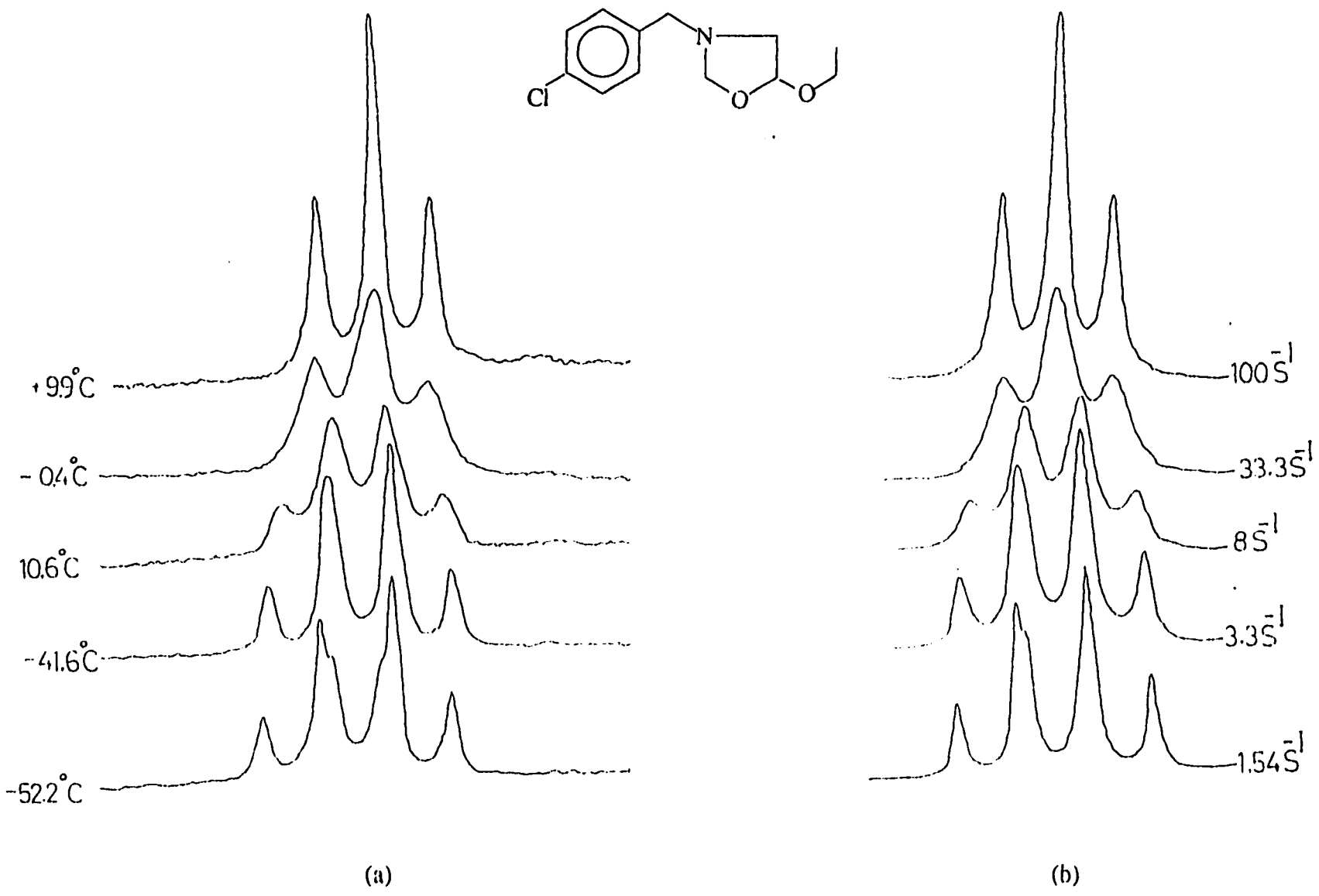

Figure A.2 ^1H spectrum of **124c**. (a) Observed (b) Calculated.

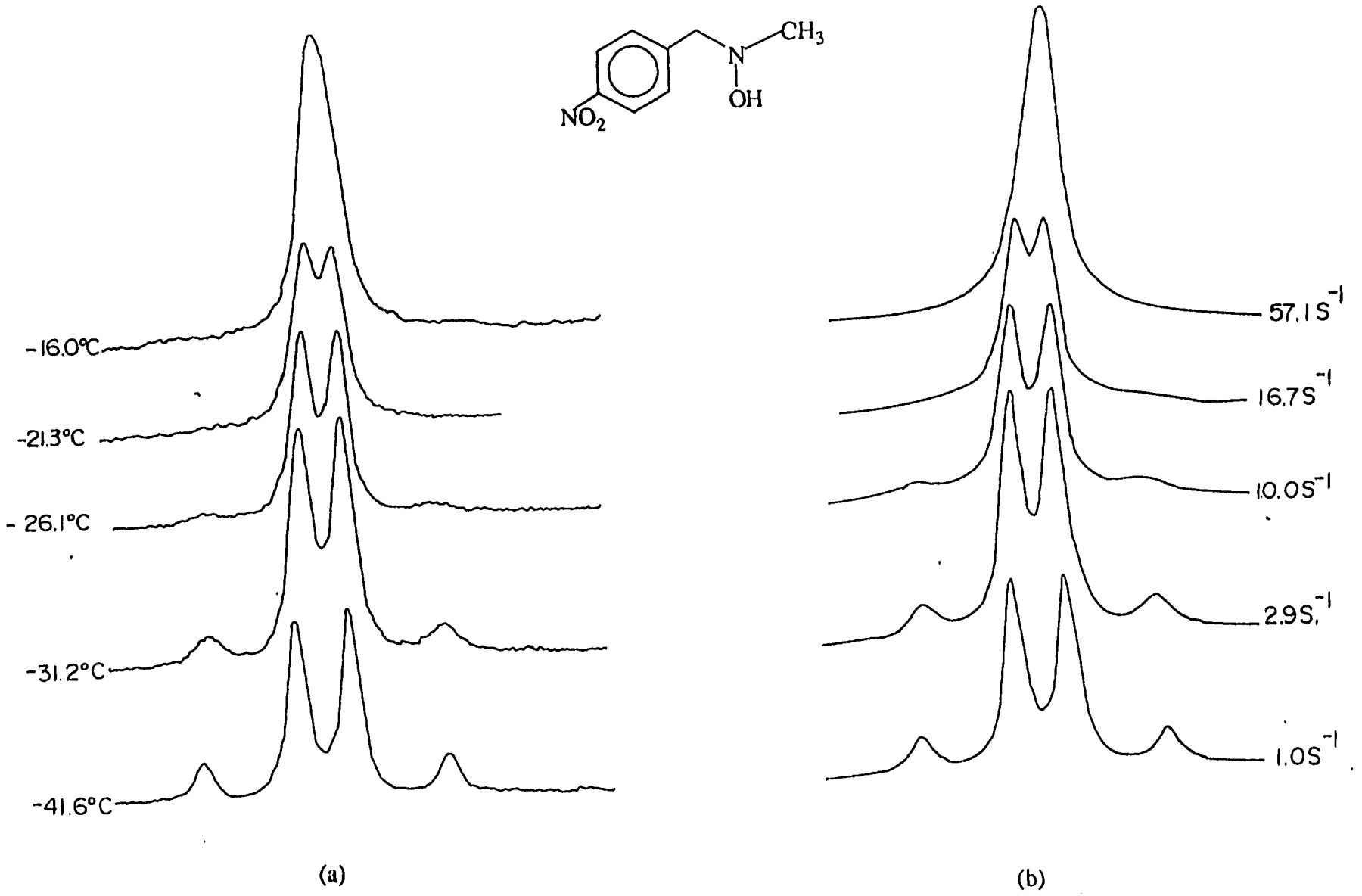

Figure A.3 ^{1}H spectrum of **108b**. (a) Observed (b) Calculated.

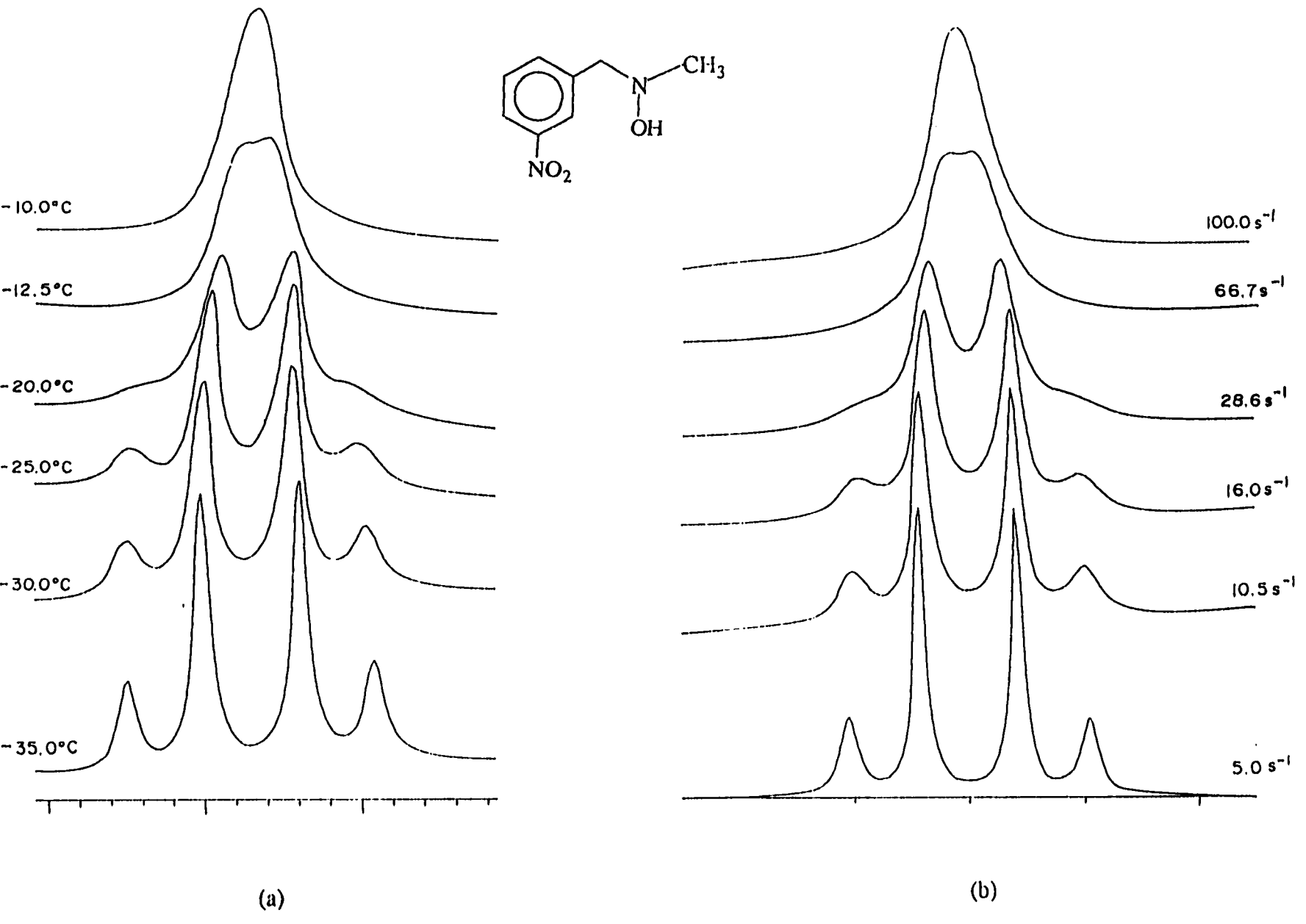

Figure A.4 ^{1}H spectrum of **108g**. (a) Observed (b) Calculated.